Current and future challenges in gravitational wave astronomy (and physics)

Lecture 1 ~ Introduction

April 21, 2026 ~ Caroline Owen

UNIVERSITA' DEGLI STUDI DI MILANO BICOCCA

Logistics

Schedule

Location: U2 - 2016

Time: 10:30 am -12:30 pm

Week 1:

Tuesday, April 21: Introduction

Thursday*, April 23: Fermi Estimates and Dimensional Analysis

Week 2:

Tuesday, April 28: Post Newtonian Binaries

Thursday*, April 30: Stationary Phase Approximation and Waveform Approximants

Week 3:

Tuesday, May 5: Bayesian Overview

Friday, May 8: Binary Parameter Estimation

Week 4:

Tuesday, May 12: Fisher Analysis and Principal Component Analysis

Friday, May 15: Wrap up and Gravity Beyond GR

Materials will be posted to the git repo: github.com/cbo17/CFCGWA_UNIMIB/

Recordings will be posted to: elearning.unimib.it/

Exam

(Only for the PhD students taking the course for credit)

10-minute presentation on your own research or a published paper discussing how it relates to the techniques or topics we have discussed in this class

2 minutes for questions

Note: I will be leaving Milan sometime in June, so we will need to schedule all exams before then

Historical overview

Historical overview

1687: Philosophiæ Naturalis Principia Mathematica

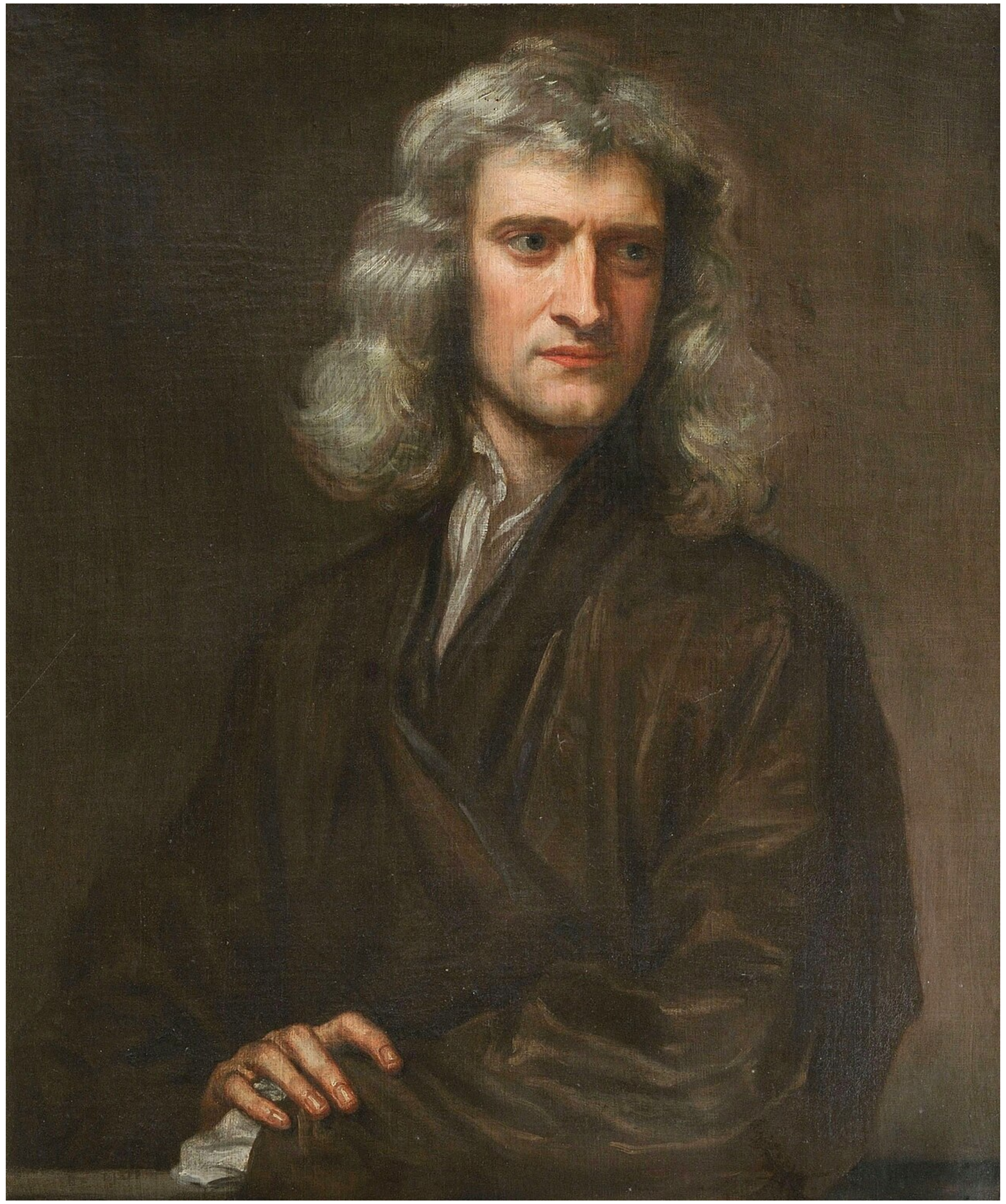

Historical overview

1687: Philosophiæ Naturalis Principia Mathematica

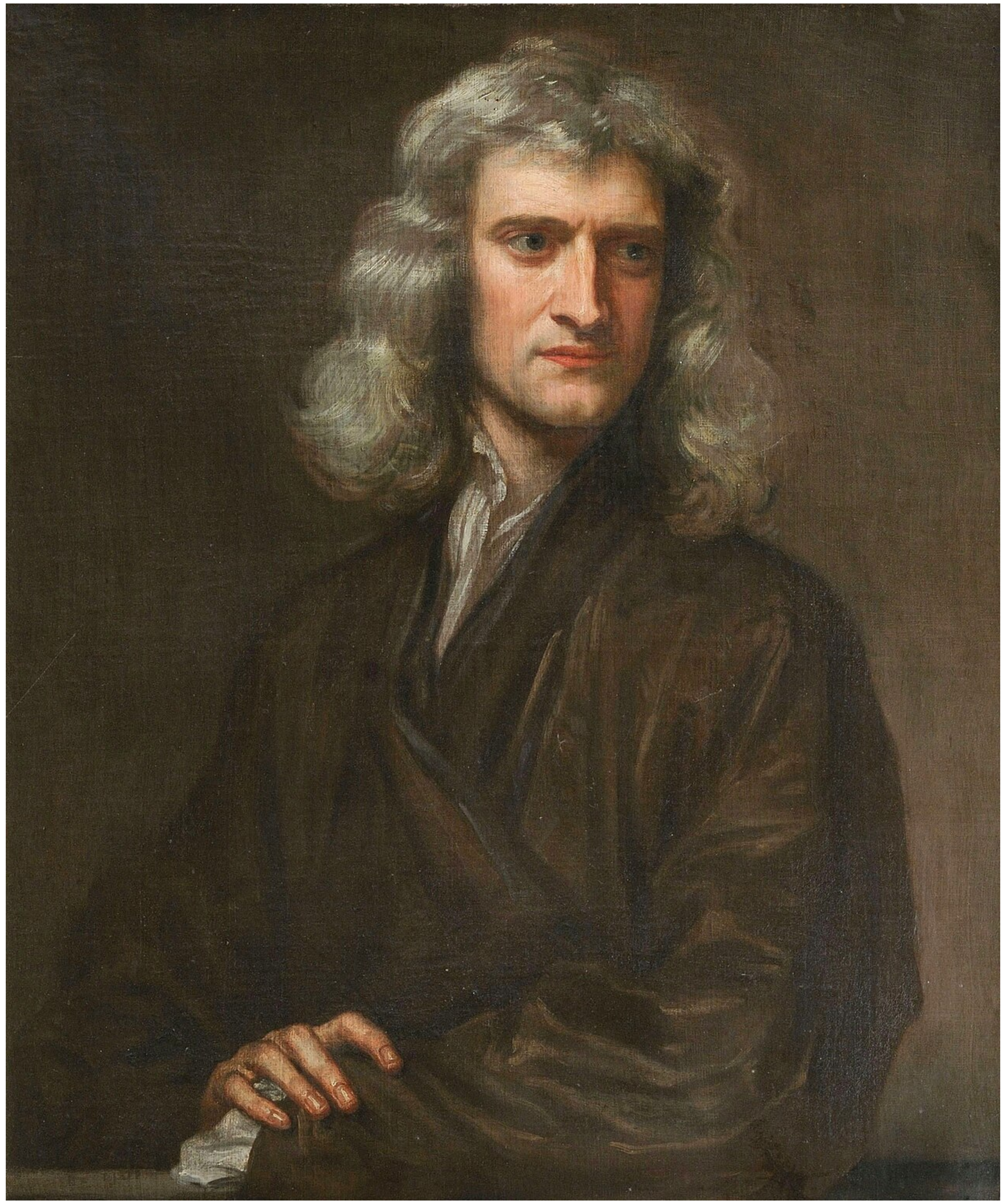

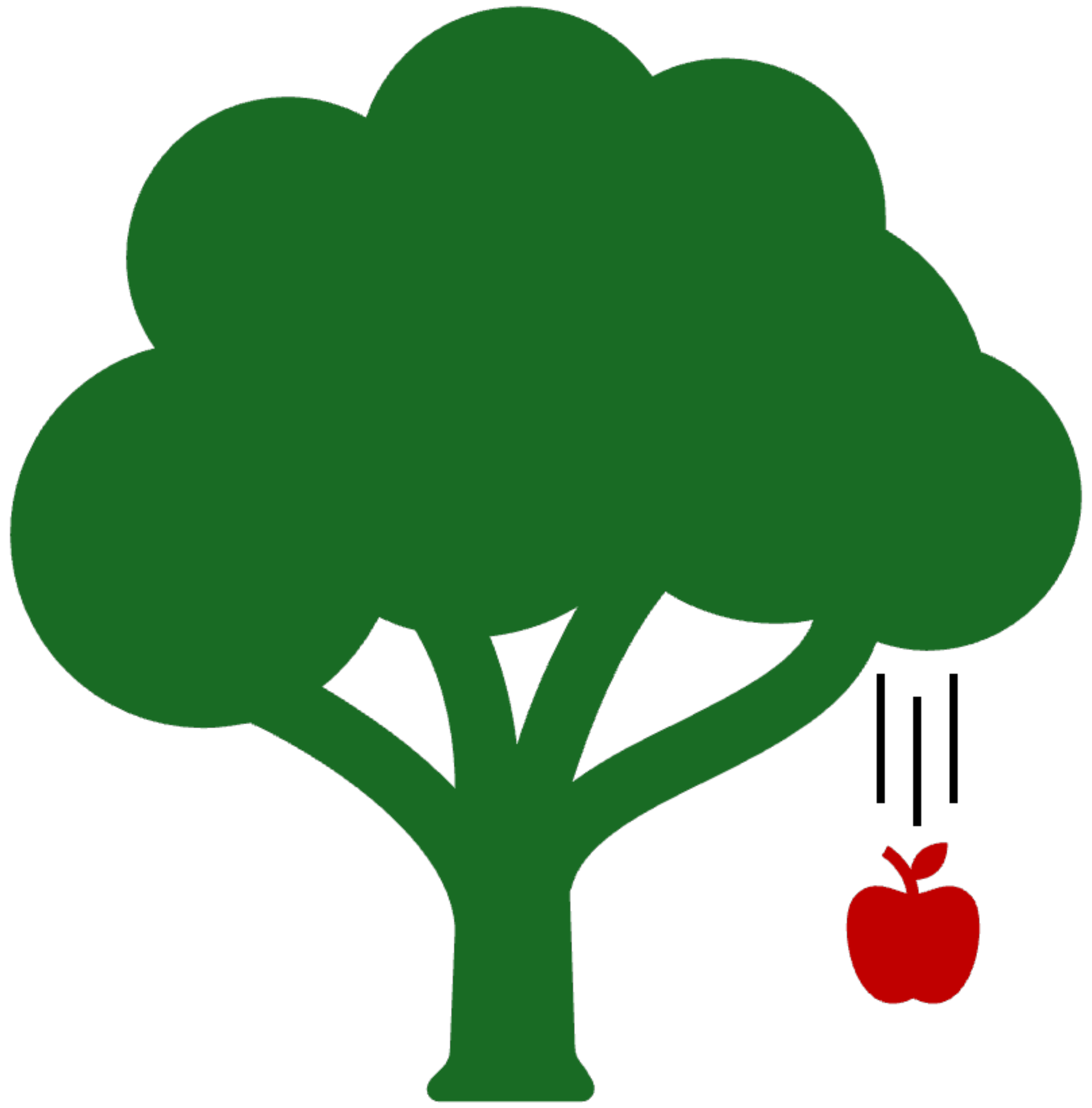

$$F = G\frac{m_1 m_2}{r^2}$$

Historical overview

1687: Philosophiæ Naturalis Principia Mathematica

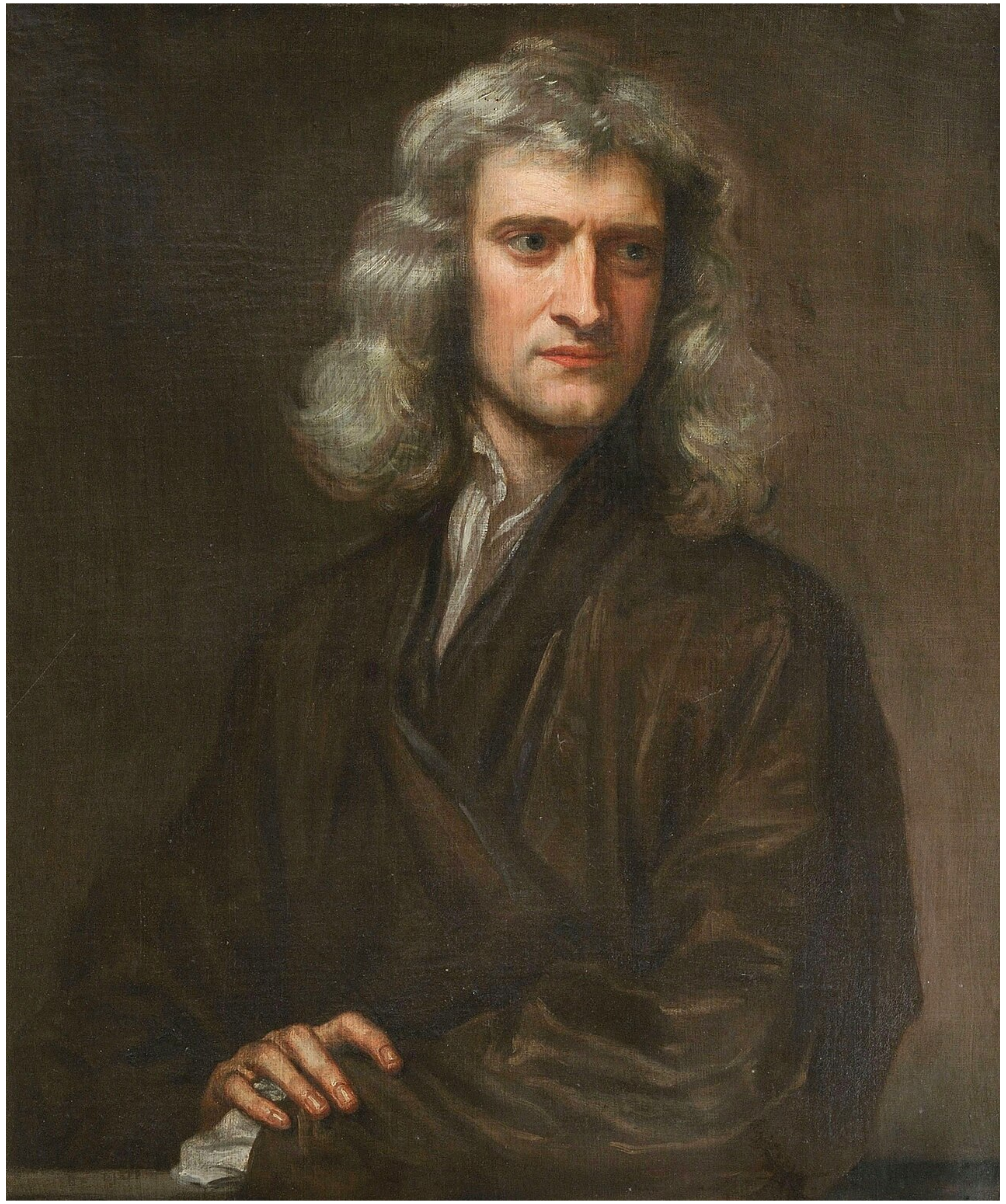

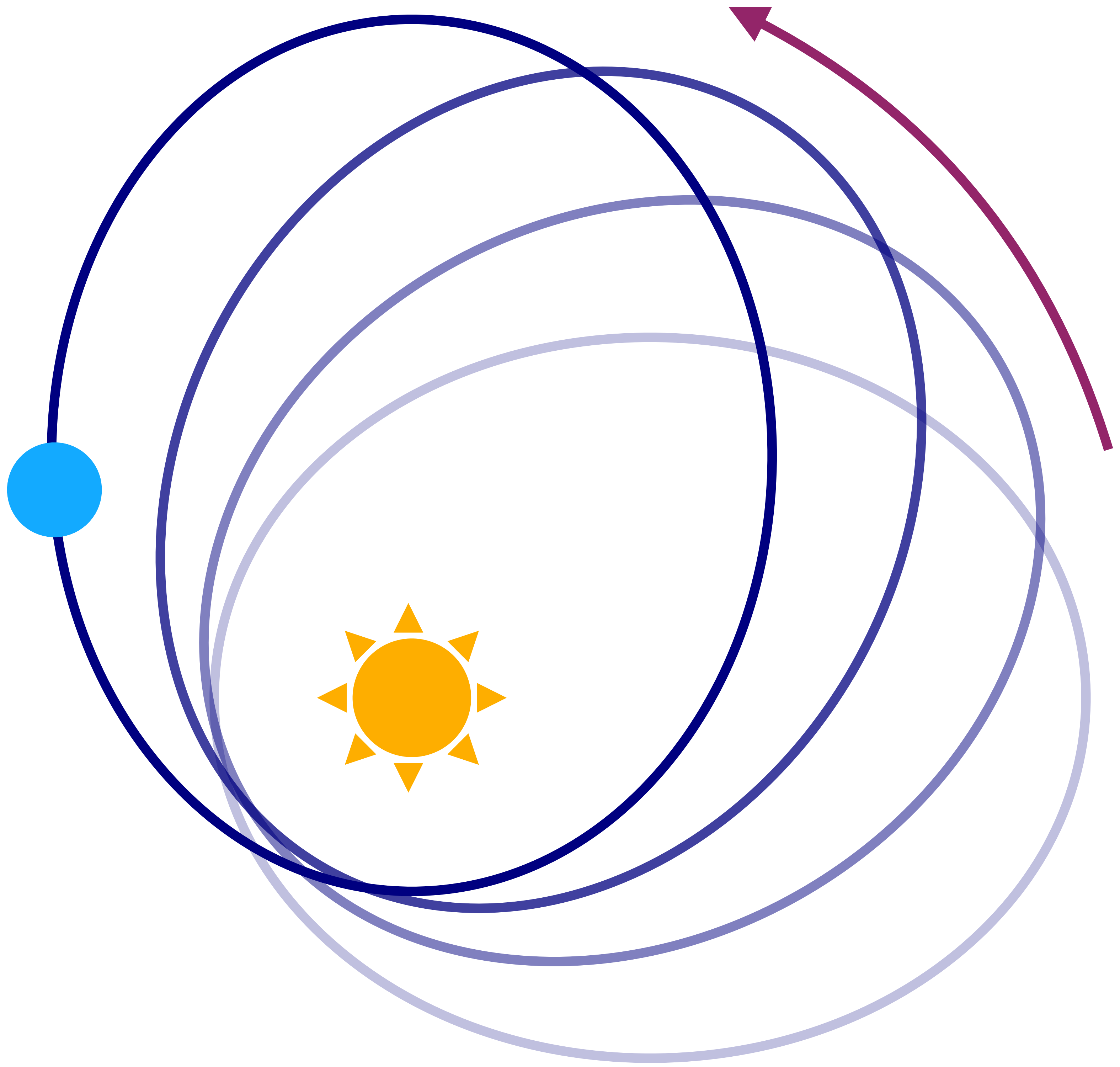

Historical overview

1687: Philosophiæ Naturalis Principia Mathematica

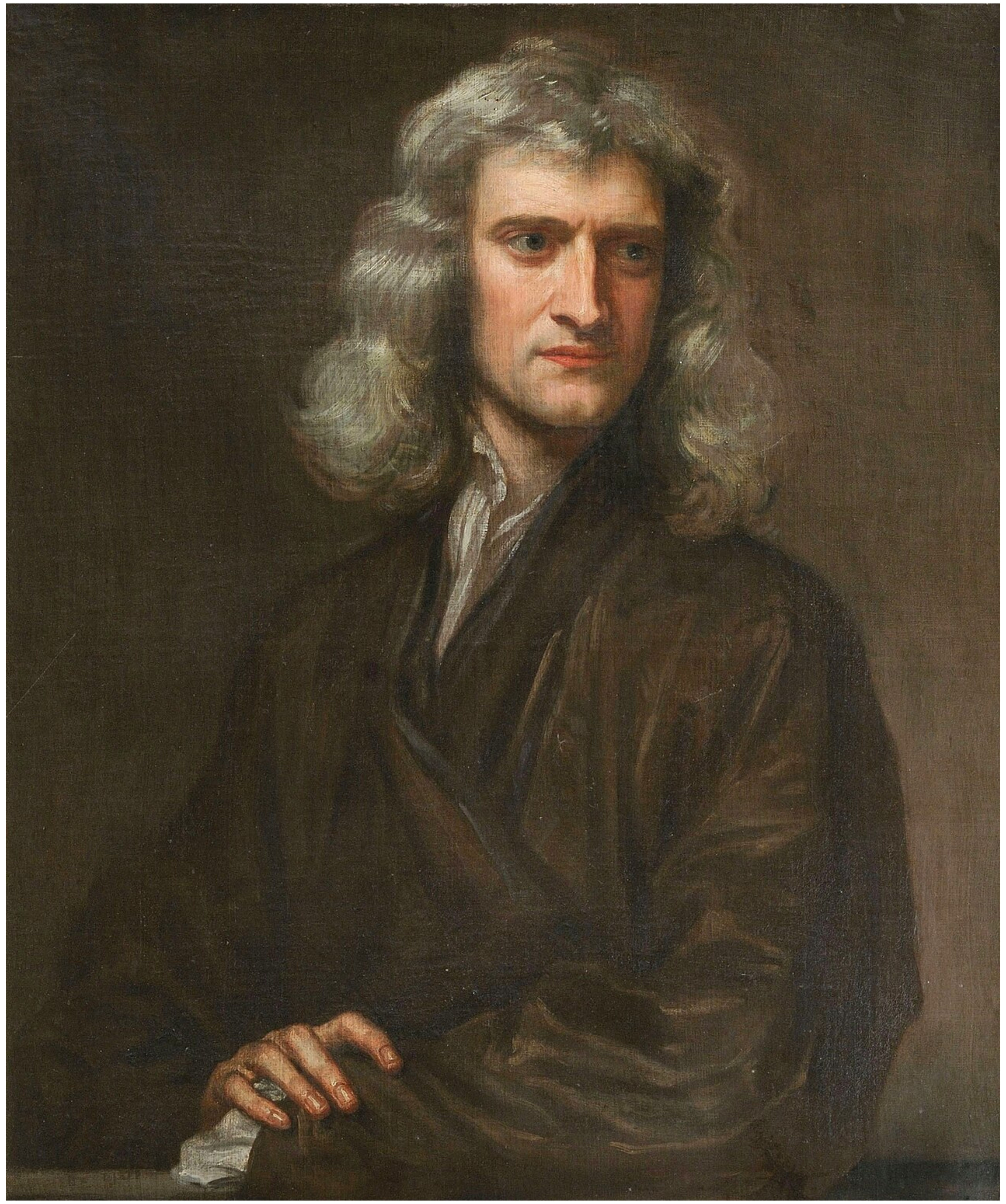

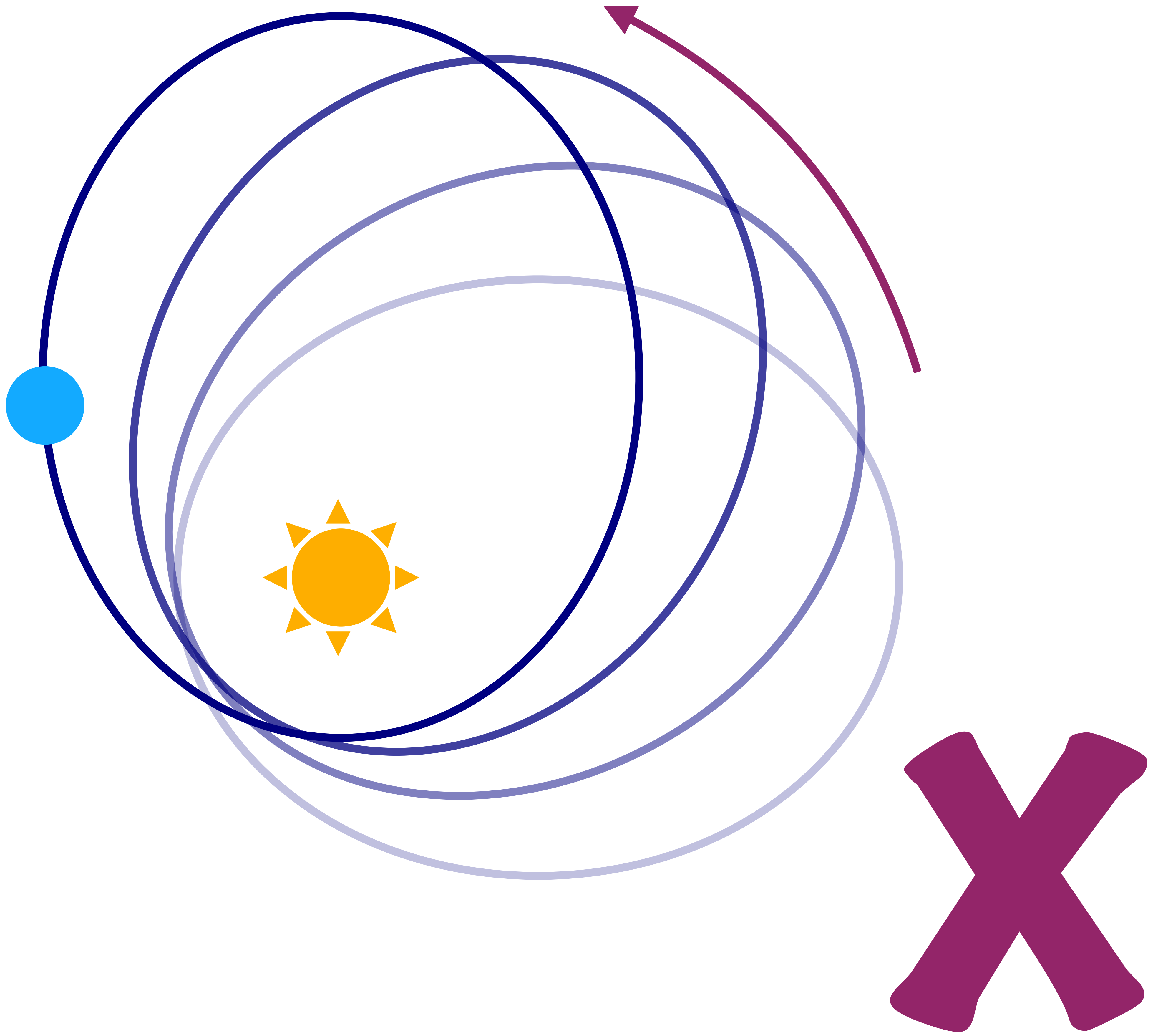

Historical overview

November 1915: *The Field Equations of Gravitation*, Albert Einstein

Die Feldgleichungen der Gravitation.

Von A. Einstein.

In zwei vor kurzem erschienenen Mitteilungen[1] habe ich gezeigt, wie man zu Feldgleichungen der Gravitation gelangen kann, die dem Postulat allgemeiner Relativität entsprechen, d. h. die in ihrer allgemeinen Fassung beliebigen Substitutionen der Raumzeitvariabeln gegenüber kovariant sind.

Der Entwicklungsgang war dabei folgender. Zunächst fand ich Gleichungen, welche die Newtonsche Theorie als Näherung enthalten und beliebigen Substitutionen von der Determinante 1 gegenüber kovariant waren. Hierauf fand ich, daß diesen Gleichungen allgemein kovariante entsprechen, falls der Skalar des Energietensors der »Materie« verschwindet. Das Koordinatensystem war dann nach der einfachen Regel zu spezialisieren, daß $\sqrt{-g}$ zu 1 gemacht wird, wodurch die Gleichungen der Theorie eine eminente Vereinfachung erfahren. Dabei mußte aber, wie erwähnt, die Hypothese eingeführt werden, daß der Skalar des Energietensors der Materie verschwinde.

Neuerdings finde ich nun, daß man ohne Hypothese über den Energietensor der Materie auskommen kann, wenn man den Energietensor der Materie in etwas anderer Weise in die Feldgleichungen einsetzt, als dies in meinen beiden früheren Mitteilungen geschehen ist. Die Feldgleichungen für das Vakuum, auf welche ich die Erklärung der Perihelbewegung des Merkur gegründet habe, bleiben von dieser Modifikation unberührt. Ich gebe hier nochmals die ganze Betrachtung, damit der Leser nicht genötigt ist, die früheren Mitteilungen unausgesetzt heranzuziehen.

Aus der bekannten Riemannschen Kovariante vierten Ranges leitet man folgende Kovariante zweiten Ranges ab:

$$G_{im} = R_{im} + S_{im} \tag{1}$$

$$R_{im} = -\sum_l \frac{\partial \begin{Bmatrix} im \\ l \end{Bmatrix}}{\partial x_l} + \sum_{l\rho} \begin{Bmatrix} il \\ \rho \end{Bmatrix} \begin{Bmatrix} m\rho \\ l \end{Bmatrix} \tag{1a}$$

$$S_{im} = \sum_l \frac{\partial \begin{Bmatrix} il \\ l \end{Bmatrix}}{\partial x_m} - \sum_{l\rho} \begin{Bmatrix} im \\ \rho \end{Bmatrix} \begin{Bmatrix} \rho l \\ l \end{Bmatrix} \tag{1b}$$

[1] Sitzungsber. XLIV, S. 778 und XLVI, S. 799, 1915.

Die allgemein kovarianten zehn Gleichungen des Gravitationsfeldes in Räumen, in denen »Materie« fehlt, erhalten wir, indem wir ansetzen

$$G_{im} = 0. \tag{2}$$

Diese Gleichungen lassen sich einfacher gestalten, wenn man das Bezugssystem so wählt, daß $\sqrt{-g} = 1$ ist. Dann verschwindet S_{im} wegen (1b), so daß man statt (2) erhält

$$R_{im} = \sum_l \frac{\partial \Gamma^l_{im}}{\partial x_l} + \sum_{\rho l} \Gamma^l_{i\rho} \Gamma^\rho_{ml} = 0 \tag{3}$$

$$\sqrt{-g} = 1. \tag{3a}$$

Dabei ist

$$\Gamma^l_{im} = -\begin{Bmatrix} im \\ l \end{Bmatrix} \tag{4}$$

gesetzt, welche Größen wir als die »Komponenten« des Gravitationsfeldes bezeichnen.

Ist in dem betrachteten Raume »Materie« vorhanden, so tritt deren Energietensor auf der rechten Seite von (2) bzw. (3) auf. Wir setzen

$$G_{im} = -\varkappa \left(T_{im} - \frac{1}{2} g_{im} T \right), \tag{2a}$$

wobei

$$\sum_{\rho\sigma} g^{\rho\sigma} T_{\rho\sigma} = \sum_\sigma T^\sigma_\sigma = T \tag{5}$$

gesetzt ist; T ist der Skalar des Energietensors der »Materie«, die rechte Seite von (2a) ein Tensor. Spezialisieren wir wieder das Koordinatensystem in der gewohnten Weise, so erhalten wir an Stelle von (2a) die äquivalenten Gleichungen

$$R_{im} = \sum_l \frac{\partial \Gamma^l_{im}}{\partial x_l} + \sum_{\rho l} \Gamma^l_{i\rho} \Gamma^\rho_{ml} = -\varkappa \left(T_{im} - \frac{1}{2} g_{im} T \right) \tag{6}$$

$$\sqrt{-g} = 1. \tag{3a}$$

Wie stets nehmen wir an, daß die Divergenz des Energietensors der Materie im Sinne des allgemeinen Differentialkalkuls verschwinde (Impulsenergiesatz). Bei der Spezialisierung der Koordinatenwahl gemäß (3a) kommt dies darauf hinaus, daß die T_{im} die Bedingungen

$$\sum_\lambda \frac{\partial T^\lambda_\sigma}{\partial x_\lambda} = -\frac{1}{2} \sum_{\mu\nu} \frac{\partial g^{\mu\nu}}{\partial x_\sigma} T_{\mu\nu} \tag{7}$$

oder

$$\sum_\lambda \frac{\partial T^\lambda_\sigma}{\partial x_\lambda} = -\sum_{\mu\nu} \Gamma^\mu_{\sigma\nu} T^\nu_\mu \tag{7a}$$

erfüllen sollen.

Multipliziert man (6) mit $\frac{\partial g^{im}}{\partial x_\sigma}$ und summiert über i und m, so erhält man[1] mit Rücksicht auf (7) und auf die aus (3a) folgende Relation

$$\frac{1}{2} \sum_{im} g_{im} \frac{\partial g^{im}}{\partial x_\sigma} = -\frac{\partial \lg \sqrt{-g}}{\partial x_\sigma} = 0$$

den Erhaltungssatz für Materie und Gravitationsfeld zusammen in der Form

$$\sum_\lambda \frac{\partial}{\partial x_\lambda} (T^\lambda_\sigma + t^\lambda_\sigma) = 0, \tag{8}$$

wobei t^λ_σ (der »Energietensor« des Gravitationsfeldes) gegeben ist durch

$$\varkappa t^\lambda_\sigma = \frac{1}{2} \delta^\lambda_\sigma \sum_{\mu\nu\alpha\beta} g^{\mu\nu} \Gamma^\alpha_{\mu\beta} \Gamma^\beta_{\nu\alpha} - \sum g^{\mu\nu} \Gamma^\alpha_{\mu\sigma} \Gamma^\lambda_{\nu\alpha}. \tag{8a}$$

Die Gründe, welche mich zur Einführung des zweiten Gliedes auf der rechten Seite von (2a) und (6) veranlaßt haben, erhellen erst aus den folgenden Überlegungen, welche den an der soeben angeführten Stelle (S. 785) gegebenen völlig analog sind.

Multiplizieren wir (6) mit g^{im} und summieren wir über die Indizes i und m, so erhalten wir nach einfacher Rechnung

$$\sum_{\alpha\beta} \frac{\partial^2 g^{\alpha\beta}}{\partial x_\alpha \partial x_\beta} - \varkappa (T + t) = 0, \tag{9}$$

wobei entsprechend (5) zur Abkürzung gesetzt ist

$$\sum_{\rho\sigma} g^{\rho\sigma} t_{\rho\sigma} = \sum_\sigma t^\sigma_\sigma = t. \tag{8b}$$

Man beachte, daß es unser Zusatzglied mit sich bringt, daß in (9) der Energietensor des Gravitationsfeldes neben dem der Materie in gleicher Weise auftritt, was in Gleichung (21) a. a. O. nicht der Fall ist.

Ferner leitet man an Stelle der Gleichung (22) a. a. O. auf dem dort angegebenen Wege mit Hilfe der Energiegleichung die Relationen ab:

$$\frac{\partial}{\partial x_\mu} \left[\sum_{\alpha\beta} \frac{\partial^2 g^{\alpha\beta}}{\partial x_\alpha \partial x_\beta} - \varkappa (T + t) \right] = 0. \tag{10}$$

Unser Zusatzglied bringt es mit sich, daß diese Gleichungen gegenüber (9) keine neue Bedingung enthalten, so daß über den Energie-

[1] Über die Ableitung vgl. Sitzungsber. XLIV, 1915, S. 784/785. Ich ersuche den Leser, für das Folgende auch die dort auf S. 785 gegebenen Entwicklungen zum Vergleiche heranzuziehen.

tensor der Materie keine andere Voraussetzung gemacht werden muß als die, daß er dem Impulsenergiesatze entspricht.

Damit ist endlich die allgemeine Relativitätstheorie als logisches Gebäude abgeschlossen. Das Relativitätspostulat in seiner allgemeinsten Fassung, welches die Raumzeitkoordinaten zu physikalisch bedeutungslosen Parametern macht, führt mit zwingender Notwendigkeit zu einer ganz bestimmten Theorie der Gravitation, welche die Perihelbewegung des Merkur erklärt. Dagegen vermag das allgemeine Relativitätspostulat uns nichts über das Wesen der übrigen Naturvorgänge zu offenbaren, was nicht schon die spezielle Relativitätstheorie gelehrt hätte. Meine in dieser Hinsicht neulich an dieser Stelle geäußerte Meinung war irrtümlich. Jede der speziellen Relativitätstheorie gemäße physikalische Theorie kann vermittels des absoluten Differentialkalkuls in das System der allgemeinen Relativitätstheorie eingereiht werden, ohne daß letztere irgendein Kriterium für die Zulässigkeit jener Theorie lieferte.

Ausgegeben am 2. Dezember.

Historical overview

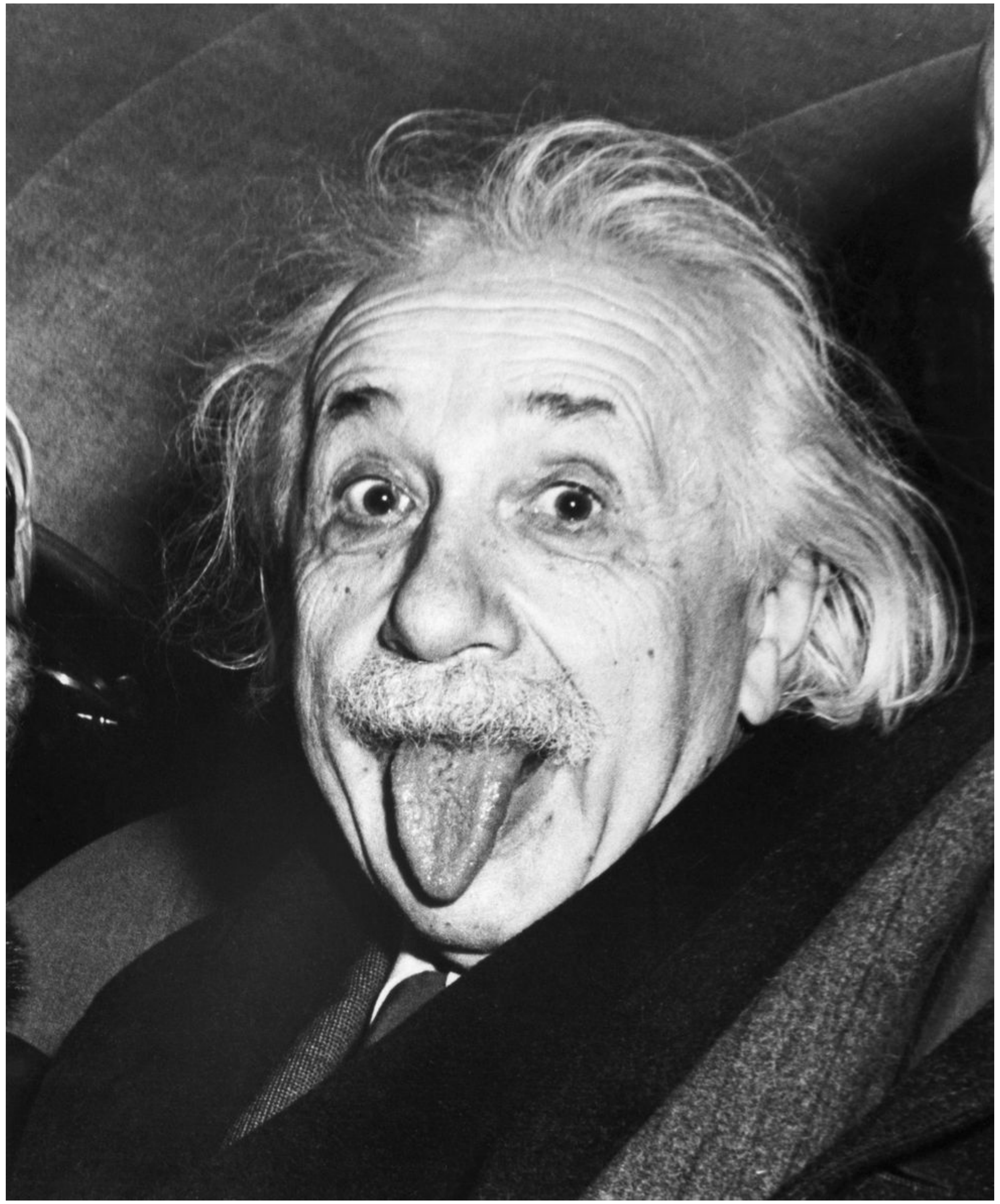

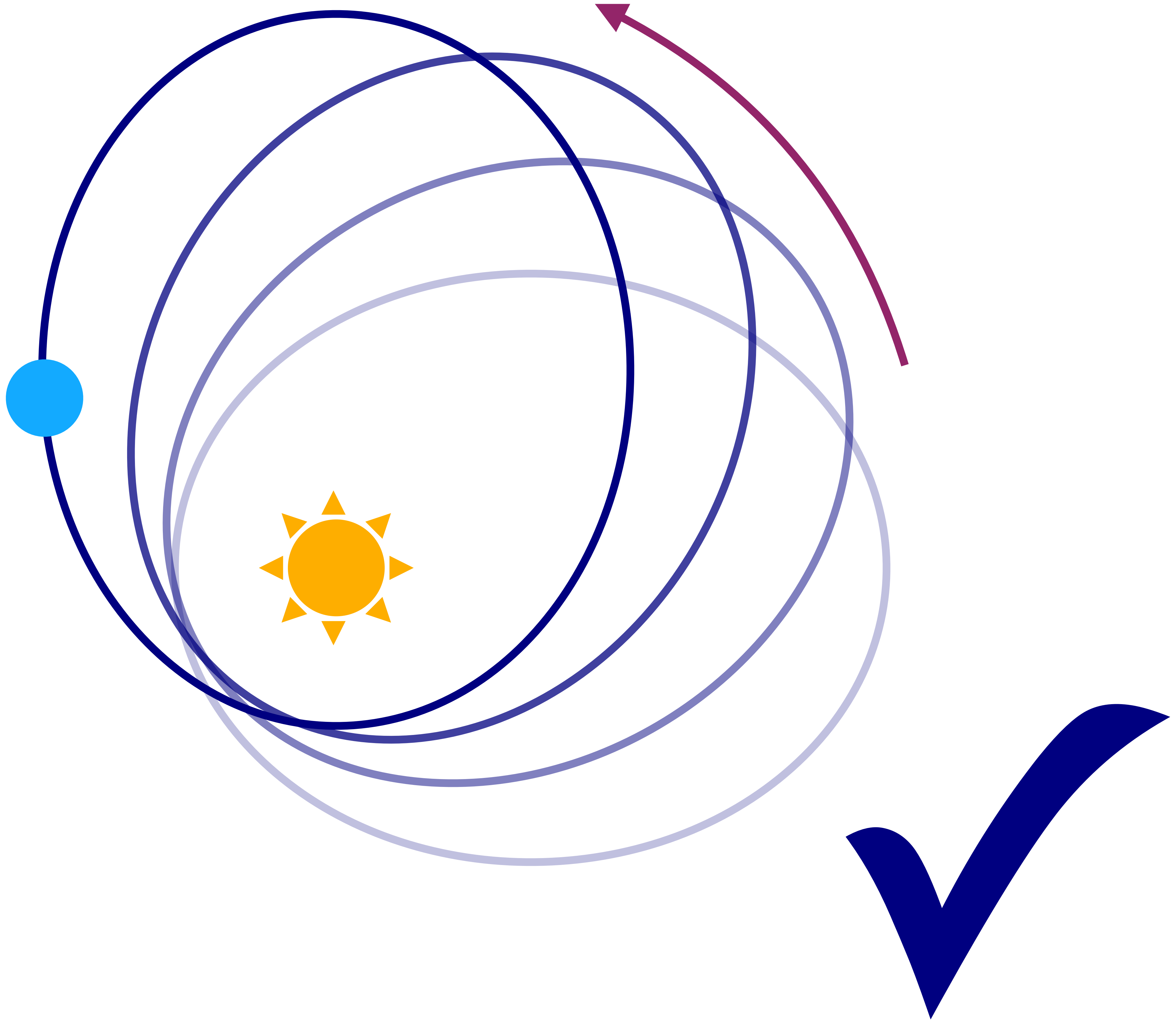

Historical overview

1919: The Eddington experiment, first confirmation of a novel prediction of GR

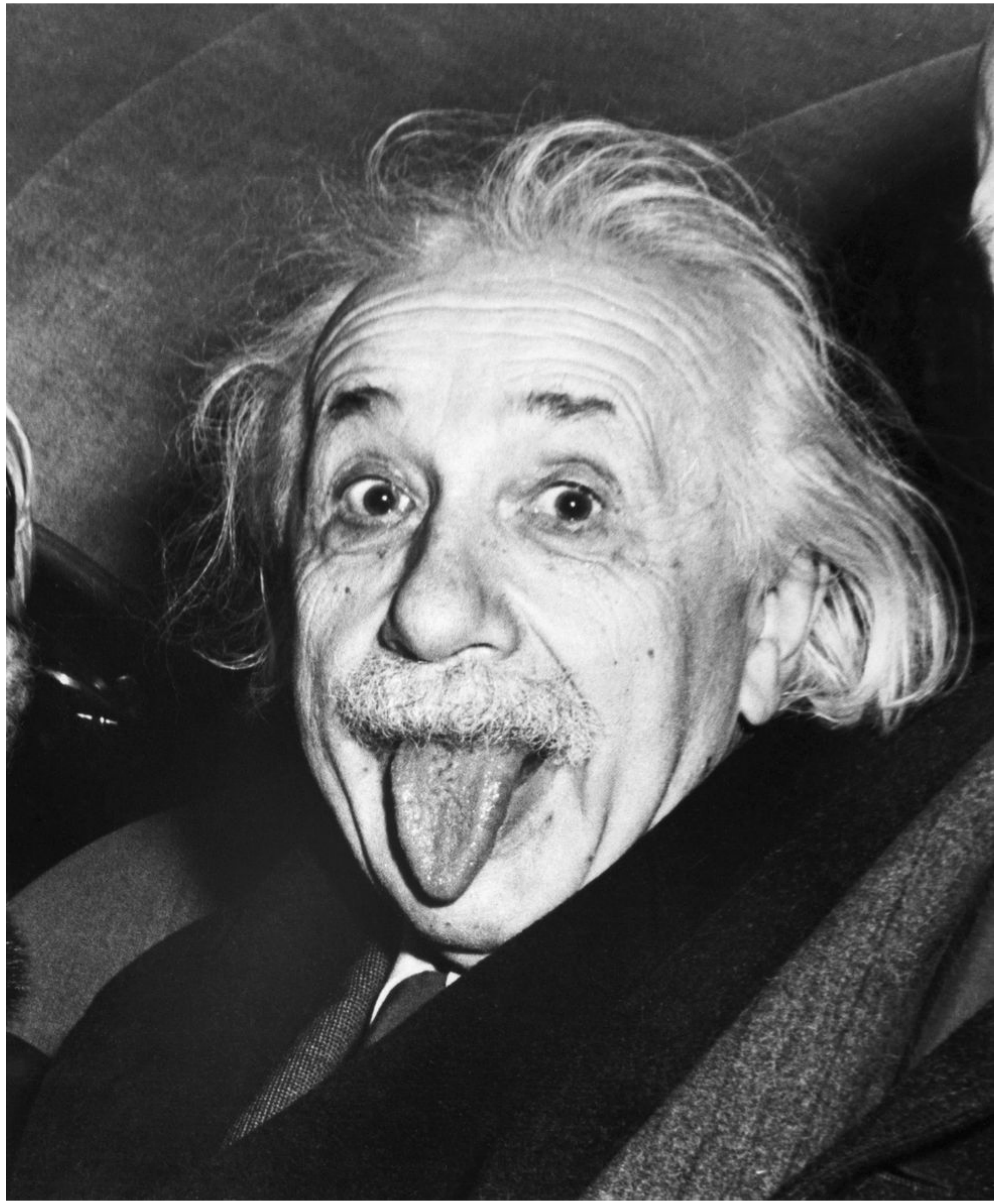

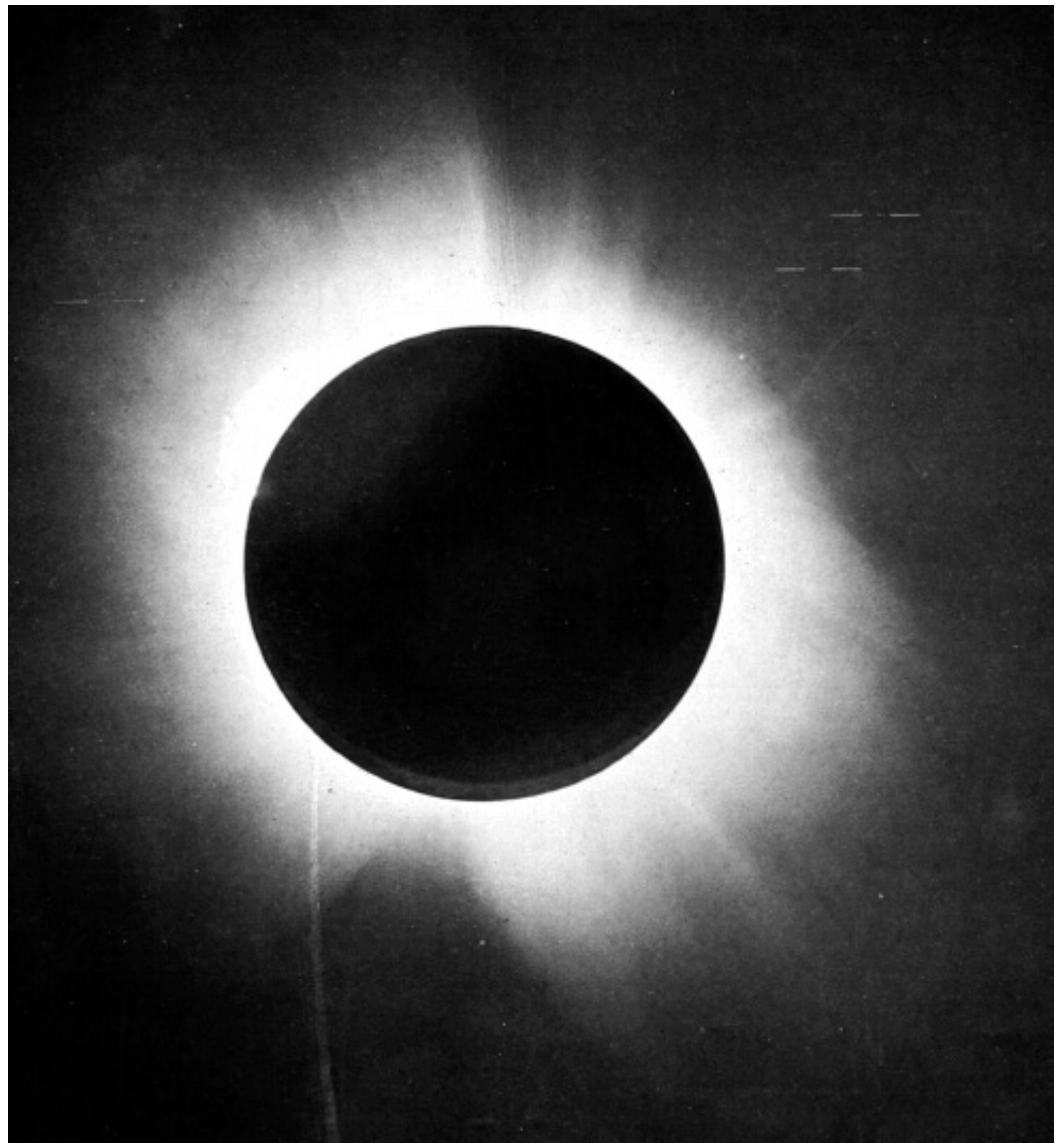

The New York Times
November 10, 1919

LIGHTS ALL ASKEW IN THE HEAVENS

Men of Science More or Less Agog Over Results of Eclipse Observations.

EINSTEIN THEORY TRIUMPHS

Stars Not Where They Seemed or Were Calculated to be, but Nobody Need Worry.

A BOOK FOR 12 WISE MEN

No More in All the World Could Comprehend It, Said Einstein When His Daring Publishers Accepted It.

Historical overview

1919: The Eddington experiment, first confirmation of a novel prediction of GR

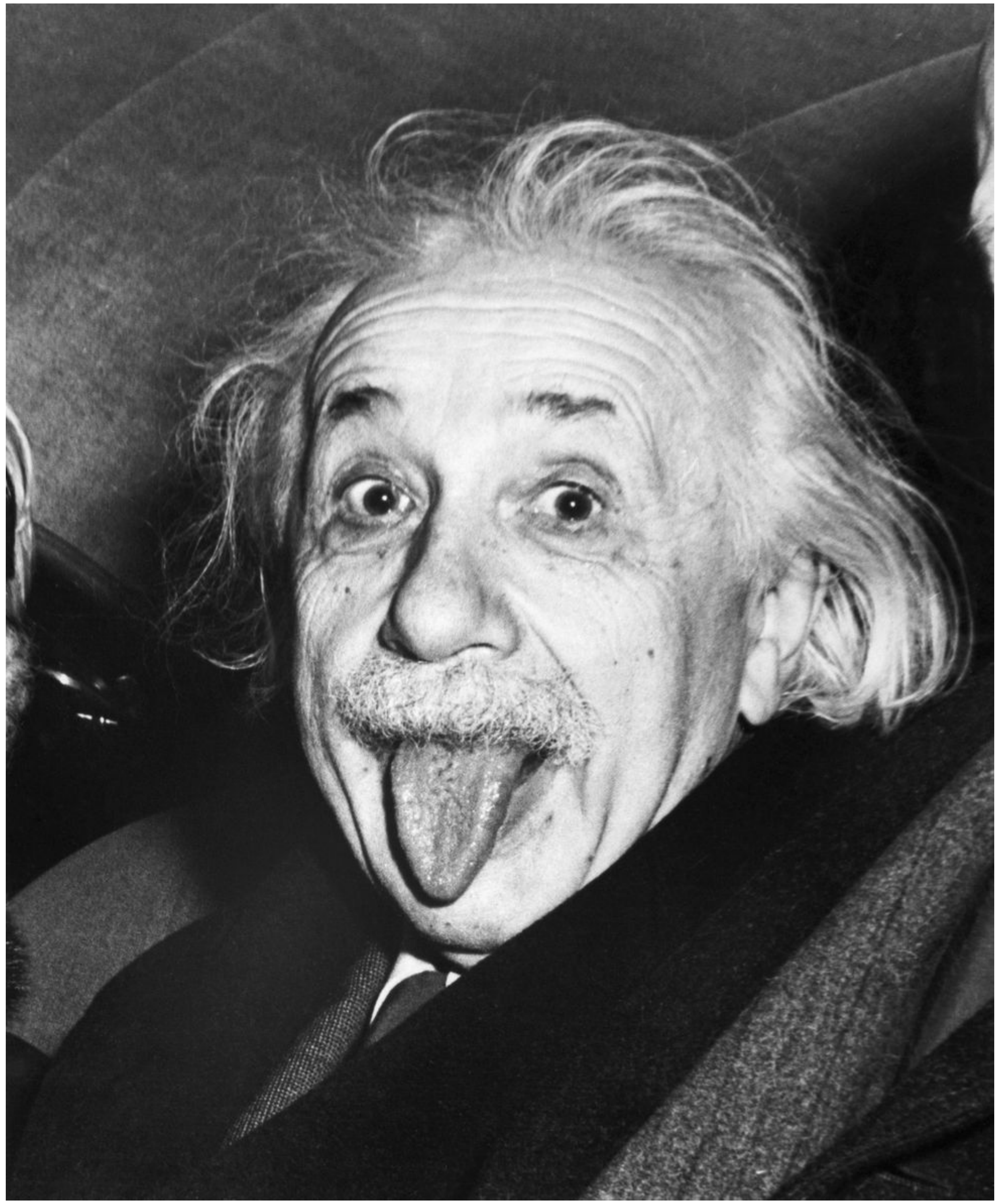

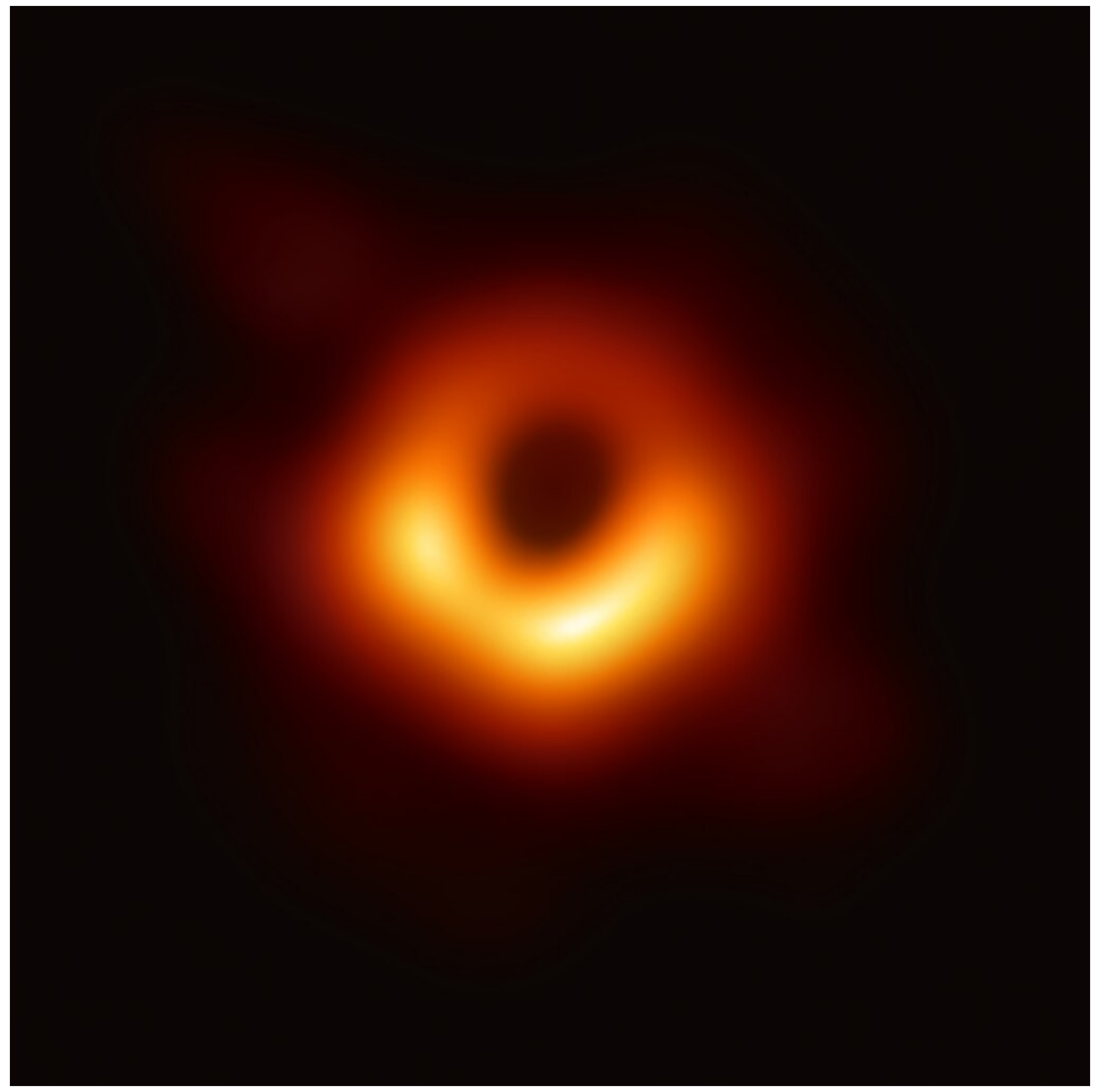

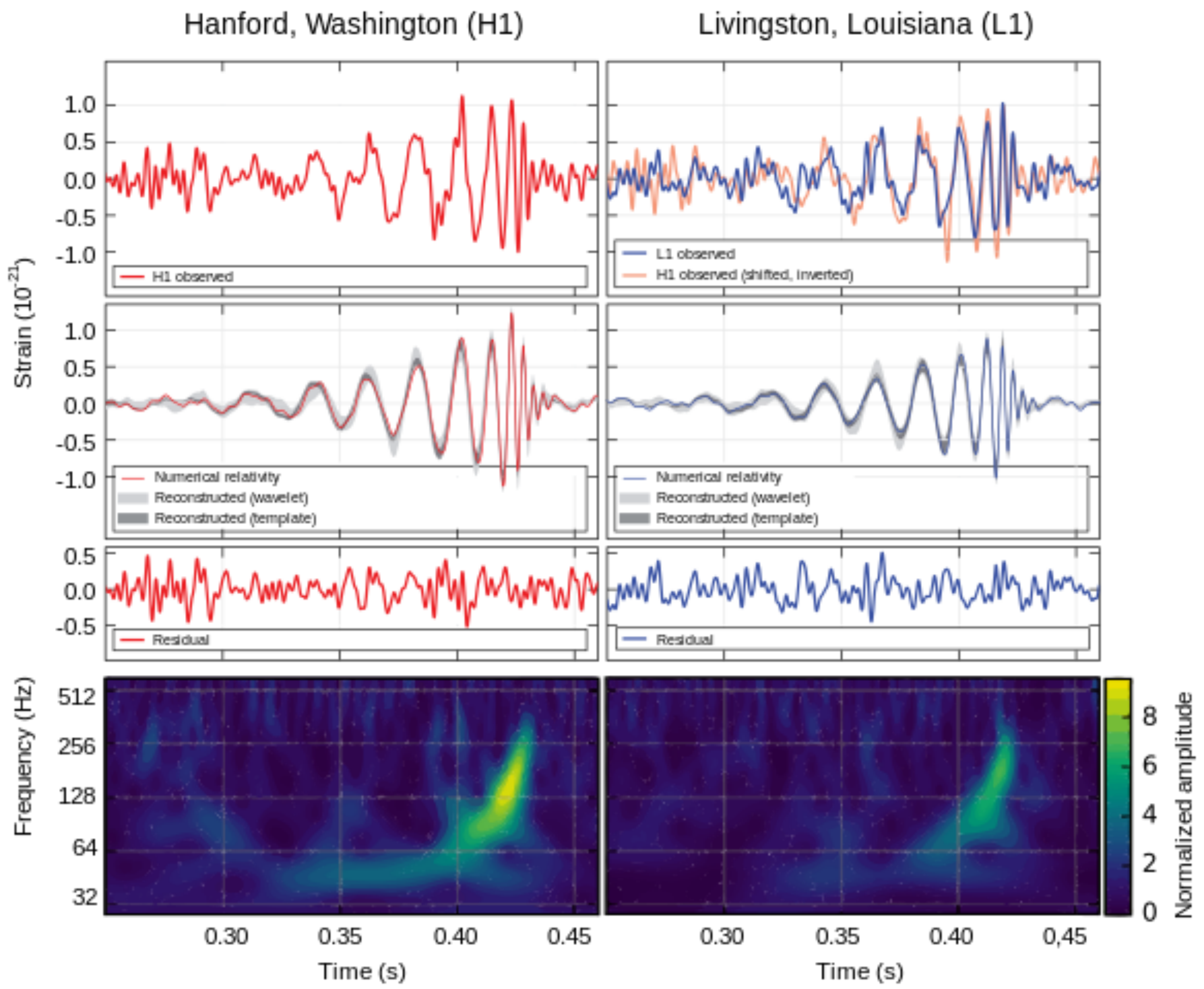

Historical overview

1916 and 1918: Einstein claims the existence of gravitational waves

"Approximate integration of the field equations of gravitation"

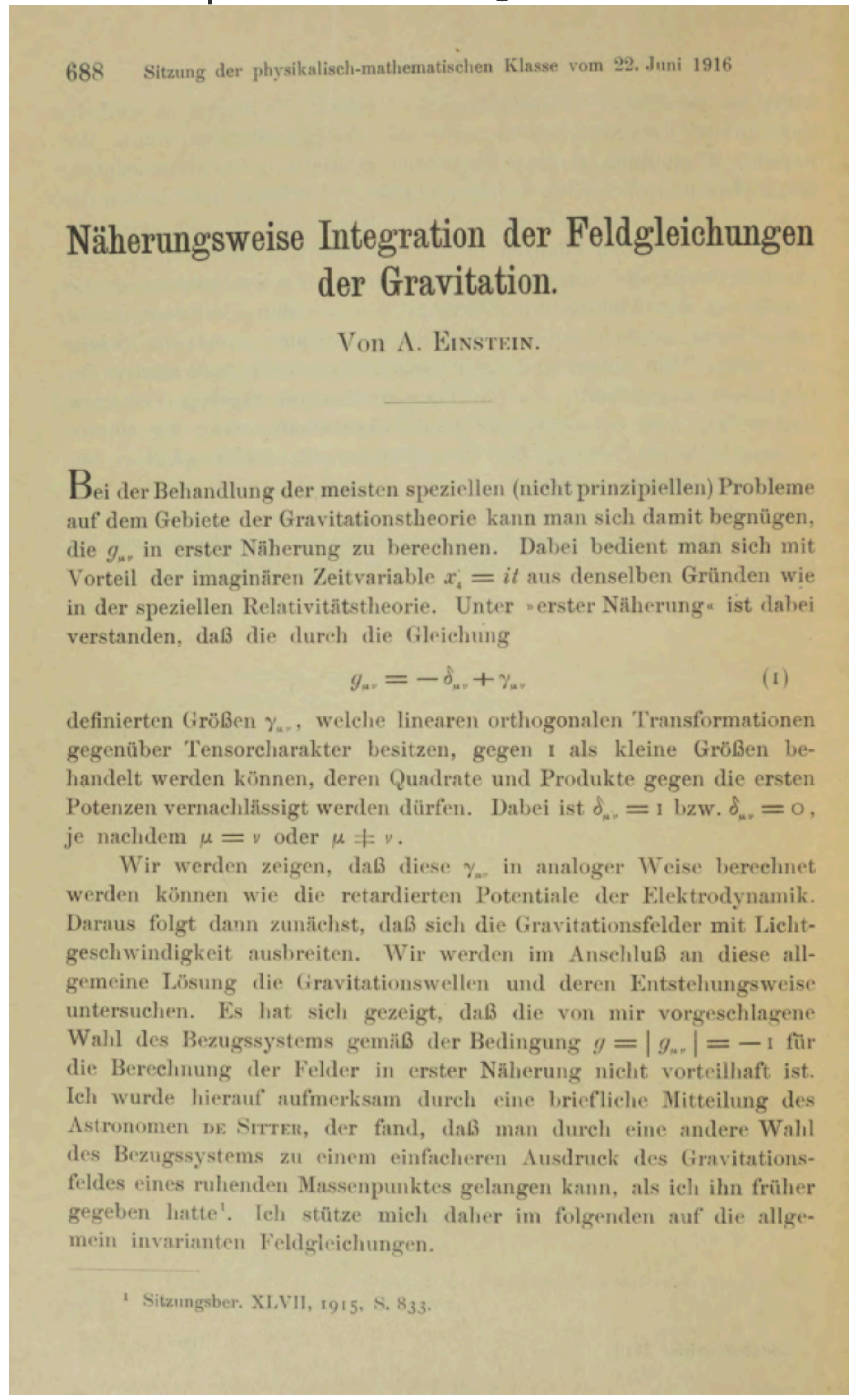

688 Sitzung der physikalisch-mathematischen Klasse vom 22. Juni 1916

Näherungsweise Integration der Feldgleichungen der Gravitation.

Von A. Einstein.

Bei der Behandlung der meisten speziellen (nicht prinzipiellen) Probleme auf dem Gebiete der Gravitationstheorie kann man sich damit begnügen, die $g_{\mu\nu}$ in erster Näherung zu berechnen. Dabei bedient man sich mit Vorteil der imaginären Zeitvariable $x_4 = it$ aus denselben Gründen wie in der speziellen Relativitätstheorie. Unter »erster Näherung« ist dabei verstanden, daß die durch die Gleichung

$$g_{\mu\nu} = -\delta_{\mu\nu} + \gamma_{\mu\nu} \qquad (1)$$

definierten Größen $\gamma_{\mu\nu}$, welche linearen orthogonalen Transformationen gegenüber Tensorcharakter besitzen, gegen 1 als kleine Größen behandelt werden können, deren Quadrate und Produkte gegen die ersten Potenzen vernachlässigt werden dürfen. Dabei ist $\delta_{\mu\nu} = 1$ bzw. $\delta_{\mu\nu} = 0$, je nachdem $\mu = \nu$ oder $\mu \neq \nu$.

Wir werden zeigen, daß diese $\gamma_{\mu\nu}$ in analoger Weise berechnet werden können wie die retardierten Potentiale der Elektrodynamik. Daraus folgt dann zunächst, daß sich die Gravitationsfelder mit Lichtgeschwindigkeit ausbreiten. Wir werden im Anschluß an diese allgemeine Lösung die Gravitationswellen und deren Entstehungsweise untersuchen. Es hat sich gezeigt, daß die von mir vorgeschlagene Wahl des Bezugssystems gemäß der Bedingung $g = |g_{\mu\nu}| = -1$ für die Berechnung der Felder in erster Näherung nicht vorteilhaft ist. Ich wurde hierauf aufmerksam durch eine briefliche Mitteilung des Astronomen de Sitter, der fand, daß man durch eine andere Wahl des Bezugssystems zu einem einfacheren Ausdruck des Gravitationsfeldes eines ruhenden Massenpunktes gelangen kann, als ich ihn früher gegeben hatte[1]. Ich stütze mich daher im folgenden auf die allgemein invarianten Feldgleichungen.

[1] Sitzungsber. XLVII, 1915, S. 833.

"On gravitational waves"

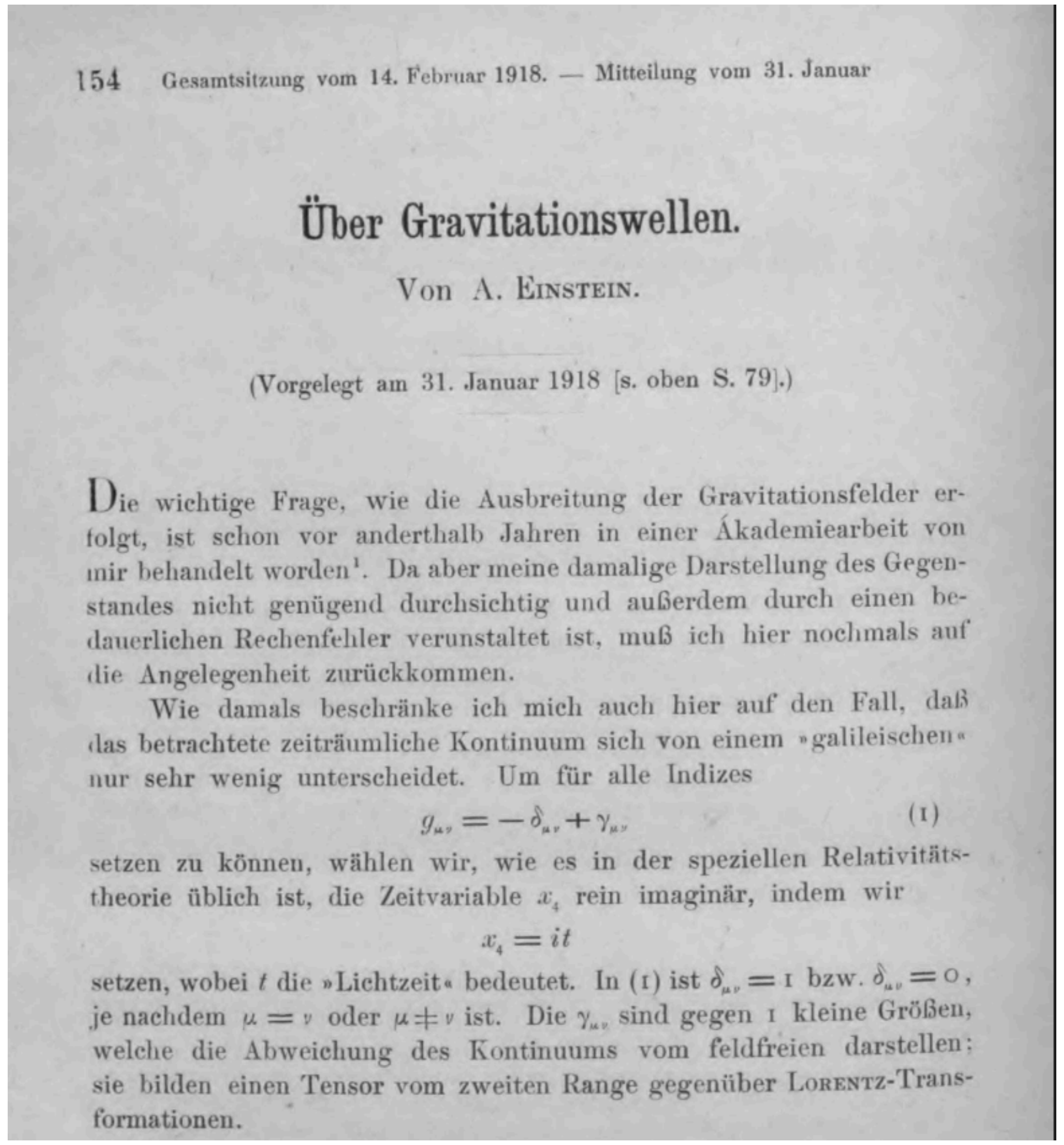

154 Gesamtsitzung vom 14. Februar 1918. — Mitteilung vom 31. Januar

Über Gravitationswellen.

Von A. Einstein.

(Vorgelegt am 31. Januar 1918 [s. oben S. 79].)

Die wichtige Frage, wie die Ausbreitung der Gravitationsfelder erfolgt, ist schon vor anderthalb Jahren in einer Akademiearbeit von mir behandelt worden[1]. Da aber meine damalige Darstellung des Gegenstandes nicht genügend durchsichtig und außerdem durch einen bedauerlichen Rechenfehler verunstaltet ist, muß ich hier nochmals auf die Angelegenheit zurückkommen.

Wie damals beschränke ich mich auch hier auf den Fall, daß das betrachtete zeiträumliche Kontinuum sich von einem »galileischen« nur sehr wenig unterscheidet. Um für alle Indizes

$$g_{\mu\nu} = -\delta_{\mu\nu} + \gamma_{\mu\nu} \qquad (1)$$

setzen zu können, wählen wir, wie es in der speziellen Relativitätstheorie üblich ist, die Zeitvariable x_4 rein imaginär, indem wir

$$x_4 = it$$

setzen, wobei t die »Lichtzeit« bedeutet. In (1) ist $\delta_{\mu\nu} = 1$ bzw. $\delta_{\mu\nu} = 0$, je nachdem $\mu = \nu$ oder $\mu \neq \nu$ ist. Die $\gamma_{\mu\nu}$ sind gegen 1 kleine Größen, welche die Abweichung des Kontinuums vom feldfreien darstellen; sie bilden einen Tensor vom zweiten Range gegenüber Lorentz-Transformationen.

Historical overview

1916 and 1918: Einstein claims the existence of gravitational waves

"Approximate integration of the field equations of gravitation"

688 Sitzung der physikalisch-mathematischen Klasse vom 22. Juni 1916

Näherungsweise Integration der Feldgleichungen der Gravitation.

Von A. Einstein.

Bei der Behandlung der meisten speziellen (nicht prinzipiellen) Probleme auf dem Gebiete der Gravitationstheorie kann man sich damit begnügen, die $g_{\mu\nu}$ in erster Näherung zu berechnen. Dabei bedient man sich mit Vorteil der imaginären Zeitvariable $x_4 = it$ aus denselben Gründen wie in der speziellen Relativitätstheorie. Unter »erster Näherung« ist dabei verstanden, daß die durch die Gleichung

$$g_{\mu\nu} = -\delta_{\mu\nu} + \gamma_{\mu\nu} \tag{1}$$

definierten Größen $\gamma_{\mu\nu}$, welche linearen orthogonalen Transformationen gegenüber Tensorcharakter besitzen, gegen 1 als kleine Größen behandelt werden können, deren Quadrate und Produkte gegen die ersten Potenzen vernachlässigt werden dürfen. Dabei ist $\delta_{\mu\nu} = 1$ bzw. $\delta_{\mu\nu} = 0$, je nachdem $\mu = \nu$ oder $\mu \neq \nu$.

Wir werden zeigen, daß diese $\gamma_{\mu\nu}$ in analoger Weise berechnet werden können wie die retardierten Potentiale der Elektrodynamik. Daraus folgt dann zunächst, daß sich die Gravitationsfelder mit Lichtgeschwindigkeit ausbreiten. Wir werden im Anschluß an diese allgemeine Lösung die Gravitationswellen und deren Entstehungsweise untersuchen. Es hat sich gezeigt, daß die von mir vorgeschlagene Wahl des Bezugssystems gemäß der Bedingung $g = |g_{\mu\nu}| = -1$ für die Berechnung der Felder in erster Näherung nicht vorteilhaft ist. Ich wurde hierauf aufmerksam durch eine briefliche Mitteilung des Astronomen de Sitter, der fand, daß man durch eine andere Wahl des Bezugssystems zu einem einfacheren Ausdruck des Gravitationsfeldes eines ruhenden Massenpunktes gelangen kann, als ich ihn früher gegeben hatte[1]. Ich stütze mich daher im folgenden auf die allgemein invarianten Feldgleichungen.

[1] Sitzungsber. XLVII, 1915, S. 833.

"On gravitational waves"

154 Gesamtsitzung vom 14. Februar 1918. — Mitteilung vom 31. Januar

Über Gravitationswellen.

Von A. Einstein.

(Vorgelegt am 31. Januar 1918 [s. oben S. 79].)

Die wichtige Frage, wie die Ausbreitung der Gravitationsfelder erfolgt, ist schon vor anderthalb Jahren in einer Akademiearbeit von mir behandelt worden[1]. Da aber meine damalige Darstellung des Gegenstandes nicht genügend durchsichtig und außerdem durch einen bedauerlichen Rechenfehler verunstaltet ist, muß ich hier nochmals auf die Angelegenheit zurückkommen.

Wie damals beschränke ich mich auch hier auf den Fall, daß das betrachtete zeiträumliche Kontinuum sich von einem »galileischen« nur sehr wenig unterscheidet. Um für alle Indizes

$$g_{\mu\nu} = -\delta_{\mu\nu} + \gamma_{\mu\nu} \tag{1}$$

setzen zu können, wählen wir, wie es in der speziellen Relativitätstheorie üblich ist, die Zeitvariable x_4 rein imaginär, indem wir

$$x_4 = it$$

setzen, wobei t die »Lichtzeit« bedeutet. In (1) ist $\delta_{\mu\nu} = 1$ bzw. $\delta_{\mu\nu} = 0$, je nachdem $\mu = \nu$ oder $\mu \neq \nu$ ist. Die $\gamma_{\mu\nu}$ sind gegen 1 kleine Größen, welche die Abweichung des Kontinuums vom feldfreien darstellen; sie bilden einen Tensor vom zweiten Range gegenüber Lorentz-Transformationen.

Three types of waves:

- longitudinal-longitudinal
- transverse-longitudinal
- transverse-transverse

Historical overview

October 1922: Eddington: L-L and T-L waves propagate *"at the speed of thought"*

The Propagation of Gravitational Waves.

By A. S. Eddington, F.R.S.

(Received October 11, 1922.)

1. The problem of the propagation of disturbances of the gravitational field was investigated by Einstein in 1916, and again in 1918.* It has usually been inferred from his discussion that a change in the distribution of matter produces gravitational effects which are propagated with the speed of light; but I think that Einstein really left the question of the speed of propagation rather indefinite. His analysis shows how the co-ordinates must be chosen if it is desired to represent the gravitational potentials as propagated with the speed of light; but there is nothing to indicate that the speed of light appears in the problem, except as the result of this arbitrary choice. So far as I know, the propagation of the absolute physical condition—the altered curvature of space-time—has not hitherto been discussed.

Weyl† has classified plane gravitational waves into three types, viz.: (1) longitudinal-longitudinal; (2) longitudinal-transverse; (3) transverse-transverse. The present investigation leads to the conclusion that transverse-transverse waves are propagated with the speed of light *in all systems of co-ordinates*. Waves of the first and second types have no fixed velocity—a result which rouses suspicion as to their objective existence. Einstein had also become suspicious of these waves (in so far as they occur in his special co-ordinate-system) for another reason, because he found that they convey no energy.

They are not objective, and (like absolute velocity) are not detectable by any conceivable experiment. They are merely sinuosities in the co-ordinate-system, and the only speed of propagation relevant to them is "the speed of thought."

Historical overview

October 1922: Eddington: L-L and T-L waves propagate *"at the speed of thought"*

The Propagation of Gravitational Waves.

By A. S. Eddington, F.R.S.

(Received October 11, 1922.)

1. The problem of the propagation of disturbances of the gravitational field was investigated by Einstein in 1916, and again in 1918.* It has usually been inferred from his discussion that a change in the distribution of matter produces gravitational effects which are propagated with the speed of light; but I think that Einstein really left the question of the speed of propagation rather indefinite. His analysis shows how the co-ordinates must be chosen if it is desired to represent the gravitational potentials as propagated with the speed of light; but there is nothing to indicate that the speed of light appears in the problem, except as the result of this arbitrary choice. So far as I know, the propagation of the absolute physical condition—the altered curvature of space-time—has not hitherto been discussed.

Weyl† has classified plane gravitational waves into three types, viz.: (1) longitudinal-longitudinal; (2) longitudinal-transverse; (3) transverse-transverse. The present investigation leads to the conclusion that transverse-transverse waves are propagated with the speed of light *in all systems of co-ordinates.* Waves of the first and second types have no fixed velocity—a result which rouses suspicion as to their objective existence. Einstein had also become suspicious of these waves (in so far as they occur in his special co-ordinate-system) for another reason, because he found that they convey no energy.

They are not objective, and (like absolute velocity) are not detectable by any conceivable experiment. They are merely sinuosities in the co-ordinate-system, and the only speed of propagation relevant to them is "the speed of thought."

Historical overview

1936: A busy year

Historical overview

1936: A busy year

> *Together with a young collaborator [Rosen], I arrive at the interesting result that gravitational waves do not exist, though they have been assumed a certainty to the first approximation.*
> **~ *Einstein to Max Born***

Historical overview

1936: A busy year

> *Together with a young collaborator [Rosen], I arrive at the interesting result that gravitational waves do not exist, though they have been assumed a certainty to the first approximation.*
>
> ***~ Einstein to Max Born***

- June: Einstein and Rosen submitted "Are there any gravitational waves?" to PRL

Historical overview

1936: A busy year

> *Together with a young collaborator [Rosen], I arrive at the interesting result that gravitational waves do not exist, though they have been assumed a certainty to the first approximation.*
>
> ***~ Einstein to Max Born***

- June: Einstein and Rosen submitted "Are there any gravitational waves?" to PRL
  - Peer reviewed by Howard Percy Robertson, who found mistakes

Historical overview

1936: A busy year

> *Together with a young collaborator [Rosen], I arrive at the interesting result that gravitational waves do not exist, though they have been assumed a certainty to the first approximation.*
>
> ***~ Einstein to Max Born***

- June: Einstein and Rosen submitted "Are there any gravitational waves?" to PRL
  - Peer reviewed by Howard Percy Robertson, who found mistakes

July 27, 1936

Dear Sir.

"We (Mr. Rosen and I) had sent you our manuscript for publication and had not authorized you to show it to specialists before it is printed. I see no reason to address the—in any case erroneous—comments of your anonymous expert. On the basis of this incident I prefer to publish the paper elsewhere."

Respectfully

Einstein

P.S. Mr. Rosen, who has left for the Soviet Union, has authorized me to represent him in this matter.

Historical overview

1936: A busy year

> *Together with a young collaborator [Rosen], I arrive at the interesting result that gravitational waves do not exist, though they have been assumed a certainty to the first approximation.*
> ***~ Einstein to Max Born***

- June: Einstein and Rosen submitted "Are there any gravitational waves?" to PRL
  - Peer reviewed by Howard Percy Robertson, who found mistakes
- November: Rewrote the paper as "On gravitational waves"

July 27, 1936

Dear Sir.

"We (Mr. Rosen and I) had sent you our manuscript for publication and had not authorized you to show it to specialists before it is printed. I see no reason to address the—in any case erroneous—comments of your anonymous expert. On the basis of this incident I prefer to publish the paper elsewhere."

Respectfully

Einstein

P.S. Mr. Rosen, who has left for the Soviet Union, has authorized me to represent him in this matter.

Historical overview

1936: A busy year

> *Together with a young collaborator [Rosen], I arrive at the interesting result that gravitational waves do not exist, though they have been assumed a certainty to the first approximation.*
> ***~ Einstein to Max Born***

- June: Einstein and Rosen submitted "Are there any gravitational waves?" to PRL
  - Peer reviewed by Howard Percy Robertson, who found mistakes
- November: Rewrote the paper as "On gravitational waves"

July 27, 1936

Dear Sir.

"We (Mr. Rosen and I) had sent you our manuscript for publication and had not authorized you to show it to specialists before it is printed. I see no reason to address the—in any case erroneous—comments of your anonymous expert. On the basis of this incident I prefer to publish the paper elsewhere."

Respectfully

Einstein

P.S. Mr. Rosen, who has left for the Soviet Union, has authorized me to represent him in this matter.

ON GRAVITATIONAL WAVES.

BY

A. EINSTEIN and N. ROSEN.

ABSTRACT.

The rigorous solution for cylindrical gravitational waves is given. For the convenience of the reader the theory of gravitational waves and their production, already known in principle, is given in the first part of this paper. After encountering relationships which cast doubt on the existence of *rigorous* solutions for undulatory gravitational fields, we investigate rigorously the case of cylindrical gravitational waves. It turns out that rigorous solutions exist and that the problem reduces to the usual cylindrical waves in euclidean space.

I. APPROXIMATE SOLUTION OF THE PROBLEM OF PLANE WAVES AND THE PRODUCTION OF GRAVITATIONAL WAVES.

It is well known that the approximate method of integration of the gravitational equations of the general relativity theory leads to the existence of gravitational waves. The method used is as follows: We start with the equations

Historical overview

1936: A busy year

> *Together with a young collaborator [Rosen], I arrive at the interesting result that gravitational waves do not exist, though they have been assumed a certainty to the first approximation.*
> ***~ Einstein to Max Born***

- June: Einstein and Rosen submitted "Are there any gravitational waves?" to PRL
    - Peer reviewed by Howard Percy Robertson, who found mistakes
- November: Rewrote the paper as "On gravitational waves"

July 27, 1936

Dear Sir.

"We (Mr. Rosen and I) had sent you our manuscript for publication and had not authorized you to show it to specialists before it is printed. I see no reason to address the—in any case erroneous—comments of your anonymous expert. On the basis of this incident I prefer to publish the paper elsewhere."

Respectfully

Einstein

P.S. Mr. Rosen, who has left for the Soviet Union, has authorized me to represent him in this matter.

ON GRAVITATIONAL WAVES.

BY

A. EINSTEIN and N. ROSEN.

ABSTRACT.

The rigorous solution for cylindrical gravitational waves is given. For the convenience of the reader the theory of gravitational waves and their production, already known in principle, is given in the first part of this paper. After encountering relationships which cast doubt on the existence of *rigorous* solutions for undulatory gravitational fields, we investigate rigorously the case of cylindrical gravitational waves. It turns out that rigorous solutions exist and that the problem reduces to the usual cylindrical waves in euclidean space.

I. APPROXIMATE SOLUTION OF THE PROBLEM OF PLANE WAVES AND THE PRODUCTION OF GRAVITATIONAL WAVES.

It is well known that the approximate method of integration of the gravitational equations of the general relativity theory leads to the existence of gravitational waves. The method used is as follows: We start with the equations

Historical overview

Historical overview

1956: Felix A. E. Pirani: gravitational waves move particles as they pass through

Historical overview

1956: Felix A. E. Pirani: gravitational waves move particles as they pass through

1957: Chapel Hill Conference (GR1): Do gravitational waves carry energy?

Historical overview

1956: Felix A. E. Pirani: gravitational waves move particles as they pass through

1957: Chapel Hill Conference (GR1): Do gravitational waves carry energy?

R.P. Feynman: Yes. (Sticky beads argument)

Historical overview

1956: Felix A. E. Pirani: gravitational waves move particles as they pass through

1957: Chapel Hill Conference (GR1): Do gravitational waves carry energy?

R.P. Feynman: Yes. (Sticky beads argument)

Historical overview

1956: Felix A. E. Pirani: gravitational waves move particles as they pass through

1957: Chapel Hill Conference (GR1): Do gravitational waves carry energy?

R.P. Feynman: Yes. (Sticky beads argument)

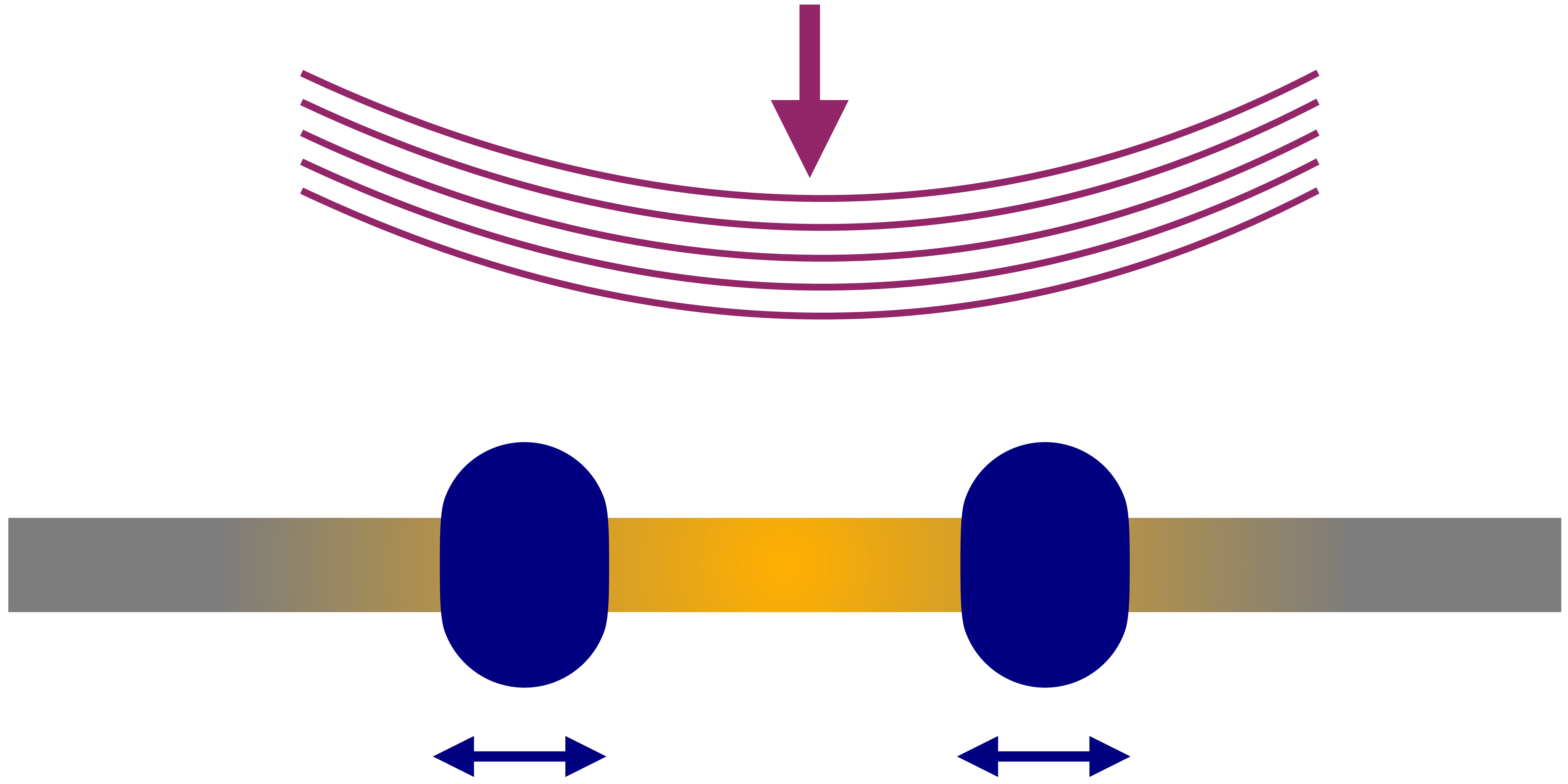

Historical overview

1956: Felix A. E. Pirani: gravitational waves move particles as they pass through

1957: Chapel Hill Conference (GR1): Do gravitational waves carry energy?

R.P. Feynman: Yes. (Sticky beads argument)

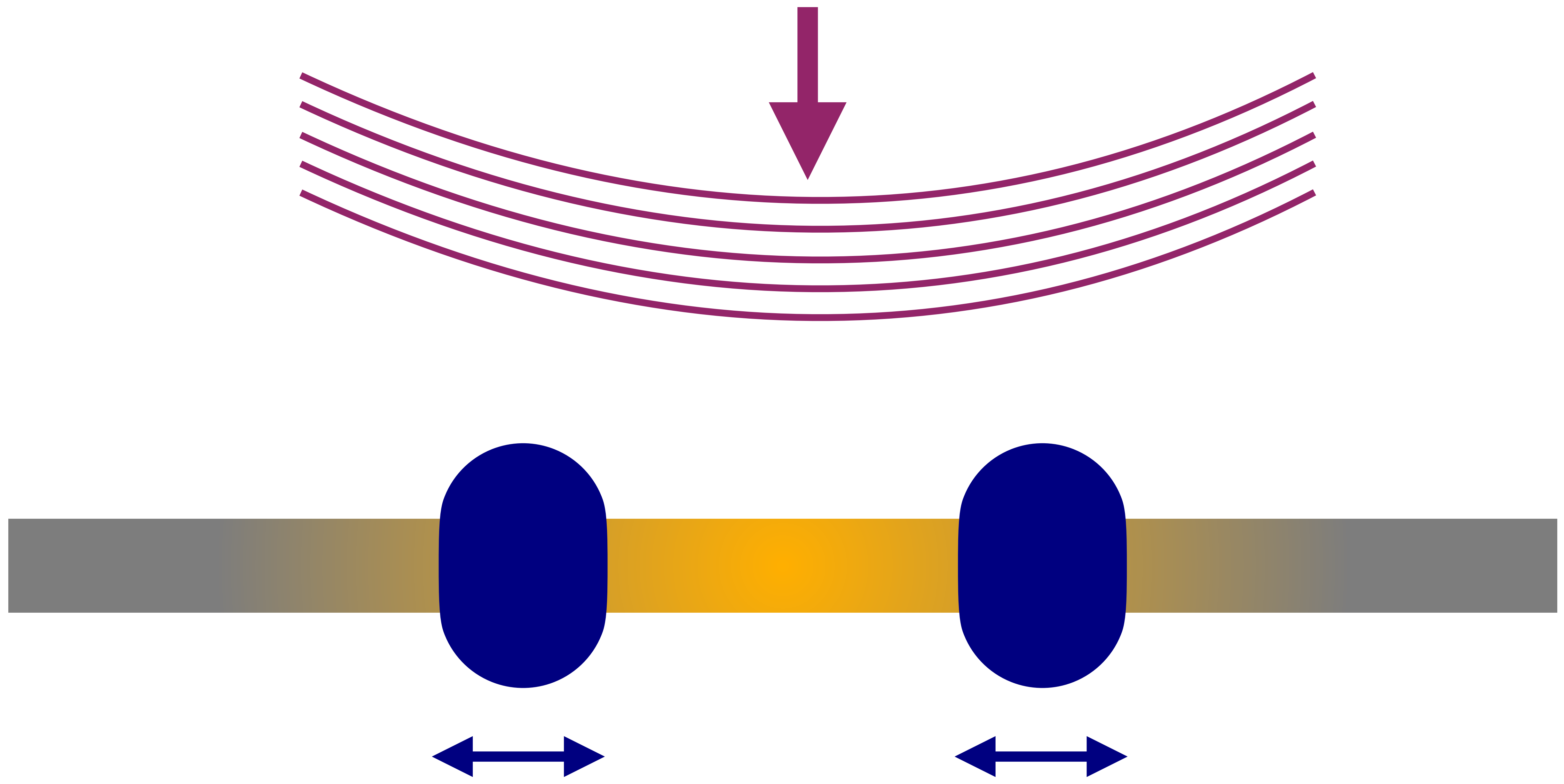

"I was surprised to find that a whole day of the conference was spent on this issue and that 'experts' were confused. That's what happens when one is considering energy conservation tensors, etc. instead of questioning, can waves do work?"

~ **R.P. Feynman**

Historical overview

1960's: John Weber claims detection using resonance bars

Historical overview

1960's: John Weber claims detection using resonance bars

EVIDENCE FOR DISCOVERY OF GRAVITATIONAL RADIATION*

J. Weber
Department of Physics and Astronomy, University of Maryland, College Park, Maryland 20742
(Received 29 April 1969)

Coincidences have been observed on gravitational-radiation detectors over a base line of about 1000 km at Argonne National Laboratory and at the University of Maryland. The probability that all of these coincidences were accidental is incredibly small. Experiments imply that electromagnetic and seismic effects can be ruled out with a high level of confidence. These data are consistent with the conclusion that the detectors are being excited by gravitational radiation.

Historical overview

1960's: John Weber claims detection using resonance bars

EVIDENCE FOR DISCOVERY OF GRAVITATIONAL RADIATION*

J. Weber
Department of Physics and Astronomy, University of Maryland, College Park, Maryland 20742
(Received 29 April 1969)

Coincidences have been observed on gravitational-radiation detectors over a base line of about 1000 km at Argonne National Laboratory and at the University of Maryland. The probability that all of these coincidences were accidental is incredibly small. Experiments imply that electromagnetic and seismic effects can be ruled out with a high level of confidence. These data are consistent with the conclusion that the detectors are being excited by gravitational radiation.

1970's: Weber's detections are debunked

Historical overview

Historical overview

1993 Nobel Prize: Russel Hulse and Joseph Taylor, "for the discovery of a new type of pulsar, a discovery that has opened up new possibilities for the study of gravitation."

DISCOVERY OF A PULSAR IN A BINARY SYSTEM

R. A. Hulse and J. H. Taylor
Department of Physics and Astronomy, University of Massachusetts, Amherst
Received 1974 October 18

ABSTRACT

We have detected a pulsar with a pulsation period that varies systematically between $0^s.058967$ and $0^s.059045$ over a cycle of $0^d.3230$. Approximately 200 independent observations over 5-minute intervals have yielded a well-sampled velocity curve which implies a binary orbit with projected semimajor axis $a_1 \sin i = 1.0\ R_\odot$, eccentricity $e = 0.615$, and mass function $f(m) = 0.13\ M_\odot$. No eclipses are observed. We infer that the unseen companion is a compact object with mass comparable to that of the pulsar. In addition to the obvious potential for determining the masses of the pulsar and its companion, this discovery makes feasible a number of studies involving the physics of compact objects, the astrophysics of close binary systems, and special- and general-relativistic effects.

Subject headings: binaries — black holes — neutron stars — pulsars — relativity

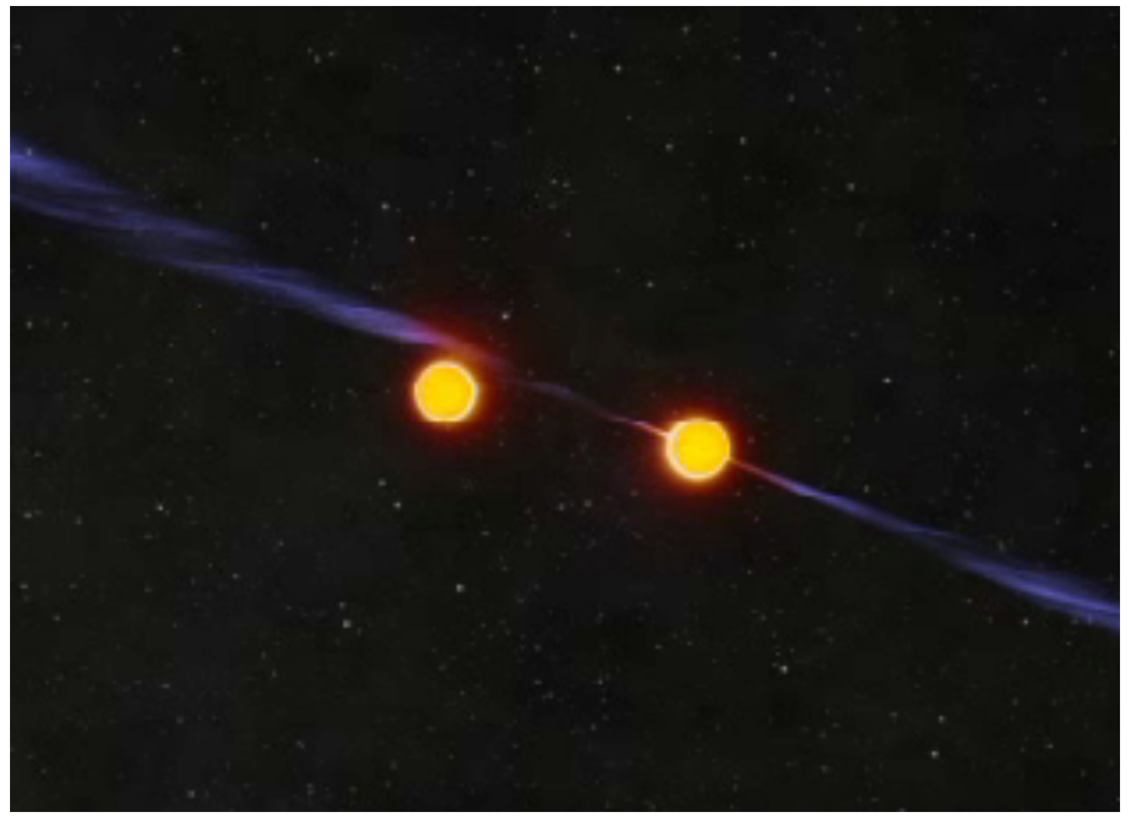

Historical overview

1993 Nobel Prize: Russel Hulse and Joseph Taylor, “for the discovery of a new type of pulsar, a discovery that has opened up new possibilities for the study of gravitation.”

DISCOVERY OF A PULSAR IN A BINARY SYSTEM

R. A. Hulse and J. H. Taylor
Department of Physics and Astronomy, University of Massachusetts, Amherst
Received 1974 October 18

ABSTRACT

We have detected a pulsar with a pulsation period that varies systematically between $0^{s}058967$ and $0^{s}059045$ over a cycle of $0^{d}3230$. Approximately 200 independent observations over 5-minute intervals have yielded a well-sampled velocity curve which implies a binary orbit with projected semimajor axis $a_1 \sin i = 1.0\ R_{\odot}$, eccentricity $e = 0.615$, and mass function $f(m) = 0.13\ M_{\odot}$. No eclipses are observed. We infer that the unseen companion is a compact object with mass comparable to that of the pulsar. In addition to the obvious potential for determining the masses of the pulsar and its companion, this discovery makes feasible a number of studies involving the physics of compact objects, the astrophysics of close binary systems, and special- and general-relativistic effects.
Subject headings: binaries — black holes — neutron stars — pulsars — relativity

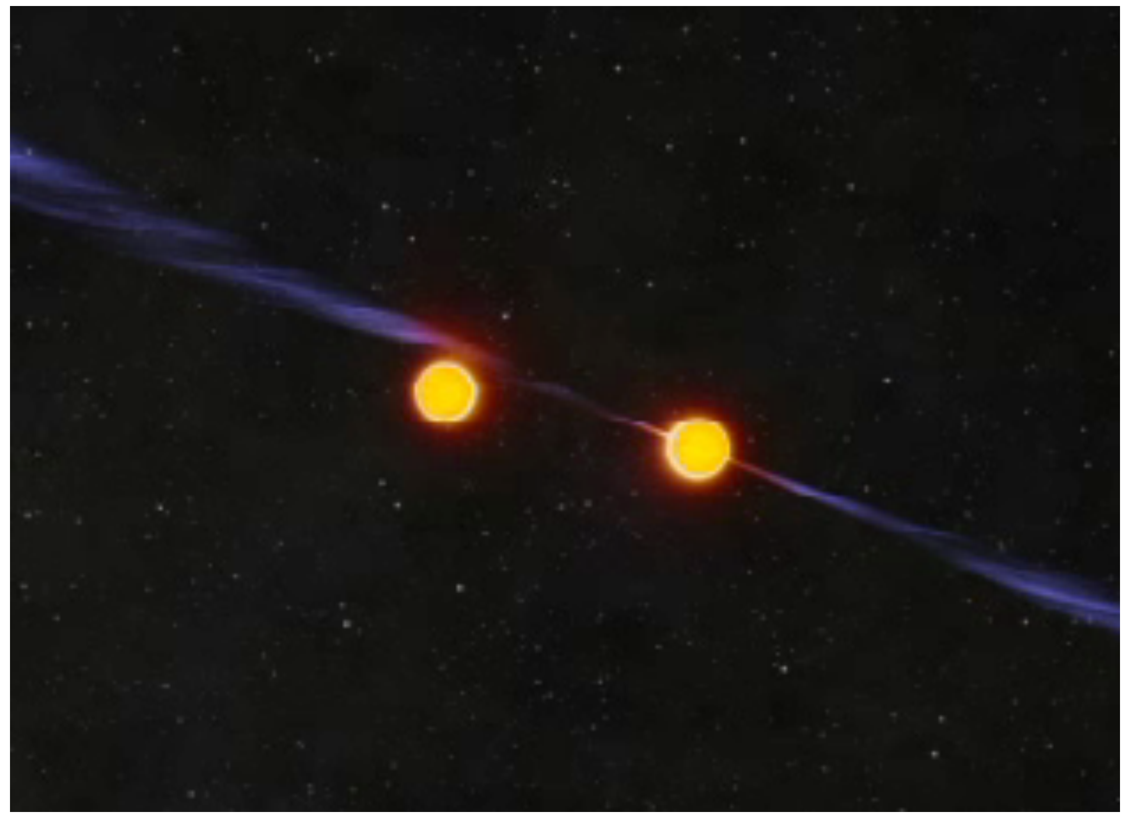

A NEW TEST OF GENERAL RELATIVITY: GRAVITATIONAL RADIATION AND THE BINARY PULSAR PSR 1913+16

J. H. Taylor and J. M. Weisberg
Department of Physics and Astronomy, University of Massachusetts, Amherst; and Joseph Henry Laboratories, Physics Department, Princeton University
Received 1981 July 2; accepted 1981 August 28

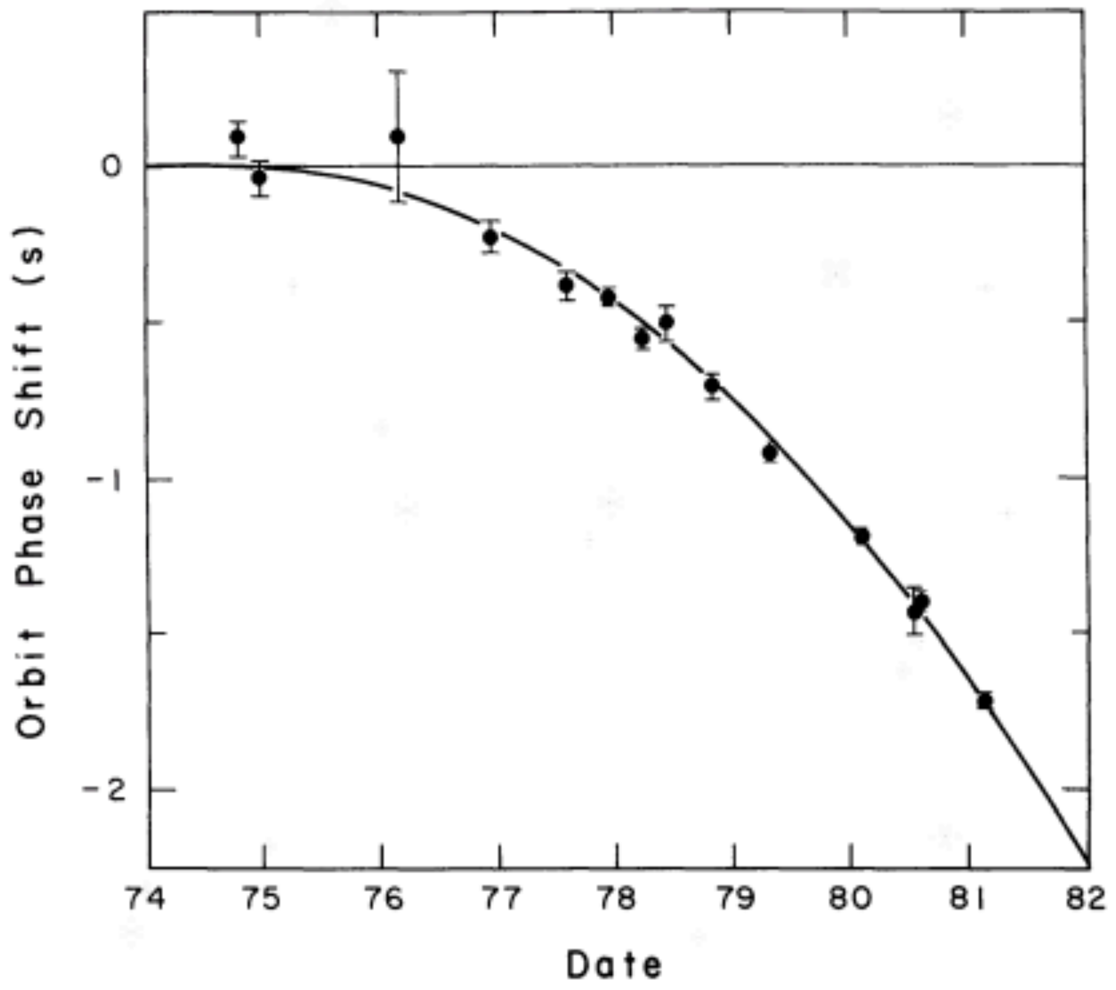

Fig. 6.—Orbital phase residuals, obtained from the data listed in Table 4. If the orbital period had remained constant, the points would be expected to lie on a straight line. The curvature of the parabola drawn through the points corresponds to the general relativistic prediction for loss of energy to gravitational radiation, or $\dot{P}_b = -2.40 \times 10^{-12}$.

Historical overview

1993 Nobel Prize: Russel Hulse and Joseph Taylor, "for the discovery of a new type of pulsar, a discovery that has opened up new possibilities for the study of gravitation."

DISCOVERY OF A PULSAR IN A BINARY SYSTEM

R. A. HULSE AND J. H. TAYLOR
Department of Physics and Astronomy, University of Massachusetts, Amherst

Received 1974 October 18

ABSTRACT

We have detected a pulsar with a pulsation period that varies systematically between $0^{s}.058967$ and $0^{s}.059045$ over a cycle of $0^{d}.3230$. Approximately 200 independent observations over 5-minute intervals have yielded a well-sampled velocity curve which implies a binary orbit with projected semimajor axis $a_1 \sin i = 1.0\, R_\odot$, eccentricity $e = 0.615$, and mass function $f(m) = 0.13\, M_\odot$. No eclipses are observed. We infer that the unseen companion is a compact object with mass comparable to that of the pulsar. In addition to the obvious potential for determining the masses of the pulsar and its companion, this discovery makes feasible a number of studies involving the physics of compact objects, the astrophysics of close binary systems, and special- and general-relativistic effects.

Subject headings: binaries — black holes — neutron stars — pulsars — relativity

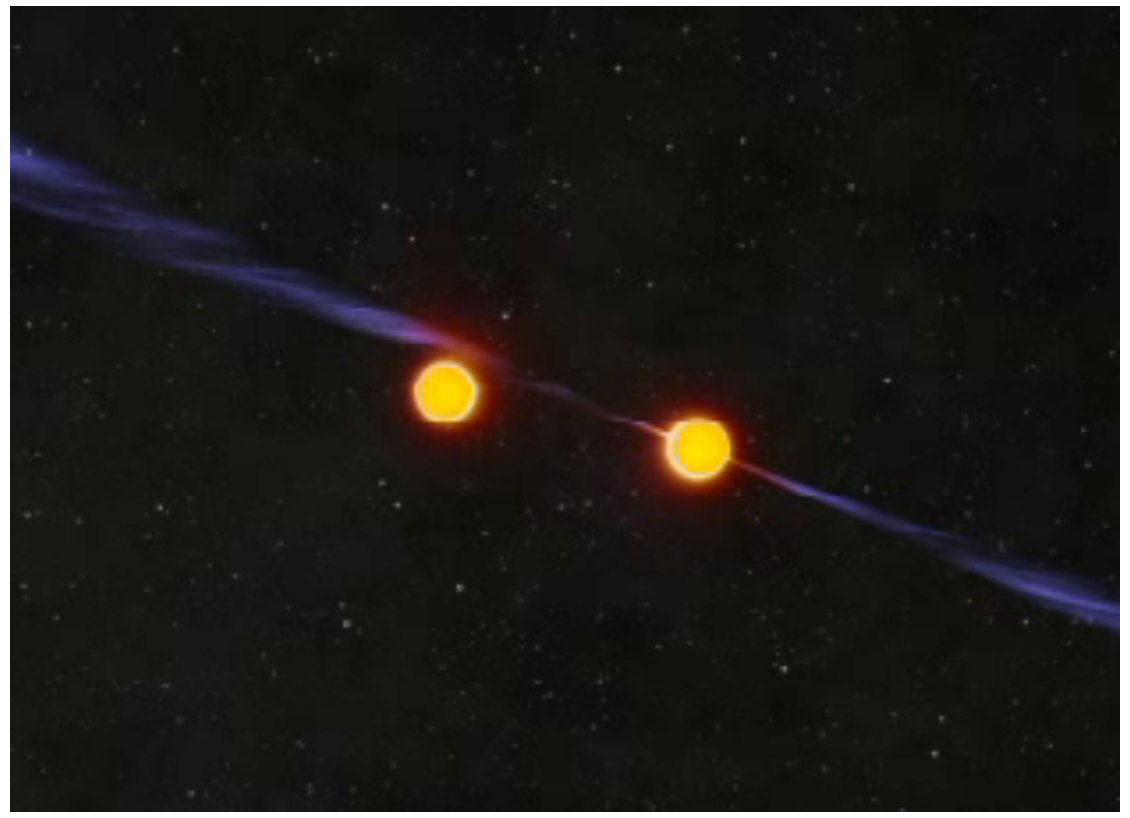

A NEW TEST OF GENERAL RELATIVITY: GRAVITATIONAL RADIATION AND THE BINARY PULSAR PSR 1913+16

J. H. TAYLOR AND J. M. WEISBERG
Department of Physics and Astronomy, University of Massachusetts, Amherst; and Joseph Henry Laboratories, Physics Department, Princeton University

Received 1981 July 2; accepted 1981 August 28

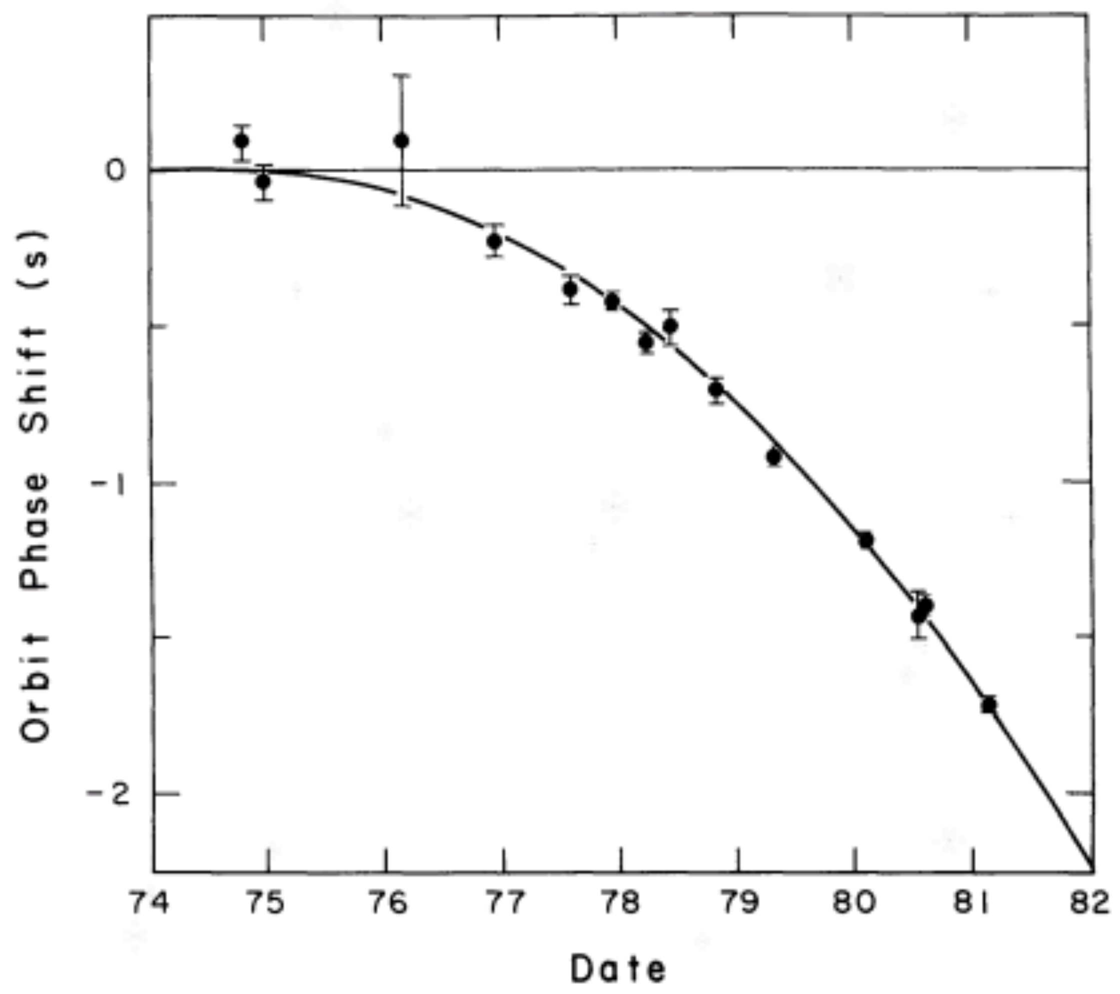

FIG. 6.—Orbital phase residuals, obtained from the data listed in Table 4. If the orbital period had remained constant, the points would be expected to lie on a straight line. The curvature of the parabola drawn through the points corresponds to the general relativistic prediction for loss of energy to gravitational radiation, or $\dot{P}_b = -2.40 \times 10^{-12}$.

Relativistic Binary Pulsar B1913+16: Thirty Years of Observations and Analysis

Joel M. Weisberg

Dept. of Physics & Astronomy, Carleton College, Northfield, MN

Joseph H. Taylor

Dept. of Physics, Princeton University, Princeton, NJ

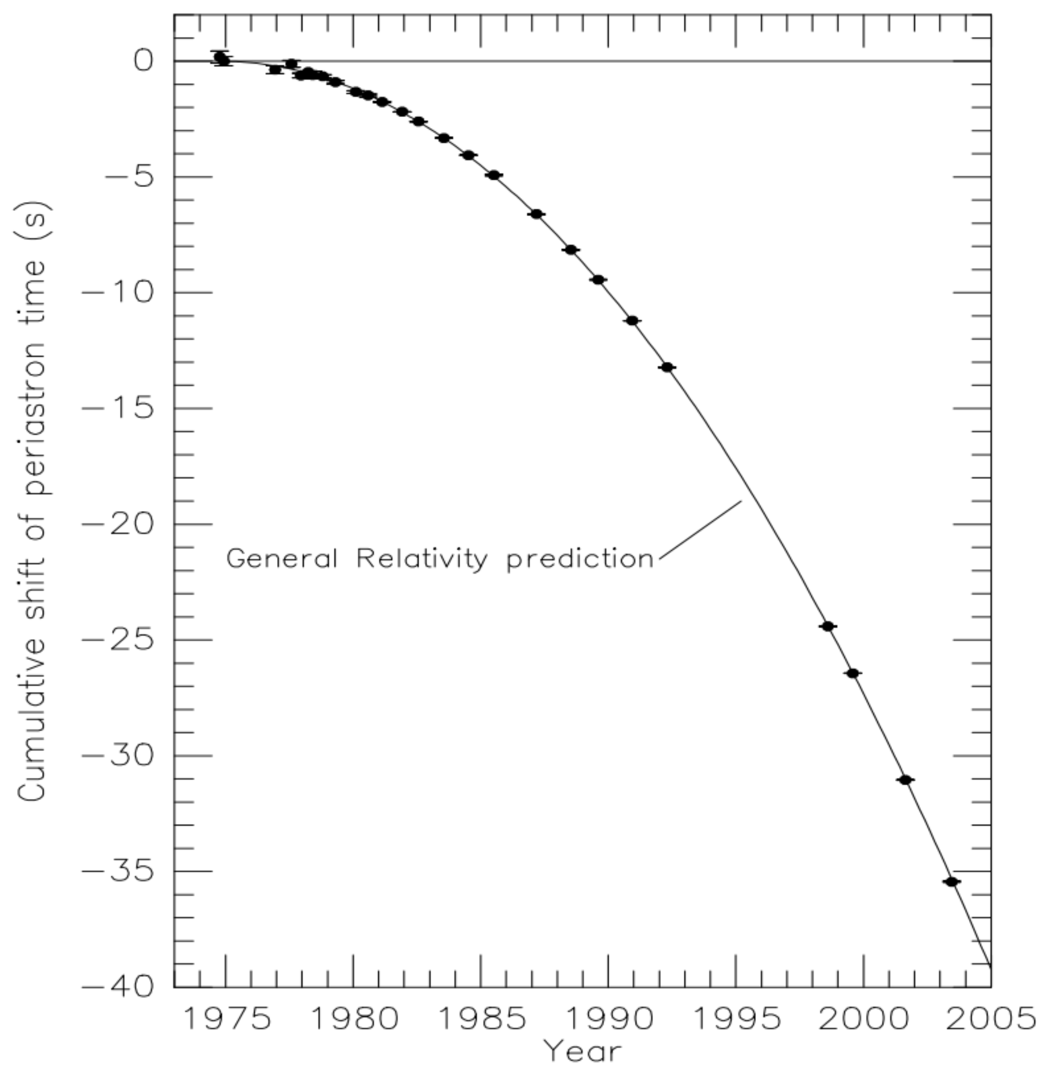

Figure 1. Orbital decay of PSR B1913+16. The data points indicate the observed change in the epoch of periastron with date while the parabola illustrates the theoretically expected change in epoch for a system emitting gravitational radiation, according to general relativity.

Historical overview

Spring 2014: BICEP2 claims to find GWs in the CMB, probably its just dust

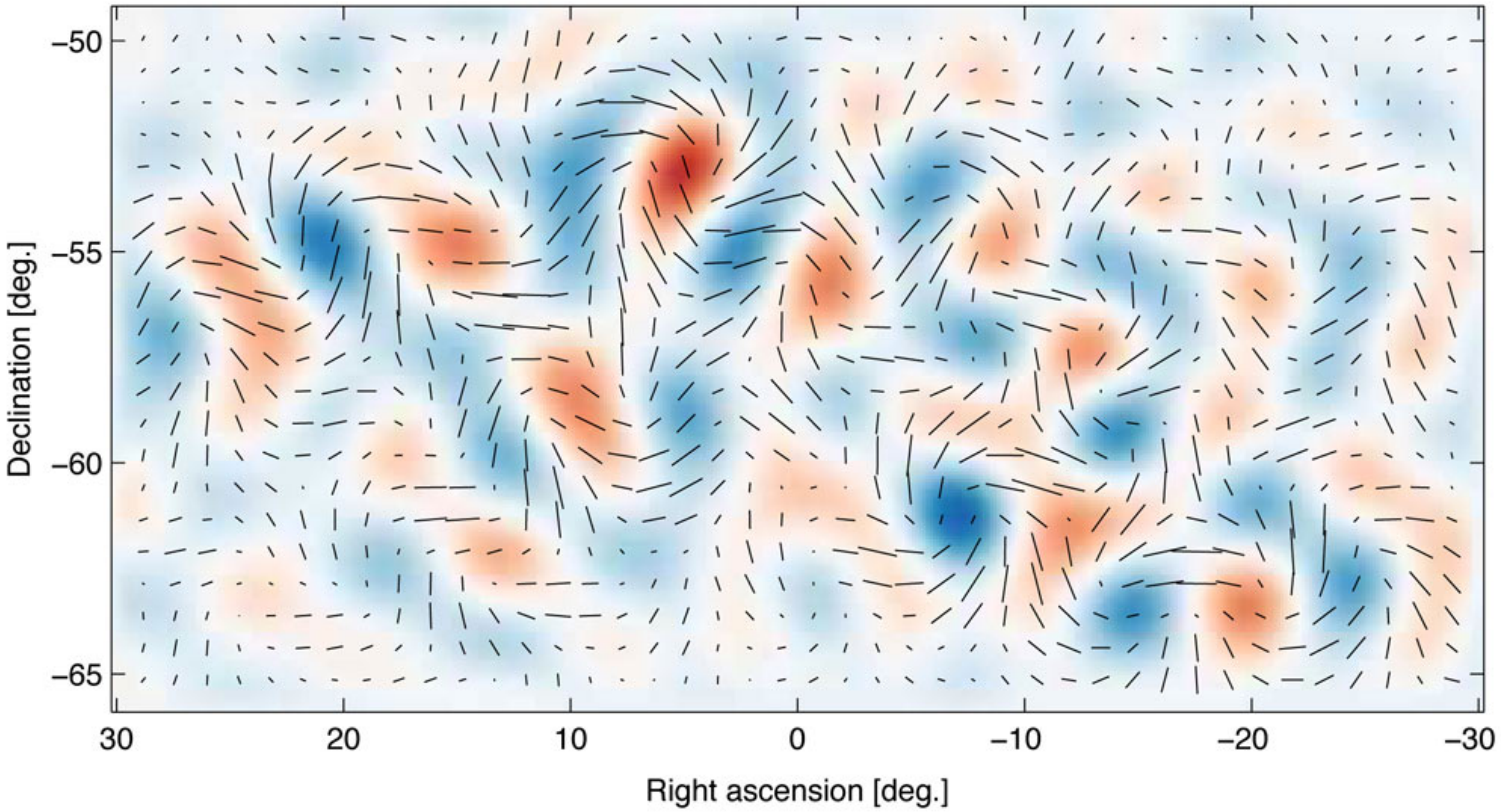

Historical overview

Spring 2014: BICEP2 claims to find GWs in the CMB, probably its just dust

arXiv > astro-ph > arXiv:1403.3985v1

Search...

Help | Adva

Astrophysics > Cosmology and Nongalactic Astrophysics

[Submitted on 17 Mar 2014 (this version), latest version 23 Jun 2014 (v3)]

BICEP2 I: Detection Of B-mode Polarization at Degree Angular Scales

BICEP2 Collaboration: P. A. R Ade (1), R. W. Aikin (2), D. Barkats (3), S. J. Benton (4), C. A. Bischoff (5), J. J. Bock (2,6), J. A. Brevik (2), I. Buder (5), E. Bullock (7), C. D. Dowell (6), L. Duband (8), J. P. Filippini (2), S. Fliescher (9), S. R. Golwala (2), M. Halpern (10), M. Hasselfield (10), S. R. Hildebrandt (2,6), G. C. Hilton (11), V. V. Hristov (2), K. D. Irwin (12,13,11), K. S. Karkare (5), J. P. Kaufman (14), B. G. Keating (14), S. A. Kernasovskiy (12), J. M. Kovac (5), C. L. Kuo (12,13), E. M. Leitch (15), M. Lueker (2), P. Mason (2), C. B. Netterfield (4), H. T. Nguyen (6), R. O'Brient (6), R. W. Ogburn IV (12,13), A. Orlando (14), C. Pryke (9,7), C. D. Reintsema (11), S. Richter (5), R. Schwarz (9), C. D. Sheehy (9,15), Z. K. Staniszewski (2,6), R. V. Sudiwala (1), G. P. Teply (2), J. E. Tolan (12), A. D. Turner (6), A. G. Vieregg (5,15), C. L. Wong (5), K. W. Yoon (12,13) ((1) Cardiff University, (2) Caltech, (3) ALMA, (4) University of Toronto, (5) Harvard/CfA, (6) NASA JPL, (7) Minnesota Institute for Astrophysics, (8) SBT Grenoble, (9) University of Minnesota, (10) University of BritishColumbia, (11) NIST, (12) Stanford University, (13) KIPAC/SLAC, (14) UCSD, (15) University of Chicago)

We report results from the BICEP2 experiment, a Cosmic Microwave Background (CMB) polarimeter specifically designed to search for the signal of inflationary gravitational waves in the B-mode power spectrum around l=80. The telescope comprised a 26 cm aperture all-cold refracting optical system equipped with a focal plane of 512 antenna coupled transition edge sensor (TES) 150 GHz bolometers each with temperature sensitivity of approx. 300 this http URL(s). BICEP2 observed from the South Pole for three seasons from 2010 to 2012. A low-foreground region of sky with an effective area of 380 square degrees was observed to a depth of 87 nK-degrees in Stokes Q and U. In this paper we describe the observations, data reduction, maps, simulations and results. We find an excess of B-mode power over the base lensed-LCDM expectation in the range 30<l<150, inconsistent with the null hypothesis at a significance of $> 5\sigma$. Through jackknife tests and simulations based on detailed calibration measurements we show that systematic contamination is much smaller than the observed excess. We also estimate potential foreground signals and find that available models predict these to be considerably smaller than the observed signal. These foreground models possess no significant cross-correlation with our maps. Additionally, cross-correlating BICEP2 against 100 GHz maps from the BICEP1 experiment, the excess signal is confirmed with 3σ significance and its spectral index is found to be consistent with that of the CMB, disfavoring synchrotron or dust at 2.3σ and 2.2σ, respectively. The observed B-mode power spectrum is well-fit by a lensed-LCDM + tensor theoretical model with tensor/scalar ratio $r = 0.20^{+0.07}_{-0.05}$, with r=0 disfavored at 7.0σ. Subtracting the best available estimate for foreground dust modifies the likelihood slightly so that r=0 is disfavored at 5.9σ.

Historical overview

Spring 2014: BICEP2 claims to find GWs in the CMB, probably its just dust

arXiv > astro-ph > arXiv:1403.3985v3

Search...

Help | Adva

Astrophysics > Cosmology and Nongalactic Astrophysics

[Submitted on 17 Mar 2014 (v1), last revised 23 Jun 2014 (this version, v3)]

BICEP2 I: Detection Of B-mode Polarization at Degree Angular Scales

P. A. R Ade (1), R. W. Aikin (2), D. Barkats (3), S. J. Benton (4), C. A. Bischoff (5), J. J. Bock (2,6), J. A. Brevik (2), I. Buder (5), E. Bullock (7), C. D. Dowell (6), L. Duband (8), J. P. Filippini (2), S. Fliescher (9), S. R. Golwala (2), M. Halpern (10), M. Hasselfield (10), S. R. Hildebrandt (2,6), G. C. Hilton (11), V. V. Hristov (2), K. D. Irwin (12,13,11), K. S. Karkare (5), J. P. Kaufman (14), B. G. Keating (14), S. A. Kernasovskiy (12), J. M. Kovac (5), C. L. Kuo (12,13), E. M. Leitch (15), M. Lueker (2), P. Mason (2), C. B. Netterfield (4,16), H. T. Nguyen (6), R. O'Brient (6), R. W. Ogburn IV (12,13), A. Orlando (14), C. Pryke (9,7), C. D. Reintsema (11), S. Richter (5), R. Schwarz (9), C. D. Sheehy (9,15), Z. K. Staniszewski (2,6), R. V. Sudiwala (1), G. P. Teply (2), J. E. Tolan (12), A. D. Turner (6), A. G. Vieregg (5,15), C. L. Wong (5), K. W. Yoon (12,13) ((1) Cardiff University, (2) Caltech, (3) ALMA, (4) University of Toronto, (5) Harvard/CfA, (6) NASA JPL, (7) Minnesota Institute for Astrophysics, (8) SBT Grenoble, (9) University of Minnesota, (10) University of British Columbia, (11) NIST, (12) Stanford University, (13) KIPAC/SLAC, (14) UCSD, (15) University of Chicago, (16) Canadian Institute for Advanced Research)

(abridged for arXiv) We report results from the BICEP2 experiment, a cosmic microwave background (CMB) polarimeter specifically designed to search for the signal of inflationary gravitational waves in the B-mode power spectrum around $\ell \sim 80$. The telescope comprised a 26 cm aperture all-cold refracting optical system equipped with a focal plane of 512 antenna coupled transition edge sensor 150 GHz bolometers each with temperature sensitivity of $\approx 300\mu\mathrm{K}_{\mathrm{CMB}}\sqrt{s}$. BICEP2 observed from the South Pole for three seasons from 2010 to 2012. A low-foreground region of sky with an effective area of 380 square deg was observed to a depth of 87 nK deg in Stokes Q and U. We find an excess of B-mode power over the base lensed-LCDM expectation in the range $30 < \ell < 150$, inconsistent with the null hypothesis at a significance of $> 5\sigma$. Through jackknife tests and simulations we show that systematic contamination is much smaller than the observed excess. We also examine a number of available models of polarized dust emission and find that at their default parameter values they predict power $\sim (5-10)\times$ smaller than the observed excess signal. However, these models are not sufficiently constrained to exclude the possibility of dust emission bright enough to explain the entire excess signal. Cross correlating BICEP2 against 100 GHz maps from the BICEP1 experiment, the excess signal is confirmed and its spectral index is found to be consistent with that of the CMB, disfavoring dust at 1.7σ. The observed B-mode power spectrum is well fit by a lensed-LCDM + tensor theoretical model with tensor-to-scalar ratio $r = 0.20^{+0.07}_{-0.05}$, with $r = 0$ disfavored at 7.0σ. Accounting for the contribution of foreground dust will shift this value downward by an amount which will be better constrained with upcoming data sets.

Historical overview

Historical overview

1970s-1980s: Interferometer detectors are proposed

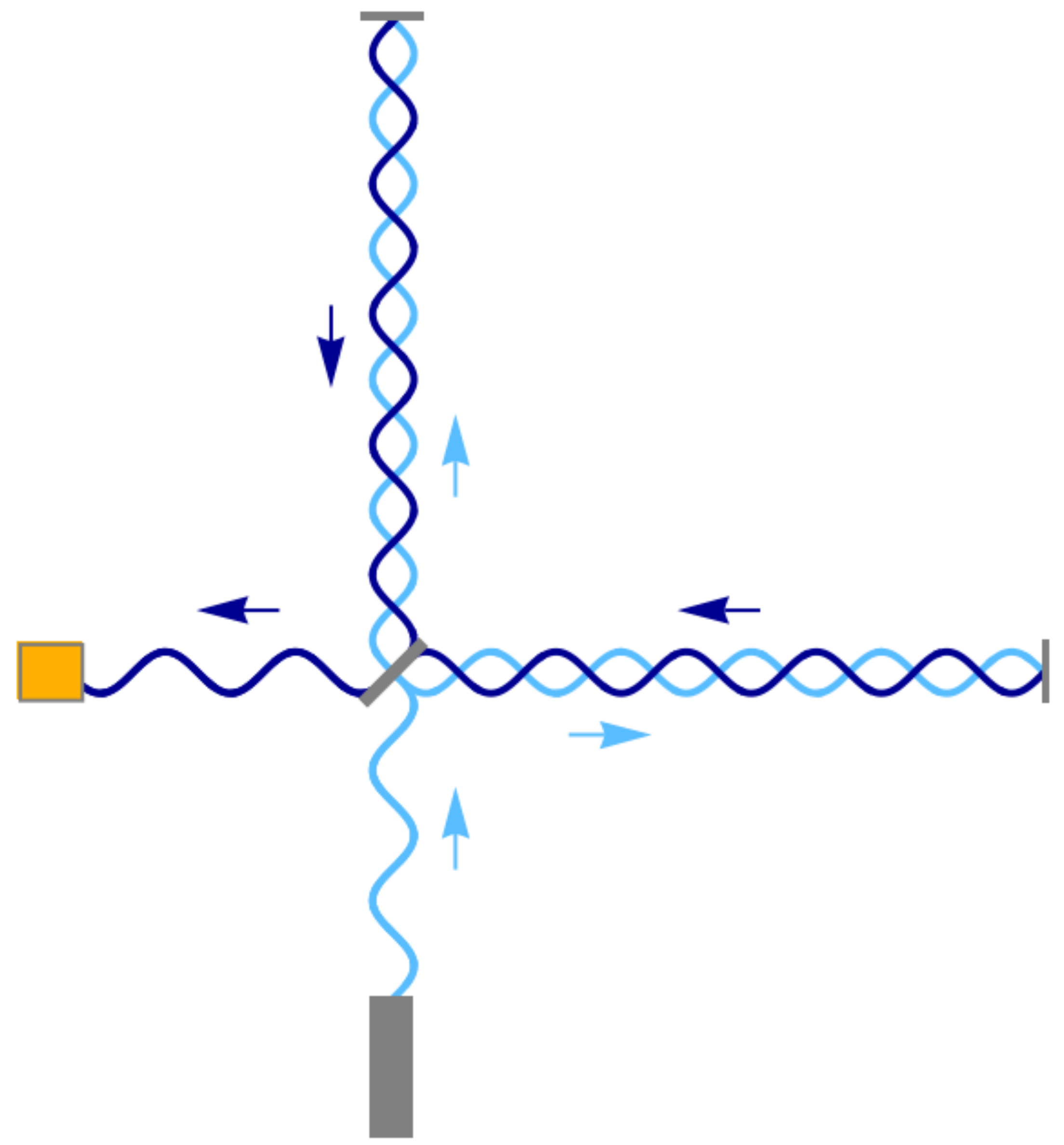

Historical overview

1970s-1980s: Interferometer detectors are proposed

1984: LIGO (Laser Interferometer Gravitational-wave Observatory) is founded

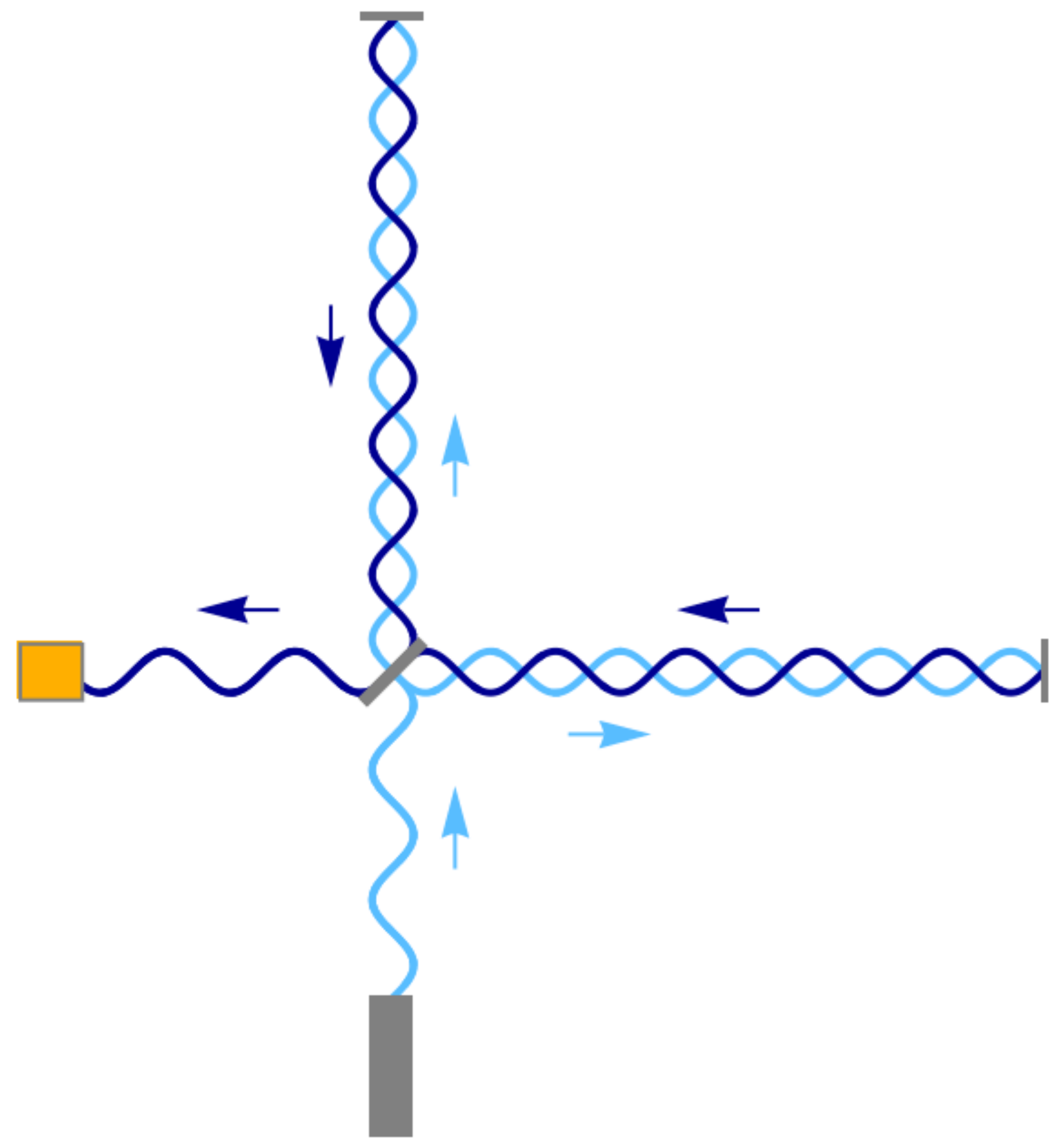

Historical overview

1970s-1980s: Interferometer detectors are proposed

1984: LIGO (Laser Interferometer Gravitational-wave Observatory) is founded

1989: Virgo is founded

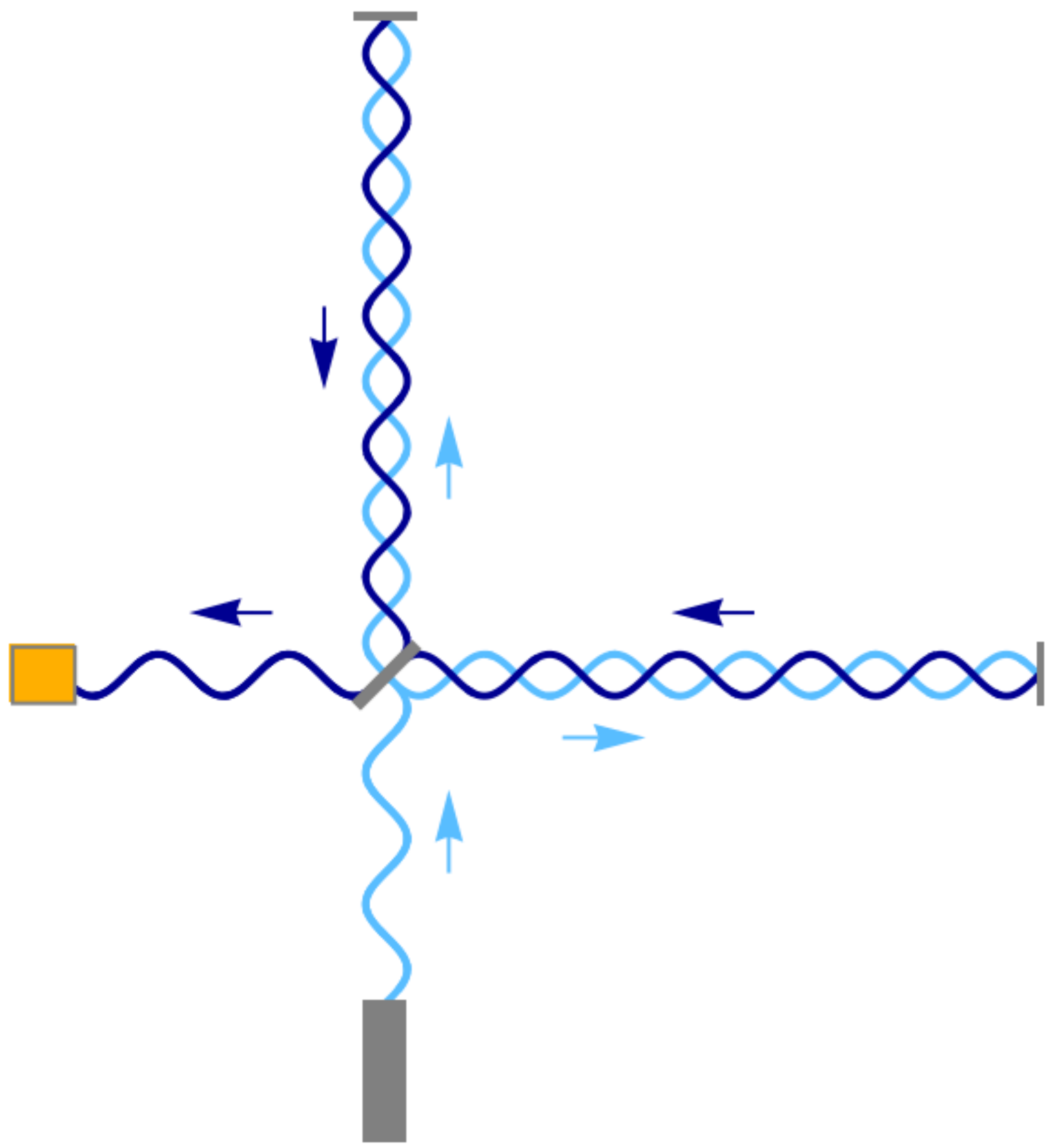

Historical overview

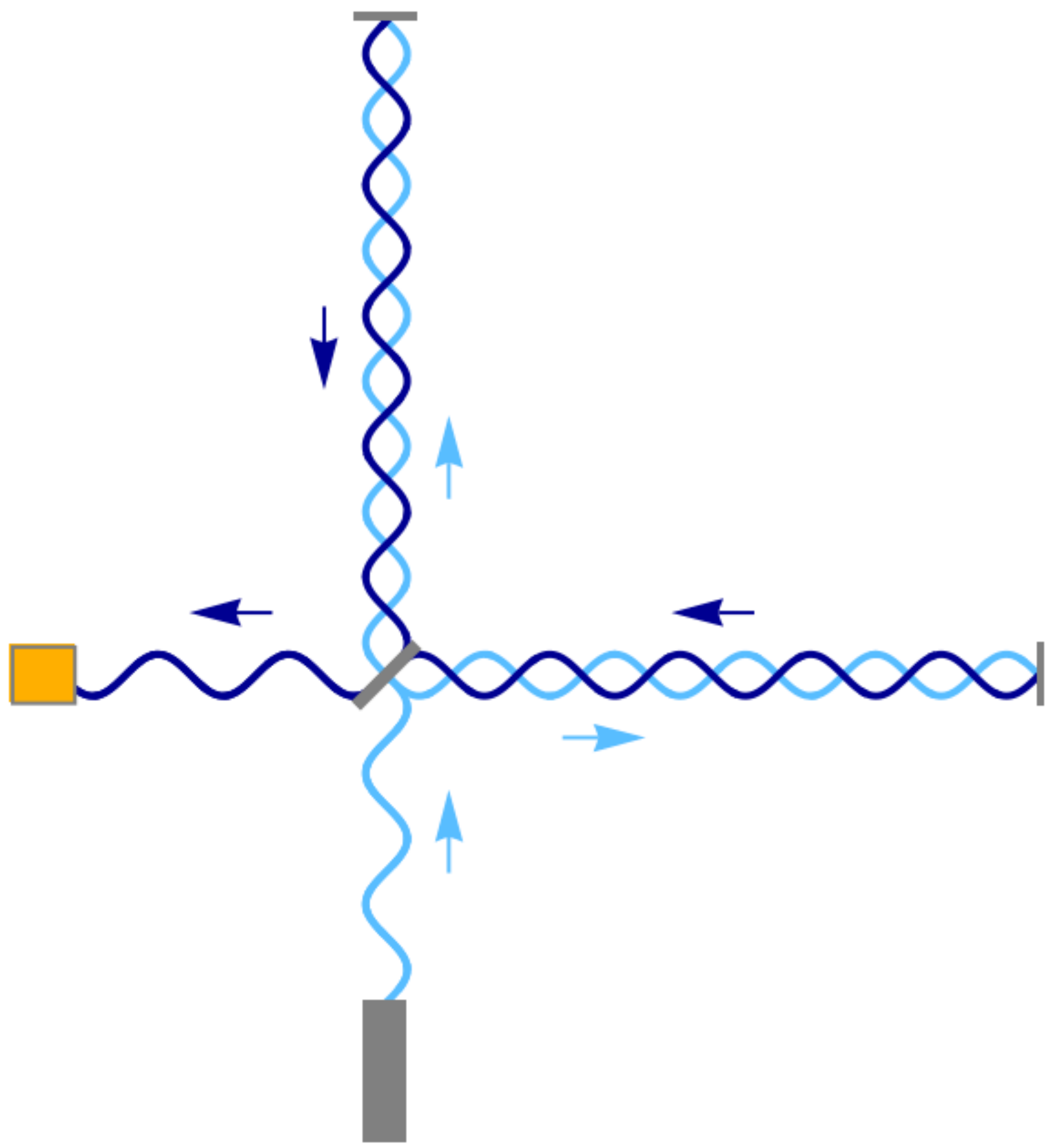

1970s-1980s: Interferometer detectors are proposed

1984: LIGO (Laser Interferometer Gravitational-wave Observatory) is founded

1989: Virgo is founded

Late 1990s-early 2000s: First-generation detectors are built (LIGO, Virgo, GEO)

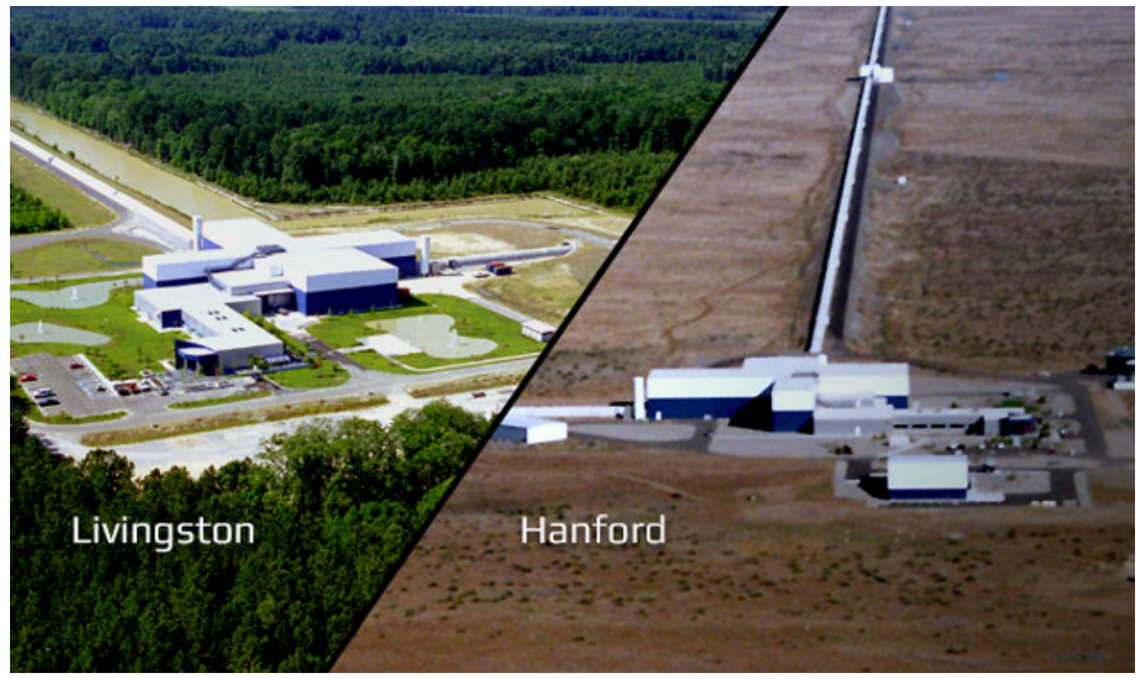

LIGO

Virgo

Historical overview

1970s-1980s: Interferometer detectors are proposed

1984: LIGO (Laser Interferometer Gravitational-wave Observatory) is founded

1989: Virgo is founded

Late 1990s-early 2000s: First-generation detectors are built (LIGO, Virgo, GEO)

Early 2010s: Second-generation upgrades (Advanced LIGO, Advanced Virgo)

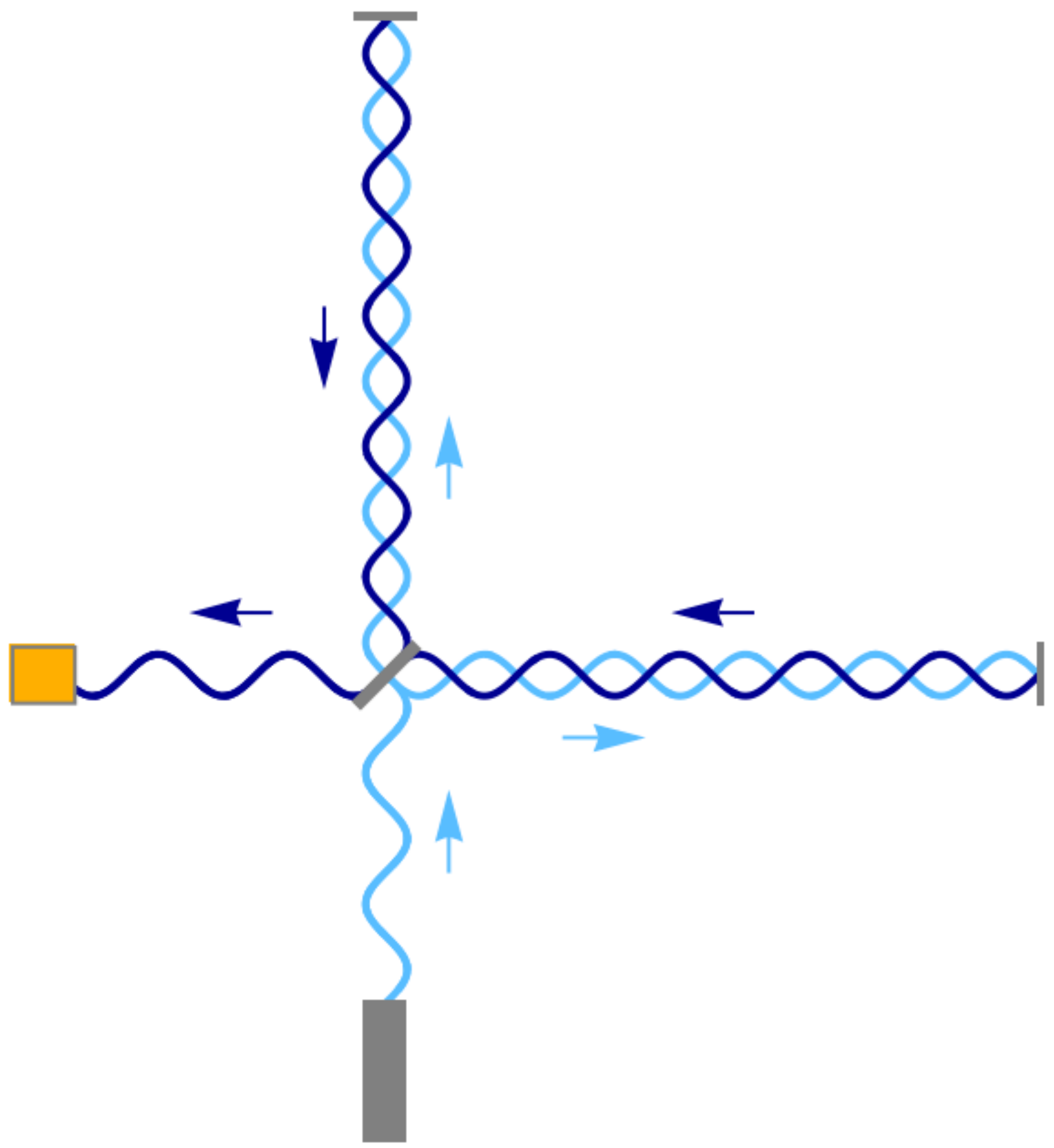

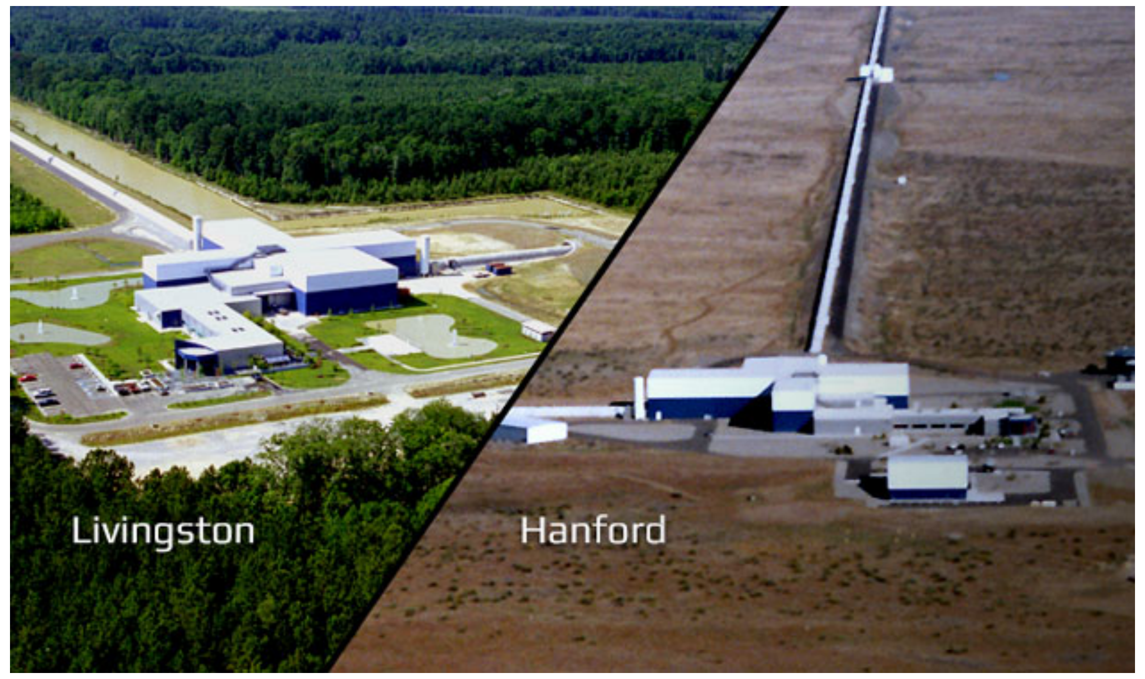

LIGO

Virgo

Historical overview

1970s-1980s: Interferometer detectors are proposed

1984: LIGO (Laser Interferometer Gravitational-wave Observatory) is founded

1989: Virgo is founded

Late 1990s-early 2000s: First-generation detectors are built (LIGO, Virgo, GEO)

Early 2010s: Second-generation upgrades (Advanced LIGO, Advanced Virgo)

2020: KAGRA is completed in Japan, LIGO-Virgo-KAGRA Collaboration

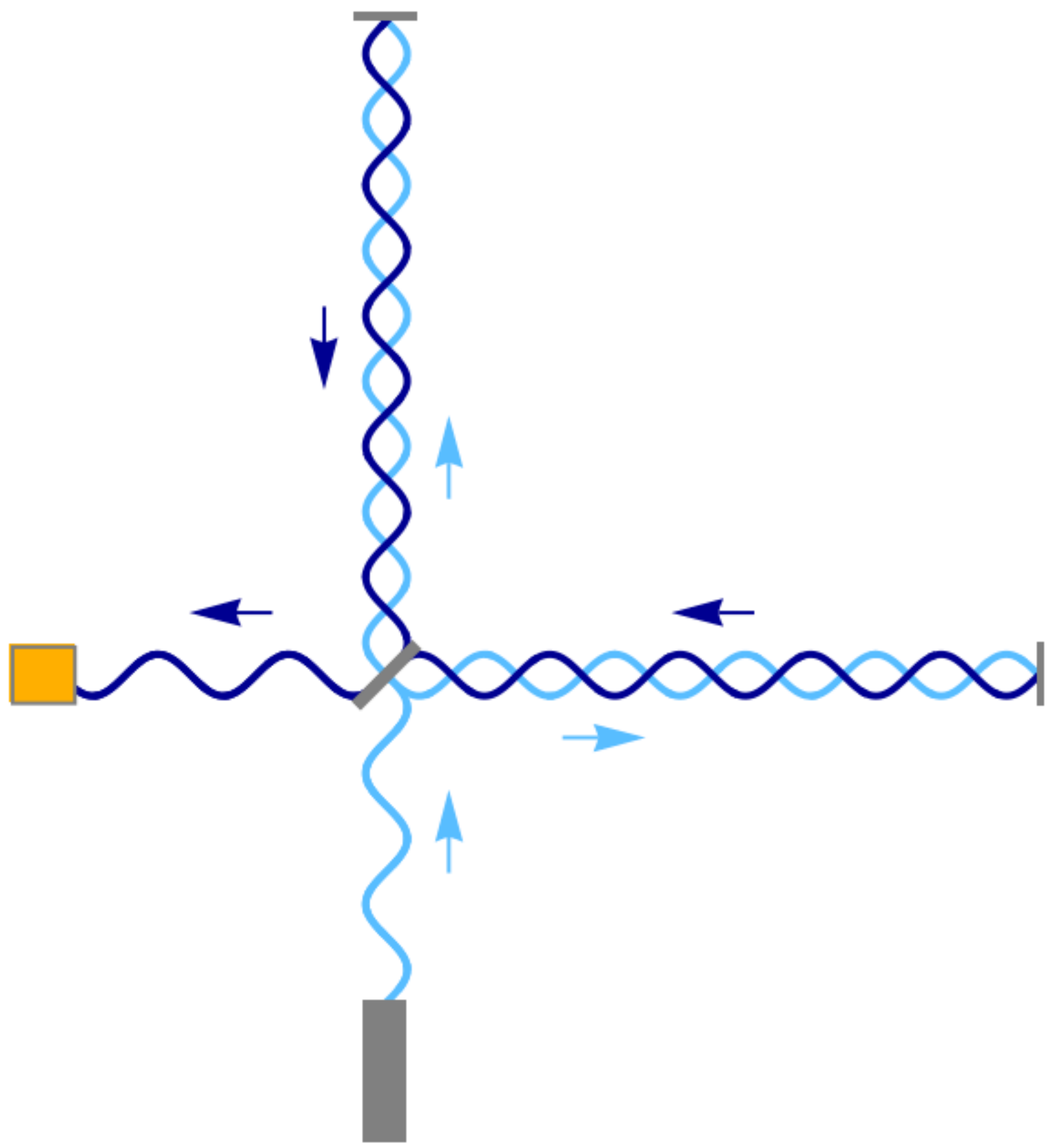

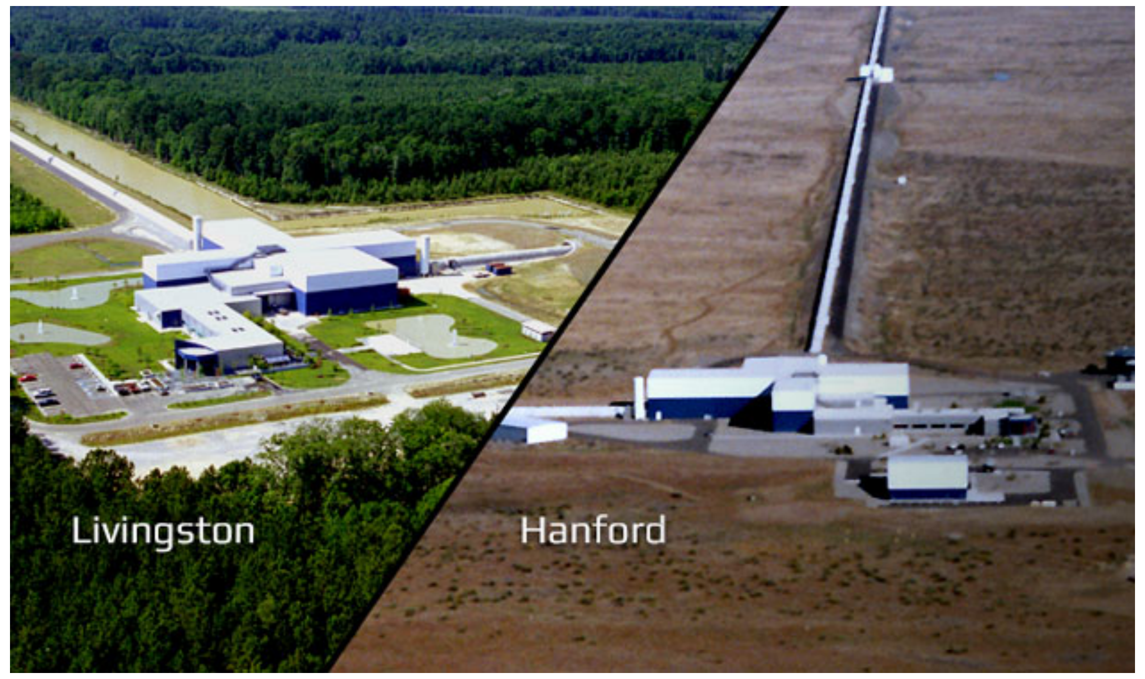

LIGO


Virgo

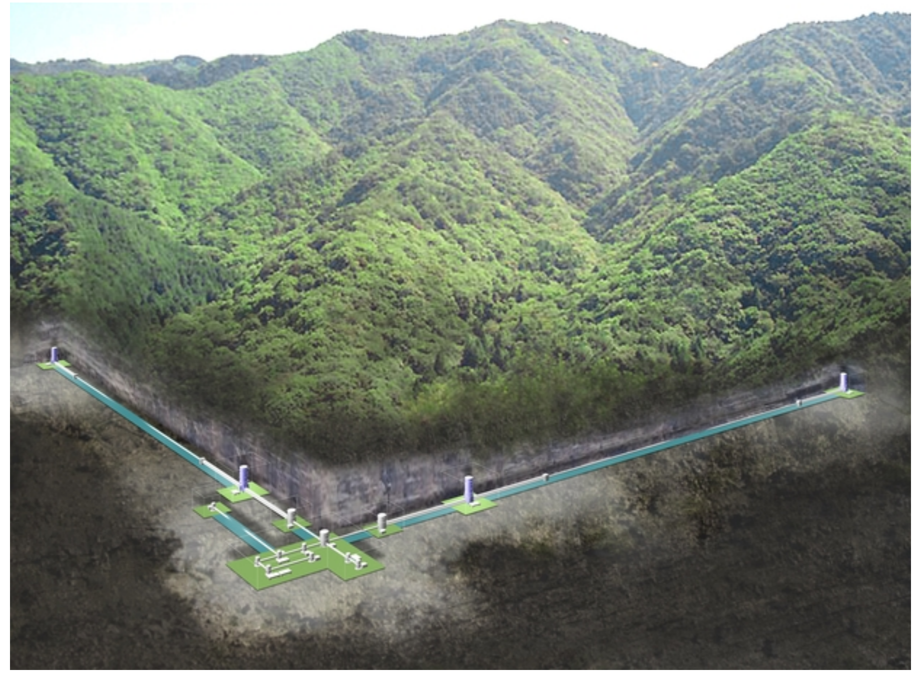
KAGRA

Historical overview

Historical overview

September 2015: The first direct observation of a gravitational wave: GW150914

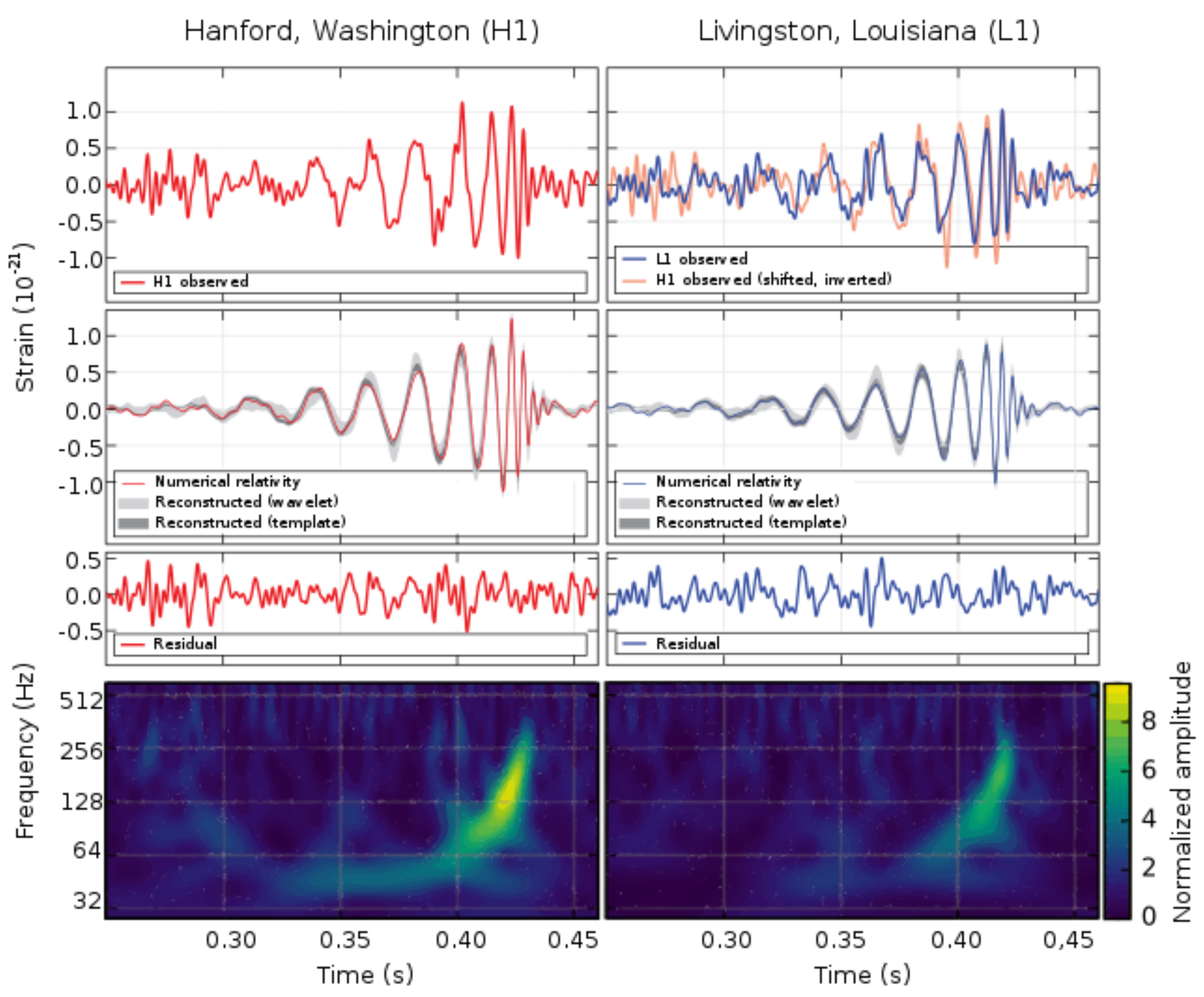

Historical overview

September 2015: The first direct observation of a gravitational wave: GW150914

February 2016: The detection is announced to the public

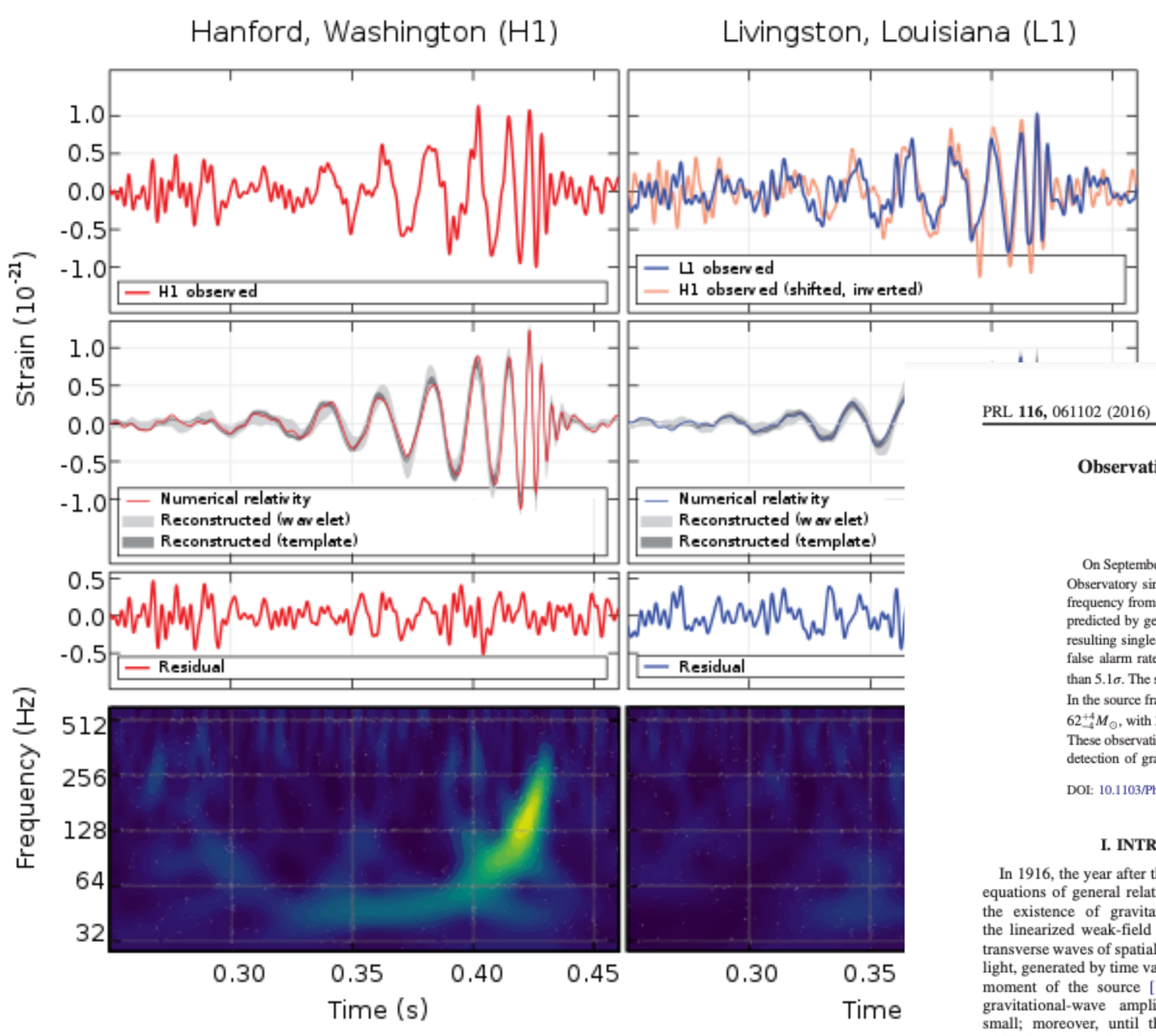

Selected for a Viewpoint in *Physics*
PRL **116,** 061102 (2016) PHYSICAL REVIEW LETTERS week ending 12 FEBRUARY 2016

Observation of Gravitational Waves from a Binary Black Hole Merger

B. P. Abbott *et al.*[*]
(LIGO Scientific Collaboration and Virgo Collaboration)
(Received 21 January 2016; published 11 February 2016)

On September 14, 2015 at 09:50:45 UTC the two detectors of the Laser Interferometer Gravitational-Wave Observatory simultaneously observed a transient gravitational-wave signal. The signal sweeps upwards in frequency from 35 to 250 Hz with a peak gravitational-wave strain of 1.0×10^{-21}. It matches the waveform predicted by general relativity for the inspiral and merger of a pair of black holes and the ringdown of the resulting single black hole. The signal was observed with a matched-filter signal-to-noise ratio of 24 and a false alarm rate estimated to be less than 1 event per 203 000 years, equivalent to a significance greater than 5.1σ. The source lies at a luminosity distance of 410^{+160}_{-180} Mpc corresponding to a redshift $z = 0.09^{+0.03}_{-0.04}$. In the source frame, the initial black hole masses are $36^{+5}_{-4} M_\odot$ and $29^{+4}_{-4} M_\odot$, and the final black hole mass is $62^{+4}_{-4} M_\odot$, with $3.0^{+0.5}_{-0.5} M_\odot c^2$ radiated in gravitational waves. All uncertainties define 90% credible intervals. These observations demonstrate the existence of binary stellar-mass black hole systems. This is the first direct detection of gravitational waves and the first observation of a binary black hole merger.

DOI: 10.1103/PhysRevLett.116.061102

I. INTRODUCTION

In 1916, the year after the final formulation of the field equations of general relativity, Albert Einstein predicted the existence of gravitational waves. He found that the linearized weak-field equations had wave solutions: transverse waves of spatial strain that travel at the speed of light, generated by time variations of the mass quadrupole moment of the source [1,2]. Einstein understood that gravitational-wave amplitudes would be remarkably small; moreover, until the Chapel Hill conference in 1957 there was significant debate about the physical reality of gravitational waves [3].

Also in 1916, Schwarzschild published a solution for the field equations [4] that was later understood to describe a black hole [5,6], and in 1963 Kerr generalized the solution to rotating black holes [7]. Starting in the 1970s theoretical work led to the understanding of black hole quasinormal modes [8–10], and in the 1990s higher-order post-Newtonian calculations [11] preceded extensive analytical studies of relativistic two-body dynamics [12,13]. These advances, together with numerical relativity breakthroughs in the past decade [14–16], have enabled modeling of binary black hole mergers and accurate predictions of their gravitational waveforms. While numerous black hole candidates have now been identified through electromagnetic observations [17–19], black hole mergers have not previously been observed.

The discovery of the binary pulsar system PSR B1913+16 by Hulse and Taylor [20] and subsequent observations of its energy loss by Taylor and Weisberg [21] demonstrated the existence of gravitational waves. This discovery, along with emerging astrophysical understanding [22], led to the recognition that direct observations of the amplitude and phase of gravitational waves would enable studies of additional relativistic systems and provide new tests of general relativity, especially in the dynamic strong-field regime.

Experiments to detect gravitational waves began with Weber and his resonant mass detectors in the 1960s [23], followed by an international network of cryogenic resonant detectors [24]. Interferometric detectors were first suggested in the early 1960s [25] and the 1970s [26]. A study of the noise and performance of such detectors [27], and further concepts to improve them [28], led to proposals for long-baseline broadband laser interferometers with the potential for significantly increased sensitivity [29–32]. By the early 2000s, a set of initial detectors was completed, including TAMA 300 in Japan, GEO 600 in Germany, the Laser Interferometer Gravitational-Wave Observatory (LIGO) in the United States, and Virgo in Italy. Combinations of these detectors made joint observations from 2002 through 2011, setting upper limits on a variety of gravitational-wave sources while evolving into a global network. In 2015, Advanced LIGO became the first of a significantly more sensitive network of advanced detectors to begin observations [33–36].

A century after the fundamental predictions of Einstein and Schwarzschild, we report the first direct detection of gravitational waves and the first direct observation of a binary black hole system merging to form a single black hole. Our observations provide unique access to the

[*]Full author list given at the end of the article.

Historical overview

September 2015: The first direct observation of a gravitational wave: GW150914

February 2016: The detection is announced to the public

December 2017: The Nobel prize is awarded to Rainer Weiss, Barry Barish, Kip Thorne, “for decisive contributions to the LIGO detector and the observation of gravitational waves”

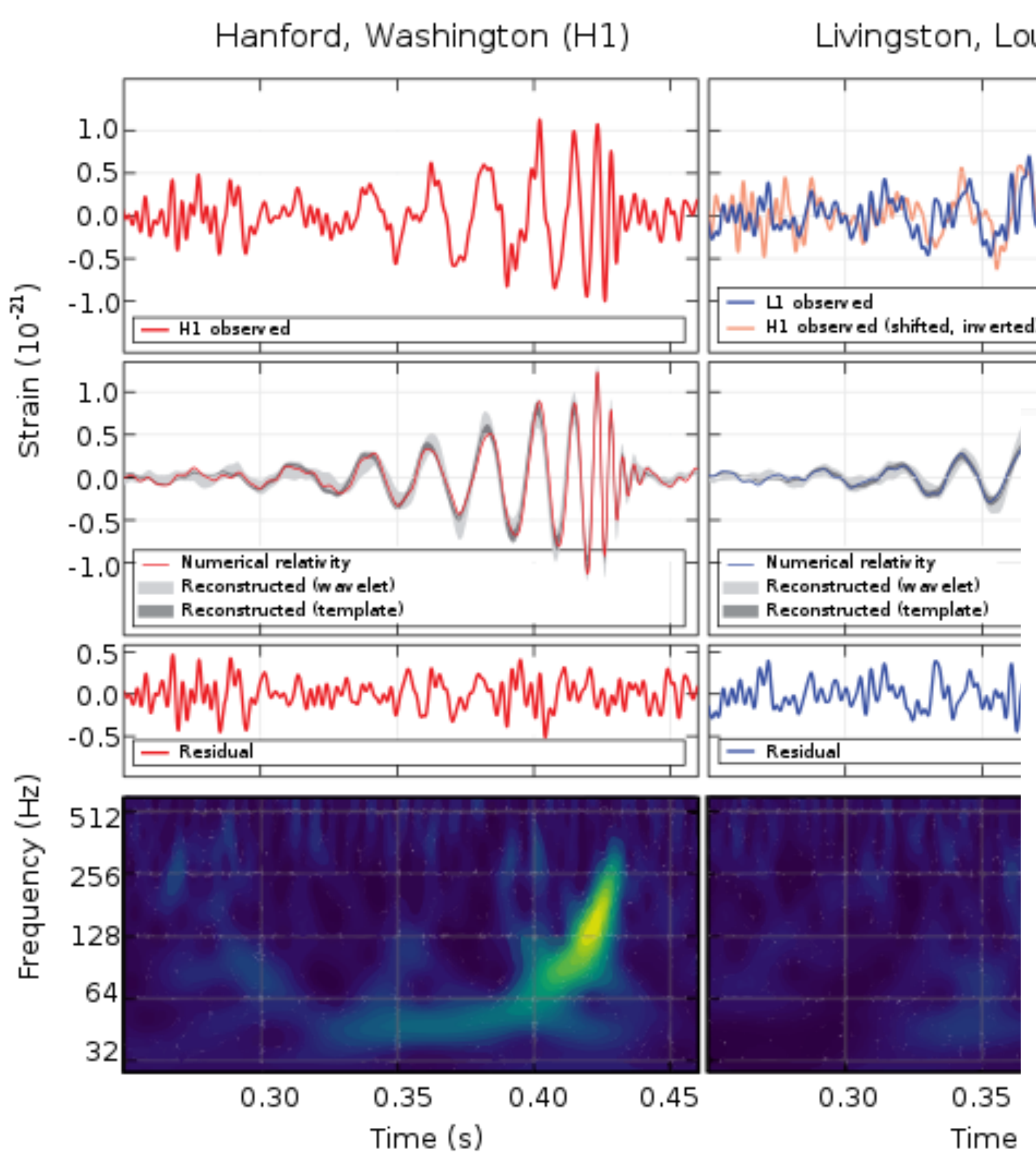

Selected for a Viewpoint in *Physics*
PRL **116,** 061102 (2016) PHYSICAL REVIEW LETTERS week ending 12 FEBRUARY 2016

Observation of Gravitational Waves from a Binary Black Hole Merger

B. P. Abbott *et al.**
(LIGO Scientific Collaboration and Virgo Collaboration)

(Received 21 January 2016; published 11 February 2016)

On September 14, 2015 at 09:50:45 UTC the two detectors of the Laser Interferometer Gravitational-Wave Observatory simultaneously observed a transient gravitational-wave signal. The signal sweeps upwards in frequency from 35 to 250 Hz with a peak gravitational-wave strain of 1.0×10^{-21}. It matches the waveform predicted by general relativity for the inspiral and merger of a pair of black holes and the ringdown of the resulting single black hole. The signal was observed with a matched-filter signal-to-noise ratio of 24 and a false alarm rate estimated to be less than 1 event per 203 000 years, equivalent to a significance greater than 5.1σ. The source lies at a luminosity distance of 410^{+160}_{-180} Mpc corresponding to a redshift $z = 0.09^{+0.03}_{-0.04}$. In the source frame, the initial black hole masses are $36^{+5}_{-4} M_\odot$ and $29^{+4}_{-4} M_\odot$, and the final black hole mass is $62^{+4}_{-4} M_\odot$, with $3.0^{+0.5}_{-0.5} M_\odot c^2$ radiated in gravitational waves. All uncertainties define 90% credible intervals. These observations demonstrate the existence of binary stellar-mass black hole systems. This is the first direct detection of gravitational waves and the first observation of a binary black hole merger.

DOI: 10.1103/PhysRevLett.116.061102

I. INTRODUCTION

In 1916, the year after the final formulation of the field equations of general relativity, Albert Einstein predicted the existence of gravitational waves. He found that the linearized weak-field equations had wave solutions: transverse waves of spatial strain that travel at the speed of light, generated by time variations of the mass quadrupole moment of the source [1,2]. Einstein understood that gravitational-wave amplitudes would be remarkably small; moreover, until the Chapel Hill conference in 1957 there was significant debate about the physical reality of gravitational waves [3].

Also in 1916, Schwarzschild published a solution for the field equations [4] that was later understood to describe a black hole [5,6], and in 1963 Kerr generalized the solution to rotating black holes [7]. Starting in the 1970s theoretical work led to the understanding of black hole quasinormal modes [8–10], and in the 1990s higher-order post-Newtonian calculations [11] preceded extensive analytical studies of relativistic two-body dynamics [12,13]. These advances, together with numerical relativity breakthroughs in the past decade [14–16], have enabled modeling of binary black hole mergers and accurate predictions of

The discovery of the binary pulsar system PSR B1913+16 by Hulse and Taylor [20] and subsequent observations of its energy loss by Taylor and Weisberg [21] demonstrated the existence of gravitational waves. This discovery, along with emerging astrophysical understanding [22], led to the recognition that direct observations of the amplitude and phase of gravitational waves would enable studies of additional relativistic systems and provide new tests of general relativity, especially in the dynamic strong-field regime.

Experiments to detect gravitational waves began with Weber and his resonant mass detectors in the 1960s [23], followed by an international network of cryogenic resonant detectors [24]. Interferometric detectors were first suggested in the early 1960s [25] and the 1970s [26]. A study of the noise and performance of such detectors [27], and further concepts to improve them [28], led to proposals for long-baseline broadband laser interferometers with the potential for significantly increased sensitivity [29–32]. By the early 2000s, a set of initial detectors was completed, including TAMA 300 in Japan, GEO 600 in Germany, the Laser Interferometer Gravitational-Wave Observatory (LIGO) in the United States, and Virgo in Combinations of these detectors made joint obser- s from 2002 through 2011, setting upper limits on a y of gravitational-wave sources while evolving into al network. In 2015, Advanced LIGO became the f a significantly more sensitive network of advanced ors to begin observations [33–36].

entury after the fundamental predictions of Einstein chwarzschild, we report the first direct detection of ational waves and the first direct observation of a black hole system merging to form a single black Our observations provide unique access to the

Published by the American Physical Society

Historical overview

June 2023: Pulsar timing array collaborations (NANOGrav, EPTA, PPTA, InPTA, CPTA) find evidence for a gravitational wave background

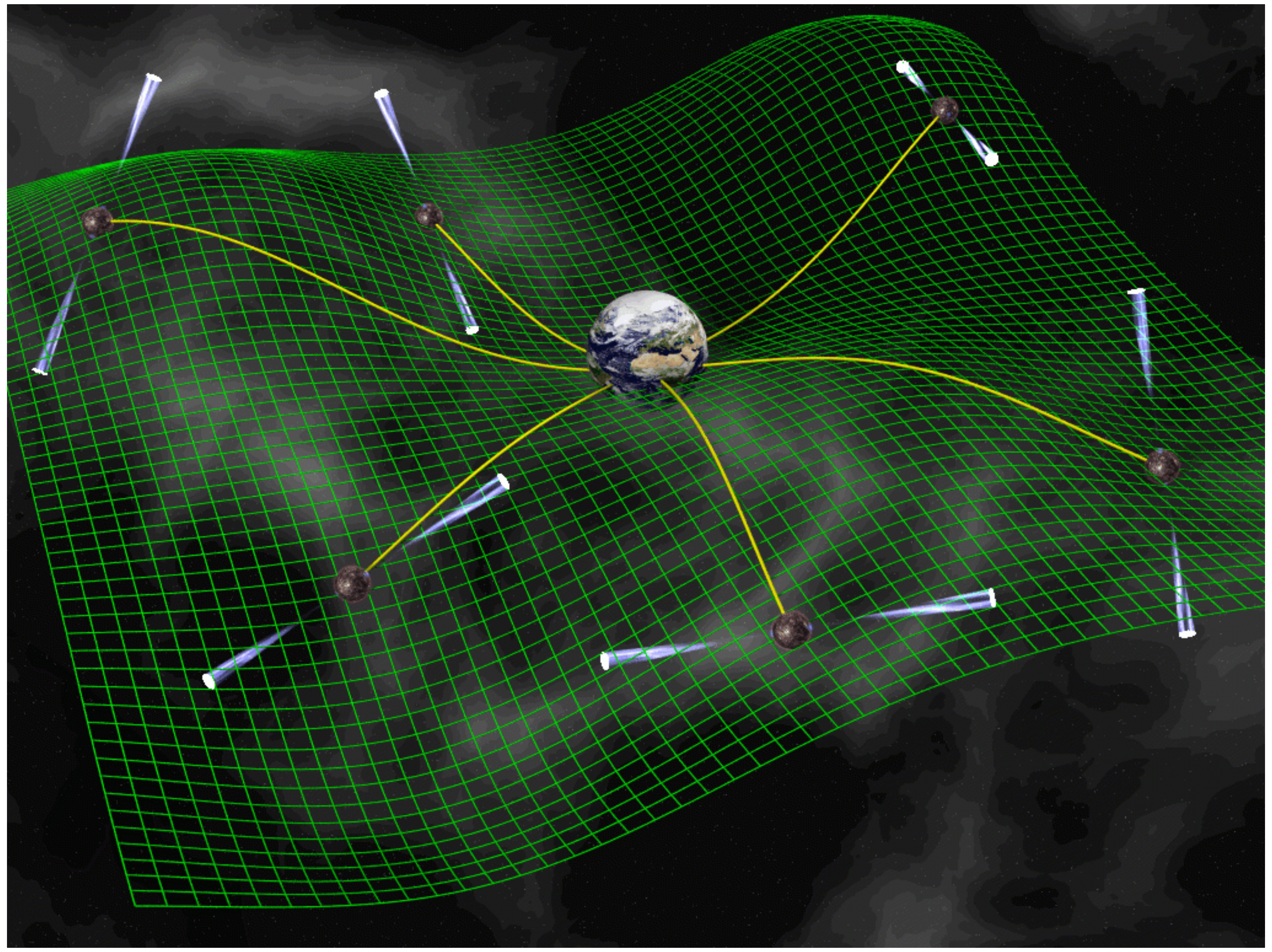

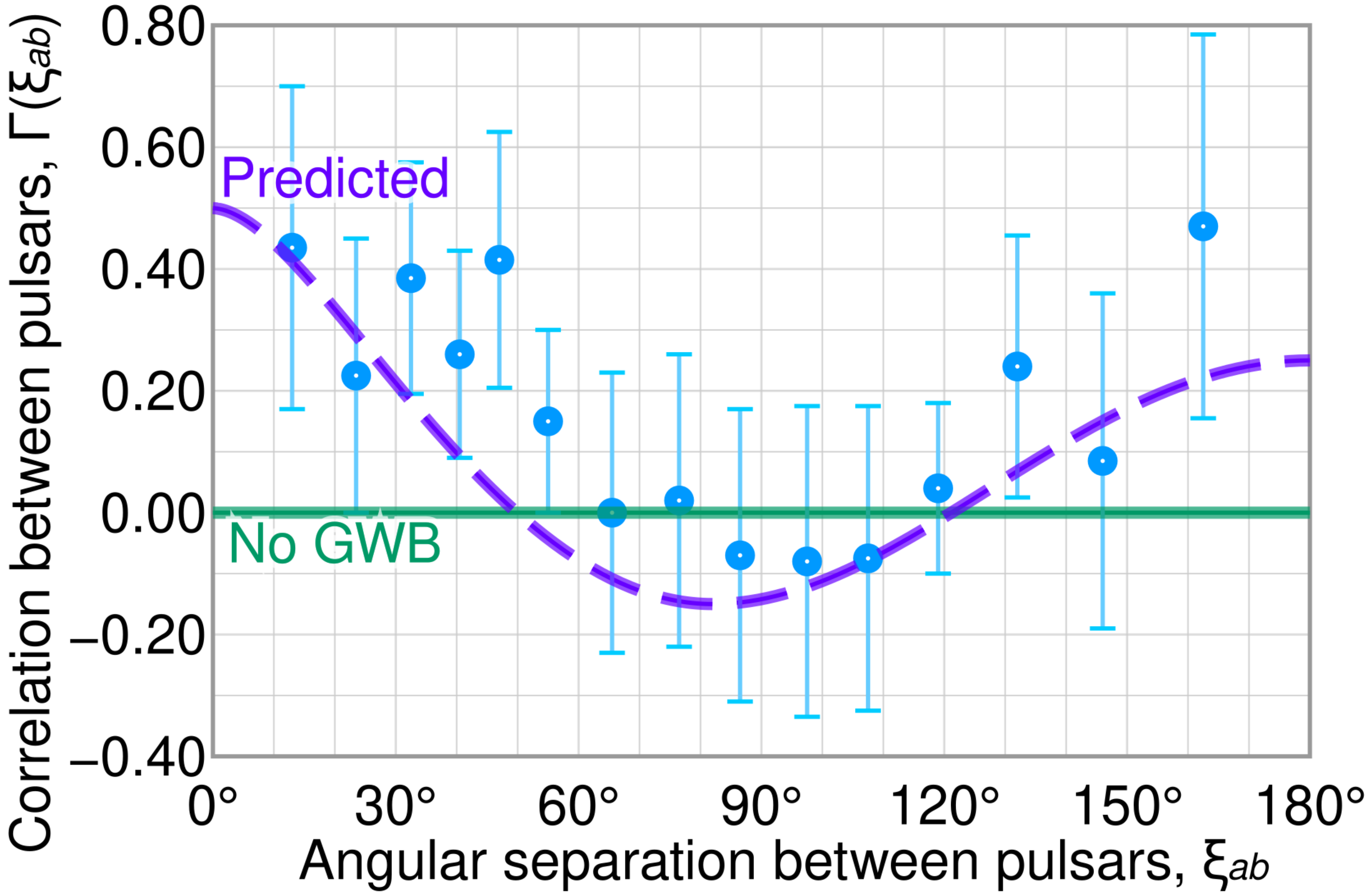

The LVK Collaboration today

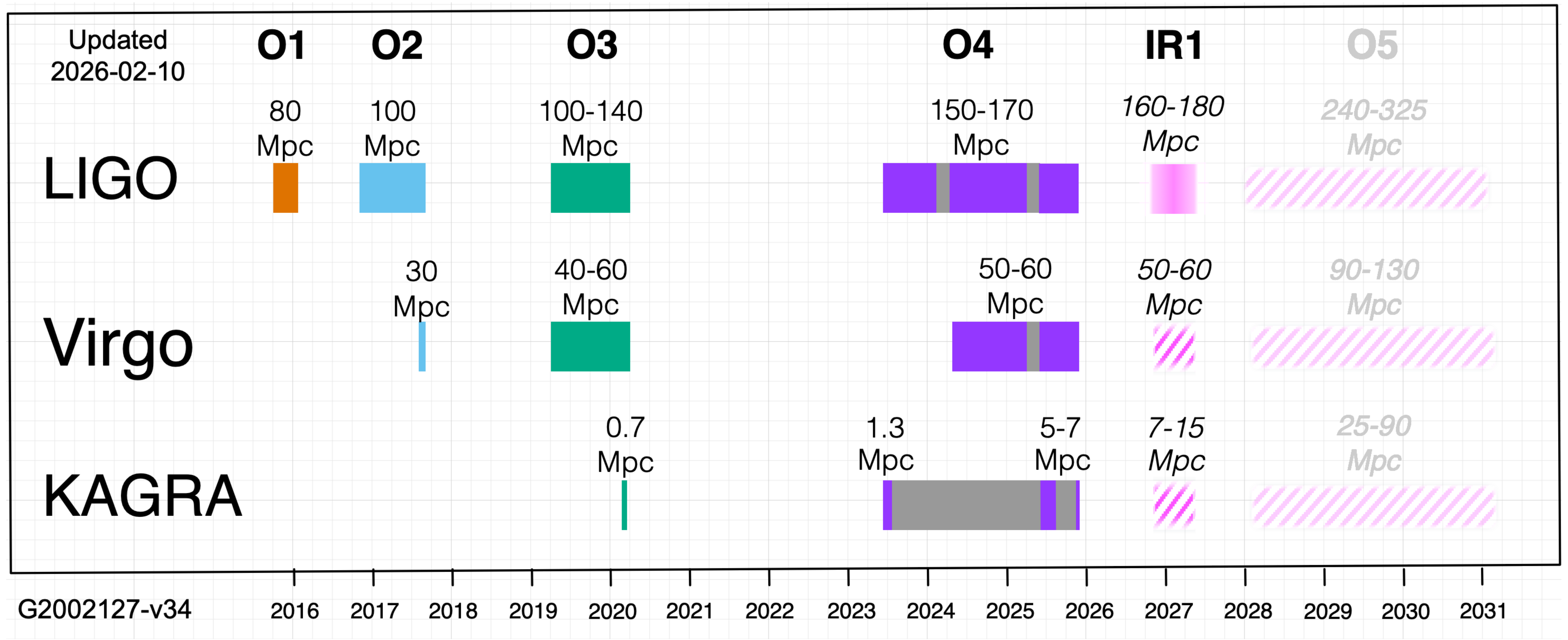

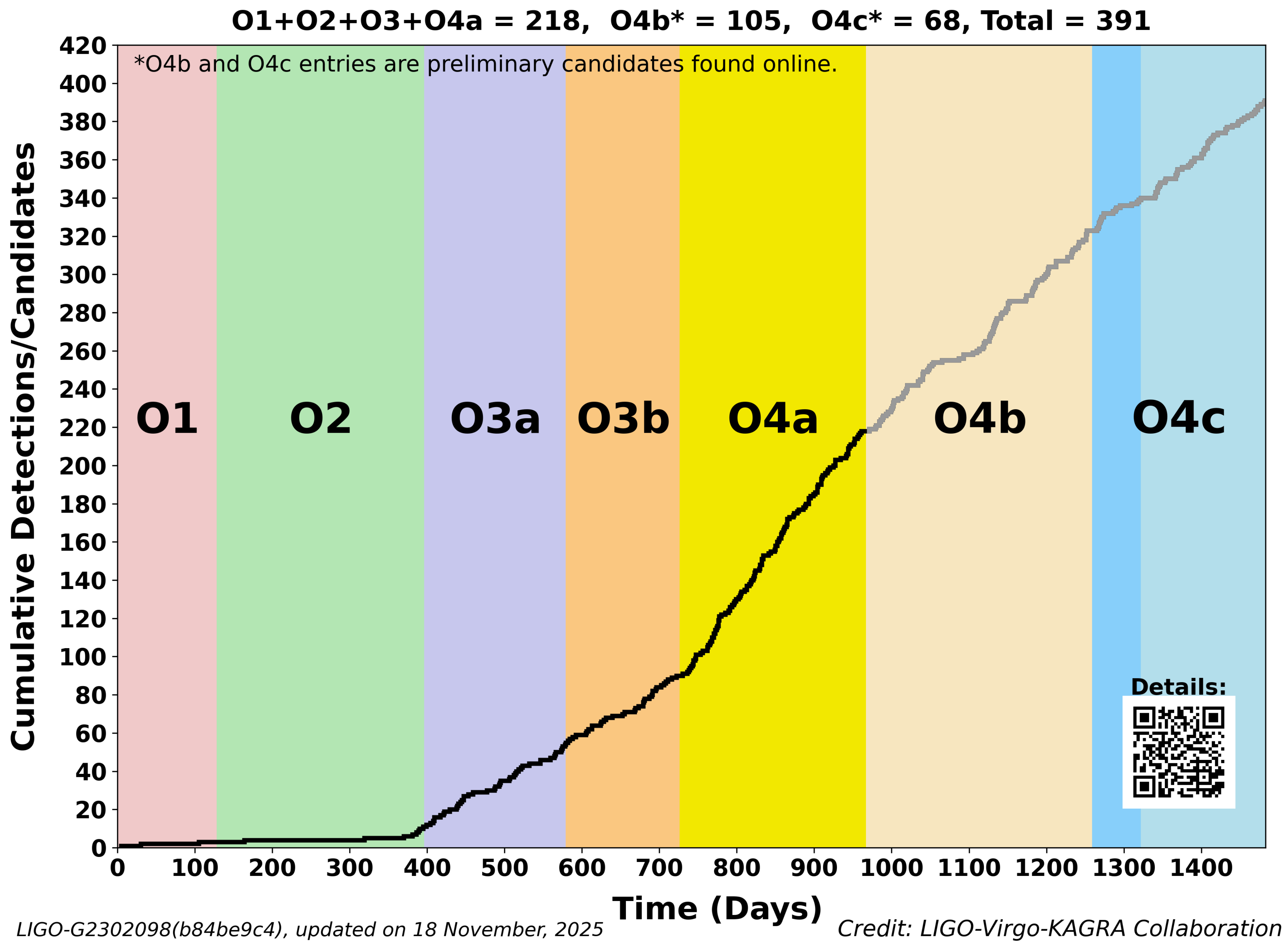

Gravitational Wave Transient Catalogs

GWTC-1: O1 + O2

GWTC-2: O1 + O2 + O3a

GWTC-3: O1 + O2 + O3a + O3b

GWTC-4: O1 + O2 + O3a + O3b + O4a

Gravitational wave equation

Gravitational wave equation

$$R_{\mu\nu} - \frac{1}{2} g_{\mu\nu} R = \frac{8\pi G}{c^4} T^{\mu\nu}$$

Gravitational wave equation

$$R_{\mu\nu} - \frac{1}{2}g_{\mu\nu}R = \frac{8\pi G}{c^4}T^{\mu\nu}$$

$$\eta_{\mu\nu} = \mathrm{diag}(-1,1,1,1)$$

$$h_{\mu\nu} \ll 1$$

$$g_{\mu\nu} = \eta_{\mu\nu} + h_{\mu\nu}$$

Gravitational wave equation

$$R_{\mu\nu} - \frac{1}{2}g_{\mu\nu}R = \frac{8\pi G}{c^4}T^{\mu\nu}$$

$\eta_{\mu\nu} = \text{diag}(-1,1,1,1)$

$h_{\mu\nu} \ll 1$

$$g_{\mu\nu} = \eta_{\mu\nu} + h_{\mu\nu}$$

Trace reverse: $\bar{h}_{\mu\nu} = h_{\mu\nu} - \frac{1}{2}h\eta_{\mu\nu}$

Lorenz gauge: $\partial_\mu \bar{h}^{\mu\nu} = 0$

$$\Box \bar{h}_{\mu\nu} = -\frac{16\pi G}{c^4}T^{\mu\nu}$$

Polarizations

Polarizations

Gravitational waves are transverse, traceless, and the metric is always symmetric:

Polarizations

Gravitational waves are transverse, traceless, and the metric is always symmetric:

$$h^{\mu\nu}(t) = \begin{pmatrix} 0 & 0 & 0 & 0 \\ 0 & h_+(t) & h_\times(t) & 0 \\ 0 & h_\times(t) & -h_+(t) & 0 \\ 0 & 0 & 0 & 0 \end{pmatrix}$$

Propagation direction: $\hat{z}$

Polarizations

Gravitational waves are transverse, traceless, and the metric is always symmetric:

$$h^{\mu\nu}(t) = \begin{pmatrix} 0 & 0 & 0 & 0 \\ 0 & h_+(t) & h_\times(t) & 0 \\ 0 & h_\times(t) & -h_+(t) & 0 \\ 0 & 0 & 0 & 0 \end{pmatrix}$$

Propagation direction: $\hat{z}$

For a binary with phase evolution $\phi(t)$:

$$h_+(t) = A(t)\cos\left[2\phi(t)\right] \quad h_\times(t) = A(t)\sin\left[2\phi(t)\right]$$

Polarizations

Gravitational waves are transverse, traceless, and the metric is always symmetric:

$$h^{\mu\nu}(t) = \begin{pmatrix} 0 & 0 & 0 & 0 \\ 0 & h_+(t) & h_\times(t) & 0 \\ 0 & h_\times(t) & -h_+(t) & 0 \\ 0 & 0 & 0 & 0 \end{pmatrix}$$

Propagation direction: $\hat{z}$

For a binary with phase evolution $\phi(t)$:

$$h_+(t) = A(t)\cos\left[2\phi(t)\right] \quad h_\times(t) = A(t)\sin\left[2\phi(t)\right]$$

Solving the geodesic deviation equation gives us the relative motion of test particles:

Polarizations

Gravitational waves are transverse, traceless, and the metric is always symmetric:

$$h^{\mu\nu}(t) = \begin{pmatrix} 0 & 0 & 0 & 0 \\ 0 & h_+(t) & h_\times(t) & 0 \\ 0 & h_\times(t) & -h_+(t) & 0 \\ 0 & 0 & 0 & 0 \end{pmatrix}$$

Propagation direction: $\hat{z}$

For a binary with phase evolution $\phi(t)$:

$$h_+(t) = A(t)\cos\left[2\phi(t)\right] \quad h_\times(t) = A(t)\sin\left[2\phi(t)\right]$$

Solving the geodesic deviation equation gives us the relative motion of test particles:

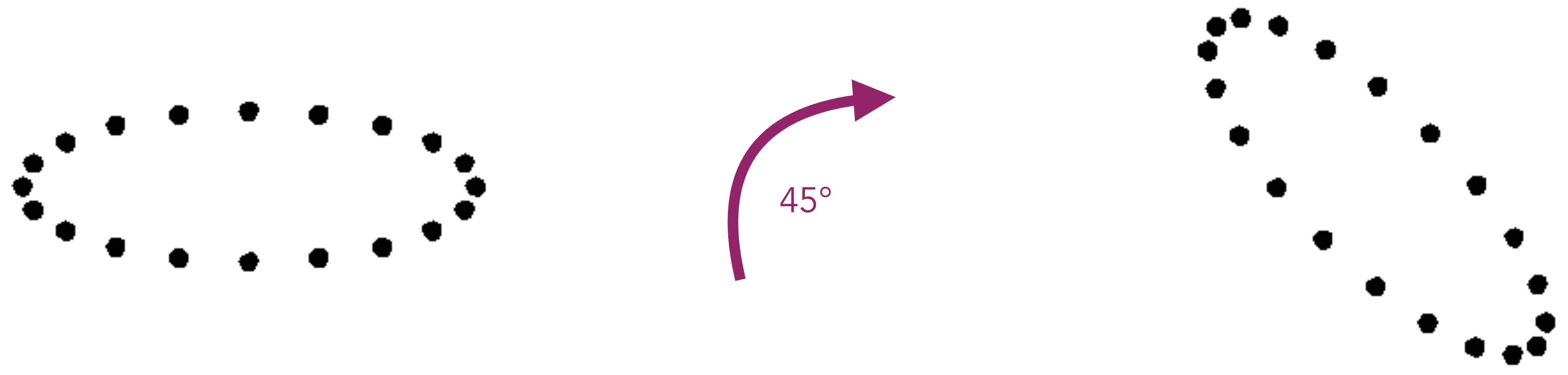

Propagation direction: ⊙

What is h?

What is h?

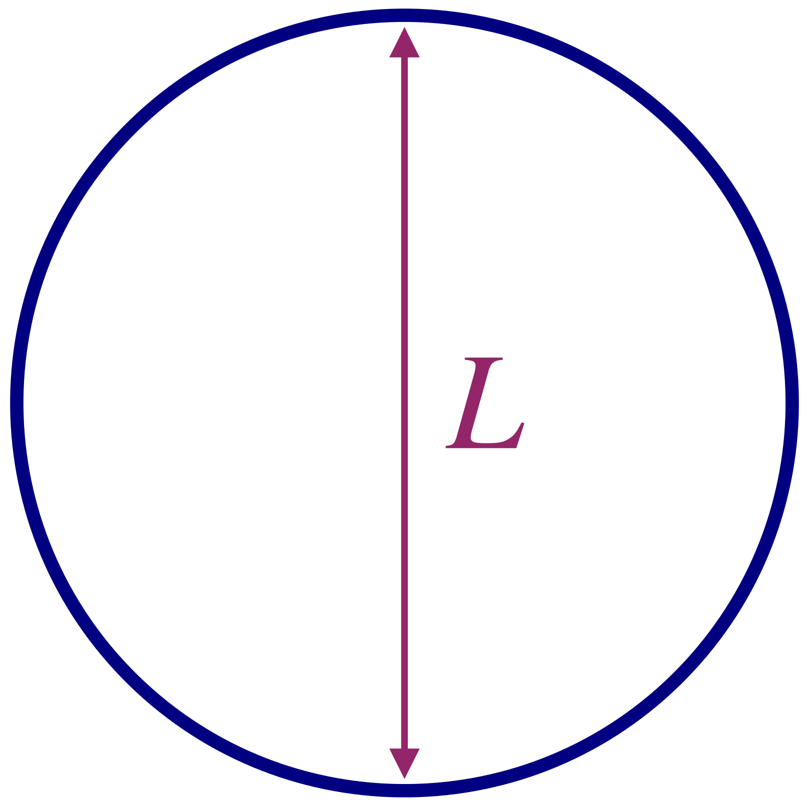

What is h?

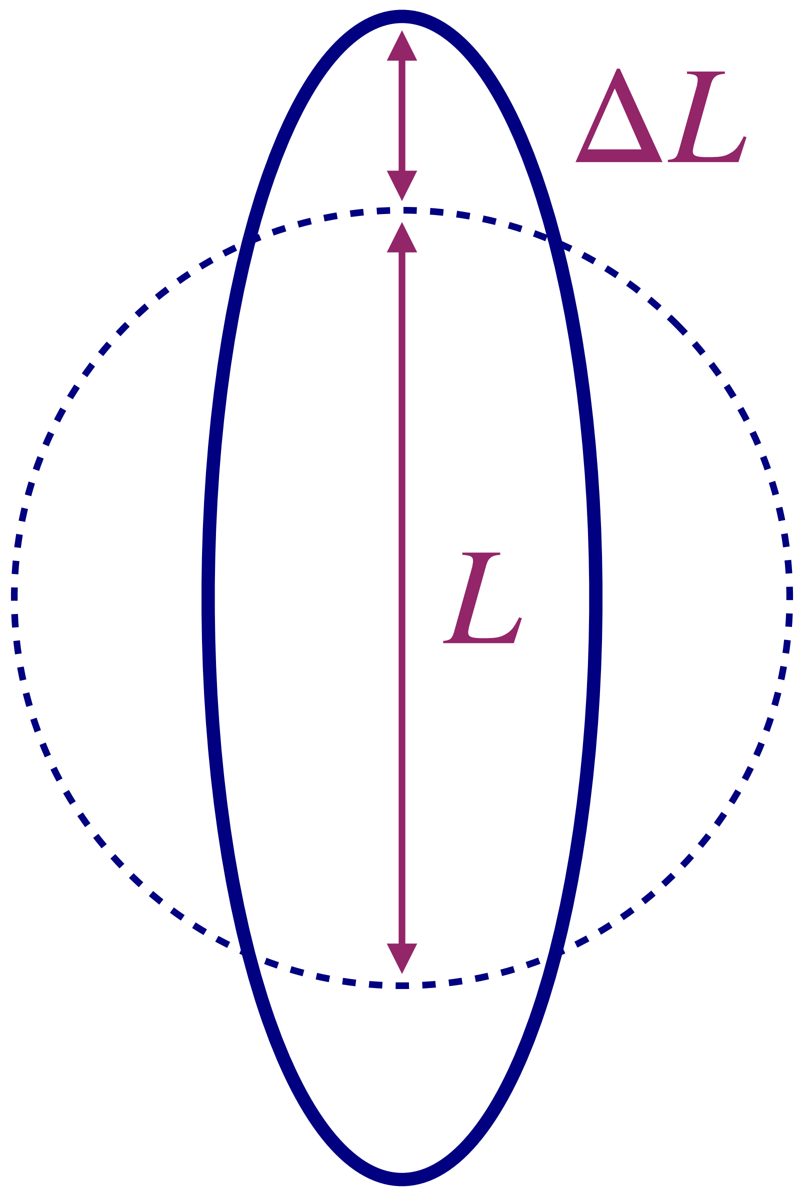

What is h?

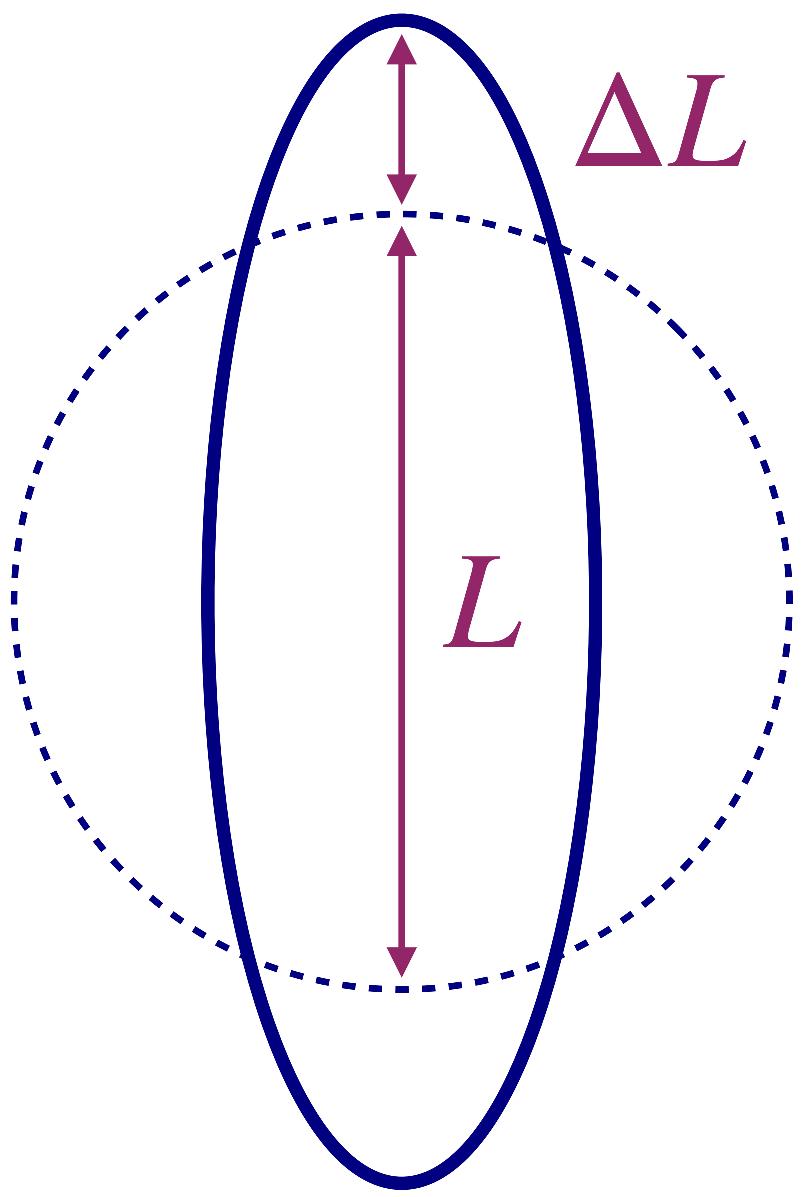

$$h \sim \frac{\Delta L}{L}$$

What is h?

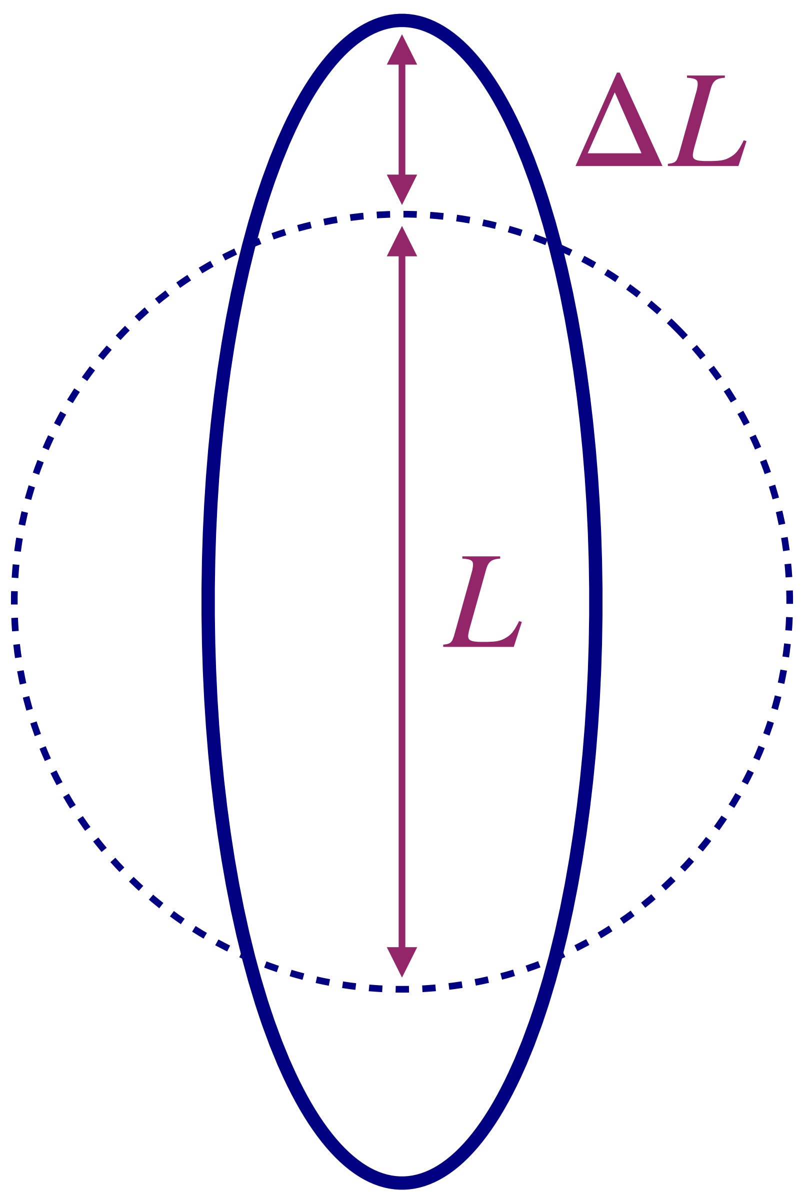

$$h \sim \frac{\Delta L}{L} \sim 10^{-22}$$

(For compact binaries observed by the LVK Collaboration)

Detector responce

Detector responce

$$h_{+,\times}(t) = h_{+,\times}(t, m_1, m_2, \boldsymbol{\chi_1}, \boldsymbol{\chi_2}, t_c, \phi_c, D_L, \iota, \ldots)$$

Detector responce

$$h_{+,\times}(t) = h_{+,\times}(t, \underbrace{m_1, m_2, \boldsymbol{\chi_1}, \boldsymbol{\chi_2}, t_c, \phi_c}_{\text{intrinsic}}, D_L, \iota, \ldots)$$

Detector responce

$$h_{+,\times}(t) = h_{+,\times}(t, \underbrace{m_1, m_2, \boldsymbol{\chi_1}, \boldsymbol{\chi_2}, t_c, \phi_c}_{\text{intrinsic}}, \underbrace{D_L, \iota}_{\text{extrinsic}}, \ldots)$$

Detector responce

$$h_{+,\times}(t) = h_{+,\times}(t, m_1, m_2, \boldsymbol{\chi_1}, \boldsymbol{\chi_2}, t_c, \phi_c, D_L, \iota, \ldots)$$

intrinsic extrinsic

Detector responce

$$h_{+,\times}(t) = h_{+,\times}(t, m_1, m_2, \chi_1, \chi_2, t_c, \phi_c, D_L, \iota, \ldots)$$

intrinsic extrinsic

The polarizations projected onto the detector:

$$h(t) = h_+(t)F_+(t) + h_\times(t)F_\times(t)$$

Detector responce

$$h_{+,\times}(t) = h_{+,\times}(t, m_1, m_2, \chi_1, \chi_2, t_c, \phi_c, D_L, \iota, \ldots)$$

intrinsic extrinsic

The polarizations projected onto the detector:

$$h(t) = h_+(t)F_+(t) + h_\times(t)F_\times(t)$$

Antenna pattern functions:

$$F_{+,\times}(t) = F_{+,\times}(t, t_c, \alpha, \delta, \psi)$$

Detector responce

$$h_{+,\times}(t) = h_{+,\times}(t, m_1, m_2, \chi_1, \chi_2, t_c, \phi_c, D_L, \iota, \ldots)$$

intrinsic extrinsic

The polarizations projected onto the detector:

$$h(t) = h_+(t)F_+(t) + h_\times(t)F_\times(t)$$

Antenna pattern functions:

$$F_{+,\times}(t) = F_{+,\times}(t, t_c, \alpha, \delta, \psi)$$

Detector responce

$$h_{+,\times}(t) = h_{+,\times}(t, m_1, m_2, \chi_1, \chi_2, t_c, \phi_c, D_L, \iota, \dots)$$

intrinsic extrinsic

The polarizations projected onto the detector:

$$h(t) = h_+(t)F_+(t) + h_\times(t)F_\times(t)$$

Antenna pattern functions:

$$F_{+,\times}(t) = F_{+,\times}(t, t_c, \alpha, \delta, \psi)$$

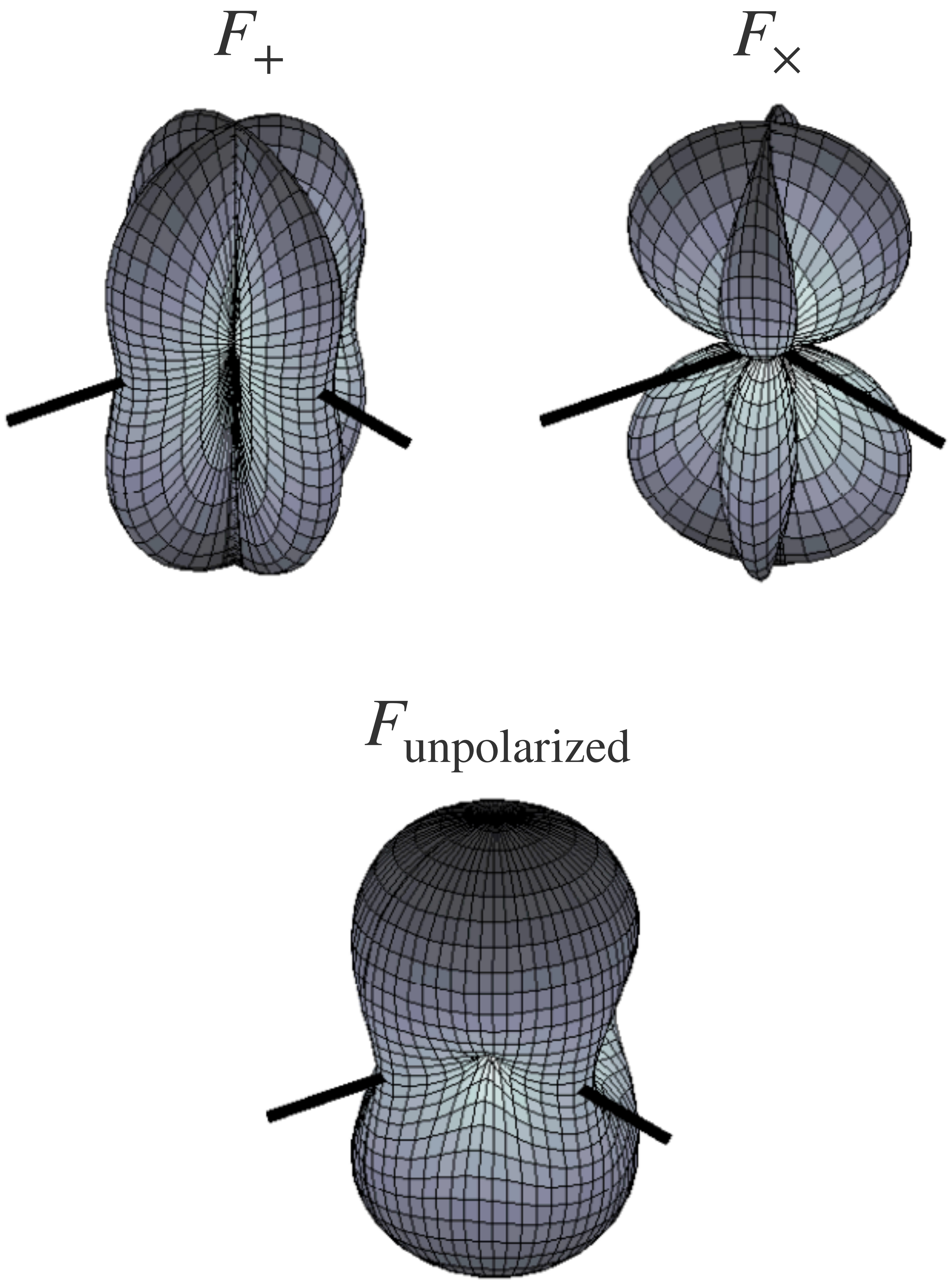

Detector responce

$$h_{+,\times}(t) = h_{+,\times}(t, m_1, m_2, \boldsymbol{\chi_1}, \boldsymbol{\chi_2}, t_c, \phi_c, D_L, \iota, \ldots)$$

intrinsic extrinsic

The polarizations projected onto the detector:

$$h(t) = h_+(t)F_+(t) + h_\times(t)F_\times(t)$$

Antenna pattern functions:

$$F_{+,\times}(t) = F_{+,\times}(t, t_c, \alpha, \delta, \psi)$$

$$\boldsymbol{\theta} = (m_1, m_2, \boldsymbol{\chi_1}, \boldsymbol{\chi_2}, t_c, \phi_c, D_L, \iota, \alpha, \delta, \psi, \ldots)$$

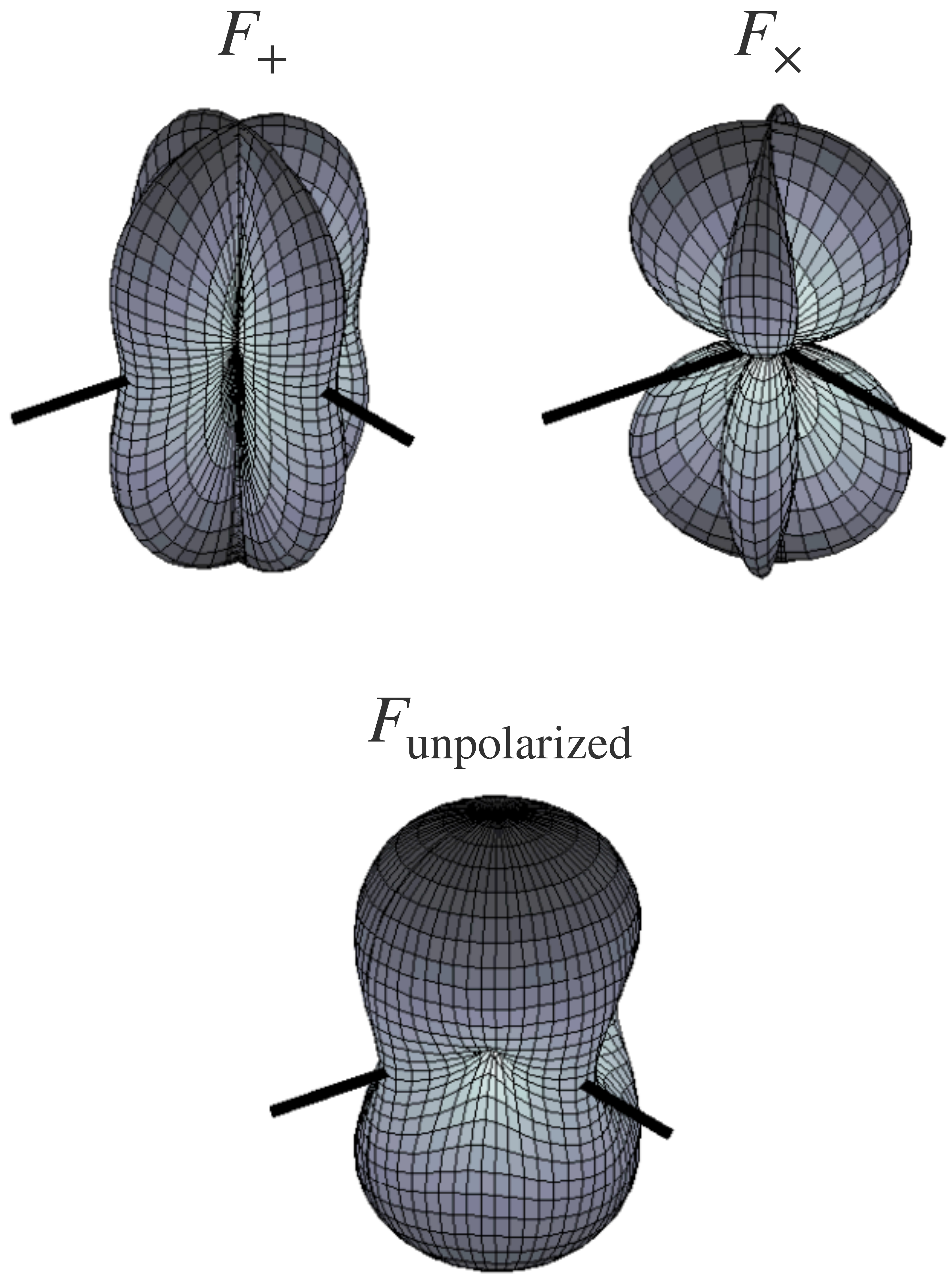

The GW spectrum

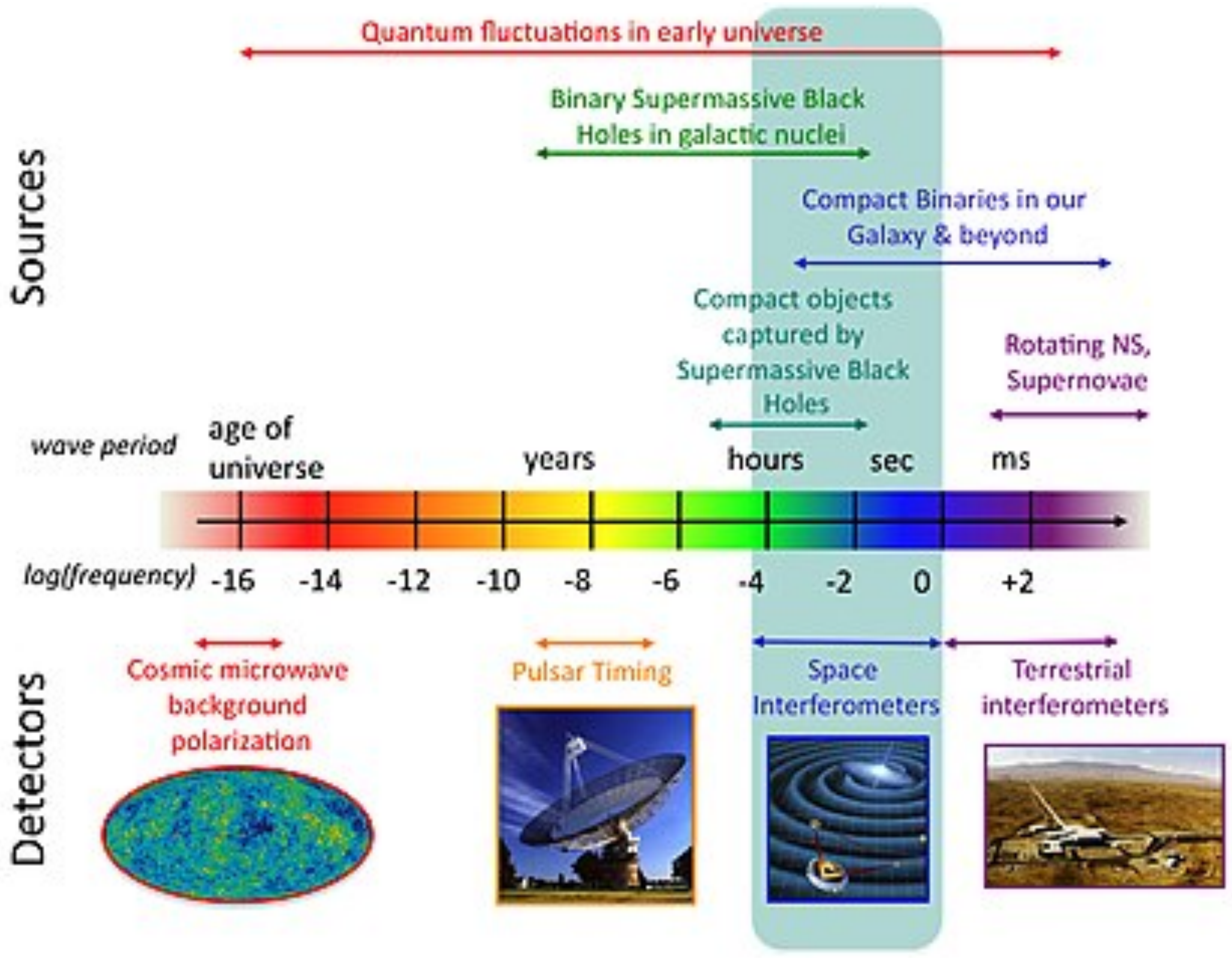

Why compact binaries?

Why compact binaries?

Experimental reasons

Why compact binaries?

Experimental reasons

- The signals can be described highly accurately with relatively few well-understood parameters

Why compact binaries?

Experimental reasons

- The signals can be described highly accurately with relatively few well-understood parameters
- Observing many cycles allows us to determine those parameters very accurately

Why compact binaries?

Experimental reasons

- The signals can be described highly accurately with relatively few well-understood parameters
- Observing many cycles allows us to determine those parameters very accurately

data =

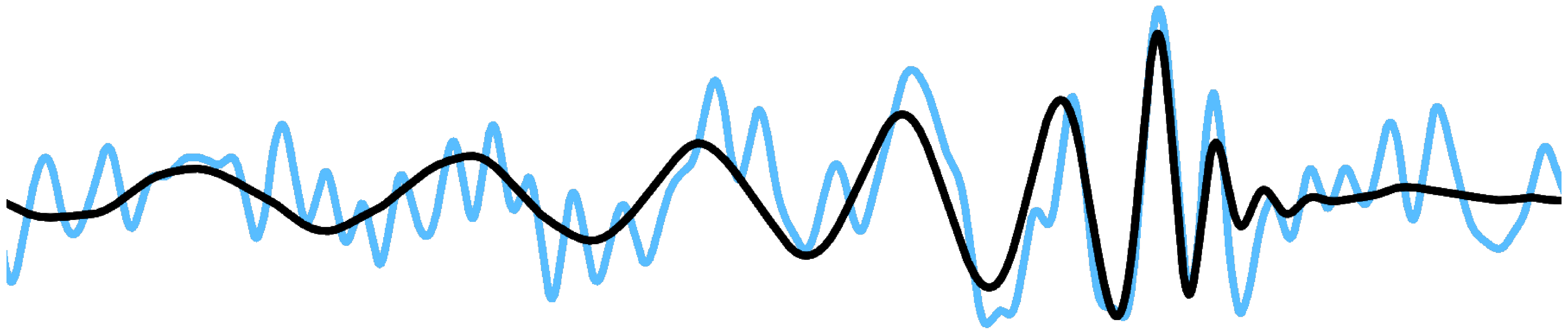

= model

Why compact binaries?

Why compact binaries?

Theoretical reasons

- Compact binary systems are extremely relativistic and exist in a physical regime we don’t have access to on Earth

Why compact binaries?

Theoretical reasons

- Compact binary systems are extremely relativistic and exist in a physical regime we don’t have access to on Earth

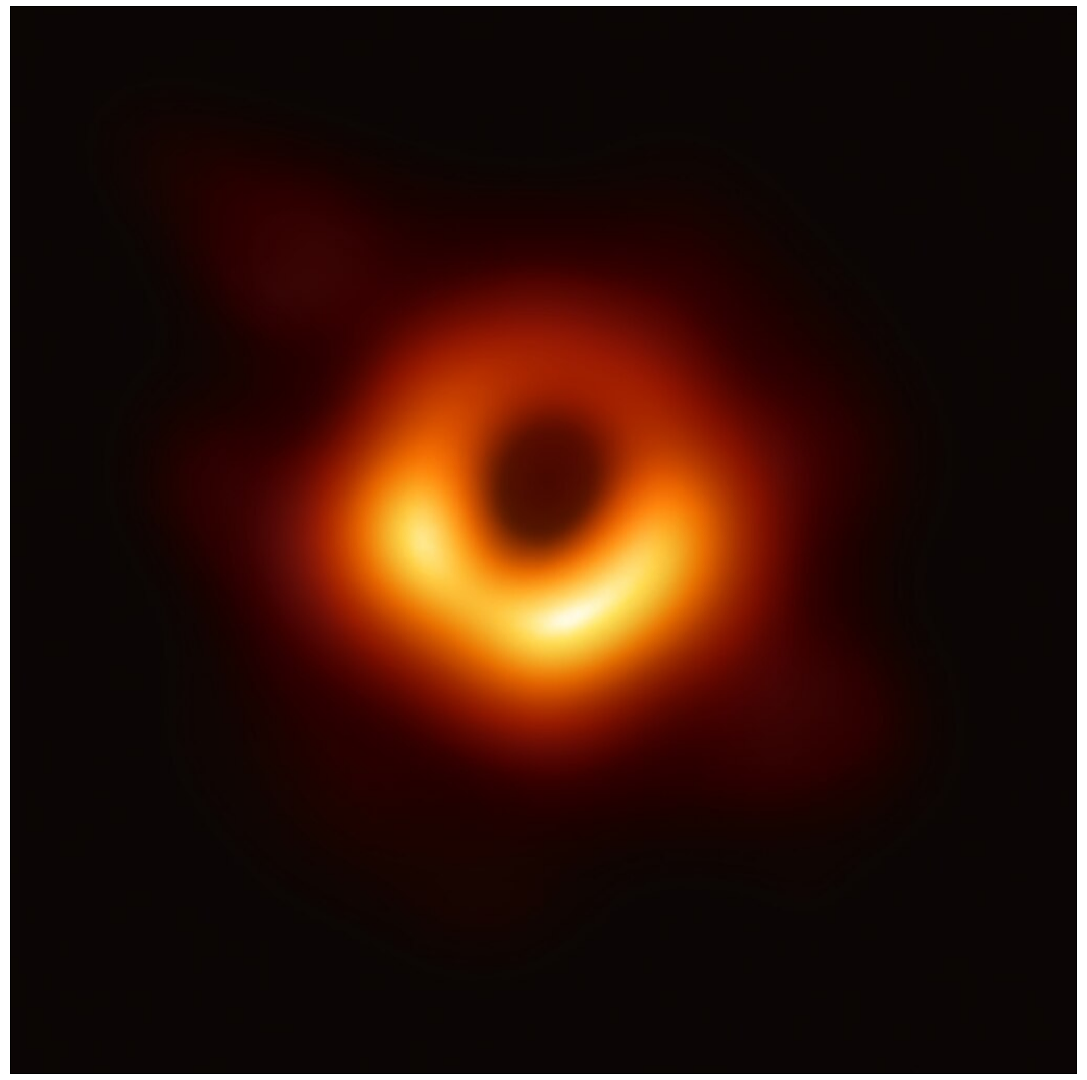

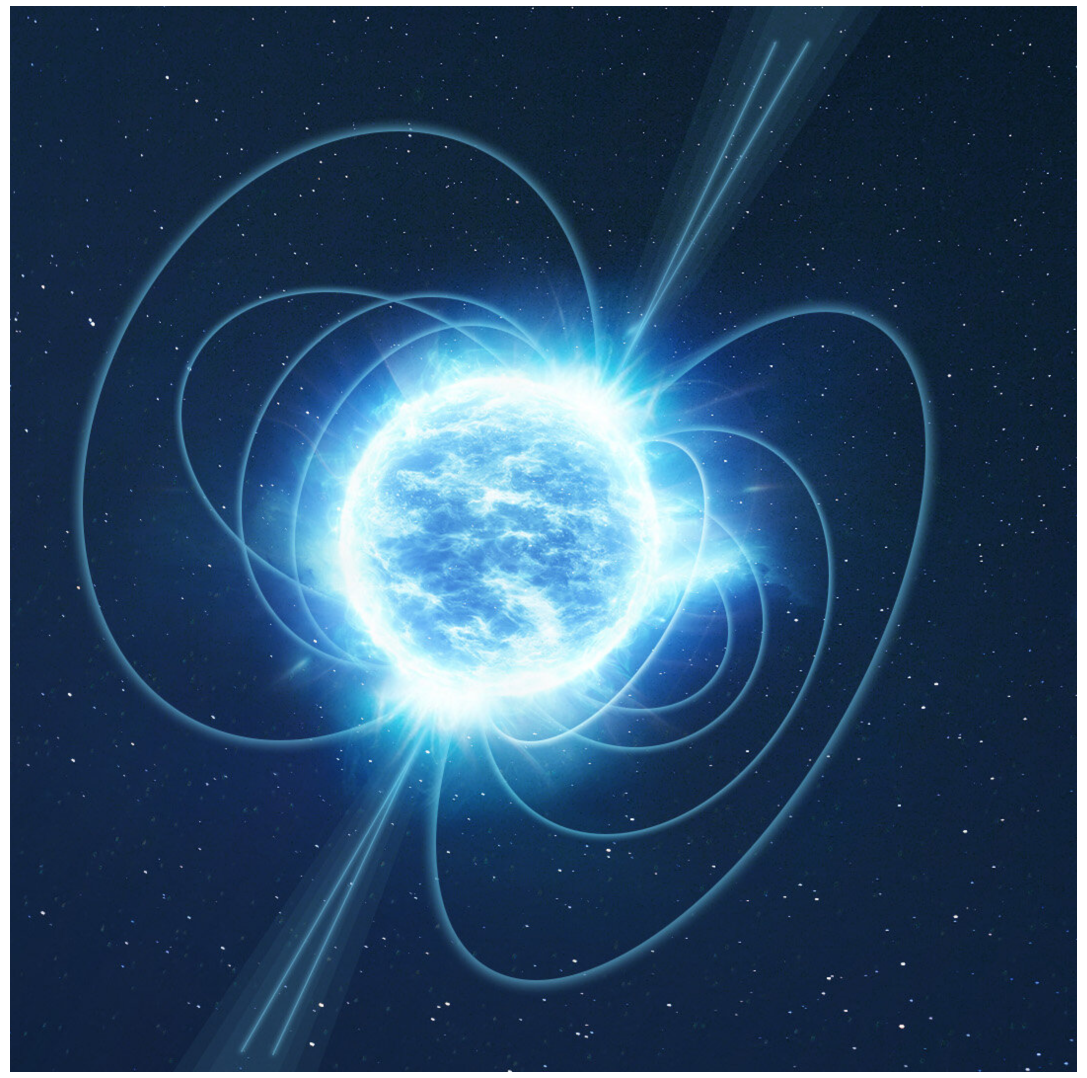

Why compact binaries?

Theoretical reasons

- Compact binary systems are extremely relativistic and exist in a physical regime we don’t have access to on Earth

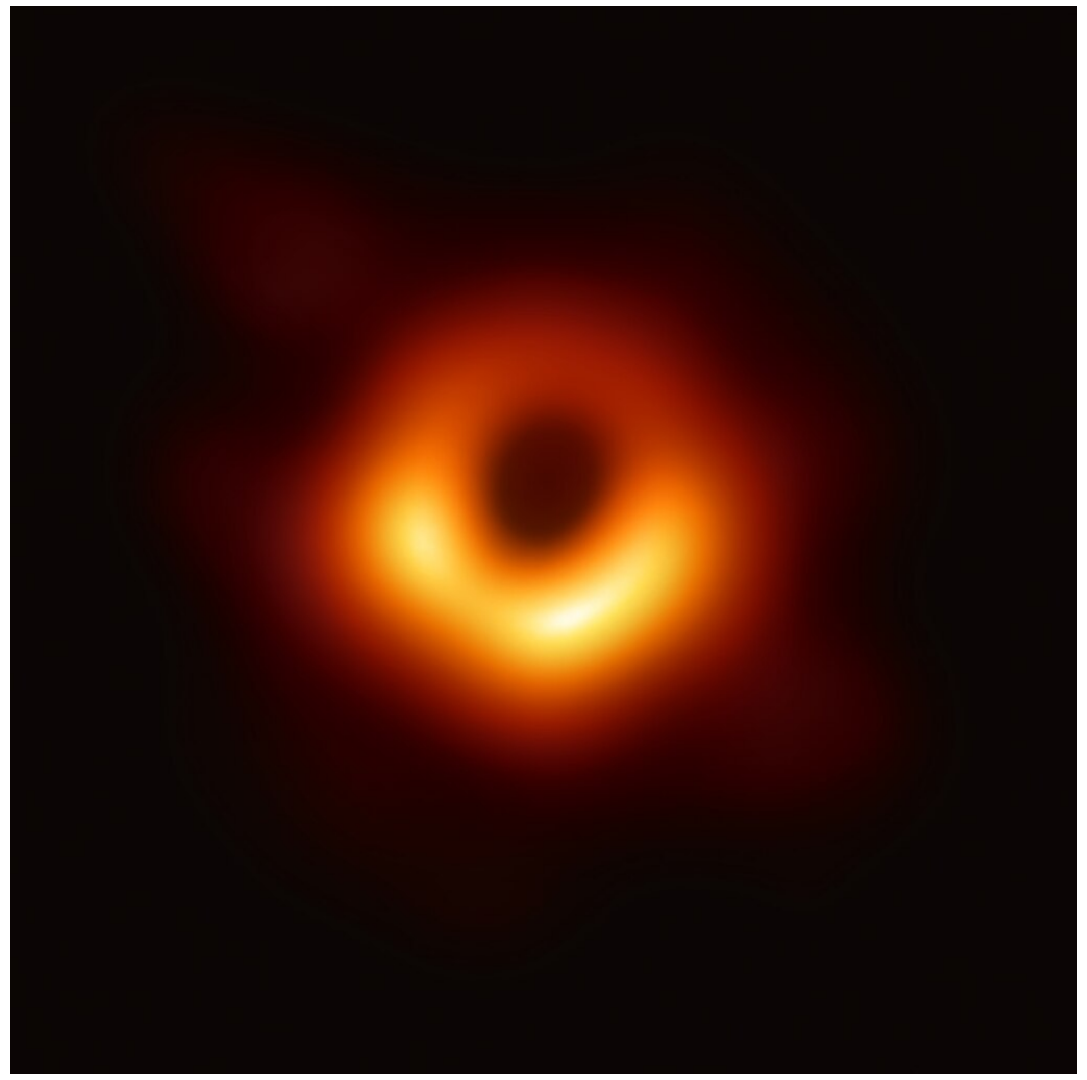

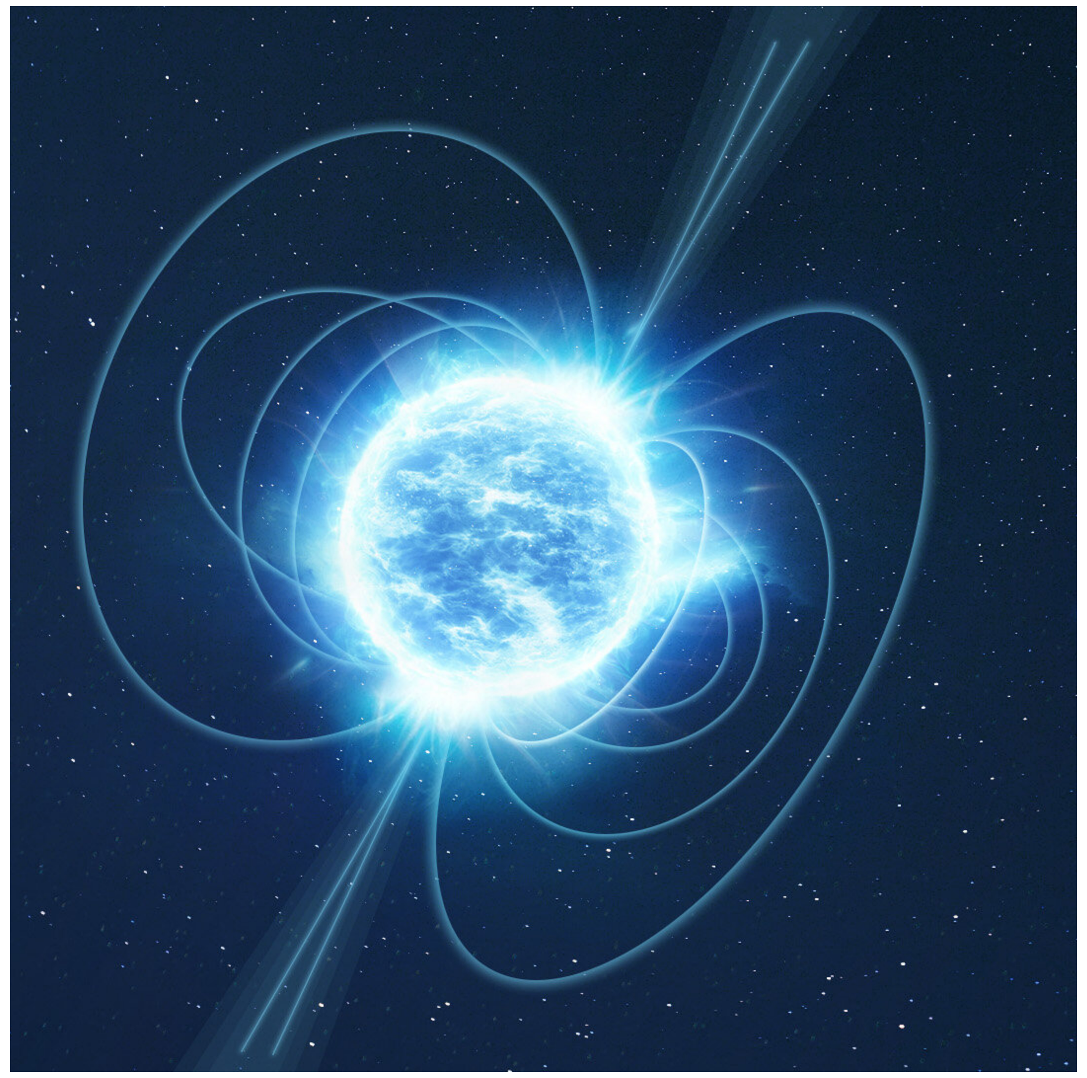

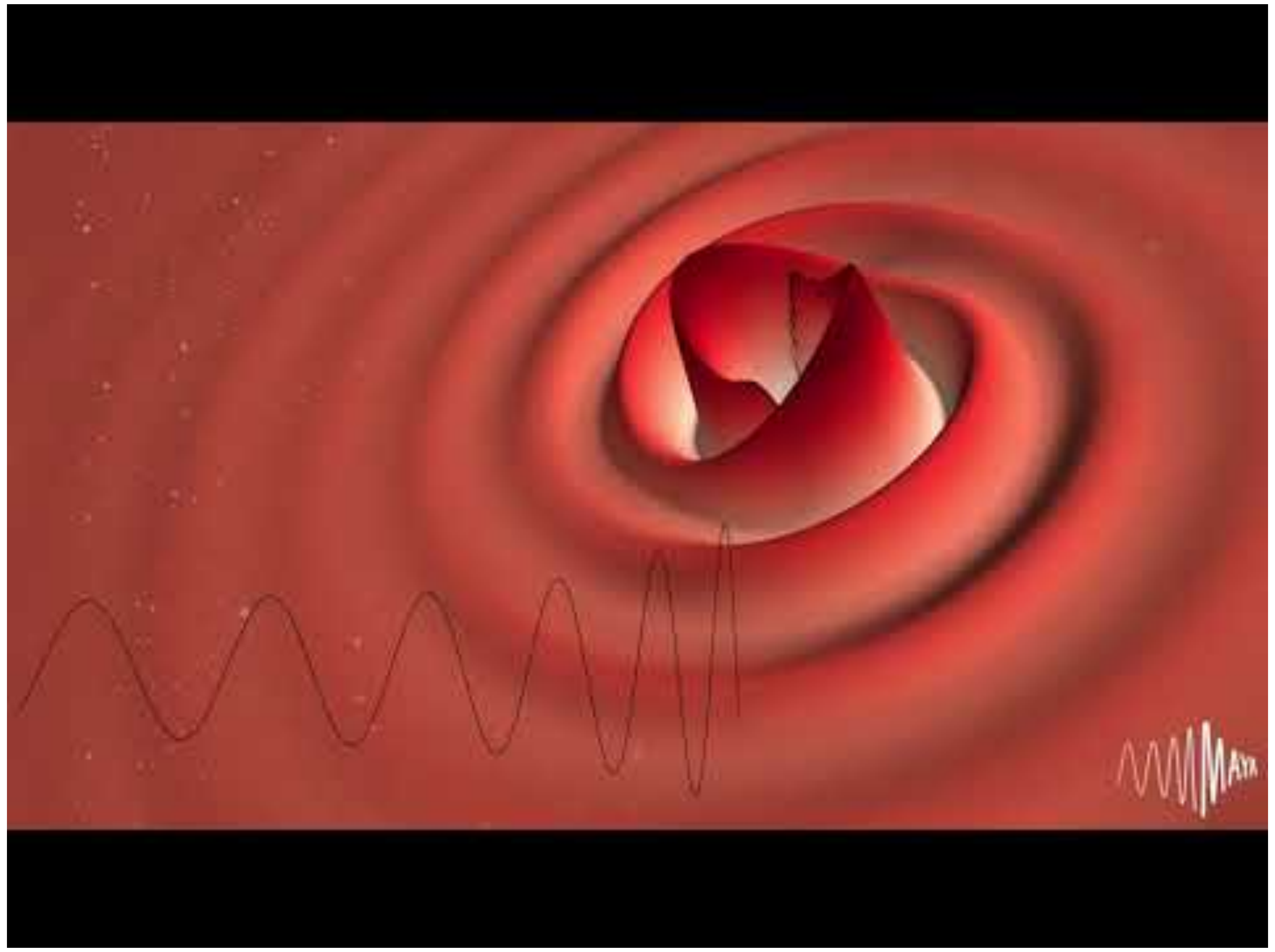

Anatomy of a binary signal

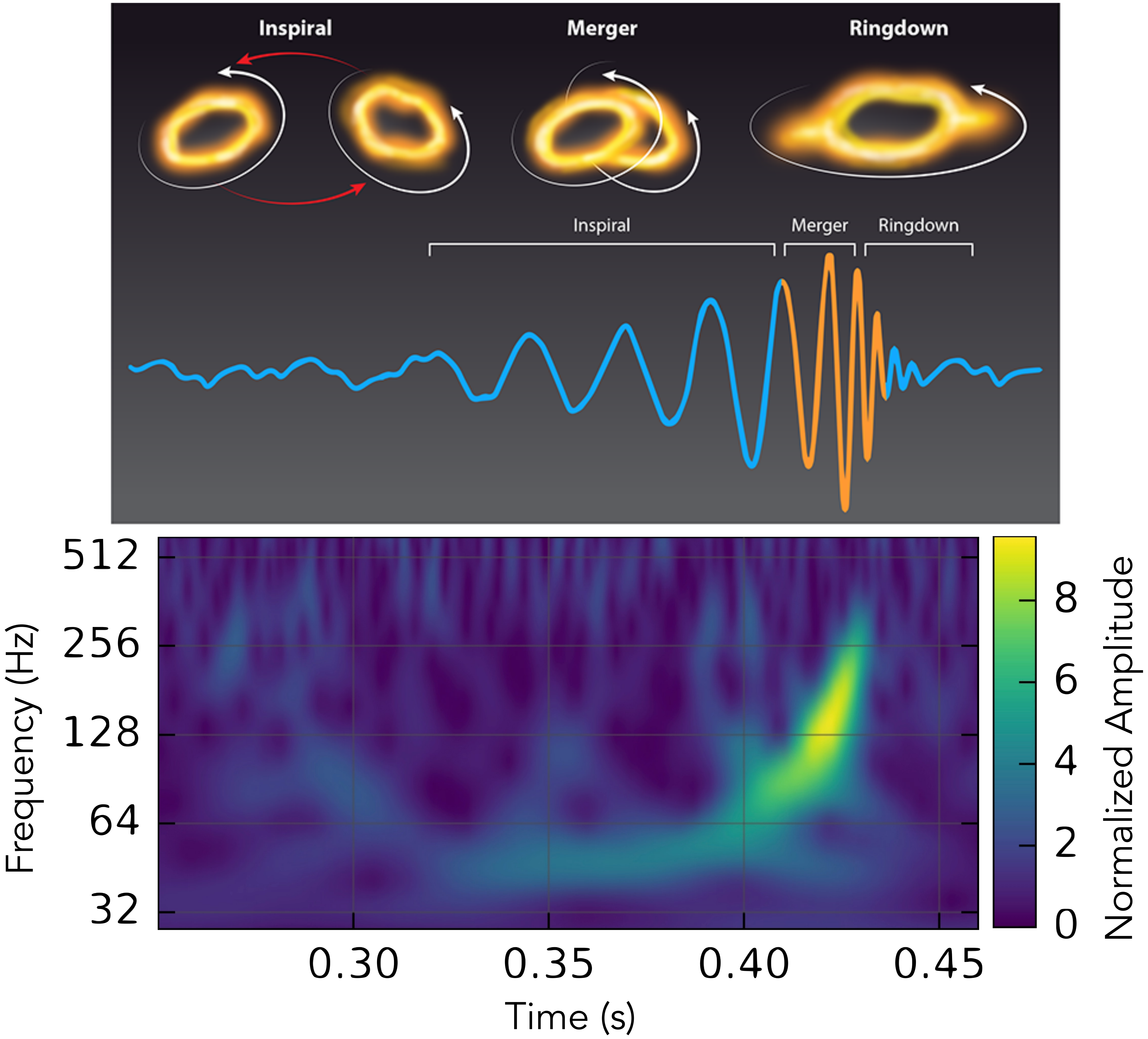

Anatomy of a binary signal

$h =$

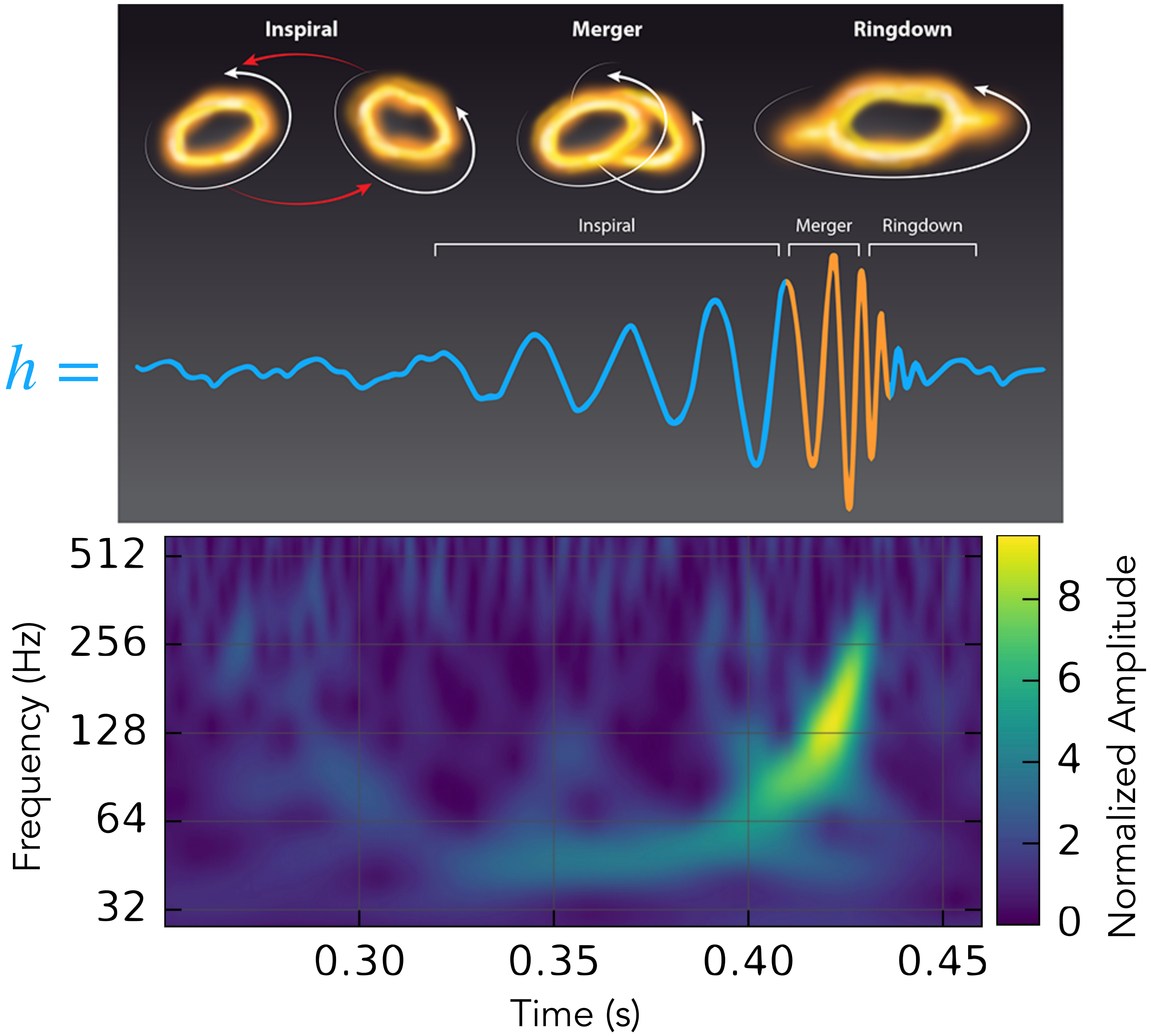

Anatomy of a binary signal

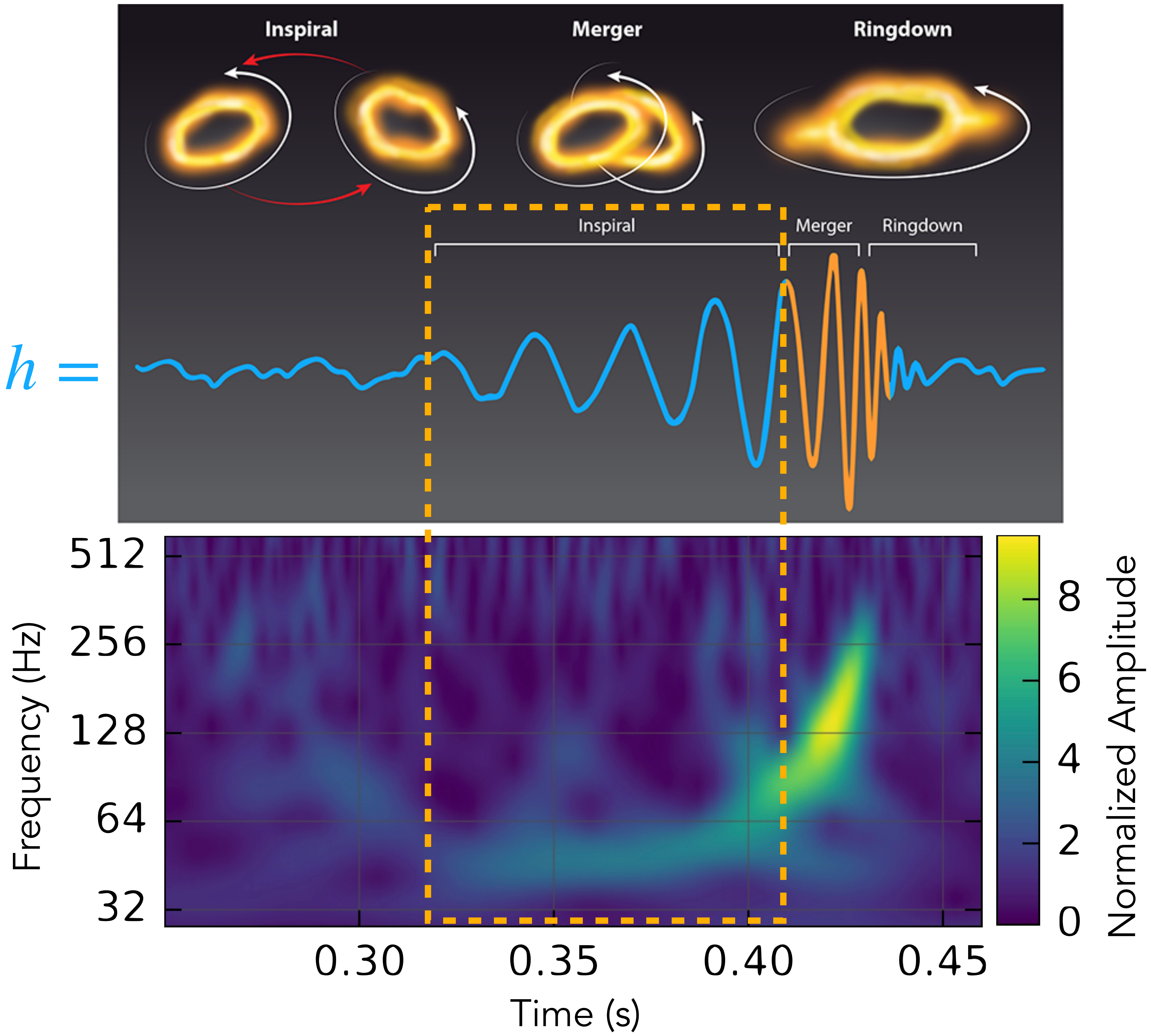

Anatomy of a binary signal

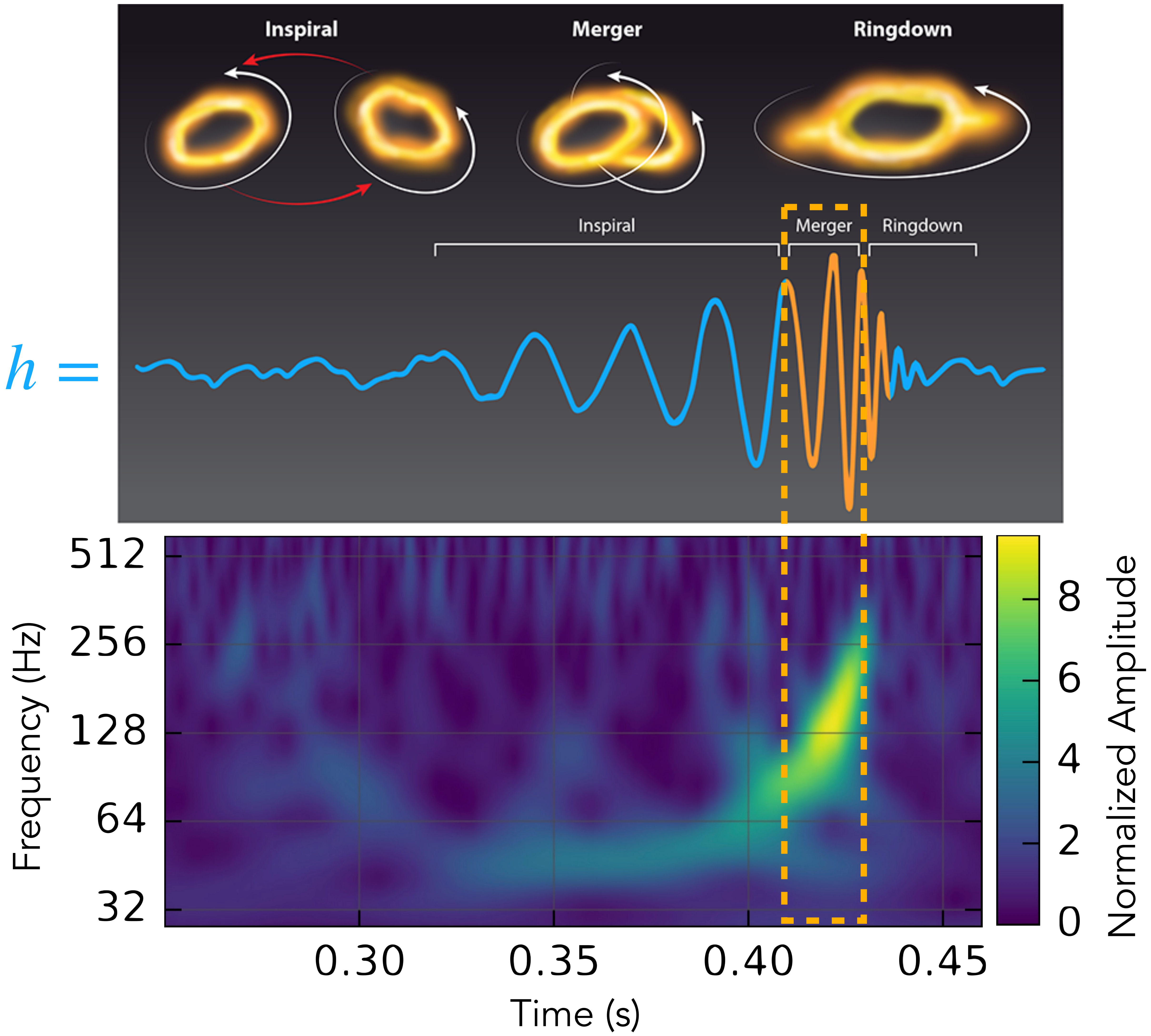

Anatomy of a binary signal

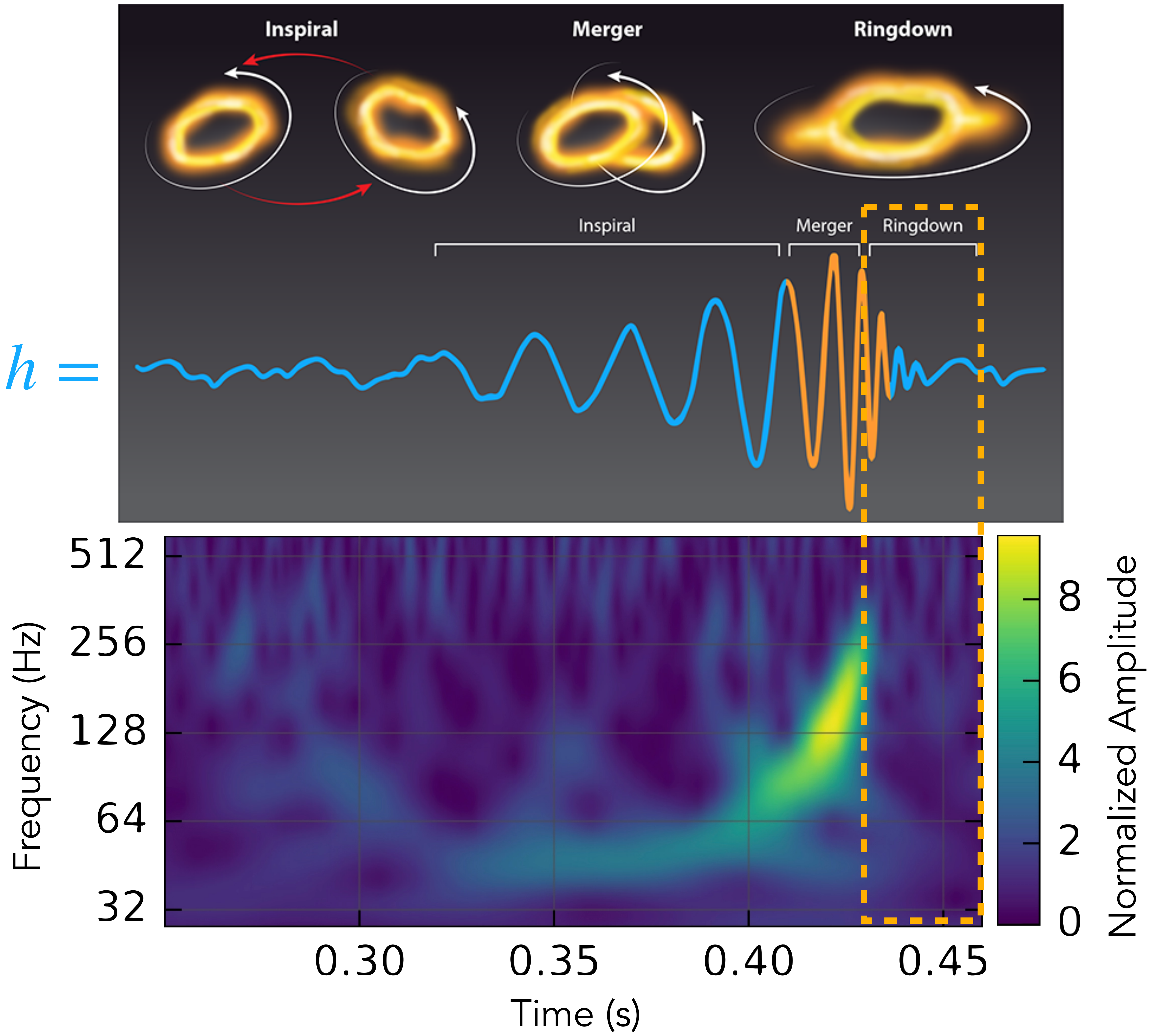

Anatomy of a binary signal

$h =$

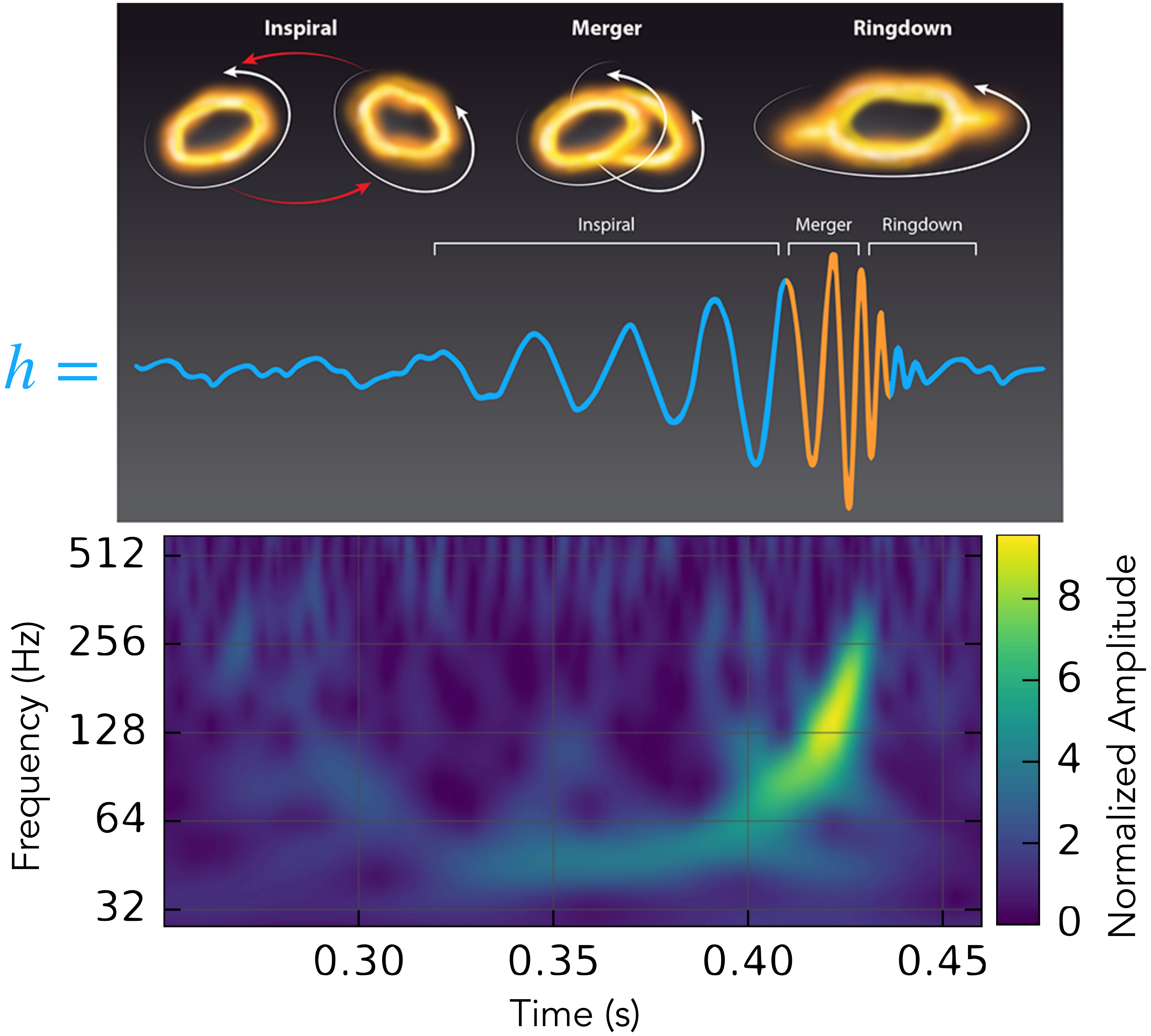

Anatomy of a binary signal

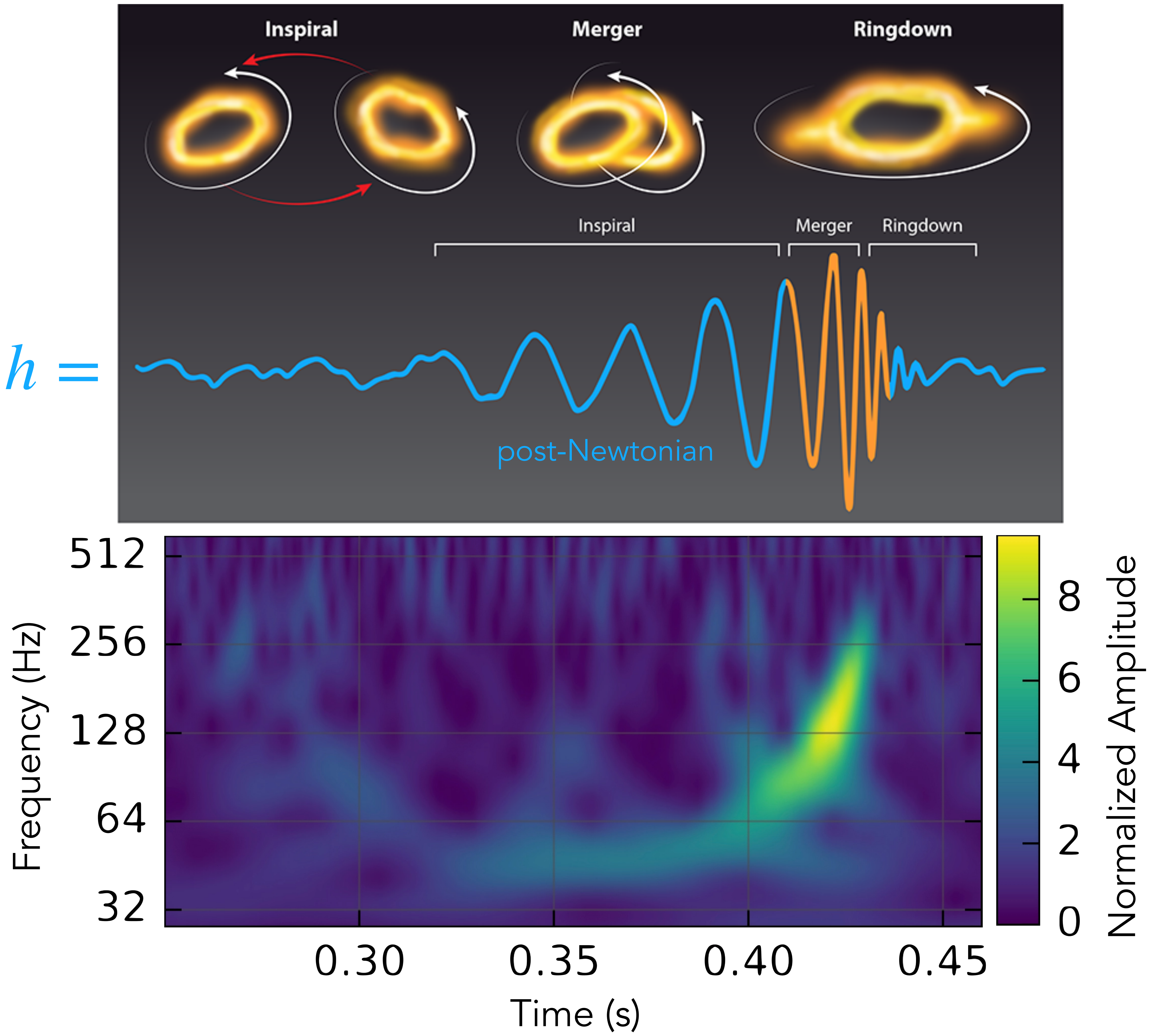

Anatomy of a binary signal

$h =$

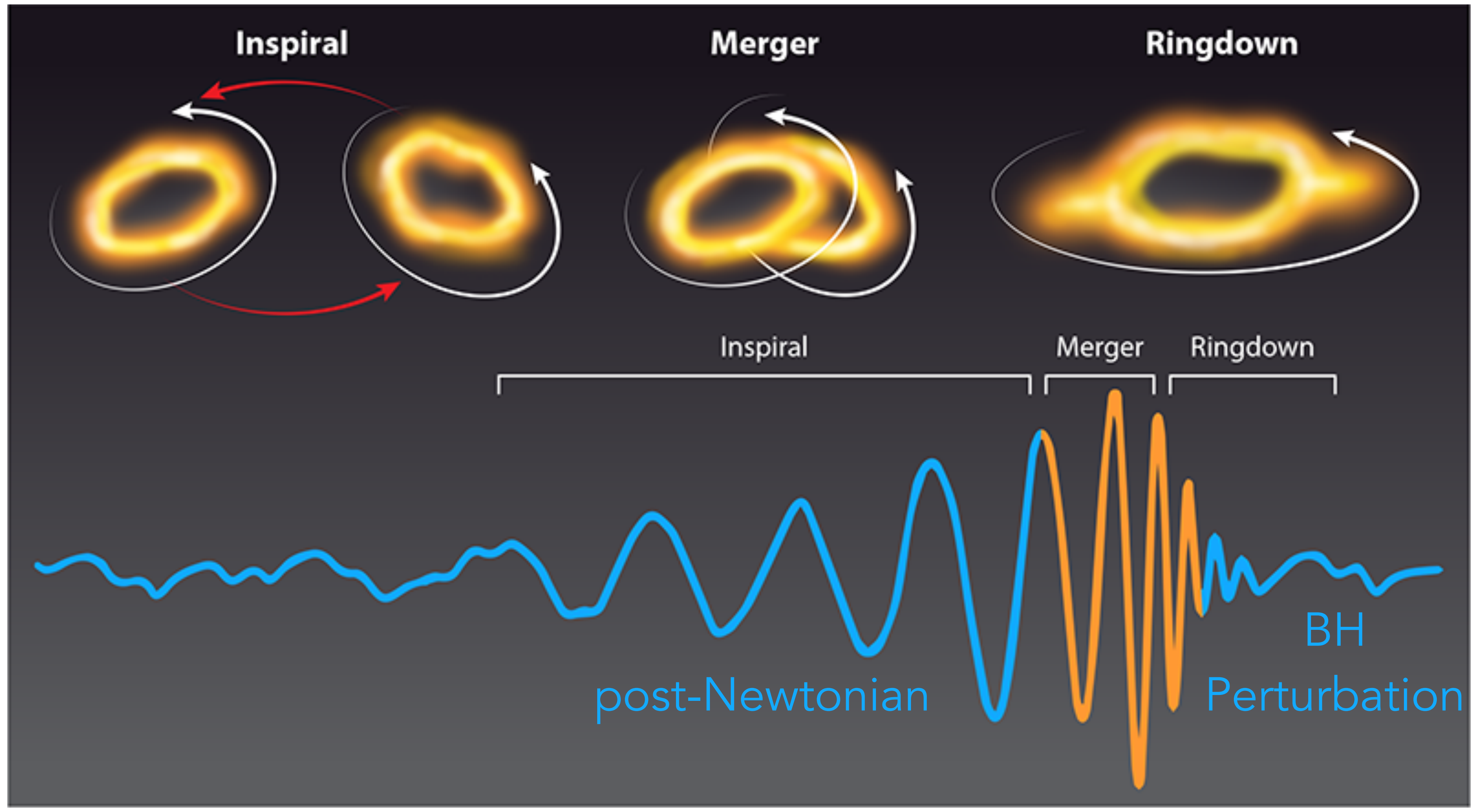

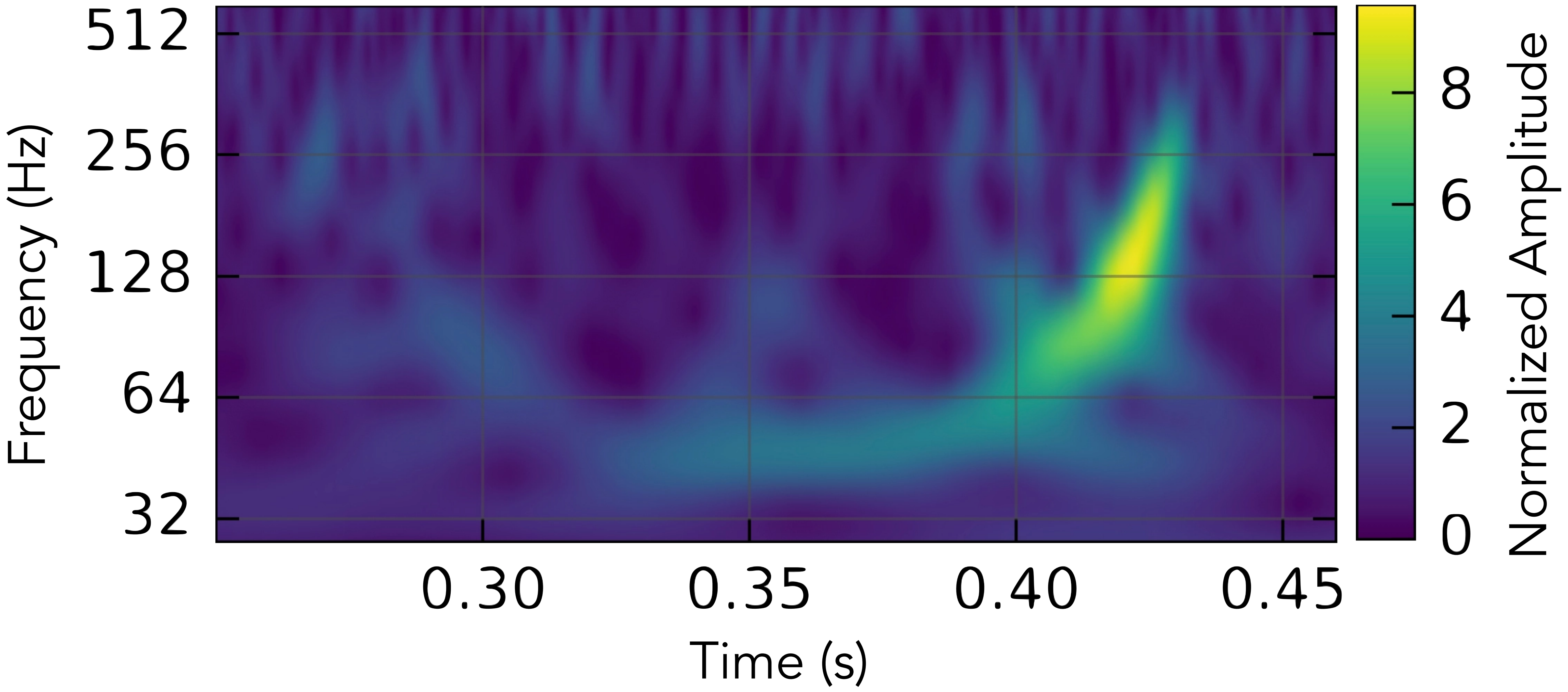

Anatomy of a binary signal

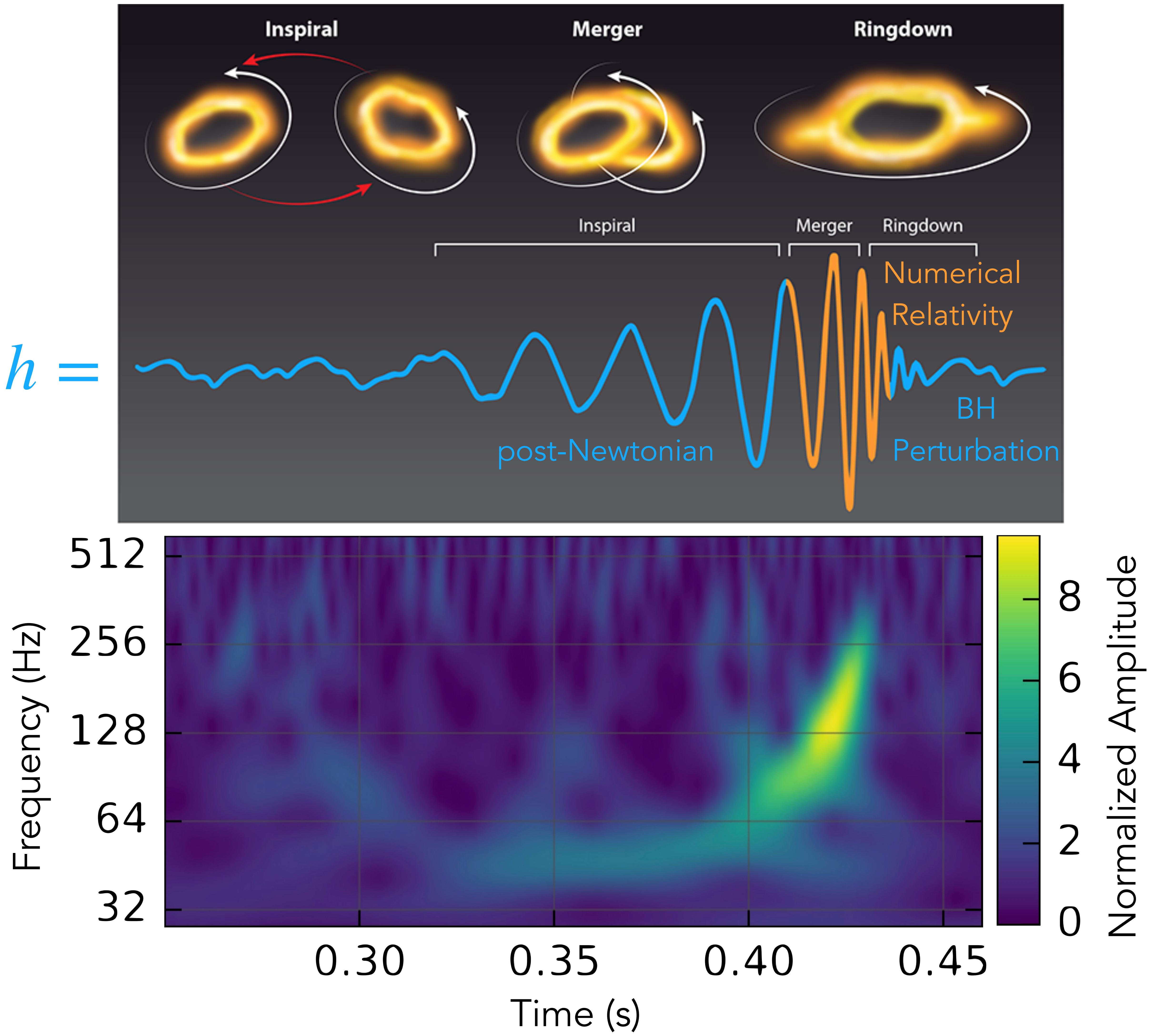

Anatomy of a binary signal

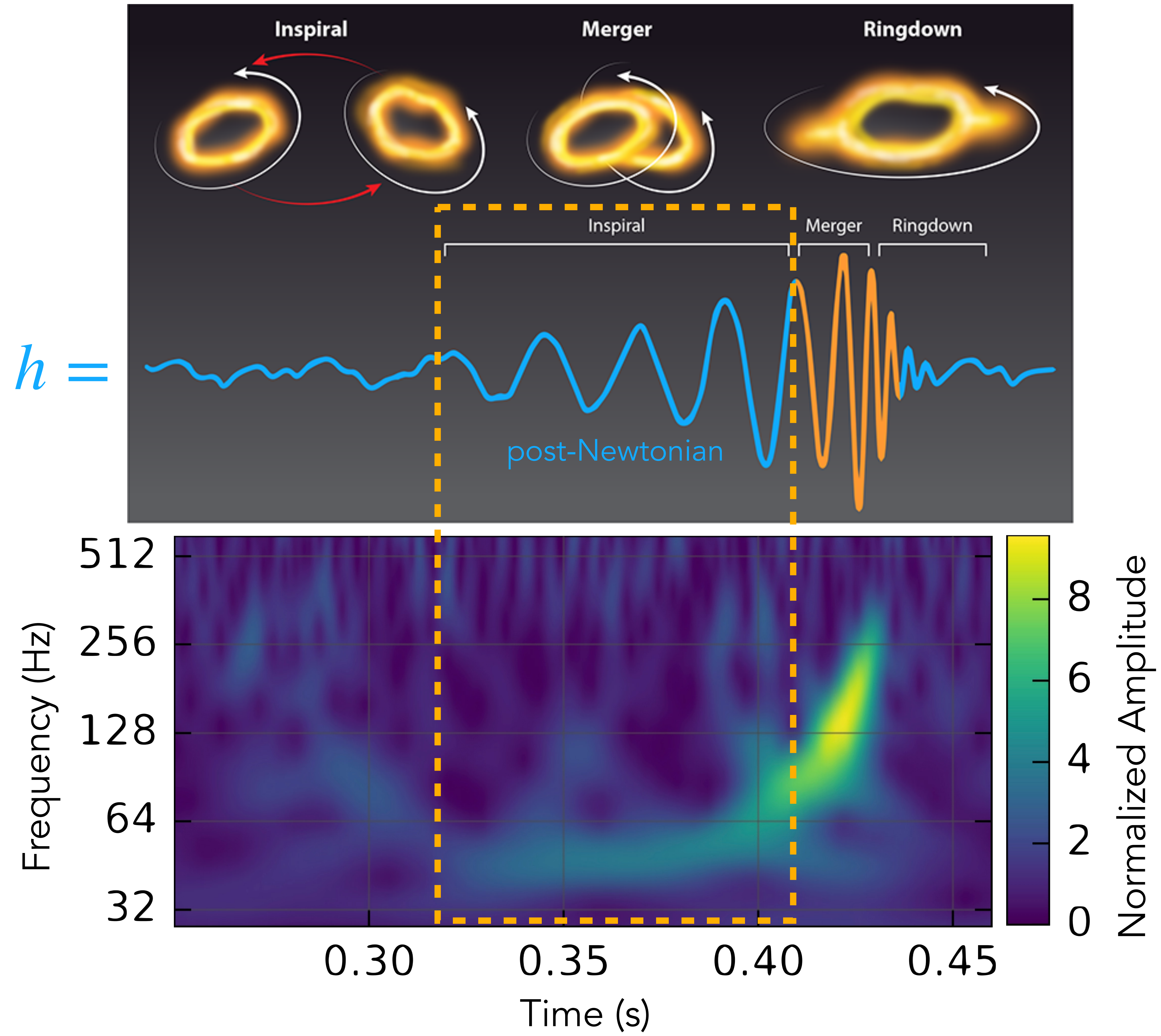

Post-Newtonian formalism

Post-Newtonian formalism

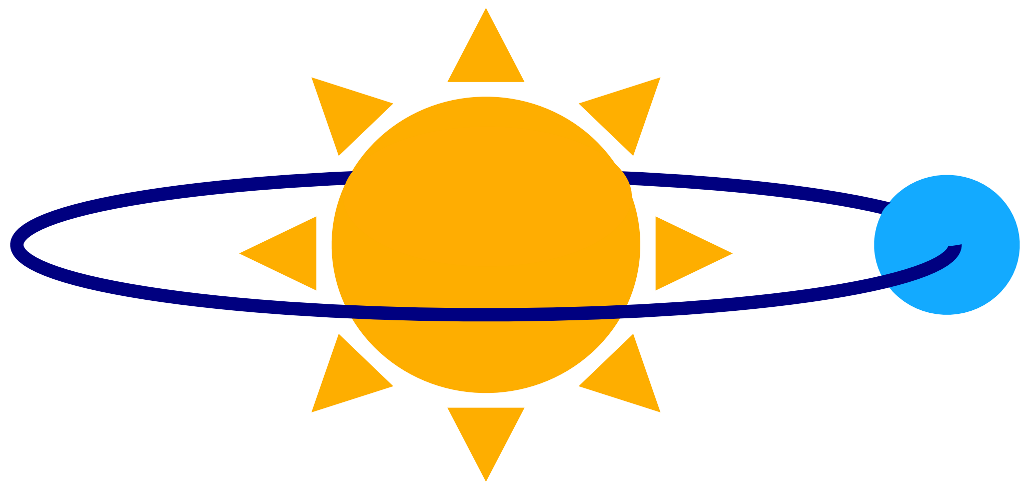

Weakest Systems

Post-Newtonian formalism

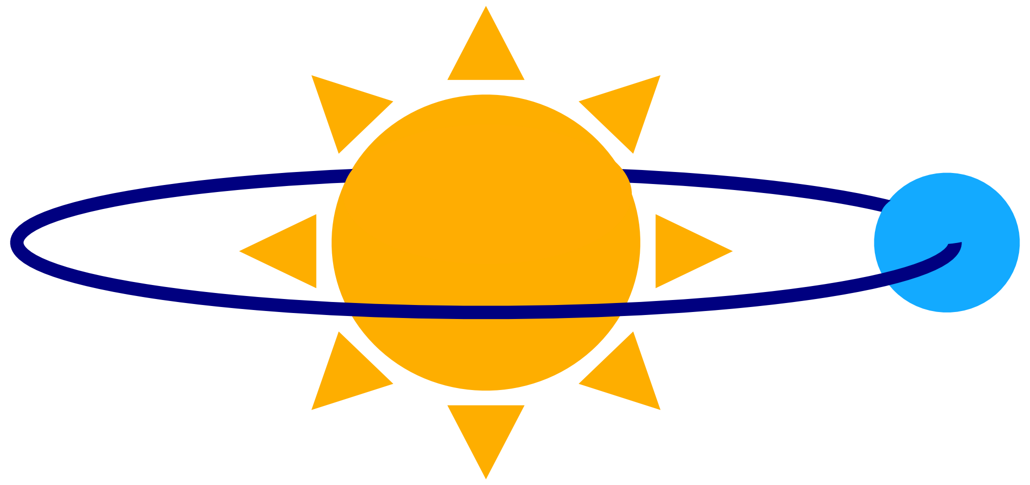

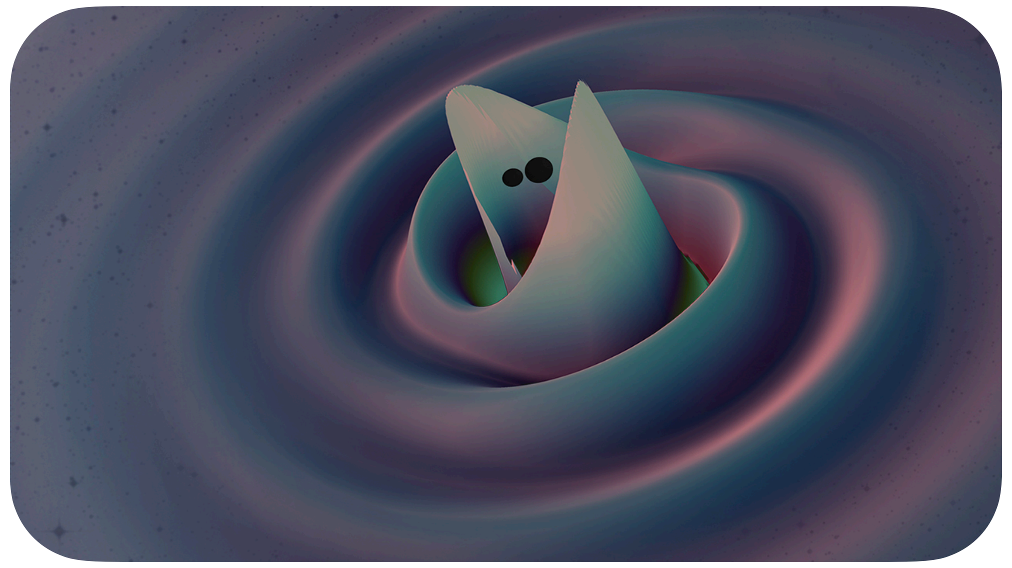

Weakest Systems

Strongest Systems

Post-Newtonian formalism

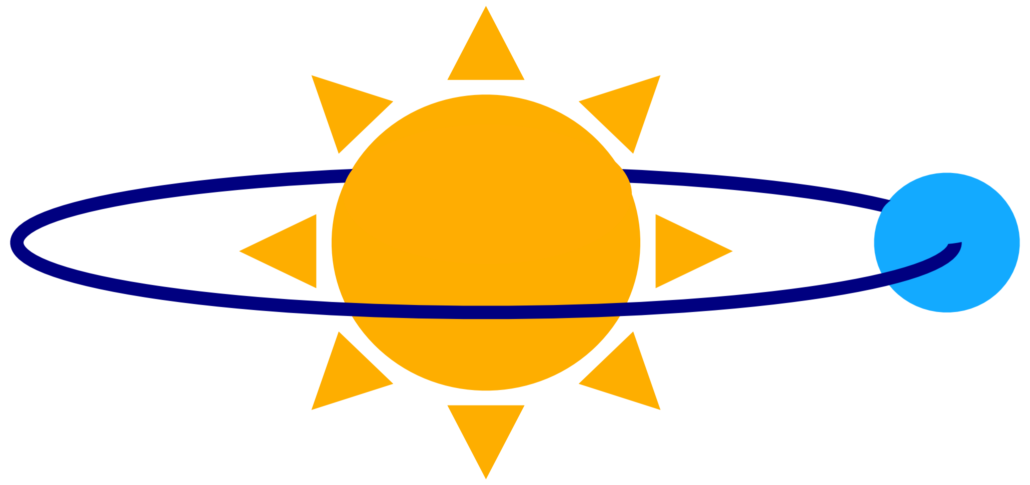

Weakest Systems

Post-Newtonian!

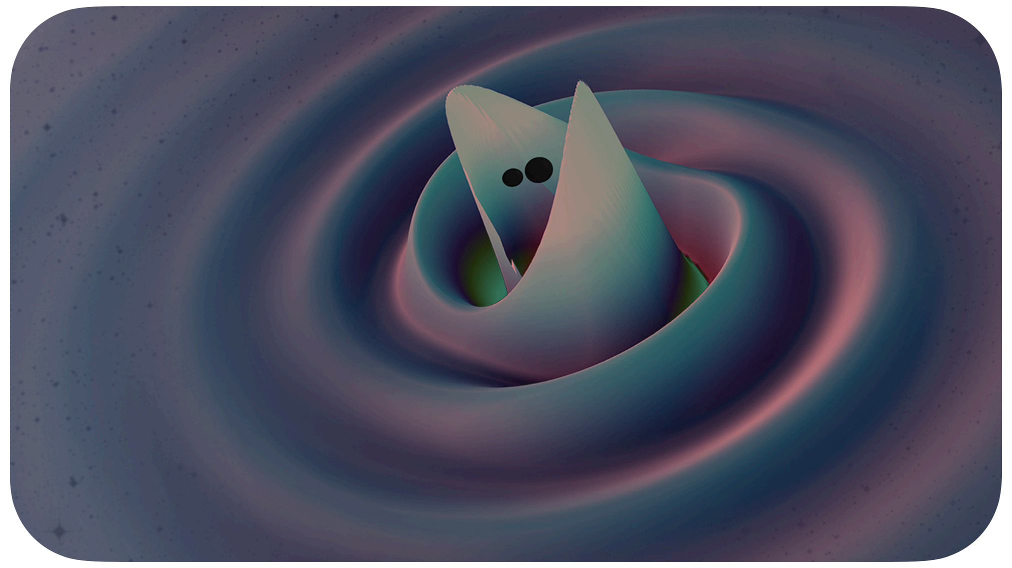

Strongest Systems

Post-Newtonian formalism

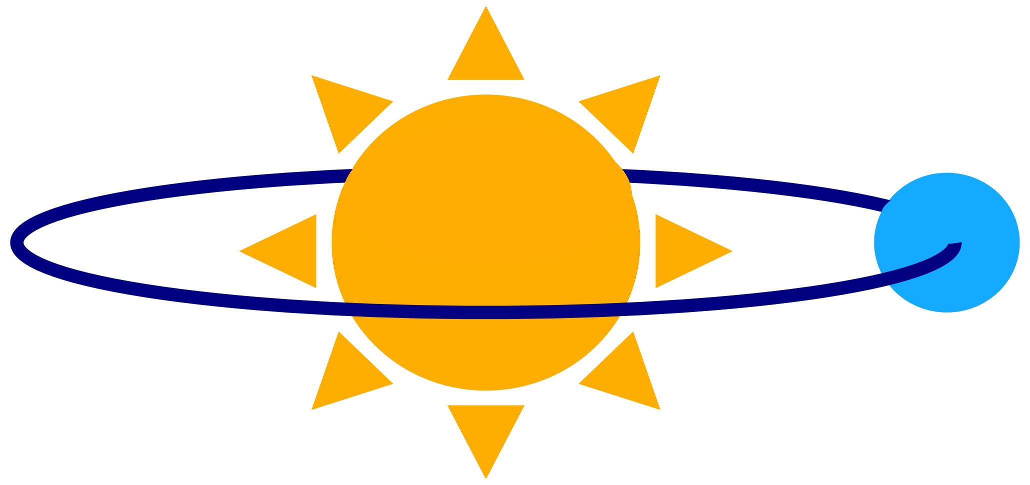

Post-Newtonian!

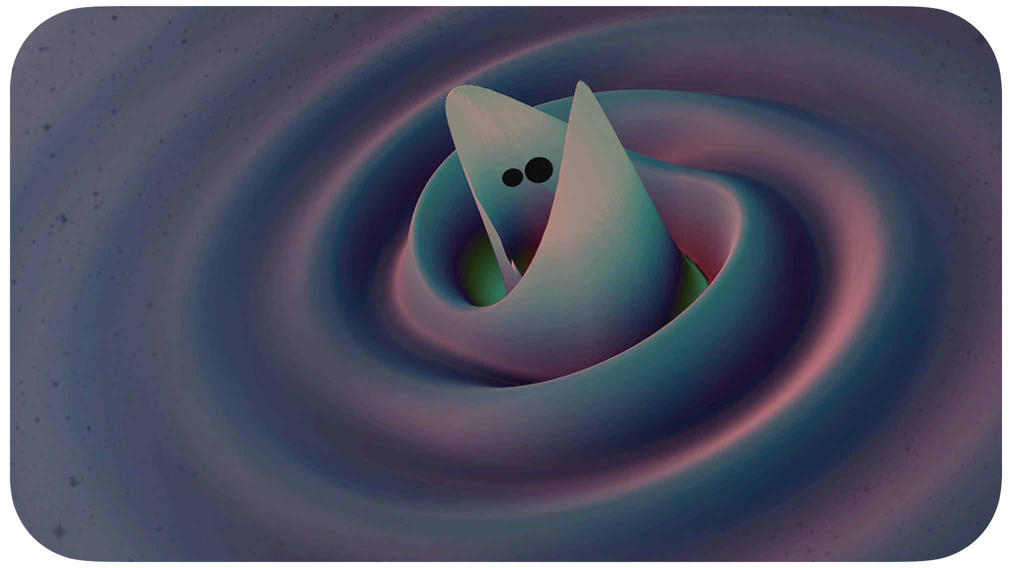

Weakest Systems ⟷ Strongest Systems

Assume:

Post-Newtonian formalism

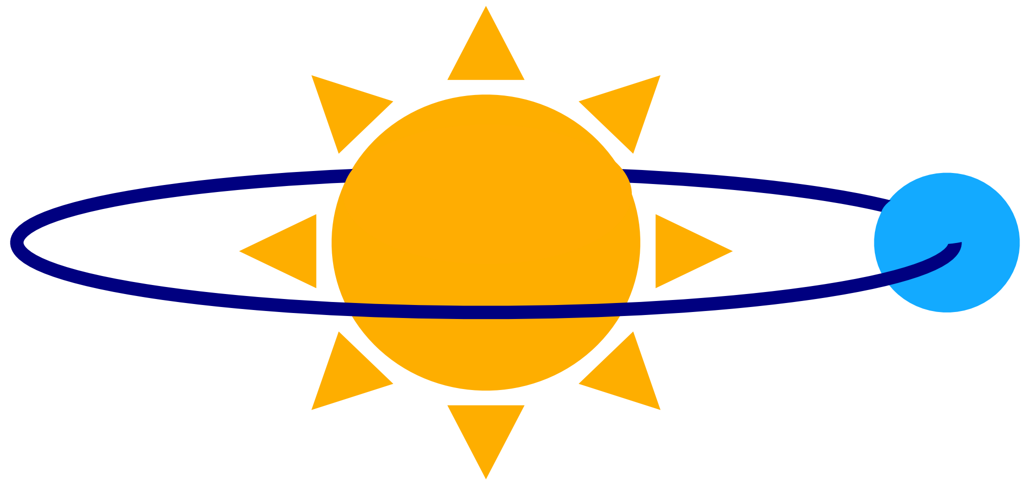

Post-Newtonian!

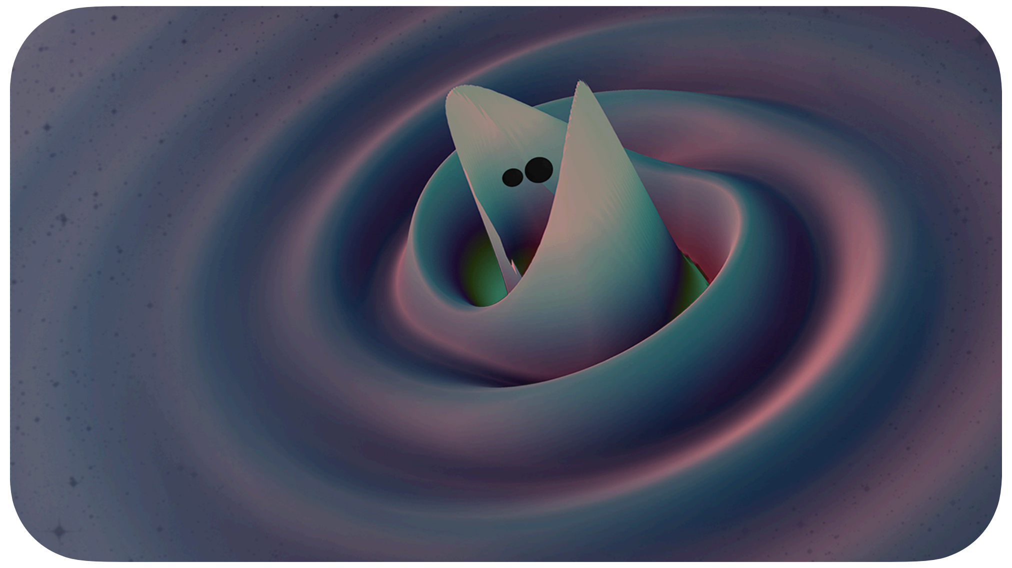

Weakest Systems ⟷ Strongest Systems

Assume: $(v/c)^2 \ll 1$

Post-Newtonian formalism

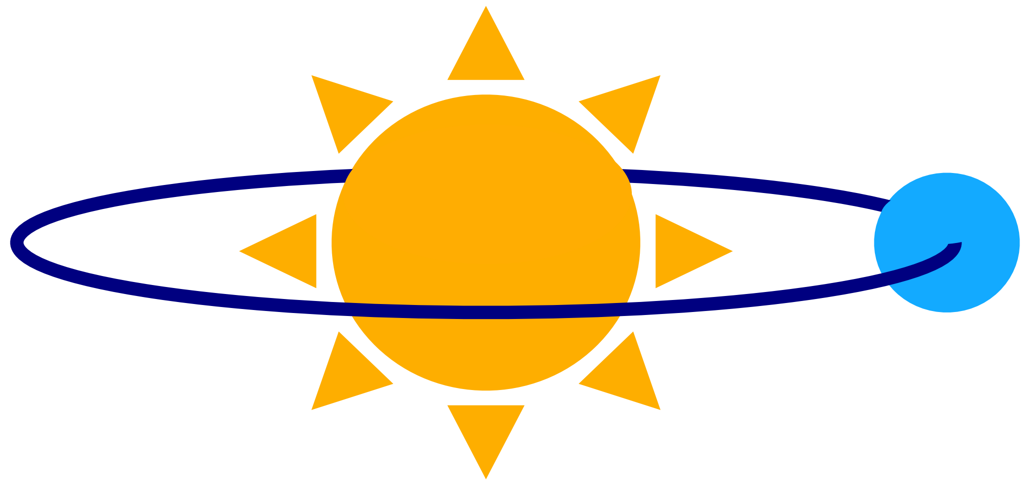

Post-
Newtonian!

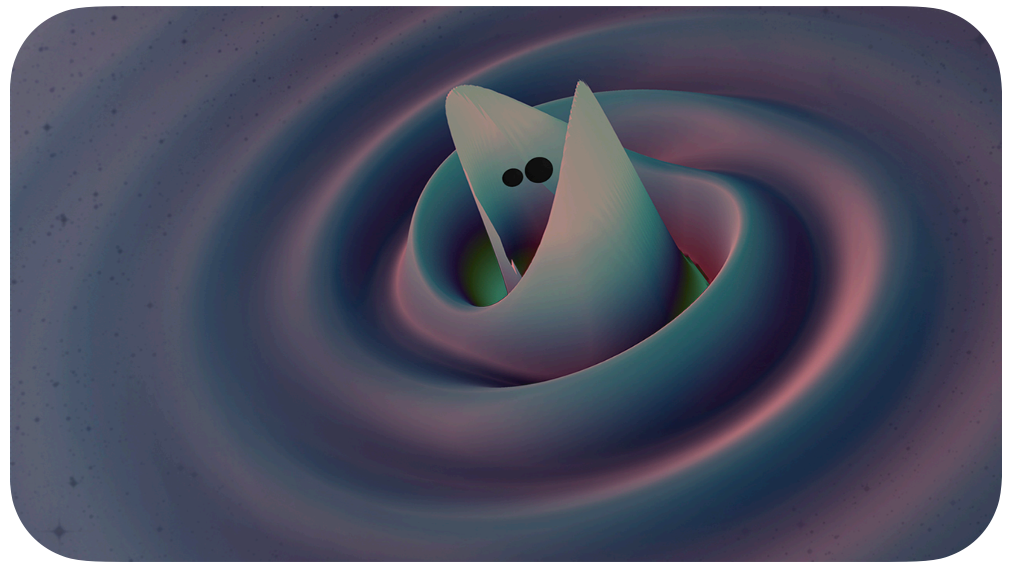

Weakest Systems ⟵ ⟶ Strongest Systems

Assume: $(v/c)^2 \ll 1$ and $Gm/rc^2 \ll 1$

Post-Newtonian formalism

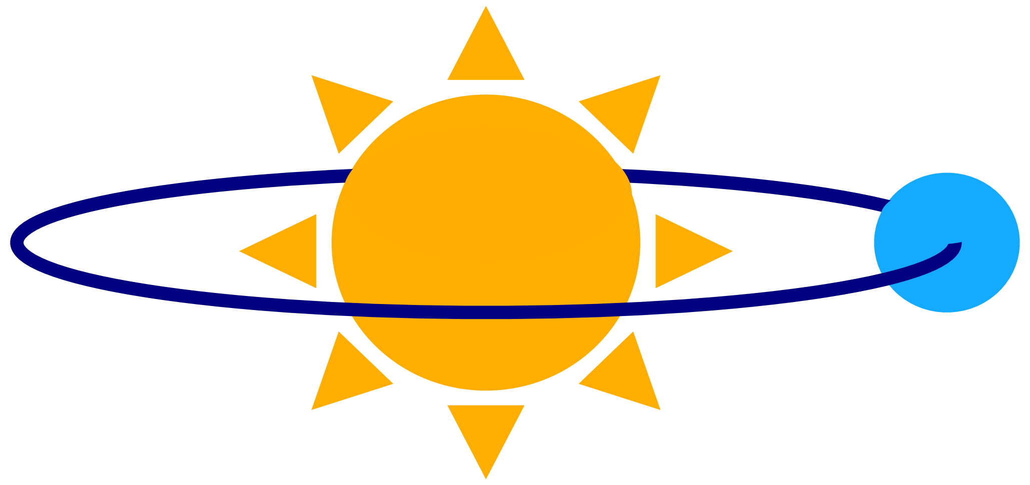

Weakest Systems

Post-Newtonian!

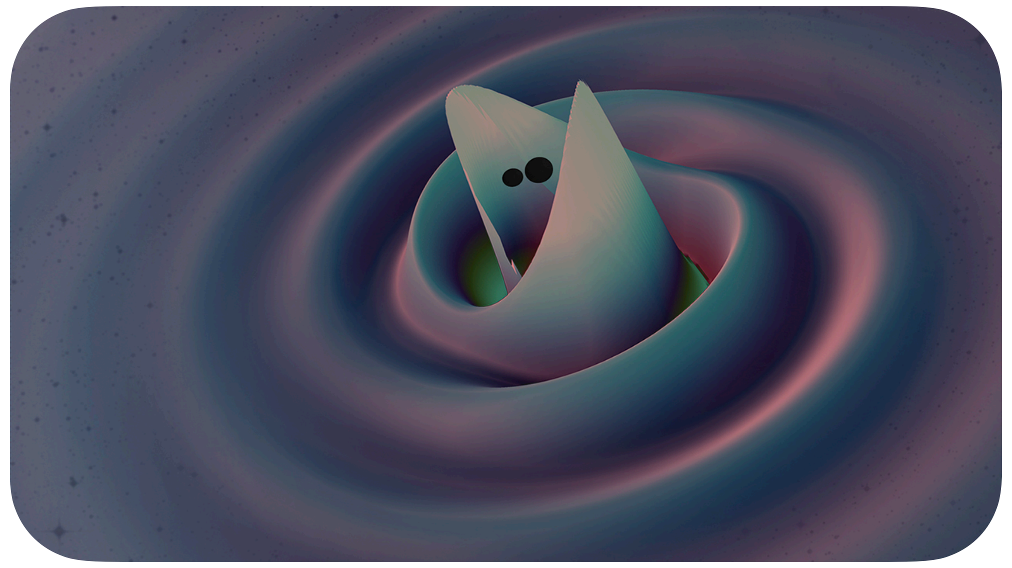

Strongest Systems

Assume: $(v/c)^2 \ll 1$ and $Gm/rc^2 \ll 1$

Circular orbits: $(v/r)^2 = \omega^2$

Post-Newtonian formalism

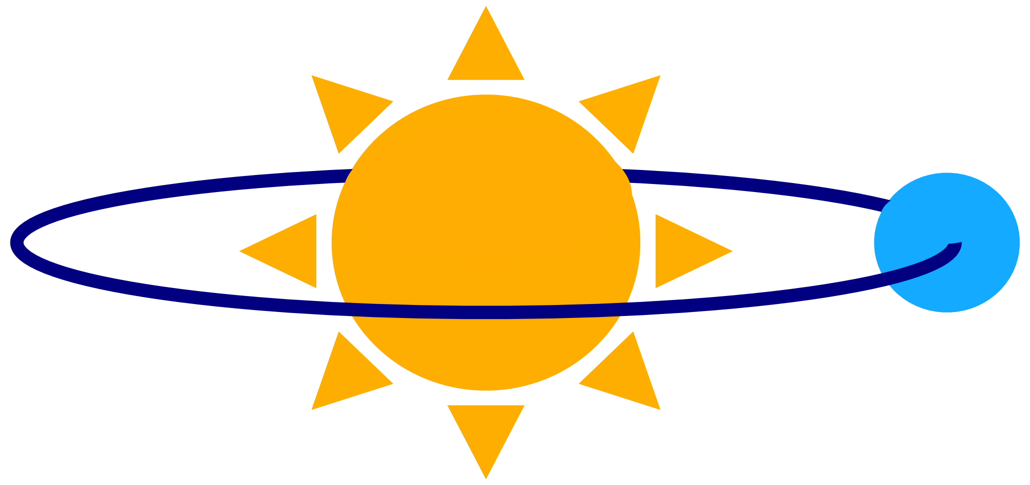

Post-Newtonian!

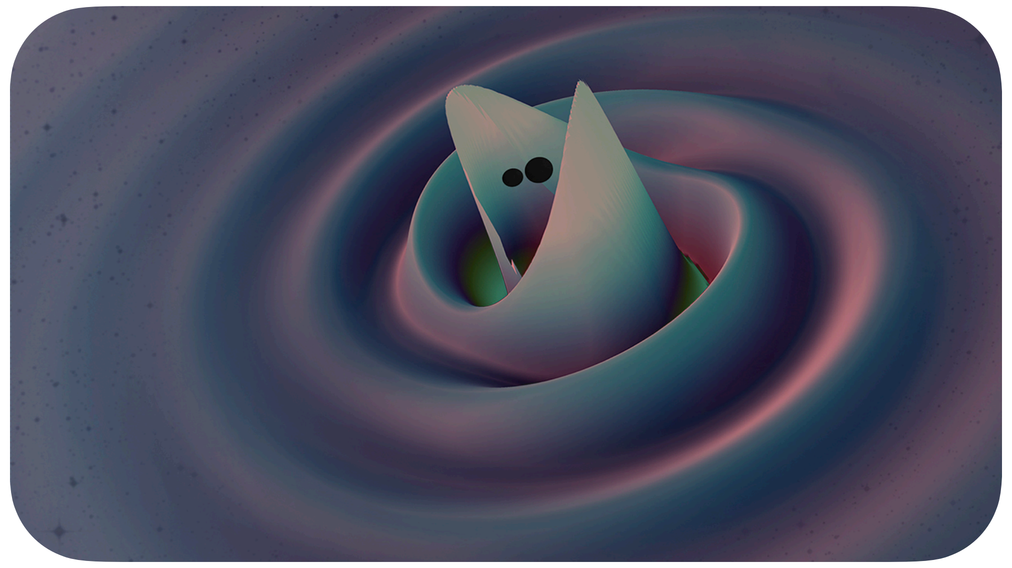

Weakest Systems

Strongest Systems

Assume: $(v/c)^2 \ll 1$ and $Gm/rc^2 \ll 1$

Circular orbits: $(v/r)^2 = \omega^2 = (Gm/r^3) + \mathcal{O}(c^{-2})$

Post-Newtonian formalism

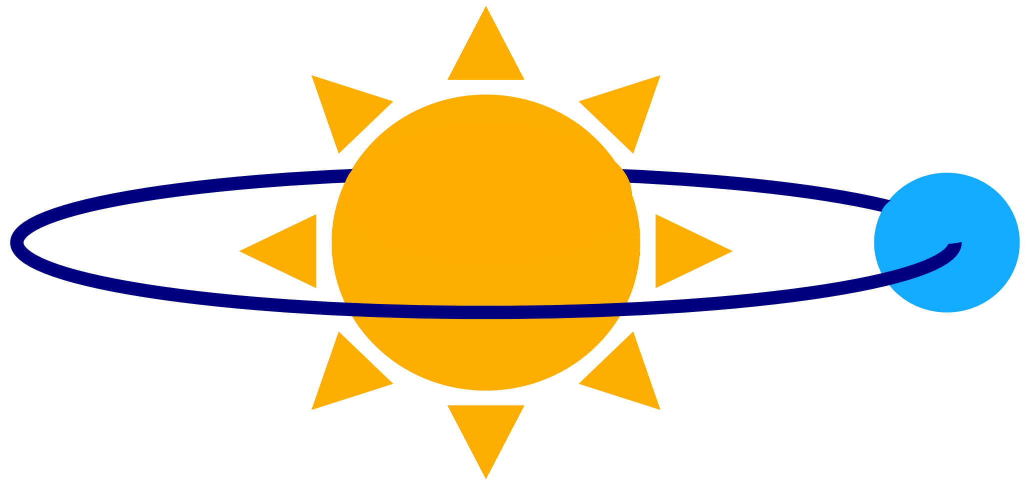

Post-Newtonian!

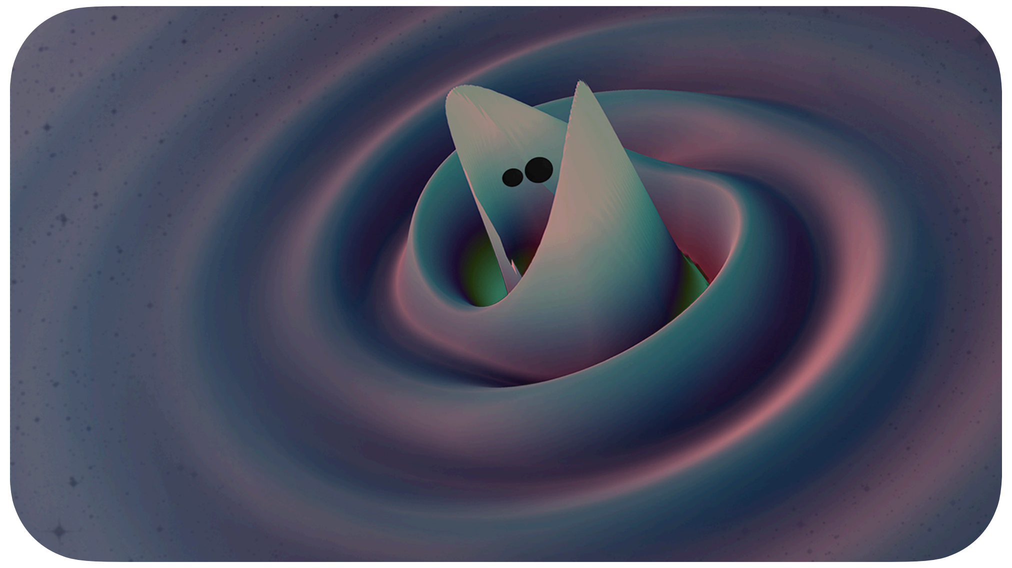

Weakest Systems ⟷ Strongest Systems

Assume: $(v/c)^2 \ll 1$ and $Gm/rc^2 \ll 1$

Circular orbits: $(v/r)^2 = \omega^2 = (Gm/r^3) + \mathcal{O}(c^{-2}) \longrightarrow x = (Gm\omega)^{2/3}/c^2$

Post-Newtonian formalism

Assume: $(v/c)^2 \ll 1$ and $Gm/rc^2 \ll 1$

Circular orbits: $(v/r)^2 = \omega^2 = (Gm/r^3) + \mathcal{O}(c^{-2}) \longrightarrow x = (Gm\omega)^{2/3}/c^2$

A nPN quantity looks something like

$$x^m \left(1 + c_1 x + \ldots + c_n x^n\right)$$

Post-Newtonian formalism

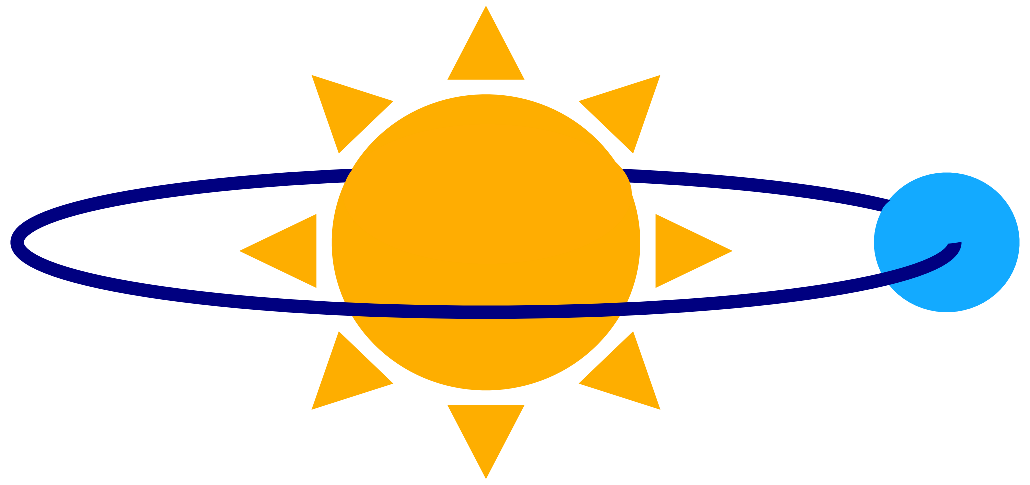

Weakest Systems

Post-Newtonian!

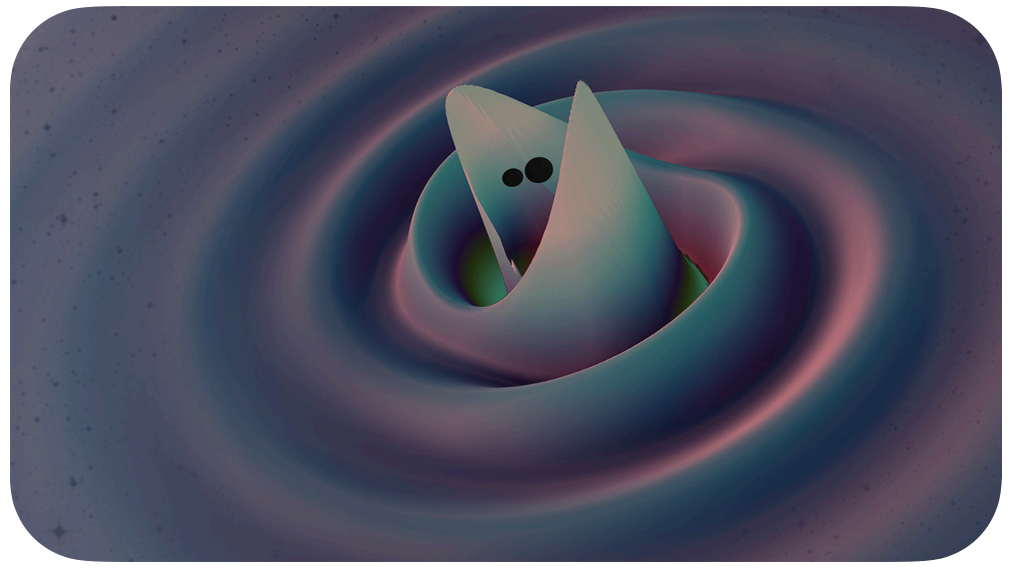

Strongest Systems

Assume: $(v/c)^2 \ll 1$ and $Gm/rc^2 \ll 1$

Circular orbits: $(v/r)^2 = \omega^2 = (Gm/r^3) + \mathcal{O}(c^{-2}) \longrightarrow x = (Gm\omega)^{2/3}/c^2$

A nPN quantity looks something like

$$x^m \left(1 + c_1 x + \ldots + c_n x^n\right)$$

Newtonian

Post-Newtonian formalism

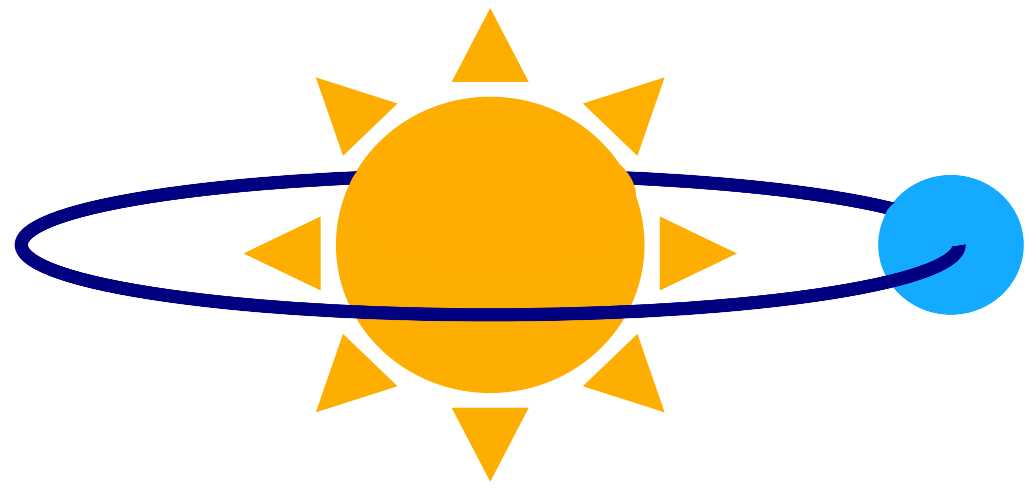

Post-Newtonian!

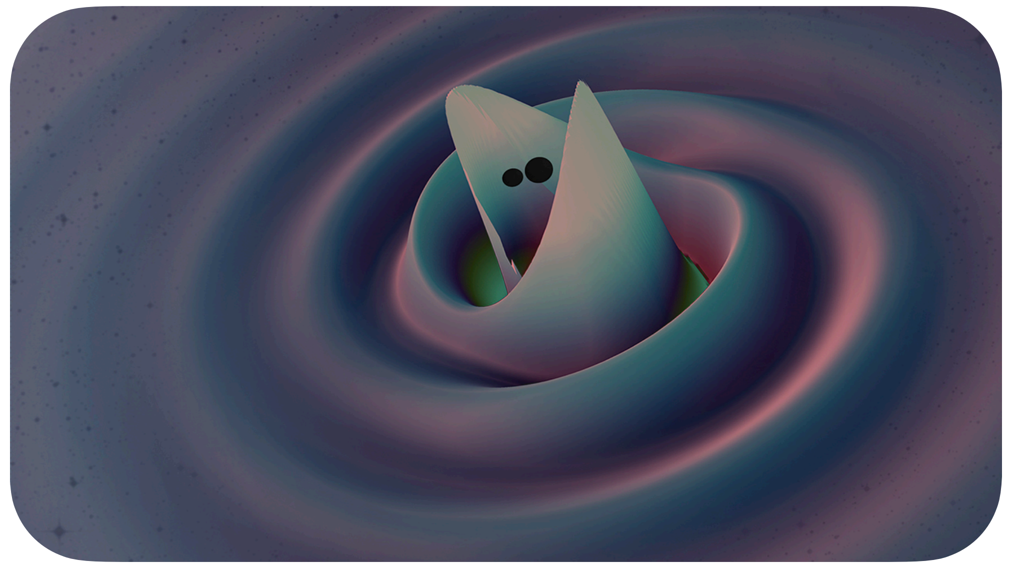

Weakest Systems

Strongest Systems

Assume: $(v/c)^2 \ll 1$ and $Gm/rc^2 \ll 1$

Circular orbits: $(v/r)^2 = \omega^2 = (Gm/r^3) + \mathcal{O}(c^{-2}) \longrightarrow x = (Gm\omega)^{2/3}/c^2$

A nPN quantity looks something like

$$x^m \left(1 + c_1 x + \ldots + c_n x^n\right)$$

1PN

Newtonian

Post-Newtonian formalism

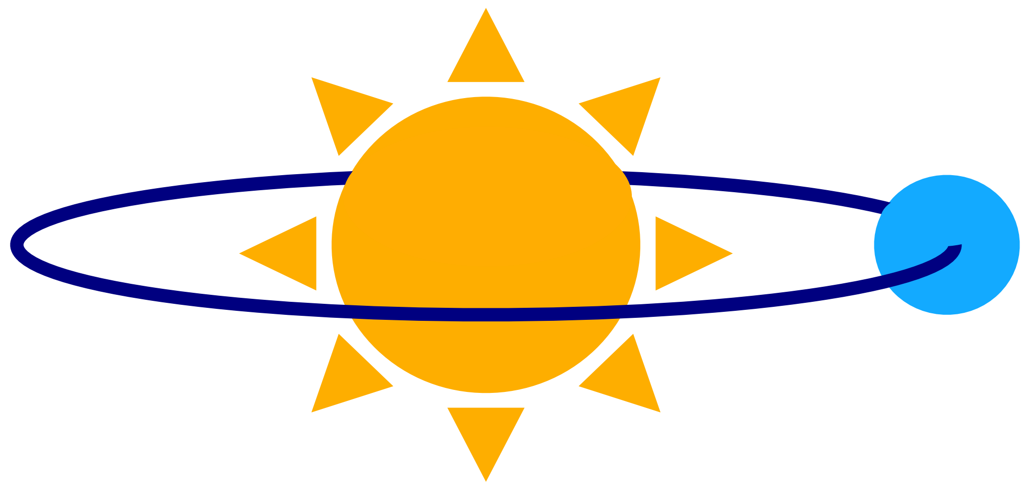

Weakest Systems

Post-Newtonian!

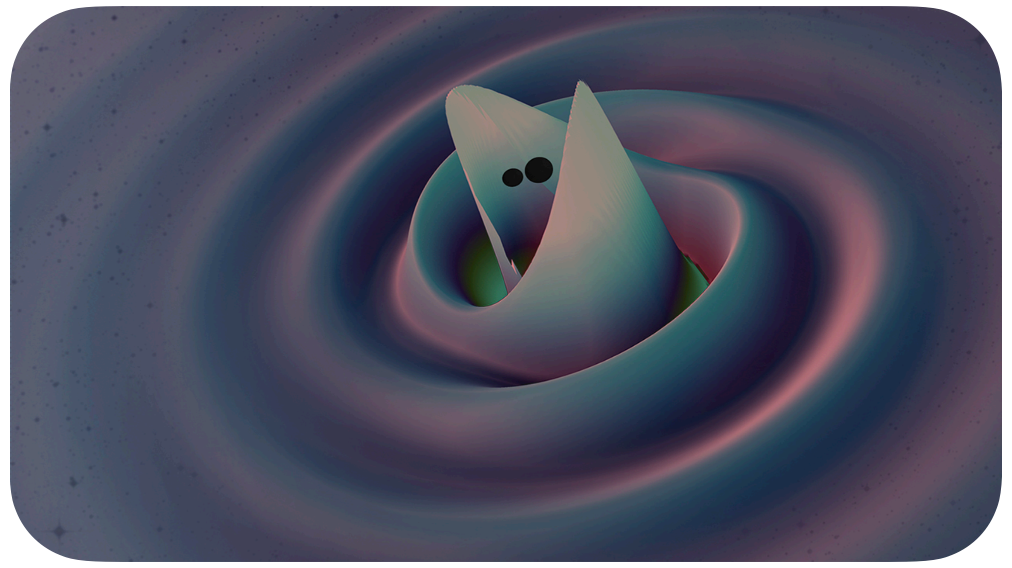

Strongest Systems

Assume: $(v/c)^2 \ll 1$ and $Gm/rc^2 \ll 1$

Circular orbits: $(v/r)^2 = \omega^2 = (Gm/r^3) + \mathcal{O}(c^{-2}) \longrightarrow x = (Gm\omega)^{2/3}/c^2$

A nPN quantity looks something like

$$x^m \left(\ldots + c_{-1}x^{-1} + 1 + c_1 x + \ldots + x^n \right)$$

-1PN

Post-Newtonian formalism

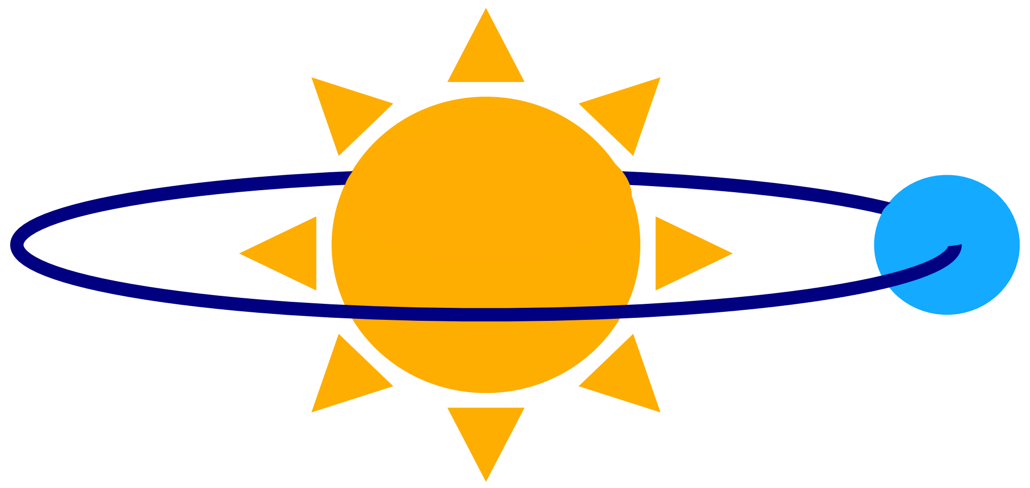

Post-Newtonian!

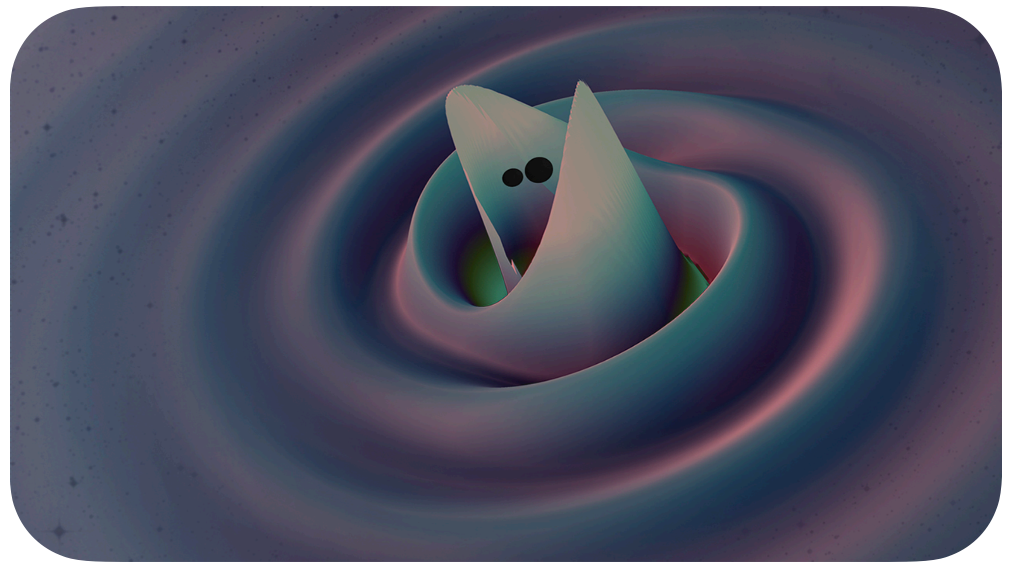

Assume: $(v/c)^2 \ll 1$ and $Gm/rc^2 \ll 1$

Circular orbits: $(v/r)^2 = \omega^2 = (Gm/r^3) + \boxed{\mathcal{O}(c^{-2})} \longrightarrow x = (Gm\omega)^{2/3}/c^2$

A nPN quantity looks something like

$$x^m \left(\ldots + c_{-1}x^{-1} + 1 + c_1 x + \ldots + x^n \right)$$

Waveform modeling

Waveform modeling

- Phenomenological:
  - Computed directly in the frequency domain
  - PN + coefficients fit to NR

Waveform modeling

- Phenomenological:
  - Computed directly in the frequency domain
  - PN + coefficients fit to NR
- Effective-one-body:
  - Single body in an effective potential
  - PN/NR/BH perturbation

Waveform modeling

- Phenomenological:
  - Computed directly in the frequency domain
  - PN + coefficients fit to NR
- Effective-one-body:
  - Single body in an effective potential
  - PN/NR/BH perturbation
- Surrogate:
  - Interpolate between NR Simulations
  - Incorporate PN/BH perturbation to deal with inspiral/ringdown

Parameter estimation

Say we have a model $h = h(\boldsymbol{\theta}) \ldots$

Parameter estimation

Say we have a model $h = h(\boldsymbol{\theta}) \ldots$

$d =$ 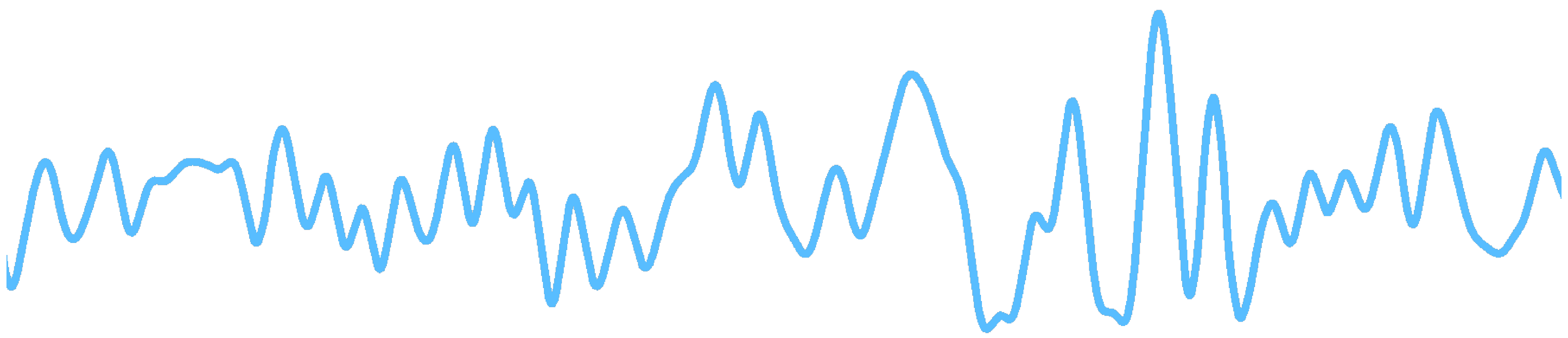

Parameter estimation

Say we have a model $h = h(\boldsymbol{\theta})\ldots$

$d =$ 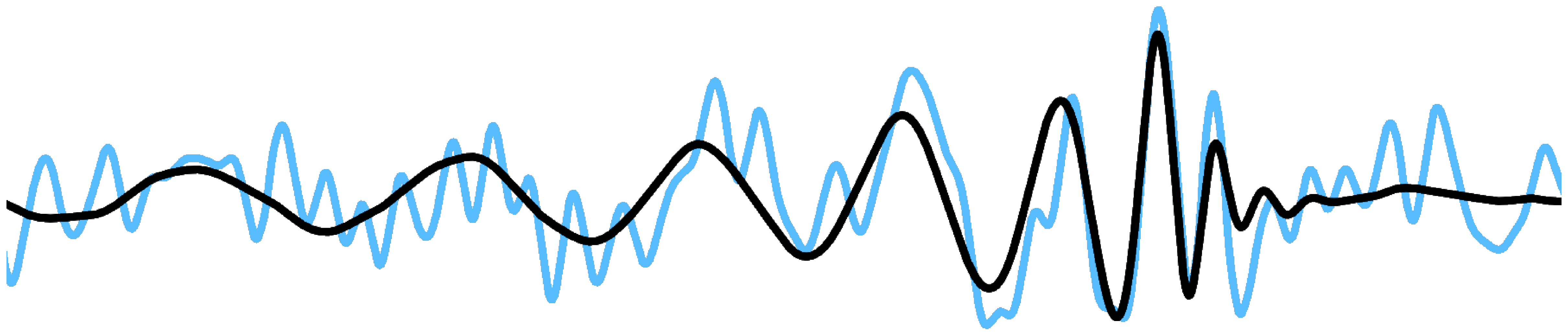 $= h(\boldsymbol{\theta})$

Parameter estimation

Say we have a model $h = h(\boldsymbol{\theta})\ldots$

$d =$

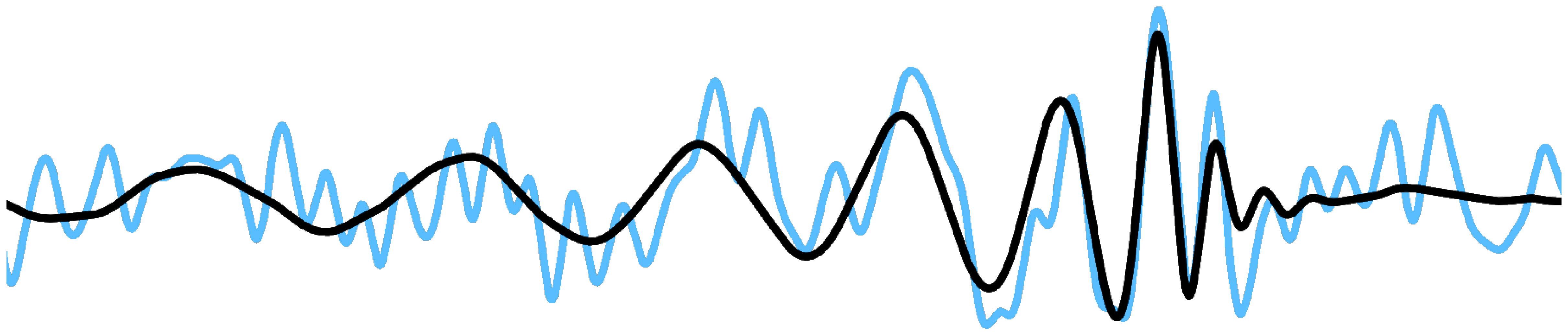

$= h(\boldsymbol{\theta})$

$$P(\boldsymbol{\theta}\,|\,d, h) = \frac{\mathscr{L}(d\,|\,\boldsymbol{\theta}, h)\pi(\boldsymbol{\theta})}{\mathscr{Z}(d)}$$

Parameter estimation

Say we have a model $h = h(\boldsymbol{\theta})\ldots$

$d =$ 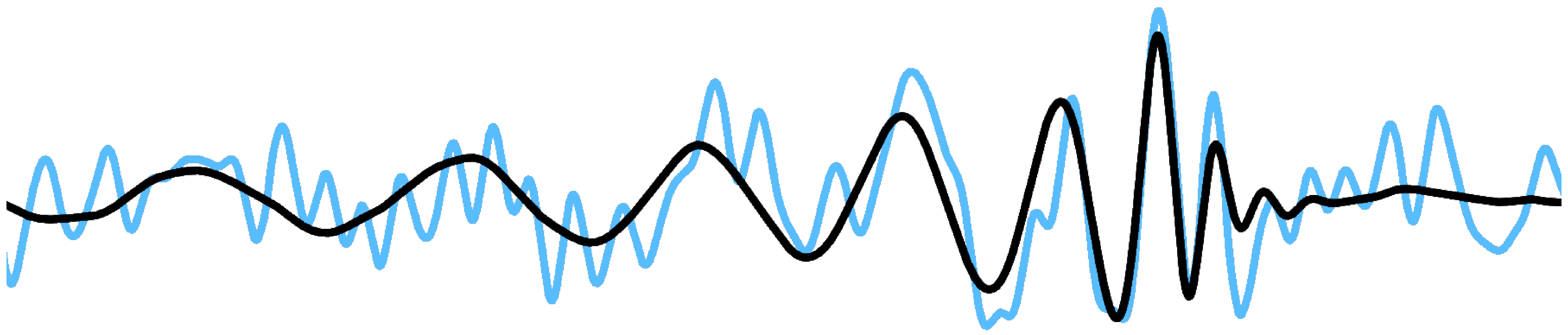 $= h(\boldsymbol{\theta})$

$$P(\boldsymbol{\theta}\,|\,d, h) = \frac{\mathscr{L}(d\,|\,\boldsymbol{\theta}, h)\pi(\boldsymbol{\theta})}{\mathscr{Z}(d)}$$

Prior: Assumptions about parameters

Parameter estimation

Say we have a model $h = h(\boldsymbol{\theta})\ldots$

$d =$ 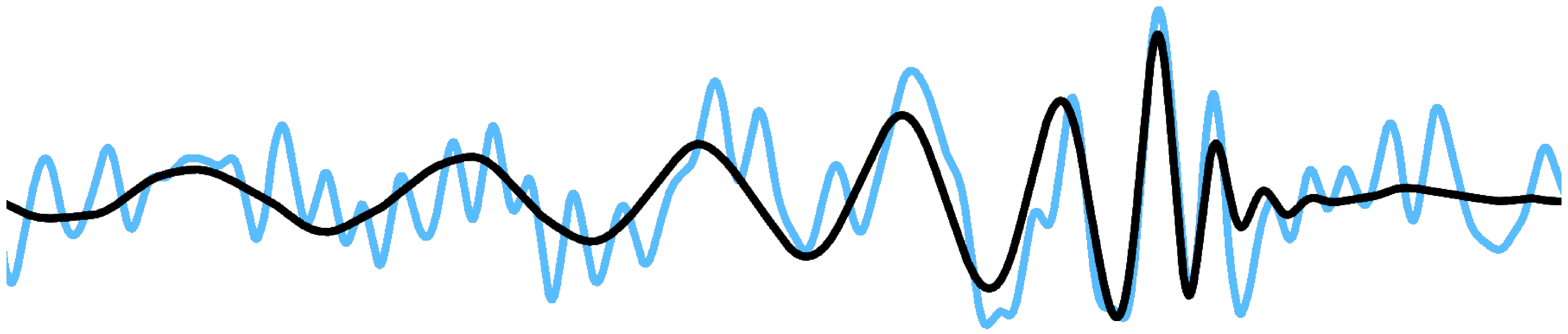 $= h(\boldsymbol{\theta})$

$$P(\boldsymbol{\theta}\,|\,d,h) = \frac{\mathscr{L}(d\,|\,\boldsymbol{\theta},h)\,\pi(\boldsymbol{\theta})}{\mathscr{Z}(d)}$$

Prior: Assumptions about parameters

Likelihood: Assumptions about data generation

Parameter estimation

Say we have a model $h = h(\boldsymbol{\theta})\ldots$

$d =$

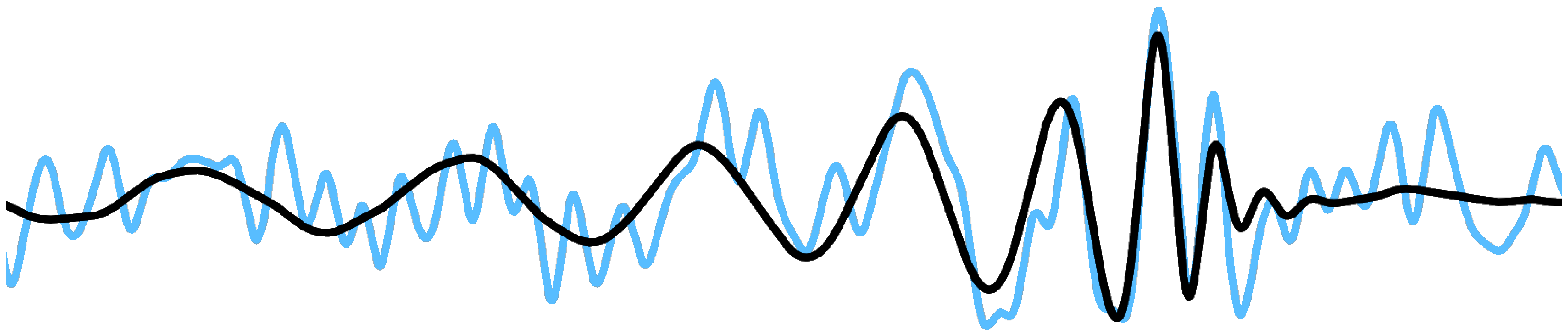

$= h(\boldsymbol{\theta})$

$$P(\boldsymbol{\theta}\,|\,d, h) = \frac{\mathscr{L}(d\,|\,\boldsymbol{\theta}, h)\pi(\boldsymbol{\theta})}{\mathcal{Z}(d)}$$

Prior: Assumptions about parameters

Likelihood: Assumptions about data generation

Evidence: Normalization (for now)

Parameter estimation

Say we have a model $h = h(\boldsymbol{\theta})\ldots$

$d =$ 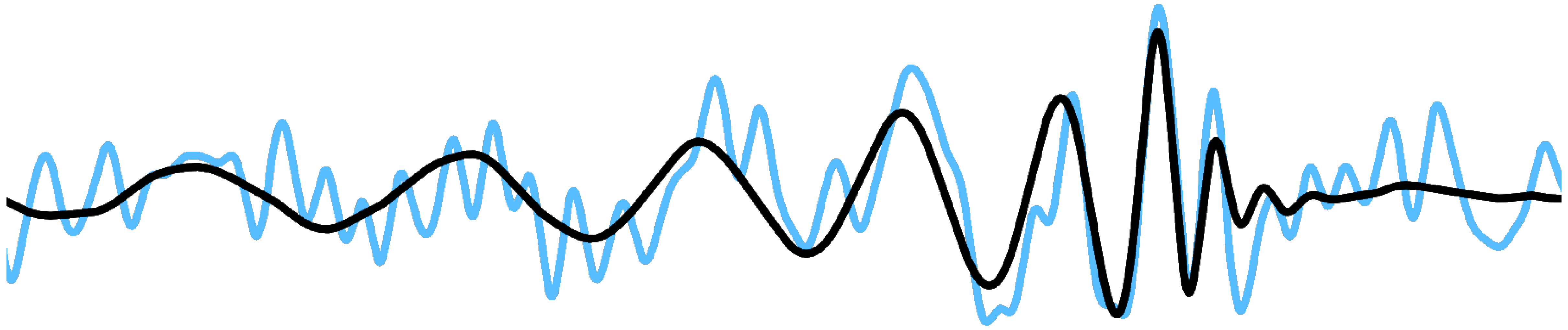 $= h(\boldsymbol{\theta})$

$$P(\boldsymbol{\theta}\,|\,d,h) = \frac{\mathscr{L}(d\,|\,\boldsymbol{\theta},h)\pi(\boldsymbol{\theta})}{\mathscr{Z}(d)}$$

Prior: Assumptions about parameters

Likelihood: Assumptions about data generation

Evidence: Normalization (for now)

Posterior: A distribution on the binary parameters

Parameter estimation

Say we have a model $h = h(\boldsymbol{\theta})\dots$

$d =$ 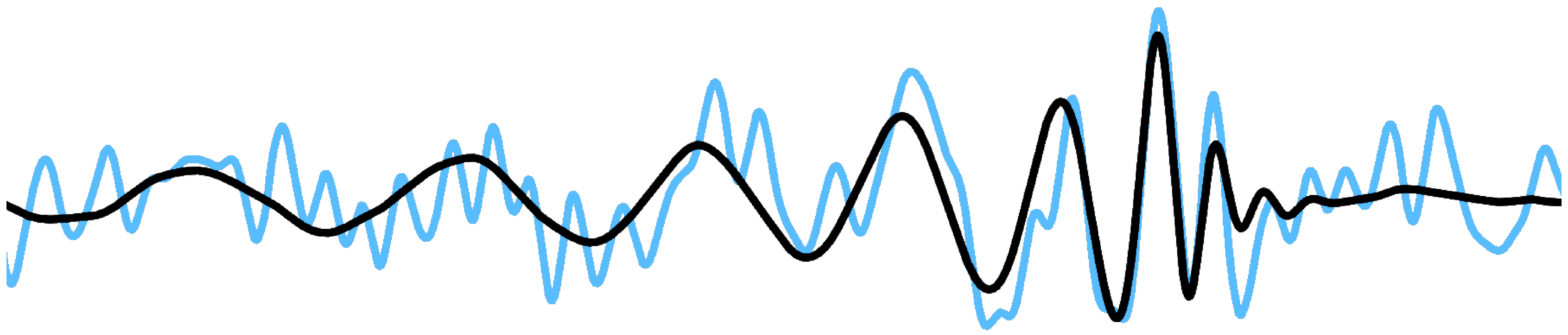 $= h(\boldsymbol{\theta})$

$$P(\boldsymbol{\theta}\,|\,d, h) = \frac{\mathscr{L}(d\,|\,\boldsymbol{\theta}, h)\pi(\boldsymbol{\theta})}{\mathscr{Z}(d)}$$

Prior: Assumptions about parameters
Likelihood: Assumptions about data generation
Evidence: Normalization (for now)

Posterior: A distribution on the binary parameters

Parameter estimation

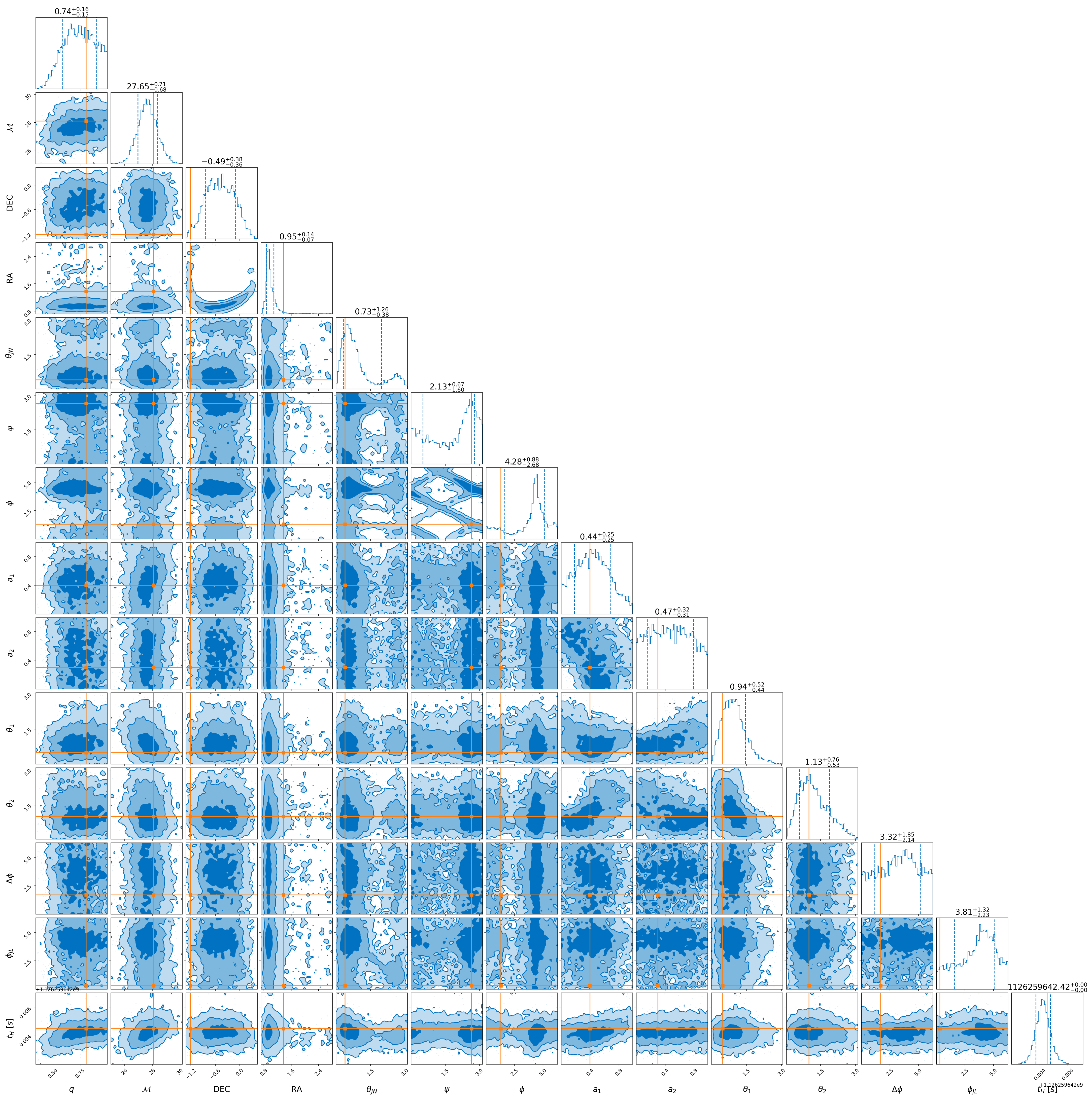

Parameter estimation

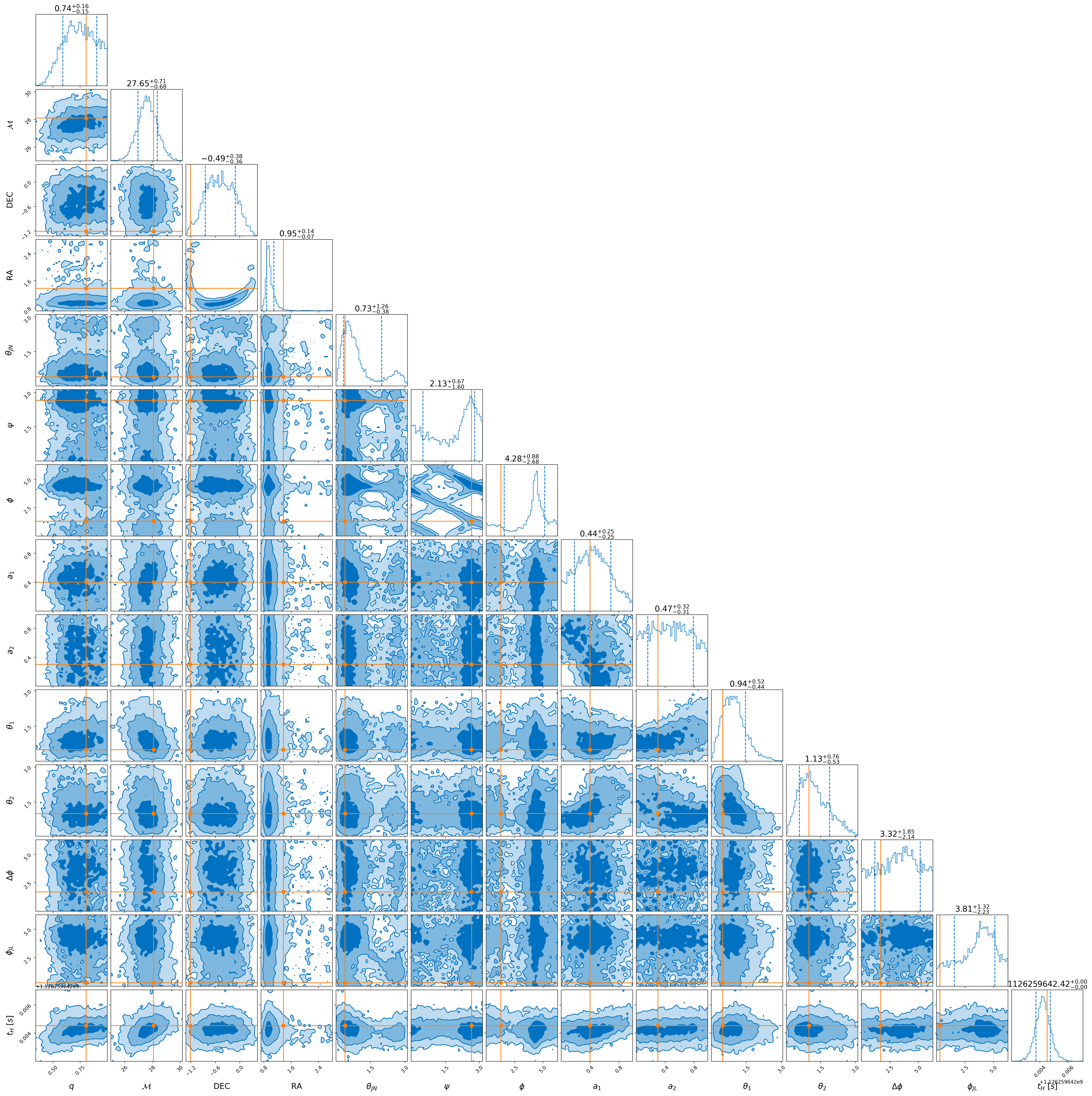

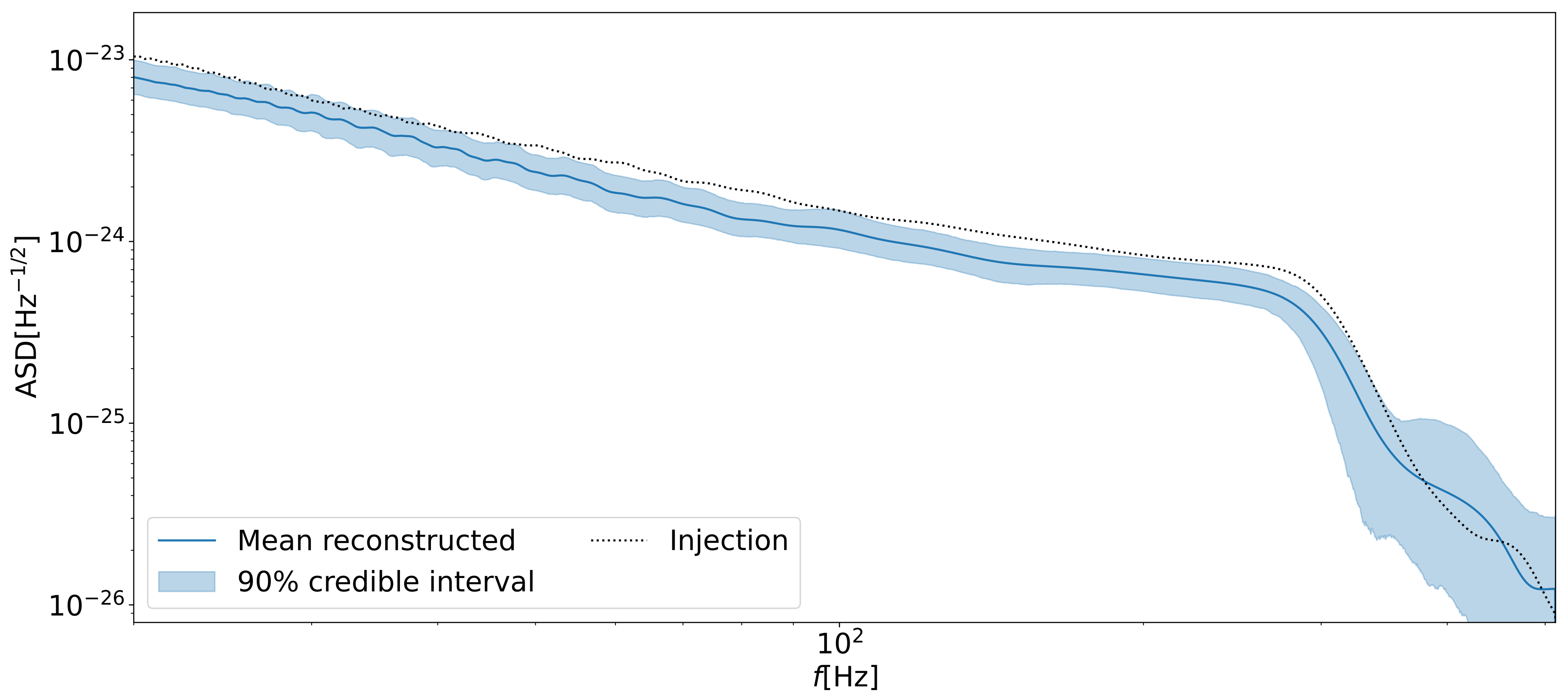

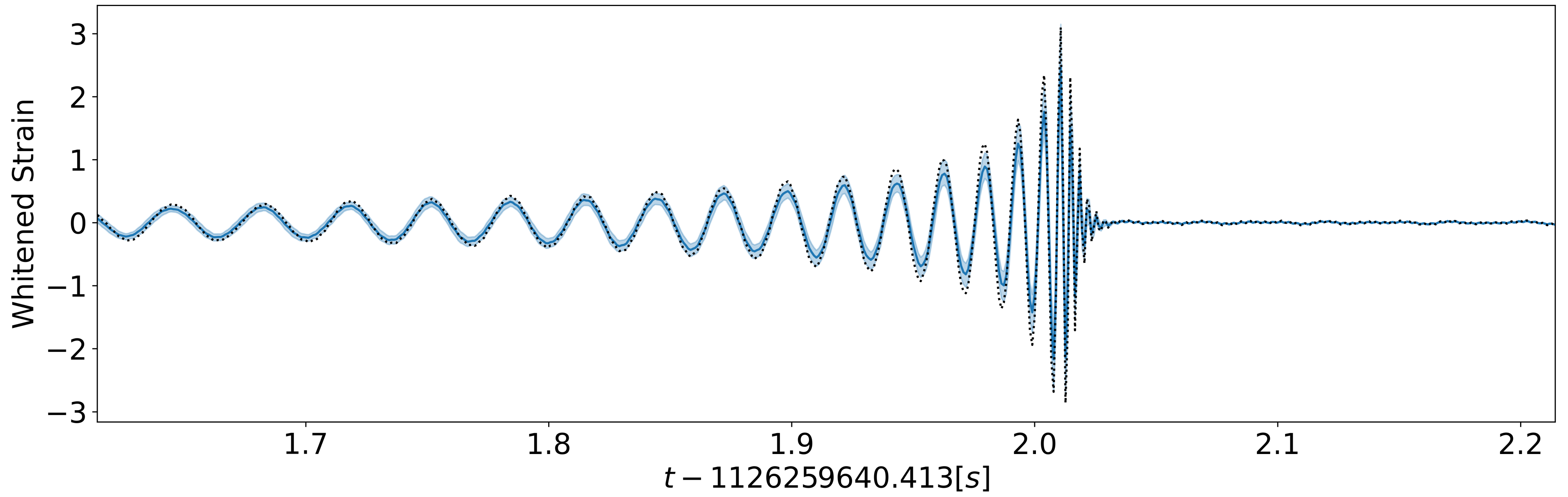

Binary parameter likelihood

Binary parameter likelihood

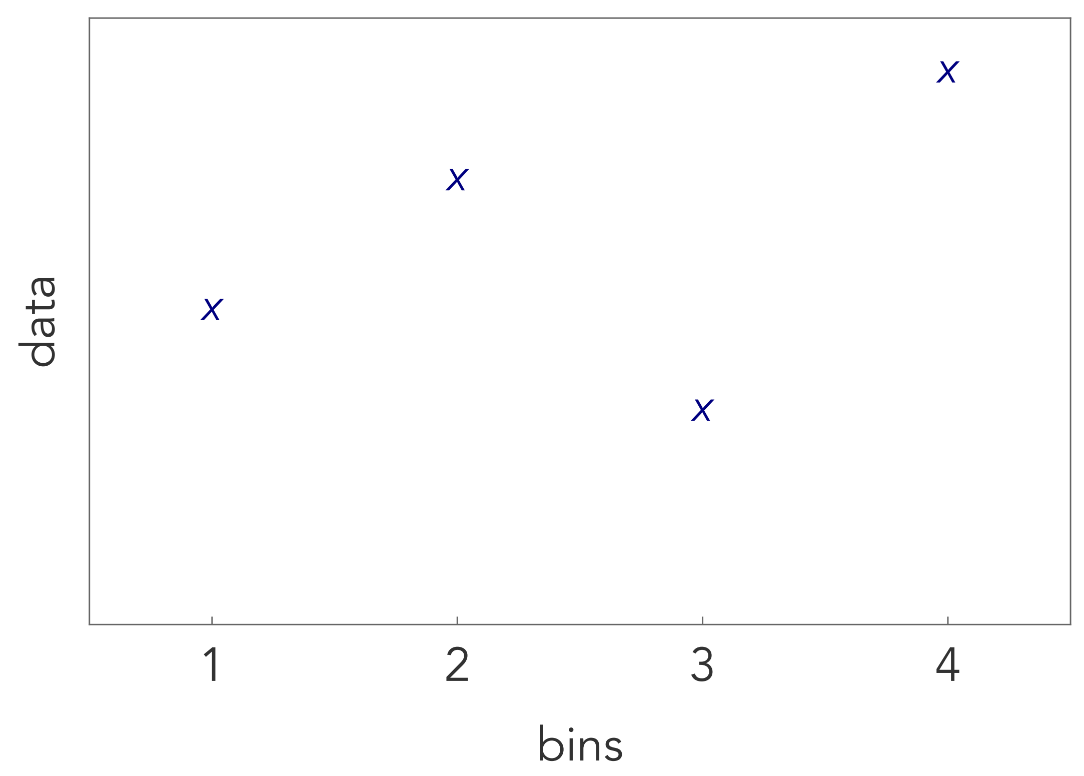

Binary parameter likelihood

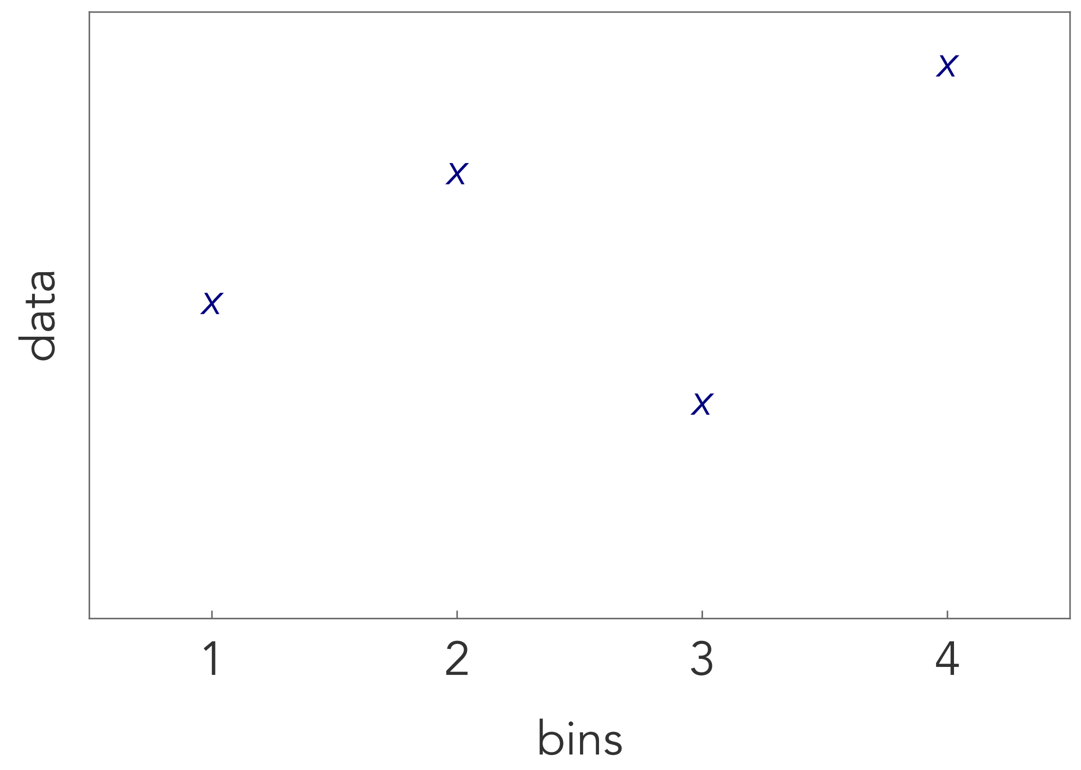

=

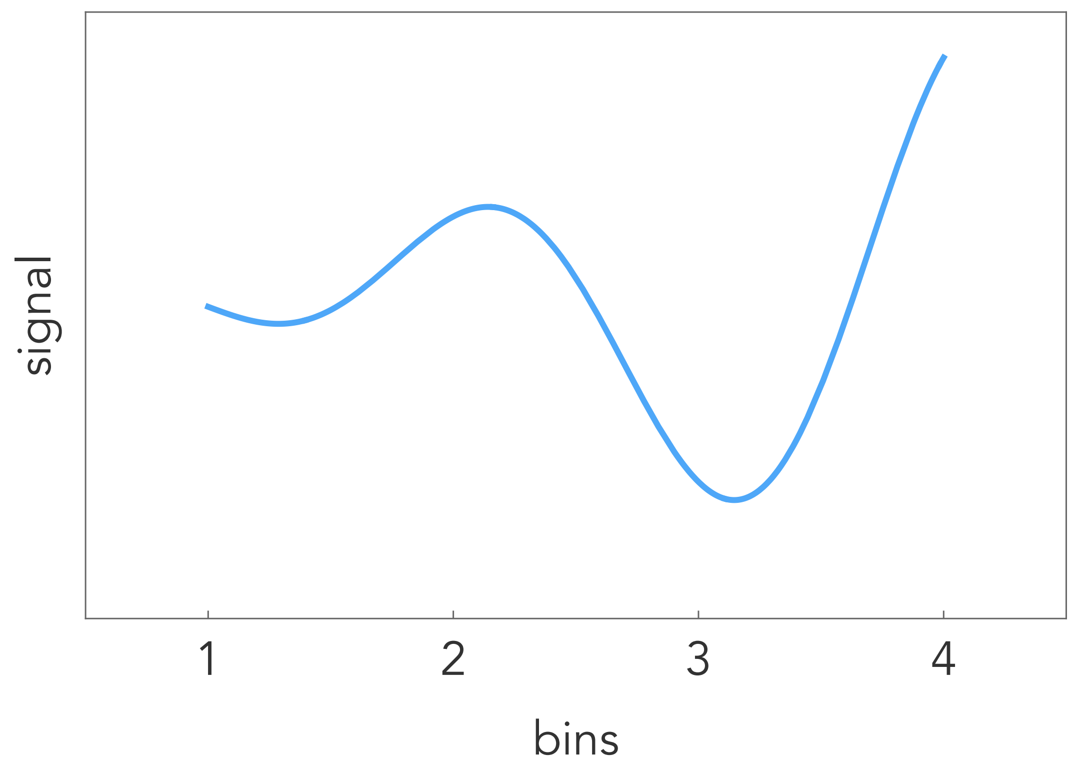

$$\text{signal} = h(i, \boldsymbol{\theta})$$

Binary parameter likelihood

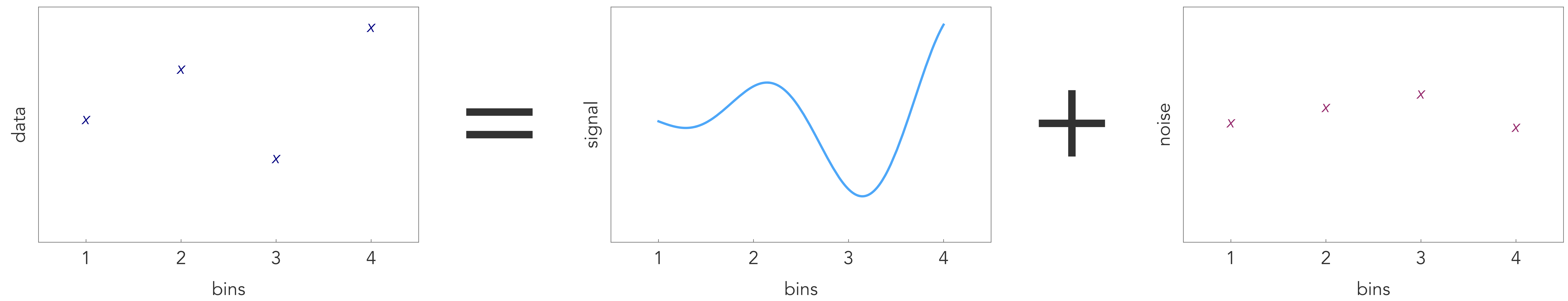

$$\text{signal} = h(i, \boldsymbol{\theta})$$

Binary parameter likelihood

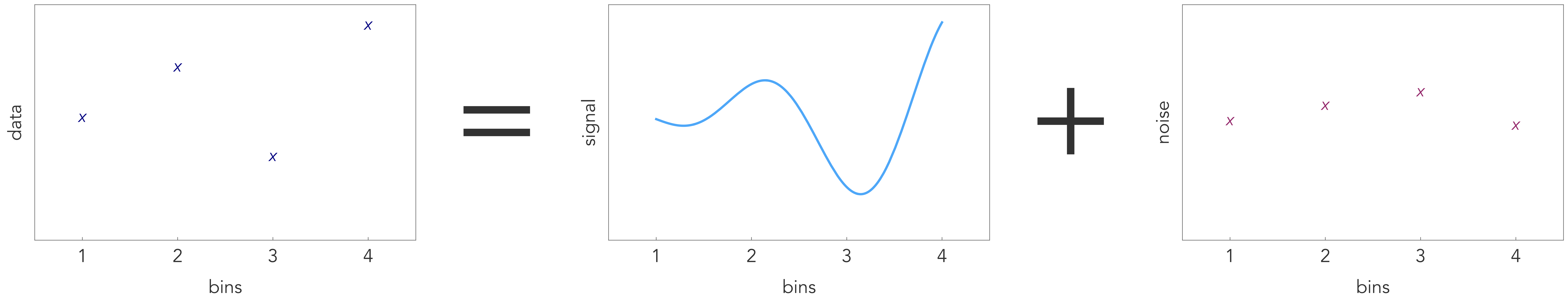

signal $= h(i, \boldsymbol{\theta})$

$$p(n_i) \propto \exp\left[-\frac{n_i^2}{2\sigma_i^2}\right]$$

Binary parameter likelihood

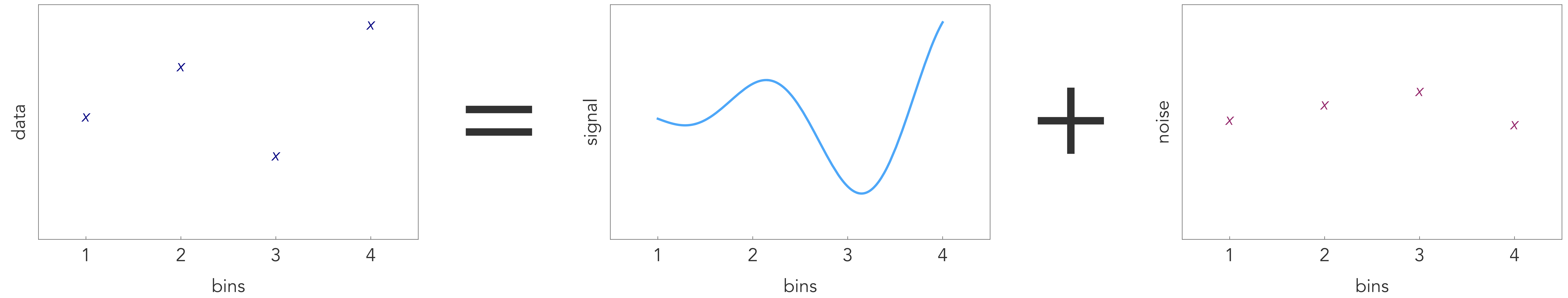

$$\text{signal} = h(i, \boldsymbol{\theta})$$

$$p(\text{noise}) \propto \exp\left[-\sum_{\text{bins}} \frac{n_i^2}{2\sigma_i^2}\right]$$

Binary parameter likelihood

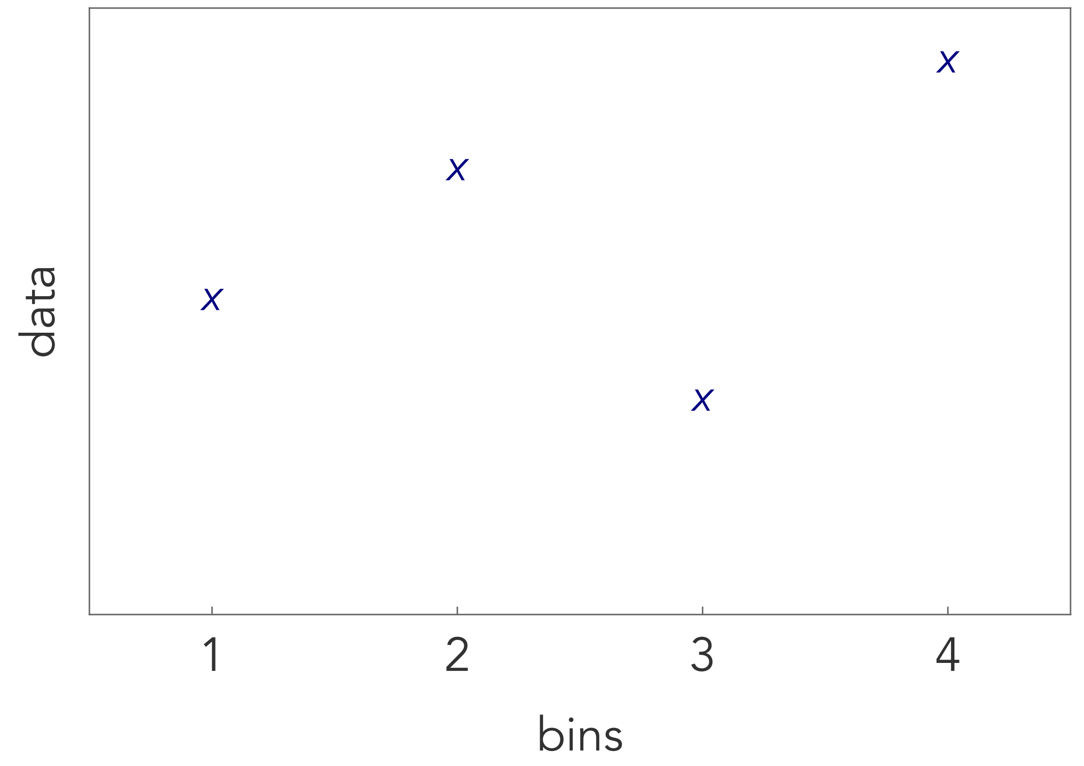

=

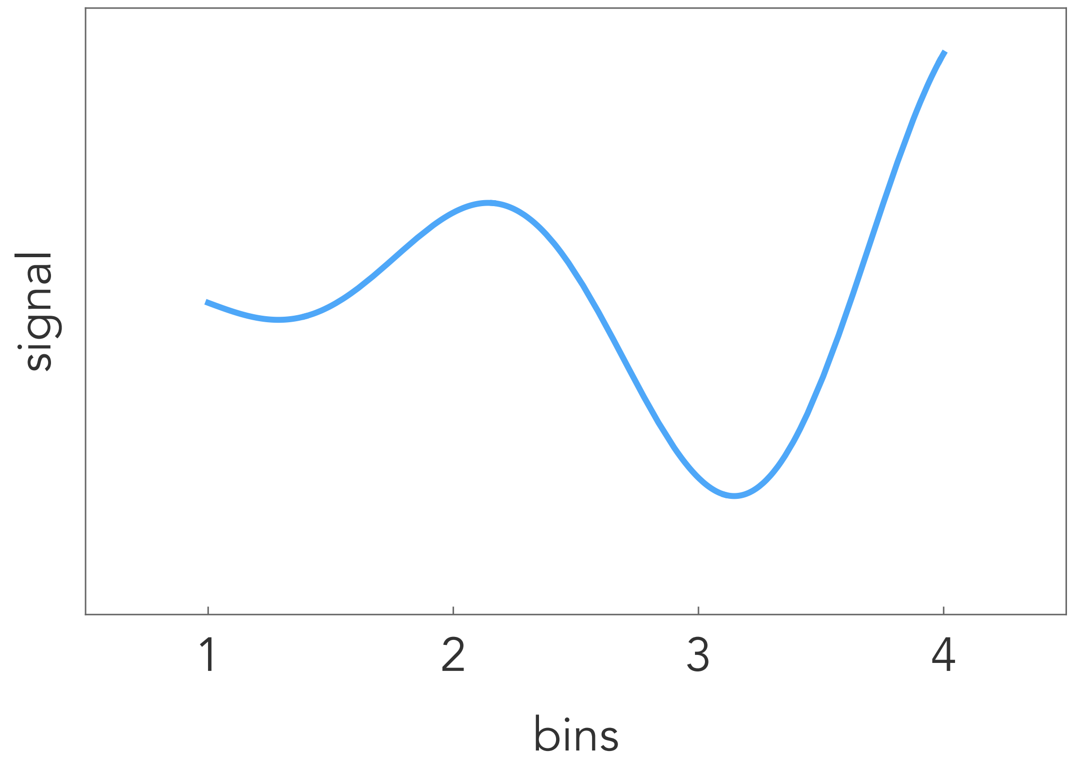

+

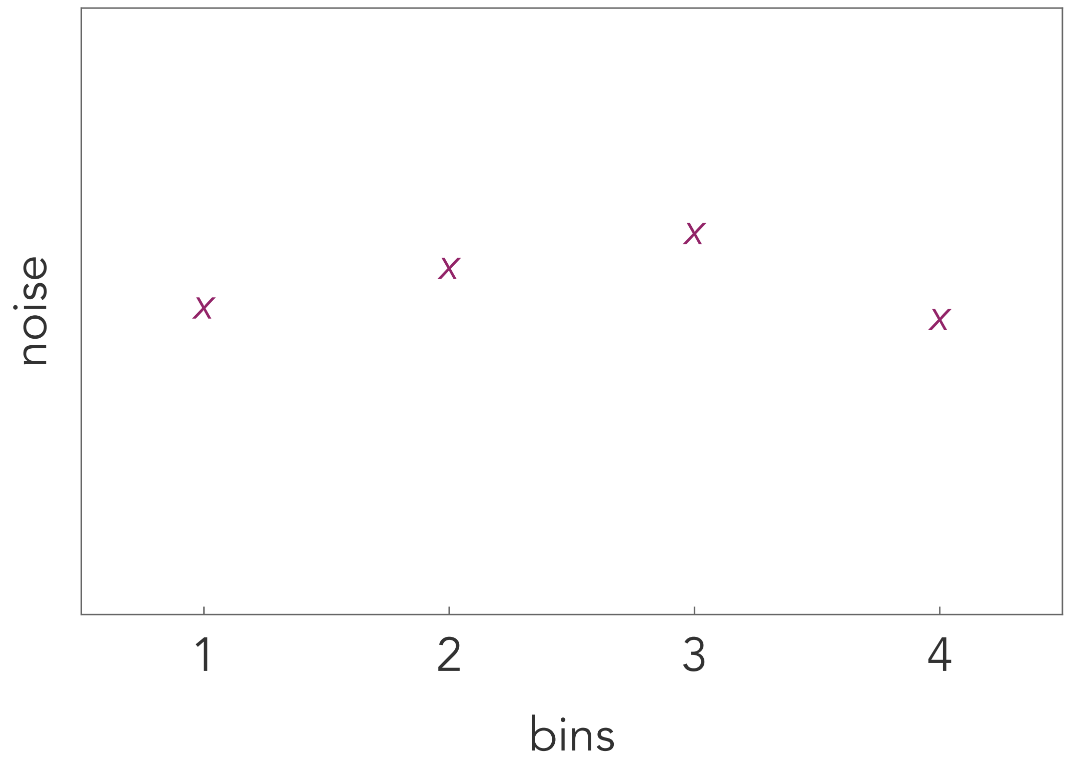

$$\text{signal} = h(i, \boldsymbol{\theta})$$

$$p(\text{noise}) \propto \exp\left[-\frac{1}{2} n_i C_{ij}^{-1} n_j\right]$$

Binary parameter likelihood

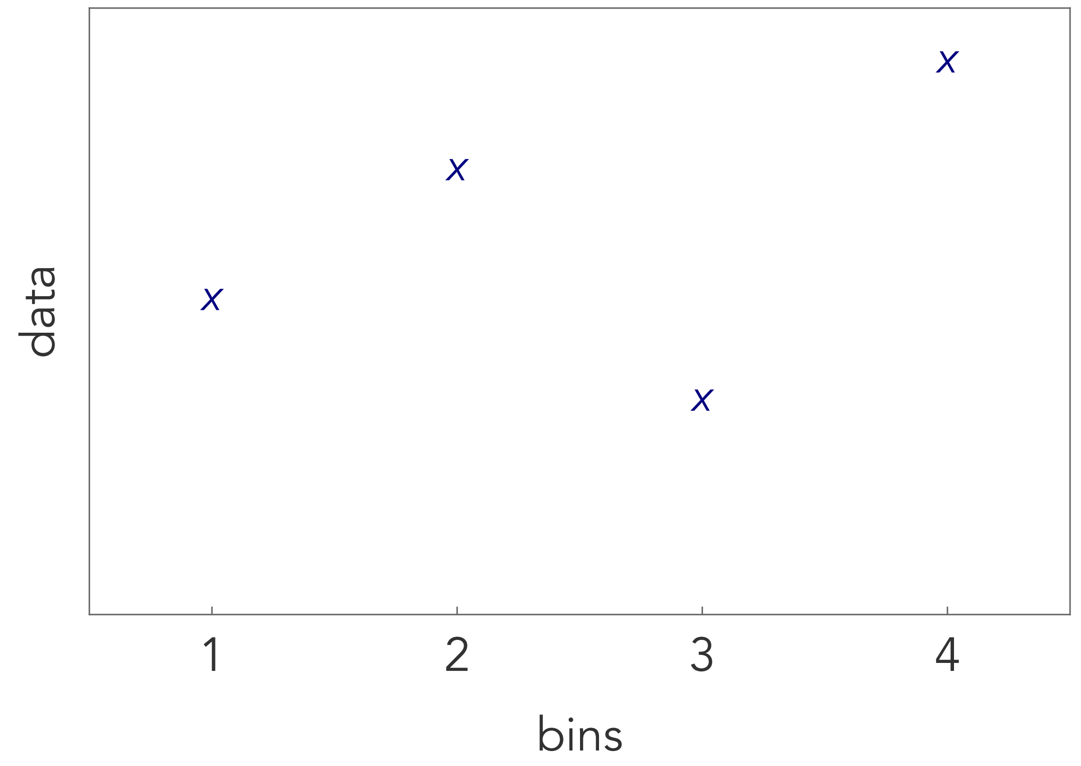

=

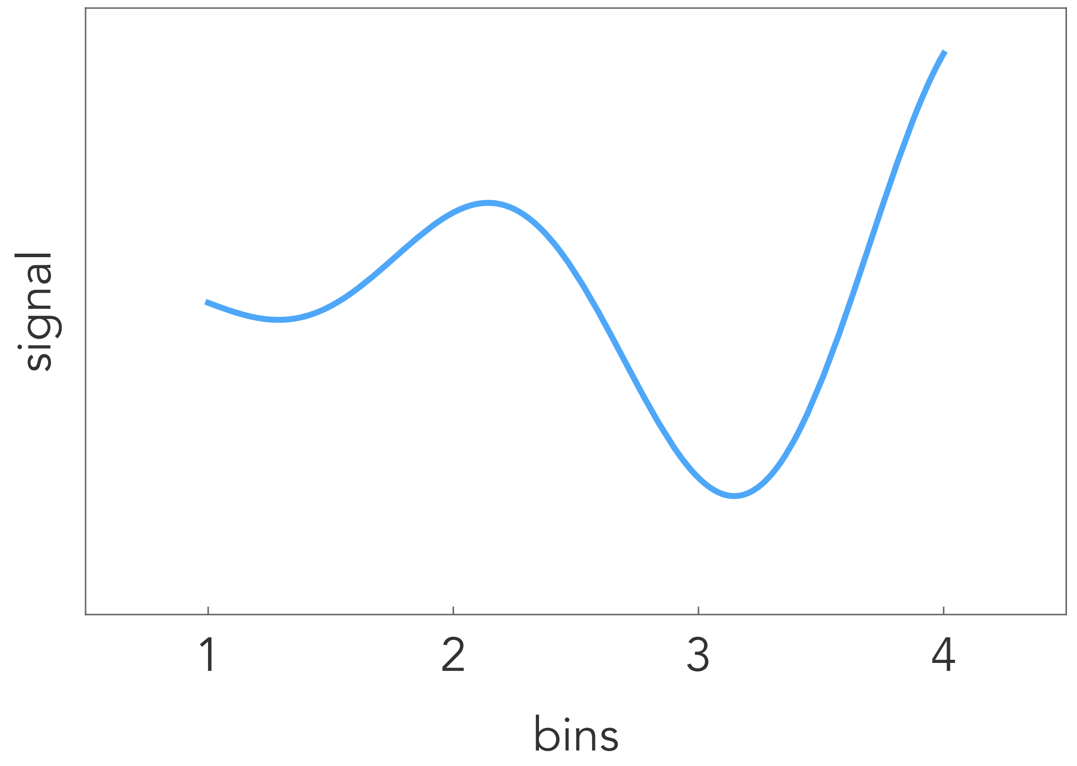

signal $= h(i, \boldsymbol{\theta})$

+

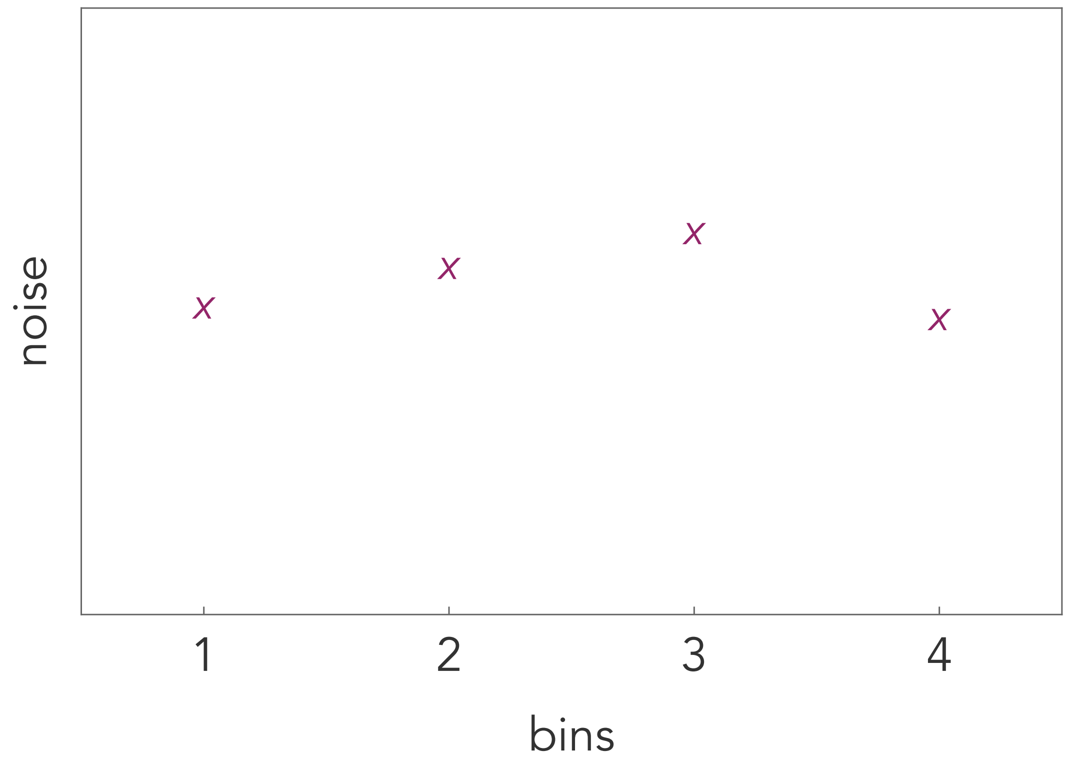

$$p(\mathrm{noise}) \propto \exp\left[-\frac{1}{2}(n\,|\,n)\right]$$

$$(a\,|\,b) = a_i C_{ij}^{-1} b_i^*$$

Binary parameter likelihood

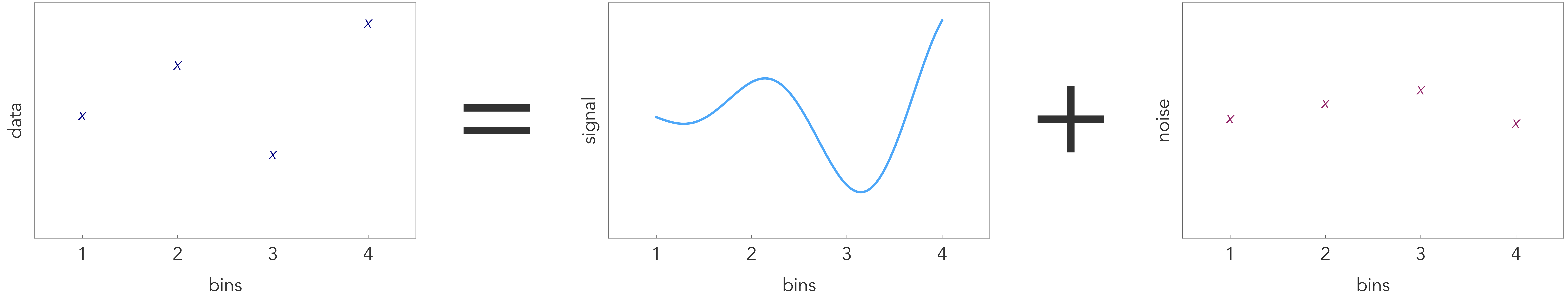

signal $= h(i, \boldsymbol{\theta})$

$$p(\text{noise}) \propto \exp\left[-\frac{1}{2}\left(d - h(\boldsymbol{\theta}) \middle| d - h(\boldsymbol{\theta})\right)\right]$$

$$(a \,|\, b) = a_i C_{ij}^{-1} b_i^{*}$$

Binary parameter likelihood

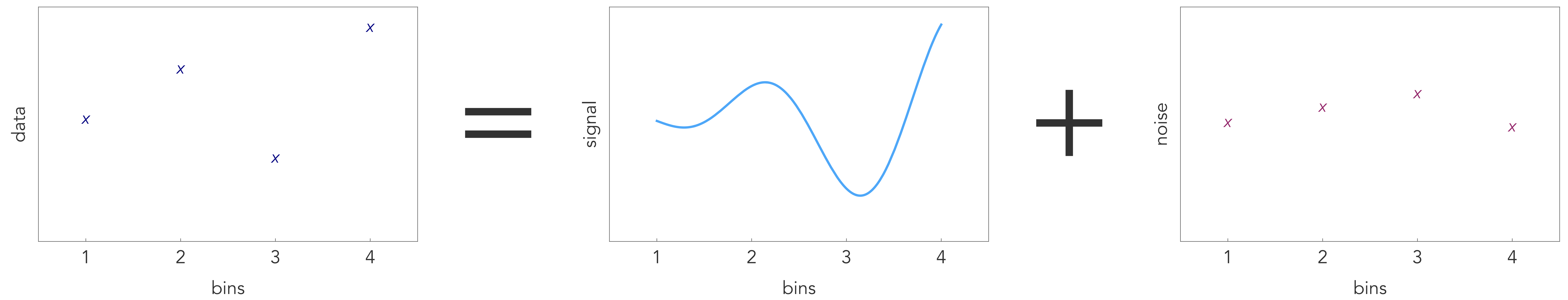

signal $= h(i, \boldsymbol{\theta})$

$$p(\text{noise}) \propto \exp\left[-\frac{1}{2}\left(d - h(\boldsymbol{\theta}) \middle| d - h(\boldsymbol{\theta})\right)\right]$$

$$(a \,|\, b) = a_i C_{ij}^{-1} b_i^*$$

Likelihood: $\mathscr{L}(d \,|\, \boldsymbol{\theta}, h) \propto \exp\left[-\frac{1}{2}\left(d - h(\boldsymbol{\theta}) \middle| d - h(\boldsymbol{\theta})\right)\right]$

Binary parameter likelihood

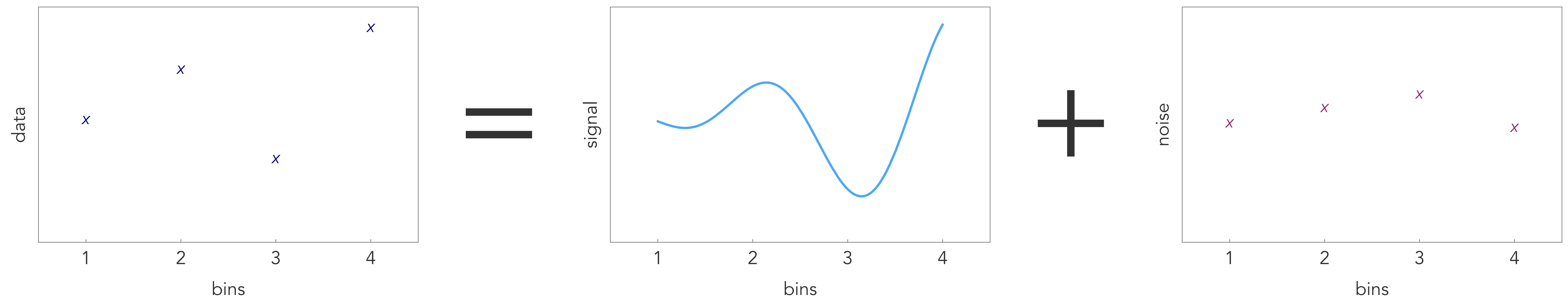

signal $= h(i, \boldsymbol{\theta})$

$$p(\text{noise}) \propto \exp\left[-\frac{1}{2}\left(d - h(\boldsymbol{\theta}) \middle| d - h(\boldsymbol{\theta})\right)\right]$$

$$(a \,|\, b) = a_i C_{ij}^{-1} b_i^*$$

Likelihood: $\mathscr{L}(d \,|\, \boldsymbol{\theta}, h) \propto \exp\left[-\frac{1}{2}\left(d - h(\boldsymbol{\theta}) \middle| d - h(\boldsymbol{\theta})\right)\right]$

What are the bins?

Binary parameter likelihood

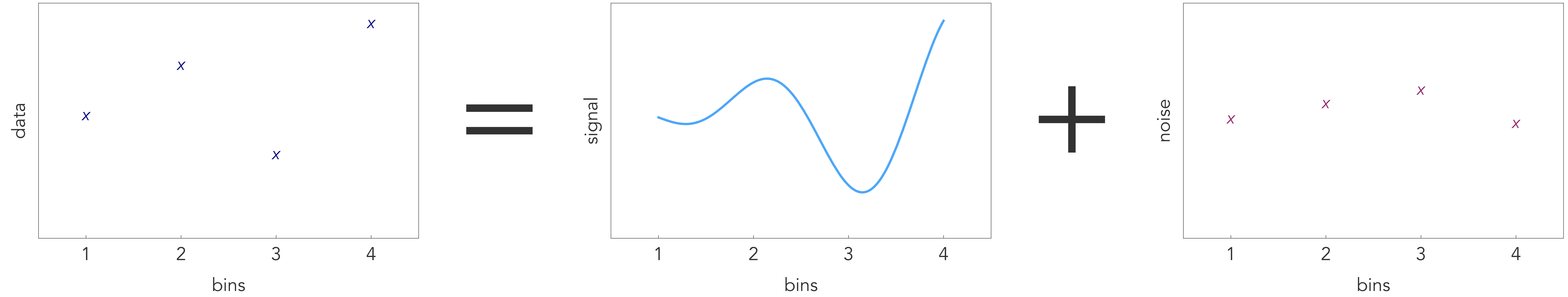

signal $= h(i, \boldsymbol{\theta})$

$$p(\text{noise}) \propto \exp\left[-\frac{1}{2}\Big(d - h(\boldsymbol{\theta})\Big| d - h(\boldsymbol{\theta})\Big)\right]$$

$$(a\,|\,b) = a_i C_{ij}^{-1} b_i^*$$

Likelihood: $\mathscr{L}(d\,|\,\boldsymbol{\theta}, h) \propto \exp\left[-\frac{1}{2}\Big(d - h(\boldsymbol{\theta})\Big| d - h(\boldsymbol{\theta})\Big)\right]$

What are the bins?

… time?

Binary parameter likelihood

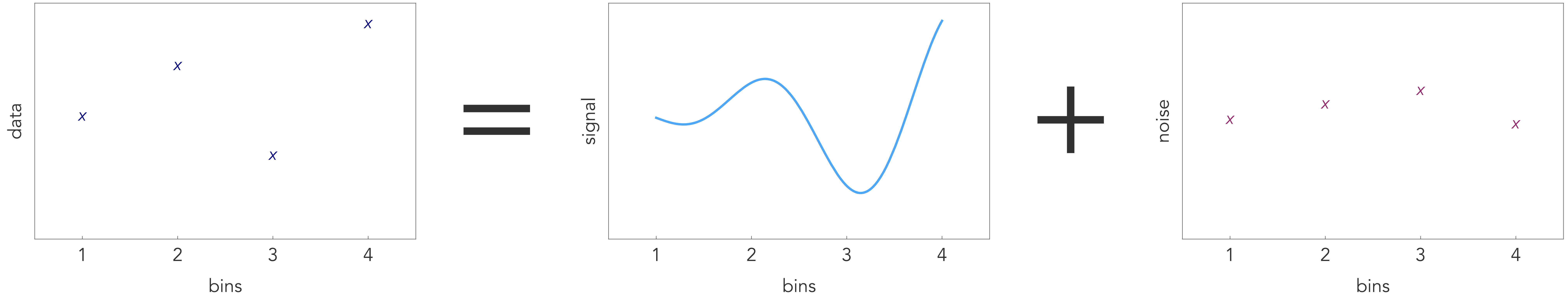

signal $= h(i, \boldsymbol{\theta})$

$$p(\text{noise}) \propto \exp\left[-\frac{1}{2}\left(d - h(\boldsymbol{\theta}) \middle| d - h(\boldsymbol{\theta})\right)\right]$$

$$(a \,|\, b) = a_i C_{ij}^{-1} b_i^*$$

Likelihood: $\mathscr{L}(d \,|\, \boldsymbol{\theta}, h) \propto \exp\left[-\frac{1}{2}\left(d - h(\boldsymbol{\theta}) \middle| d - h(\boldsymbol{\theta})\right)\right]$

What are the bins?

… time?

$$(a \,|\, b) = a(t_i) C_{ij}^{-1} b^*(t_j)$$

Binary parameter likelihood

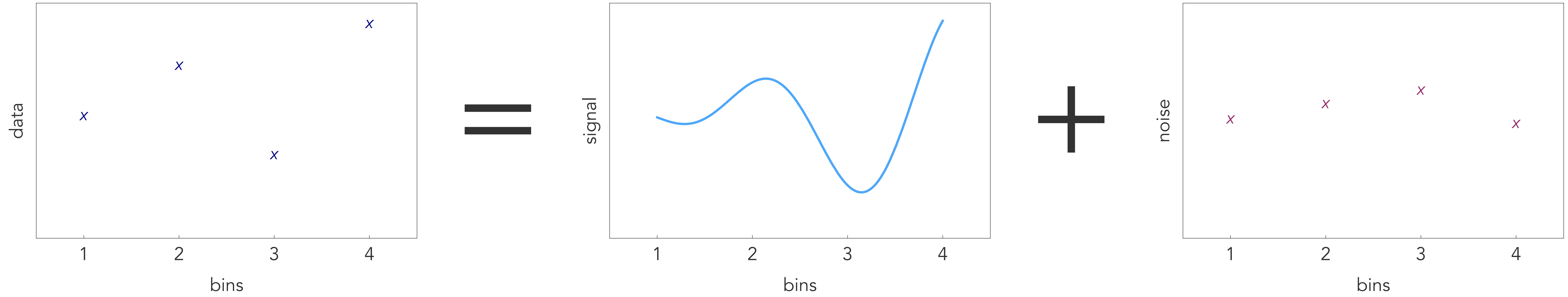

signal $= h(i, \boldsymbol{\theta})$

$$p(\text{noise}) \propto \exp\left[-\frac{1}{2}\left(d - h(\boldsymbol{\theta}) \middle| d - h(\boldsymbol{\theta})\right)\right]$$

$$(a \,|\, b) = a_i C_{ij}^{-1} b_i^*$$

Likelihood: $\mathscr{L}(d \,|\, \boldsymbol{\theta}, h) \propto \exp\left[-\frac{1}{2}\left(d - h(\boldsymbol{\theta}) \middle| d - h(\boldsymbol{\theta})\right)\right]$

What are the bins?

… time?

$$(a \,|\, b) = a(t_i) C_{ij}^{-1} b^*(t_j) \qquad i, j \in 1, \ldots, \sim 10^4$$

Binary parameter likelihood

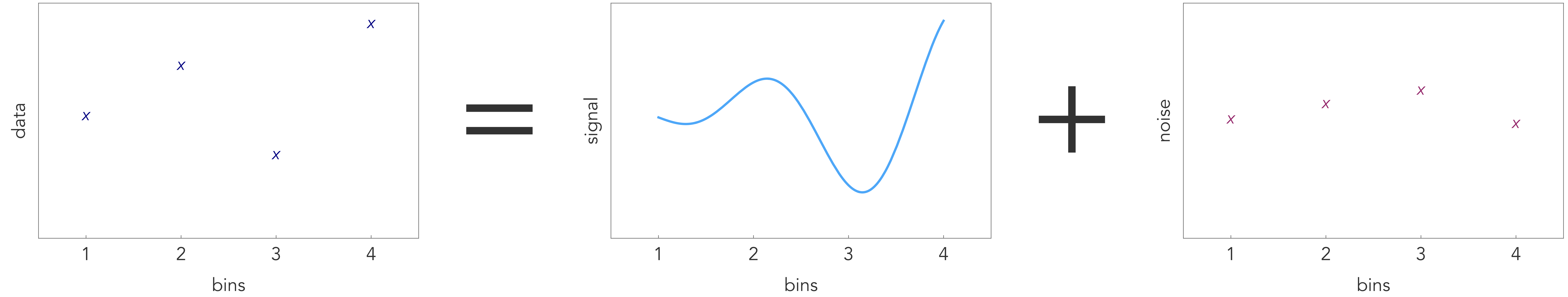

signal $= h(i, \boldsymbol{\theta})$

$$p(\text{noise}) \propto \exp\left[-\frac{1}{2}\left(d - h(\boldsymbol{\theta}) \middle| d - h(\boldsymbol{\theta})\right)\right]$$

$$(a \,|\, b) = a_i C_{ij}^{-1} b_i^*$$

Likelihood: $\mathscr{L}(d \,|\, \boldsymbol{\theta}, h) \propto \exp\left[-\frac{1}{2}\left(d - h(\boldsymbol{\theta}) \middle| d - h(\boldsymbol{\theta})\right)\right]$

What are the bins?

… time?

$$(a \,|\, b) = a(t_i) C_{ij}^{-1} b^*(t_j) \qquad i, j \in 1, \ldots, \sim 10^4$$

Inversion scales with N_{bins}^3

Binary parameter likelihood

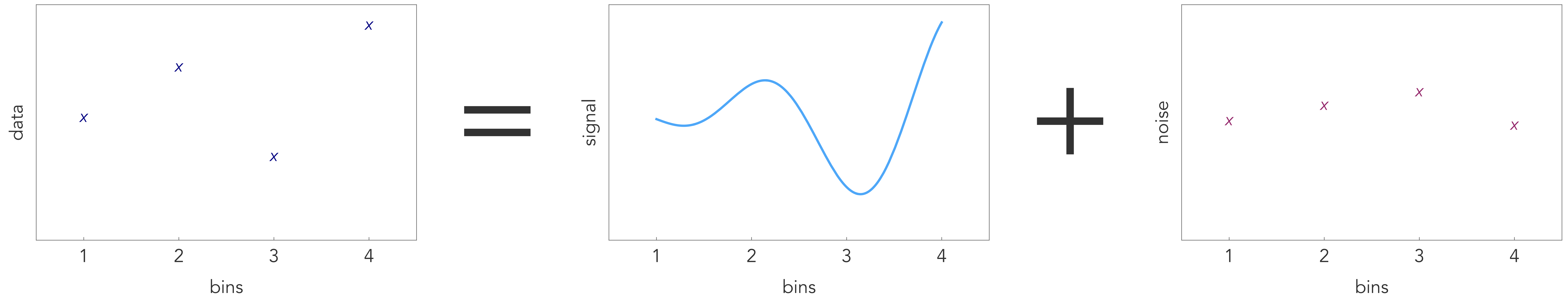

signal $= h(i, \boldsymbol{\theta})$

$$p(\text{noise}) \propto \exp\left[-\frac{1}{2}\left(d - h(\boldsymbol{\theta}) \middle| d - h(\boldsymbol{\theta})\right)\right]$$

$$(a \,|\, b) = a_i C_{ij}^{-1} b_i^*$$

Likelihood: $\mathscr{L}(d \,|\, \boldsymbol{\theta}, h) \propto \exp\left[-\frac{1}{2}\left(d - h(\boldsymbol{\theta}) \middle| d - h(\boldsymbol{\theta})\right)\right]$

What are the bins?

… time?

$$(a \,|\, b) = a(t_i) C_{ij}^{-1} b^*(t_j) \qquad i, j \in 1, \ldots, \sim 10^4$$

Inversion scales with N_{bins}^3

… frequency?

Binary parameter likelihood

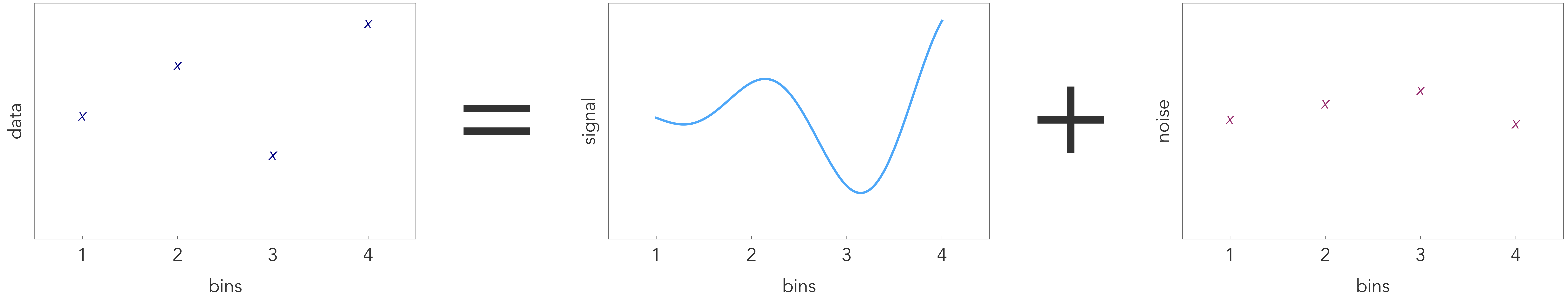

signal $= h(i, \boldsymbol{\theta})$

$$p(\text{noise}) \propto \exp\left[-\frac{1}{2}\left(d - h(\boldsymbol{\theta}) \middle| d - h(\boldsymbol{\theta})\right)\right]$$

$$(a\,|\,b) = a_i C_{ij}^{-1} b_i^*$$

Likelihood: $\mathscr{L}(d\,|\,\boldsymbol{\theta}, h) \propto \exp\left[-\frac{1}{2}\left(d - h(\boldsymbol{\theta}) \middle| d - h(\boldsymbol{\theta})\right)\right]$

What are the bins?

… time?

$$(a\,|\,b) = a(t_i) C_{ij}^{-1} b^*(t_j) \qquad i, j \in 1, \ldots, \sim 10^4$$

Inversion scales with N_{bins}^3

… frequency?

Wiener–Khinchin theorem: C_{ij} diagonalizes in the frequency domain

Binary parameter likelihood

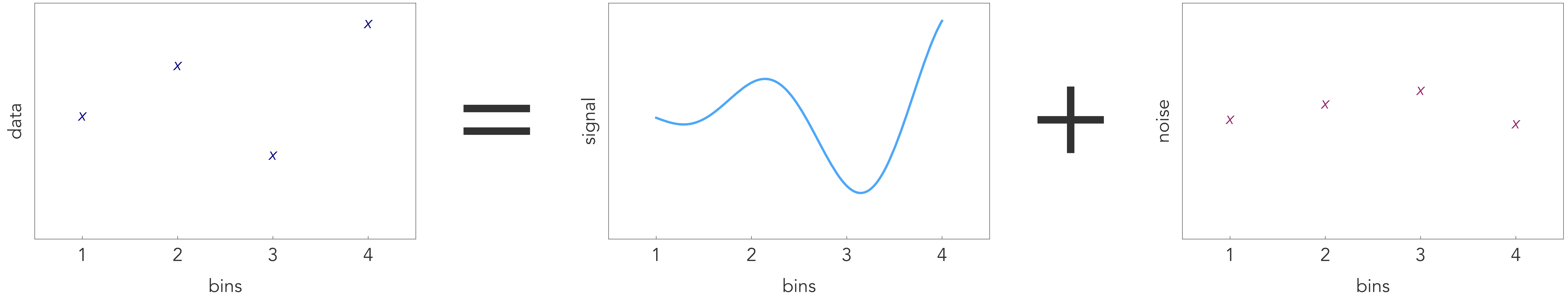

signal $= h(i, \boldsymbol{\theta})$

$$p(\text{noise}) \propto \exp\left[-\frac{1}{2}\left(d - h(\boldsymbol{\theta}) \middle| d - h(\boldsymbol{\theta})\right)\right]$$

$$(a\,|\,b) = a_i C_{ij}^{-1} b_i^*$$

Likelihood: $\mathscr{L}(d\,|\,\boldsymbol{\theta}, h) \propto \exp\left[-\frac{1}{2}\left(d - h(\boldsymbol{\theta}) \middle| d - h(\boldsymbol{\theta})\right)\right]$

What are the bins?

… time?

$(a\,|\,b) = a(t_i) C_{ij}^{-1} b^*(t_j) \qquad i, j \in 1, \ldots, \sim 10^4$

Inversion scales with N_{bins}^3

… frequency?

Wiener–Khinchin theorem: C_{ij} diagonalizes in the frequency domain

$$(a\,|\,b) = \sum_i \frac{\tilde{a}(f_i)\tilde{b}^*(f_i)}{\sigma^2(f_i)}$$

Binary parameter likelihood

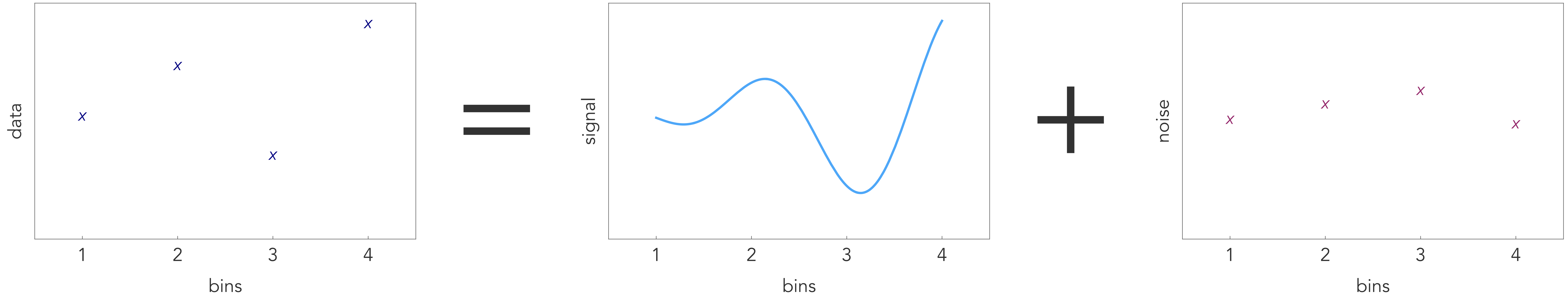

signal $= h(i, \boldsymbol{\theta})$

$$p(\text{noise}) \propto \exp\left[-\frac{1}{2}\left(d - h(\boldsymbol{\theta}) \middle| d - h(\boldsymbol{\theta})\right)\right]$$

$$(a\,|\,b) = a_i C_{ij}^{-1} b_i^*$$

Likelihood: $\mathscr{L}(d\,|\,\boldsymbol{\theta}, h) \propto \exp\left[-\frac{1}{2}\left(d - h(\boldsymbol{\theta}) \middle| d - h(\boldsymbol{\theta})\right)\right]$

What are the bins?

… time?

$$(a\,|\,b) = a(t_i) C_{ij}^{-1} b^*(t_j) \qquad i, j \in 1, \ldots, \sim 10^4$$

Inversion scales with N_{bins}^3

… frequency?

Wiener–Khinchin theorem: C_{ij} diagonalizes in the frequency domain

$$(a\,|\,b) = \sum_i \frac{\tilde{a}(f_i)\tilde{b}^*(f_i)}{\sigma^2(f_i)} \quad = 4\mathrm{Re}\int \frac{\tilde{a}(f)\tilde{b}^*(f)}{S_n(f)} df$$

Binary parameter likelihood

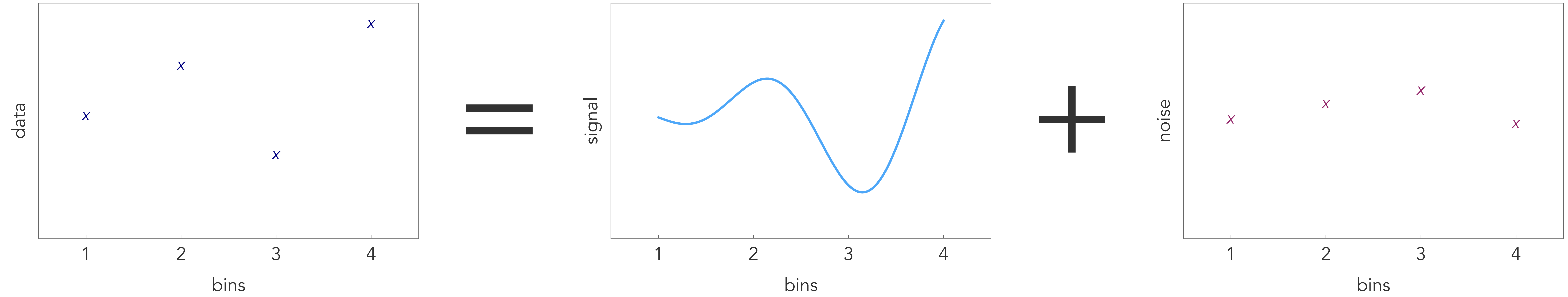

signal $= h(i, \boldsymbol{\theta})$

$$p(\text{noise}) \propto \exp\left[-\frac{1}{2}\left(d - h(\boldsymbol{\theta}) \middle| d - h(\boldsymbol{\theta})\right)\right]$$

$$(a\,|\,b) = a_i C_{ij}^{-1} b_i^*$$

Likelihood: $\mathscr{L}(d\,|\,\boldsymbol{\theta}, h) \propto \exp\left[-\frac{1}{2}\left(d - h(\boldsymbol{\theta}) \middle| d - h(\boldsymbol{\theta})\right)\right]$

What are the bins?

… time?

$$(a\,|\,b) = a(t_i) C_{ij}^{-1} b^*(t_j) \qquad i, j \in 1, \ldots, \sim 10^4$$

Inversion scales with N_{bins}^3

… frequency?

Wiener–Khinchin theorem: C_{ij} diagonalizes in the frequency domain

$$(a\,|\,b) = \sum_i \frac{\tilde{a}(f_i)\tilde{b}^*(f_i)}{\sigma^2(f_i)} \quad = 4\mathrm{Re}\int \frac{\tilde{a}(f)\tilde{b}^*(f)}{S_n(f)} df$$

$S_n(f)$ is the power spectral density (PSD)

Binary parameter likelihood

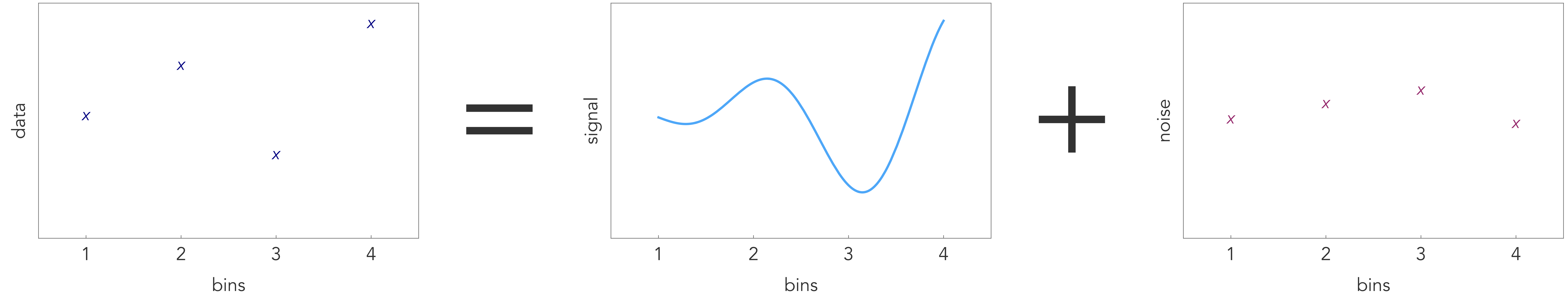

signal $= h(i, \boldsymbol{\theta})$

$$p(\text{noise}) \propto \exp\left[-\frac{1}{2}\left(d - h(\boldsymbol{\theta}) \middle| d - h(\boldsymbol{\theta})\right)\right]$$

$$(a\,|\,b) = a_i C_{ij}^{-1} b_i^*$$

Likelihood: $\mathscr{L}(d\,|\,\boldsymbol{\theta}, h) \propto \exp\left[-\frac{1}{2}\left(d - h(\boldsymbol{\theta}) \middle| d - h(\boldsymbol{\theta})\right)\right]$

What are the bins?

… time?

$$(a\,|\,b) = a(t_i) C_{ij}^{-1} b^*(t_j) \qquad i, j \in 1, \ldots, \sim 10^4$$

Inversion scales with N_{bins}^3

… frequency?

Wiener–Khinchin theorem: C_{ij} diagonalizes in the frequency domain

$$(a\,|\,b) = \sum_i \frac{\tilde{a}(f_i)\tilde{b}^*(f_i)}{\sigma^2(f_i)} \quad = 4\mathrm{Re}\int \frac{\tilde{a}(f)\tilde{b}^*(f)}{S_n(f)} df$$

$S_n(f)$ is the power spectral density (PSD)

$$\sigma^2(f) = \langle \tilde{n}(f)\tilde{n}^*(f) \rangle$$

Binary parameter likelihood

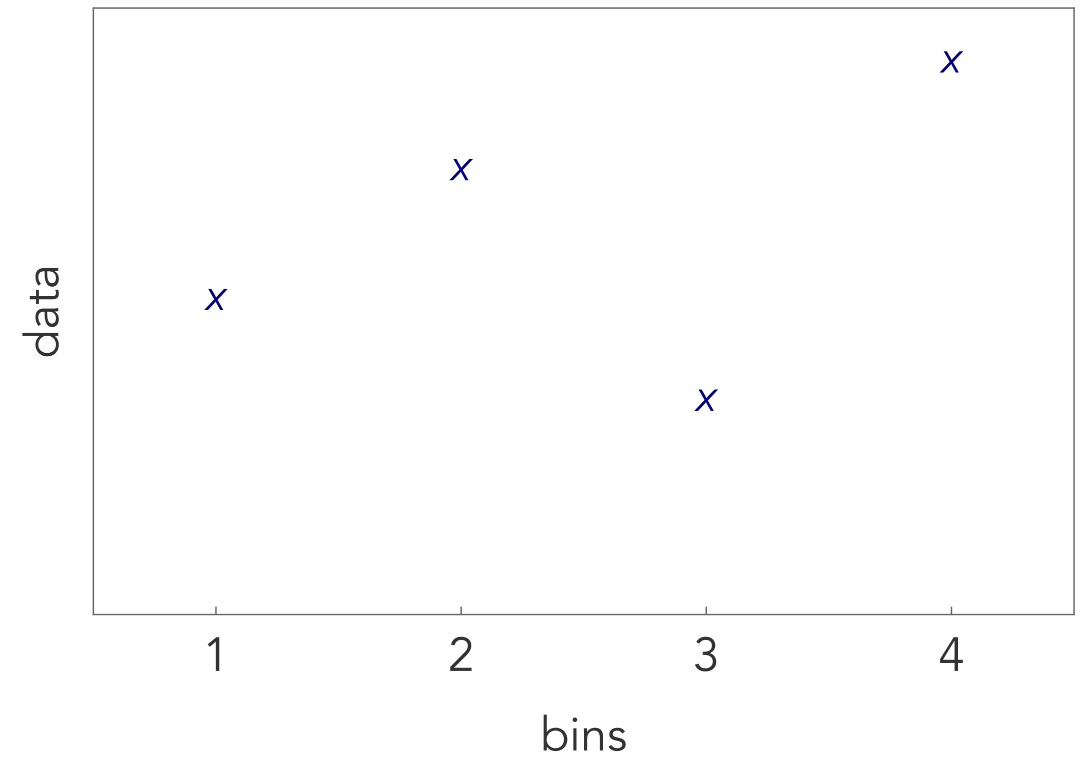

=

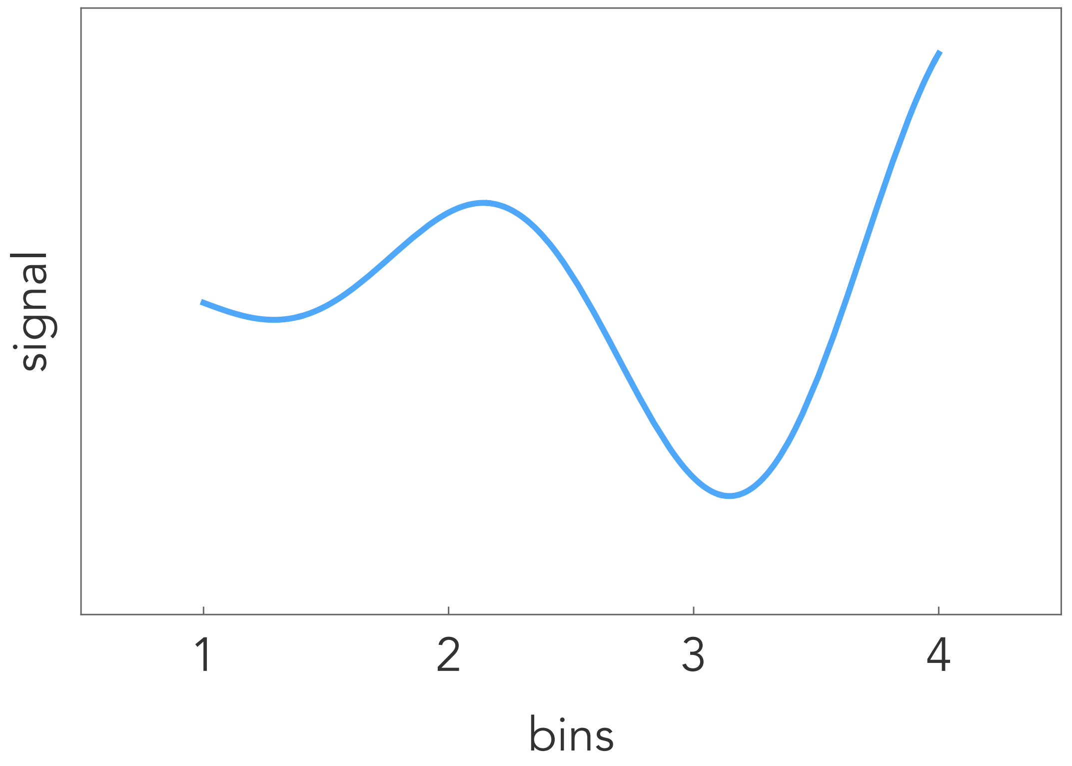

+

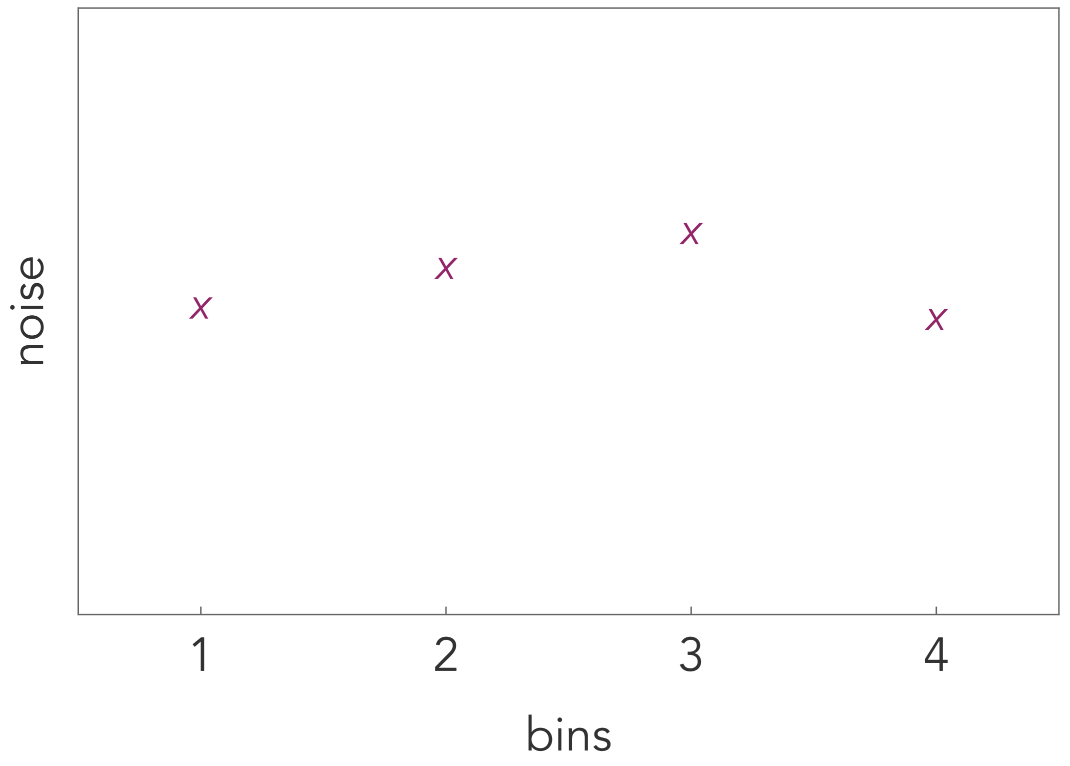

signal $= h(i, \boldsymbol{\theta})$

$$p(\text{noise}) \propto \exp\left[-\frac{1}{2}\left(d - h(\boldsymbol{\theta}) \middle| d - h(\boldsymbol{\theta})\right)\right]$$

Likelihood: $\mathscr{L}(d\,|\,\boldsymbol{\theta}, h) \propto \exp\left[-\frac{1}{2}\left(d - h(\boldsymbol{\theta}) \middle| d - h(\boldsymbol{\theta})\right)\right]$

$$(a\,|\,b) = a_i C_{ij}^{-1} b_i^*$$

What are the bins?

… time?

$$(a\,|\,b) = a(t_i) C_{ij}^{-1} b^*(t_j) \qquad i, j \in 1, \ldots, \sim 10^4$$

Inversion scales with N_{bins}^3

… frequency?

Wiener–Khinchin theorem: C_{ij} diagonalizes in the frequency domain

$$(a\,|\,b) = \sum_i \frac{\tilde{a}(f_i)\tilde{b}^*(f_i)}{\sigma^2(f_i)} = 4\mathrm{Re}\int \frac{\tilde{a}(f)\tilde{b}^*(f)}{S_n(f)} df$$

$S_n(f)$ is the power spectral density (PSD)

$$\sigma^2(f) = \langle \tilde{n}(f)\tilde{n}^*(f) \rangle$$

$$\langle \tilde{n}(f)\tilde{n}^*(f') \rangle = \frac{1}{2}\delta(f - f') S_n(f)$$

Binary parameter likelihood

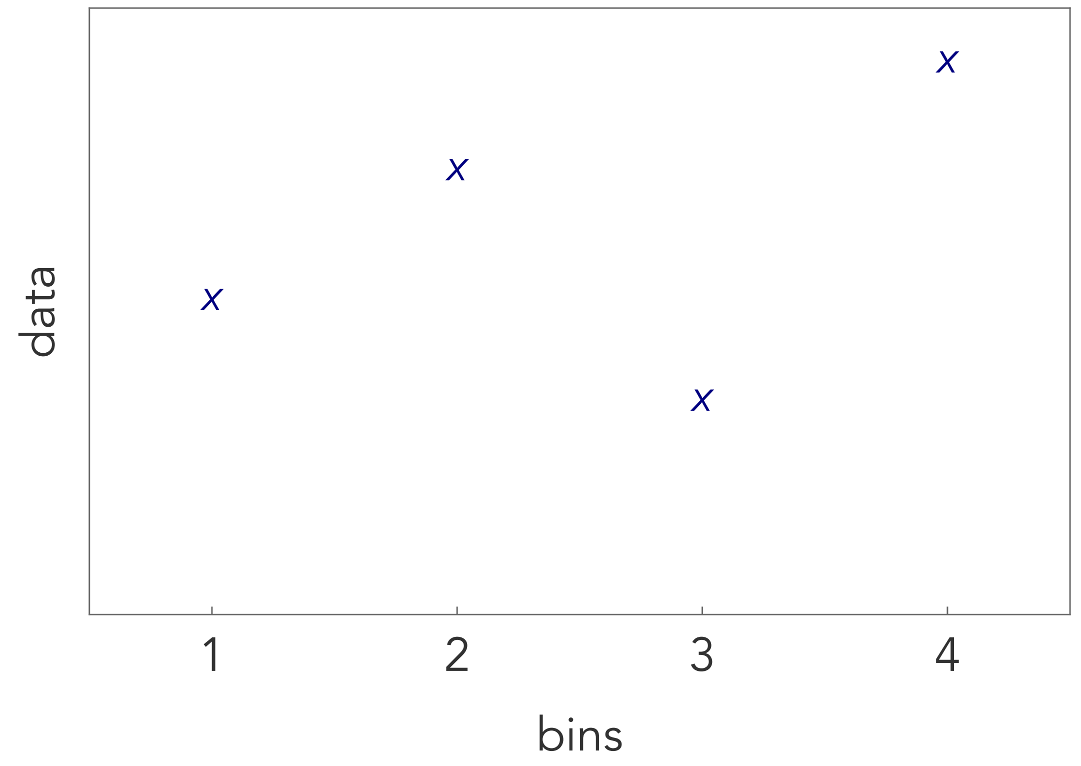

=

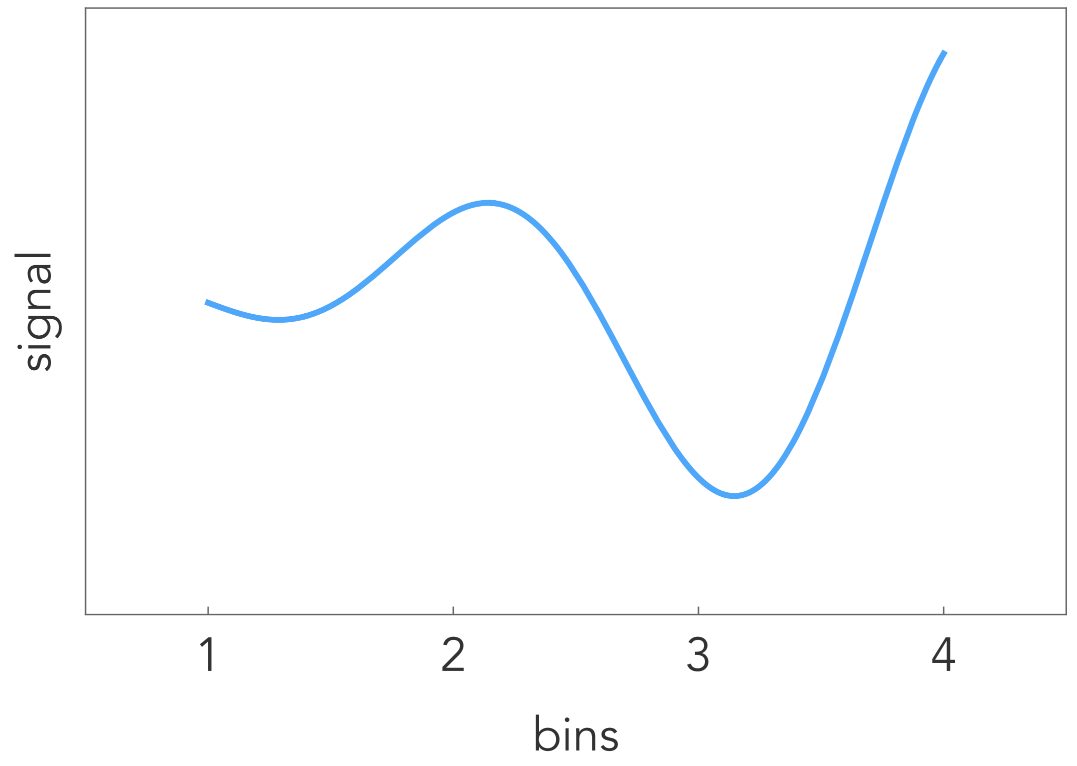

+

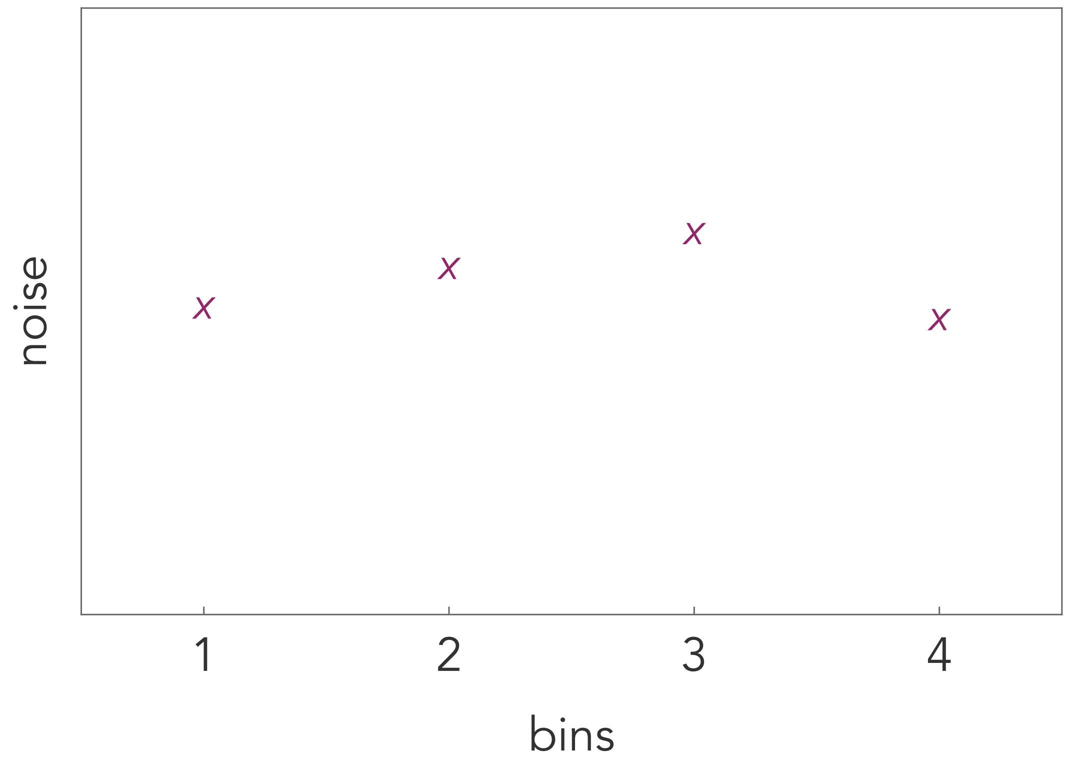

signal $= h(i, \boldsymbol{\theta})$

$$p(\mathrm{noise}) \propto \exp\left[-\frac{1}{2}\left(d - h(\boldsymbol{\theta}) \middle| d - h(\boldsymbol{\theta})\right)\right]$$

$$(a \,|\, b) = a_i C_{ij}^{-1} b_i^*$$

Likelihood: $\mathscr{L}(d \,|\, \boldsymbol{\theta}, h) \propto \exp\left[-\frac{1}{2}\left(d - h(\boldsymbol{\theta}) \middle| d - h(\boldsymbol{\theta})\right)\right]$

What are the bins?

… time?

$(a \,|\, b) = a(t_i) C_{ij}^{-1} b^*(t_j) \qquad i, j \in 1, \ldots, \sim 10^4$

Inversion scales with N_{bins}^3

… frequency?

Wiener–Khinchin theorem: C_{ij} diagonalizes in the frequency domain

$$(a \,|\, b) = \sum_i \frac{\tilde{a}(f_i)\tilde{b}^*(f_i)}{\sigma^2(f_i)} = 4\mathrm{Re}\int \frac{\tilde{a}(f)\tilde{b}^*(f)}{S_n(f)} df$$

$S_n(f)$ is the power spectral density (PSD)

$$\sigma^2(f) = \langle \tilde{n}(f)\tilde{n}^*(f) \rangle$$

$$\langle \tilde{n}(f)\tilde{n}^*(f') \rangle = \frac{1}{2}\delta(f - f') S_n(f)$$

PSD/SNR

PSD/SNR

Power Spectral Density: $S_n(f) \sim 10^{-46}\ \mathrm{Hz}^{-1}$ (for LIGO)

PSD/SNR

Power Spectral Density: $S_n(f) \sim 10^{-46}\ \mathrm{Hz}^{-1}$ (for LIGO)

Amplitude Spectral Density: $\sqrt{S_n(f)} \sim 10^{-23}\ \mathrm{Hz}^{-1/2}$ (for LIGO)

PSD/SNR

Power Spectral Density: $S_n(f) \sim 10^{-46}\ \mathrm{Hz}^{-1}$ (for LIGO)

Amplitude Spectral Density: $\sqrt{S_n(f)} \sim 10^{-23}\ \mathrm{Hz}^{-1/2}$ (for LIGO)

SNR: $\rho^2 = 4 \int \frac{\tilde{h}(f)\tilde{h}^*(f)}{S_n(f)} df = (h \,|\, h)$

PSD/SNR

Power Spectral Density: $S_n(f) \sim 10^{-46}\ \mathrm{Hz}^{-1}$ (for LIGO)

Amplitude Spectral Density: $\sqrt{S_n(f)} \sim 10^{-23}\ \mathrm{Hz}^{-1/2}$ (for LIGO)

SNR: $\rho^2 = 4 \int \frac{\tilde{h}(f)\tilde{h}^*(f)}{S_n(f)} df = (h\,|\,h)$

Characteristic Strain: $h_c(f) = 2f\tilde{h}(f)$

PSD/SNR

Power Spectral Density: $S_n(f) \sim 10^{-46}\ \mathrm{Hz}^{-1}$ (for LIGO)

Amplitude Spectral Density: $\sqrt{S_n(f)} \sim 10^{-23}\ \mathrm{Hz}^{-1/2}$ (for LIGO)

SNR: $\rho^2 = 4\int \frac{\tilde{h}(f)\tilde{h}^*(f)}{S_n(f)} df = (h\,|\,h)$

Characteristic Strain: $h_c(f) = 2f\tilde{h}(f)$

Noise Amplitude: $h_n(f) = f^{1/2}\sqrt{S_n(f)}$

PSD/SNR

Power Spectral Density: $S_n(f) \sim 10^{-46}\ \mathrm{Hz}^{-1}$ (for LIGO)

Amplitude Spectral Density: $\sqrt{S_n(f)} \sim 10^{-23}\ \mathrm{Hz}^{-1/2}$ (for LIGO)

SNR: $\rho^2 = 4\int \frac{\tilde{h}(f)\tilde{h}^*(f)}{S_n(f)} df = (h|h)$

Characteristic Strain: $h_c(f) = 2f\tilde{h}(f)$

Noise Amplitude: $h_n(f) = f^{1/2}\sqrt{S_n(f)}$

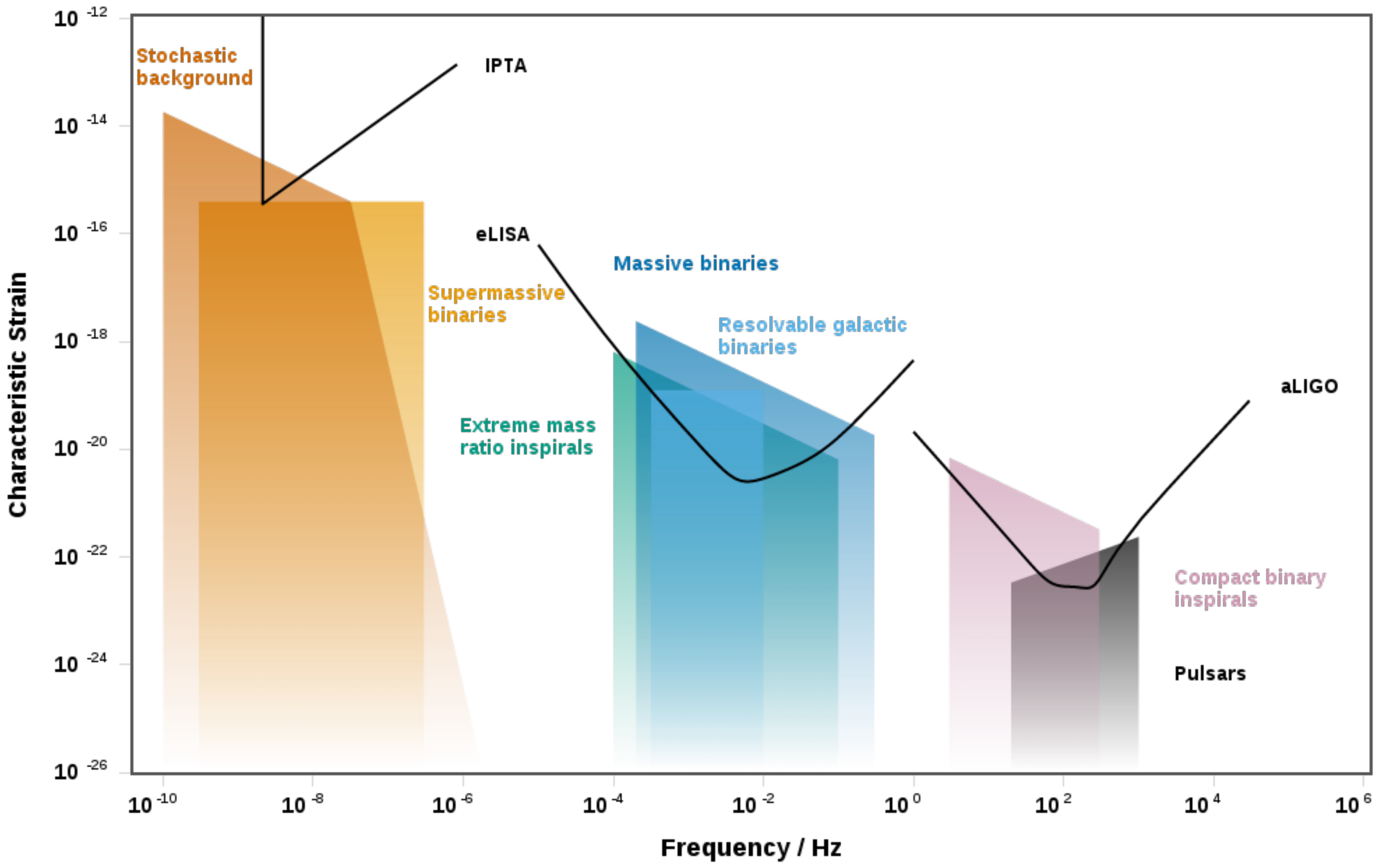

PSD/SNR

Power Spectral Density: $S_n(f) \sim 10^{-46}\ \mathrm{Hz}^{-1}$ (for LIGO)

Amplitude Spectral Density: $\sqrt{S_n(f)} \sim 10^{-23}\ \mathrm{Hz}^{-1/2}$ (for LIGO)

SNR: $\rho^2 = 4\int \frac{\tilde{h}(f)\tilde{h}^*(f)}{S_n(f)}df = (h\,|\,h)$

Characteristic Strain: $h_c(f) = 2f\tilde{h}(f)$

Noise Amplitude: $h_n(f) = f^{1/2}\sqrt{S_n(f)}$

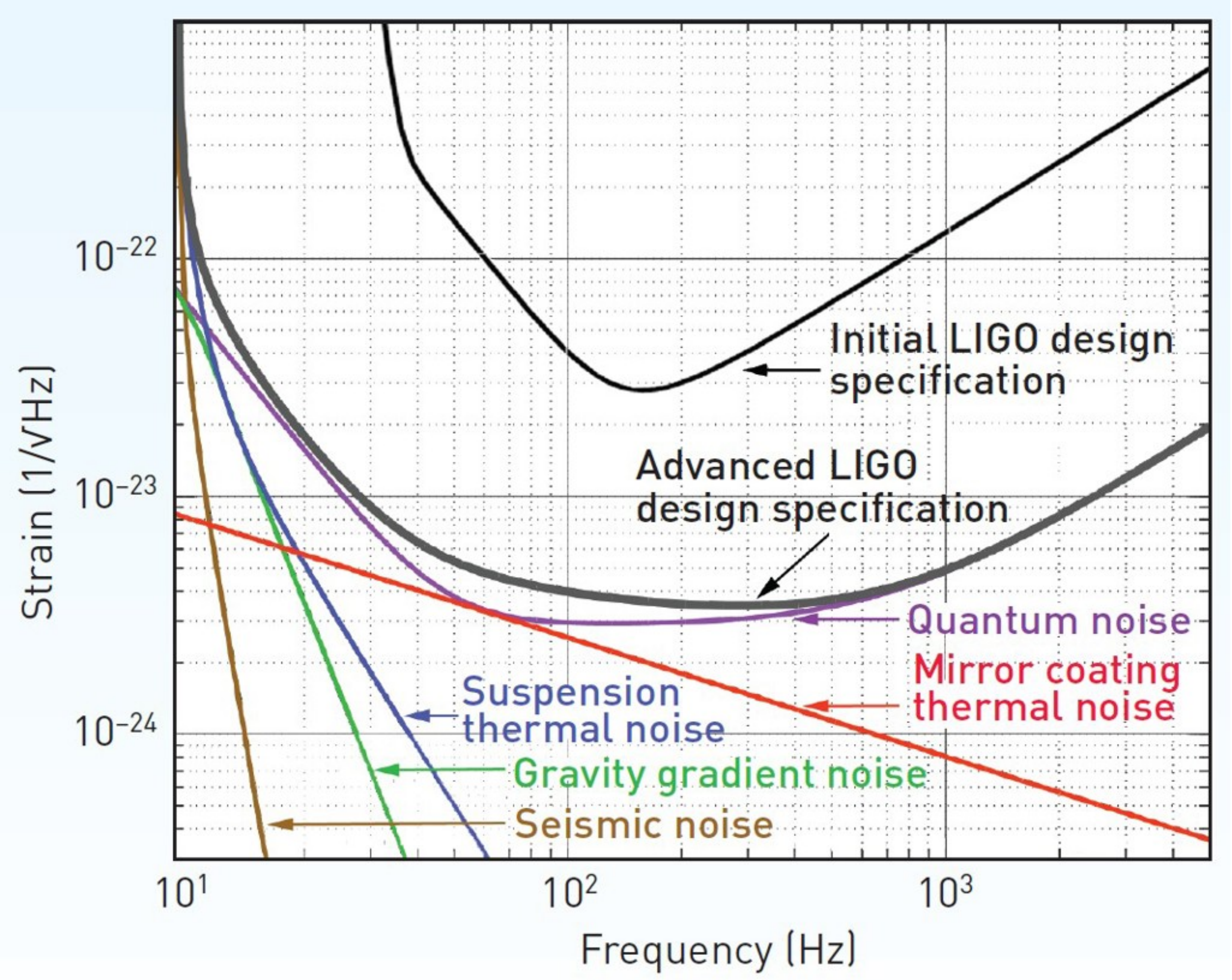

Detector frame vs source frame

Detector frame vs source frame

Our waveforms do not assume any cosmology. We measure what the source parameters would have been if the wave had traveled through a flat, static universe (detector-frame parameters). However…

Detector frame vs source frame

Our waveforms do not assume any cosmology. We measure what the source parameters would have been if the wave had traveled through a flat, static universe (detector-frame parameters). However…

The frequency is shifted by cosmic expansion: $f_{\mathrm{det}} = f_{\mathrm{src}}/(1+z)$

Detector frame vs source frame

Our waveforms do not assume any cosmology. We measure what the source parameters would have been if the wave had traveled through a flat, static universe (detector-frame parameters). However…

The frequency is shifted by cosmic expansion: $f_{\mathrm{det}} = f_{\mathrm{src}}/(1+z)$

So is the perceived distance from the source: $D_L = (1+z)D_C$

Detector frame vs source frame

Our waveforms do not assume any cosmology. We measure what the source parameters would have been if the wave had traveled through a flat, static universe (detector-frame parameters). However…

The frequency is shifted by cosmic expansion: $f_{\rm det} = f_{\rm src}/(1+z)$

So is the perceived distance from the source: $D_L = (1+z)D_C$

The leading order term of the strain is: $h \sim \dfrac{m_{\rm det}^{5/3} f_{\rm det}^{2/3}}{D_L}$

Detector frame vs source frame

Our waveforms do not assume any cosmology. We measure what the source parameters would have been if the wave had traveled through a flat, static universe (detector-frame parameters). However…

The frequency is shifted by cosmic expansion: $f_{\rm det} = f_{\rm src}/(1+z)$

So is the perceived distance from the source: $D_L = (1+z)D_C$

The leading order term of the strain is: $h \sim \dfrac{m_{\rm det}^{5/3} f_{\rm det}^{2/3}}{D_L}$

So the total mass we measure is: $m_{\rm det} = (1+z)m_{\rm src}$

Population inference

Population inference

Parameter estimation:
Learn about single events

Population inference

Parameter estimation:
Learn about single events

$$p(\boldsymbol{\theta}\,|\,d) = \frac{\mathscr{L}(d\,|\,\boldsymbol{\theta})\pi(\boldsymbol{\theta})}{\mathscr{Z}(d)}$$

$$\boldsymbol{\theta} = \{m_1, m_2, \chi_1, \chi_2, d_L \dots\}$$

$d =$ 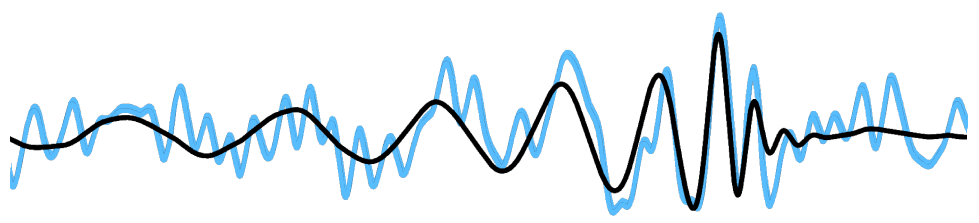 $= h$

$$\mathscr{L}(d\,|\,\boldsymbol{\theta}) \sim \exp\left[-\frac{1}{2}\big(d - h(\boldsymbol{\theta})\big)^2\right]$$

Hierarchical inference:
Learn about population properties

Population inference

Parameter estimation:
Learn about single events

$$p(\boldsymbol{\theta} \,|\, d) = \frac{\mathscr{L}(d \,|\, \boldsymbol{\theta})\pi(\boldsymbol{\theta})}{\mathscr{Z}(d)}$$

$$\boldsymbol{\theta} = \{m_1, m_2, \chi_1, \chi_2, d_L \ldots\}$$

$d =$ 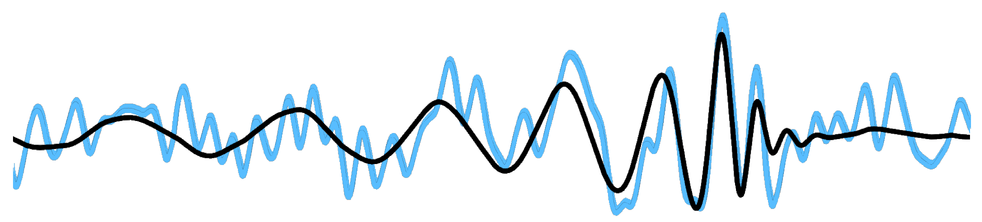 $= h$

$$\mathscr{L}(d \,|\, \boldsymbol{\theta}) \sim \exp\left[-\frac{1}{2}\big(d - h(\boldsymbol{\theta})\big)^2\right]$$

Hierarchical inference:
Learn about population properties

$$p(\boldsymbol{\Lambda} \,|\, \{d_k\}) = \frac{\mathscr{L}(\{d_k\} \,|\, \boldsymbol{\Lambda})\pi(\boldsymbol{\Lambda})}{\mathscr{Z}(\{d_k\})}$$

$\boldsymbol{\Lambda}$ = population parameters

$\{d_k\} =$ 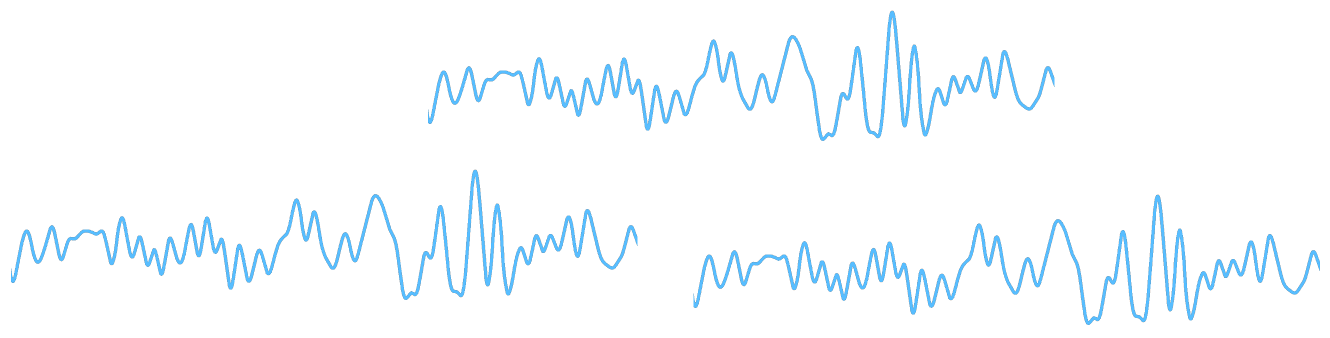

$$\mathscr{L}(\{d_k\} \,|\, \boldsymbol{\Lambda}) \sim \prod_k^n \int d\boldsymbol{\theta} \mathscr{L}(d_k \,|\, \boldsymbol{\theta}_k)\pi(\boldsymbol{\theta}_k \,|\, \boldsymbol{\Lambda})$$

Population inference

Parameter estimation:
Learn about single events

$$p(\boldsymbol{\theta}\,|\,d) = \frac{\mathscr{L}(d\,|\,\boldsymbol{\theta})\pi(\boldsymbol{\theta})}{\mathscr{Z}(d)}$$

$$\boldsymbol{\theta} = \{m_1, m_2, \chi_1, \chi_2, d_L \dots\}$$

$d =$ 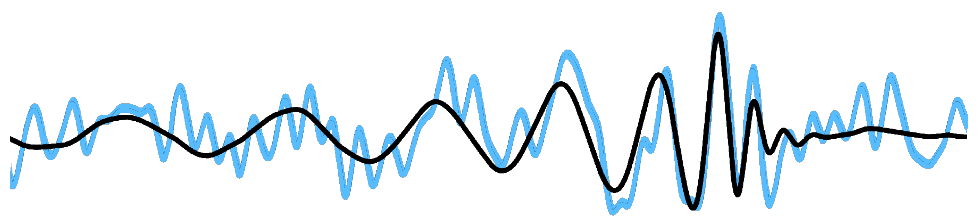 $= h$

$$\mathscr{L}(d\,|\,\boldsymbol{\theta}) \sim \exp\left[-\frac{1}{2}\big(d - h(\boldsymbol{\theta})\big)^2\right]$$

Hierarchical inference:
Learn about population properties

$$p(\boldsymbol{\Lambda}\,|\,\{d_k\}) = \frac{\mathscr{L}(\{d_k\}\,|\,\boldsymbol{\Lambda})\pi(\boldsymbol{\Lambda})}{\mathscr{Z}(\{d_k\})}$$

$\boldsymbol{\Lambda}$ = population parameters

$\{d_k\} =$ 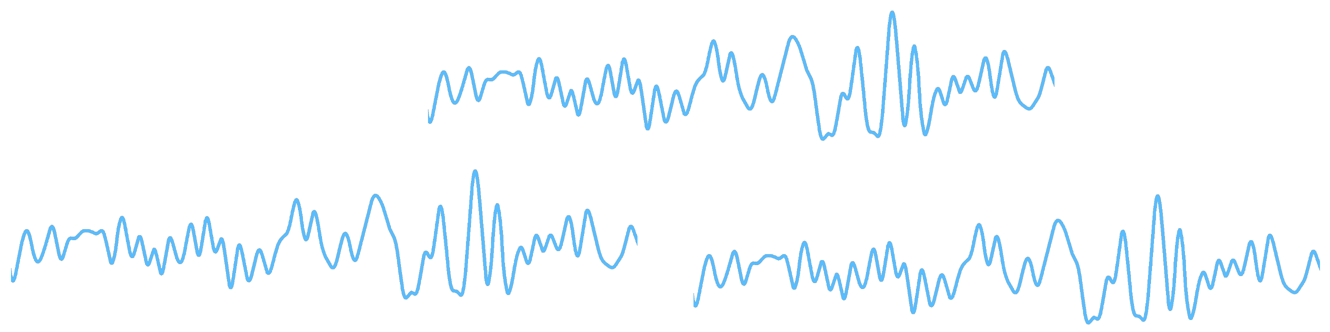

$$\mathscr{L}(\{d_k\}\,|\,\boldsymbol{\Lambda}) \sim \prod_k^n \mathscr{Z}(d_k)\frac{1}{m_k}\sum_j^{m_k}\frac{\pi(\boldsymbol{\theta}_k^j\,|\,\boldsymbol{\Lambda})}{\pi(\boldsymbol{\theta}_k^j)}$$

Population inference

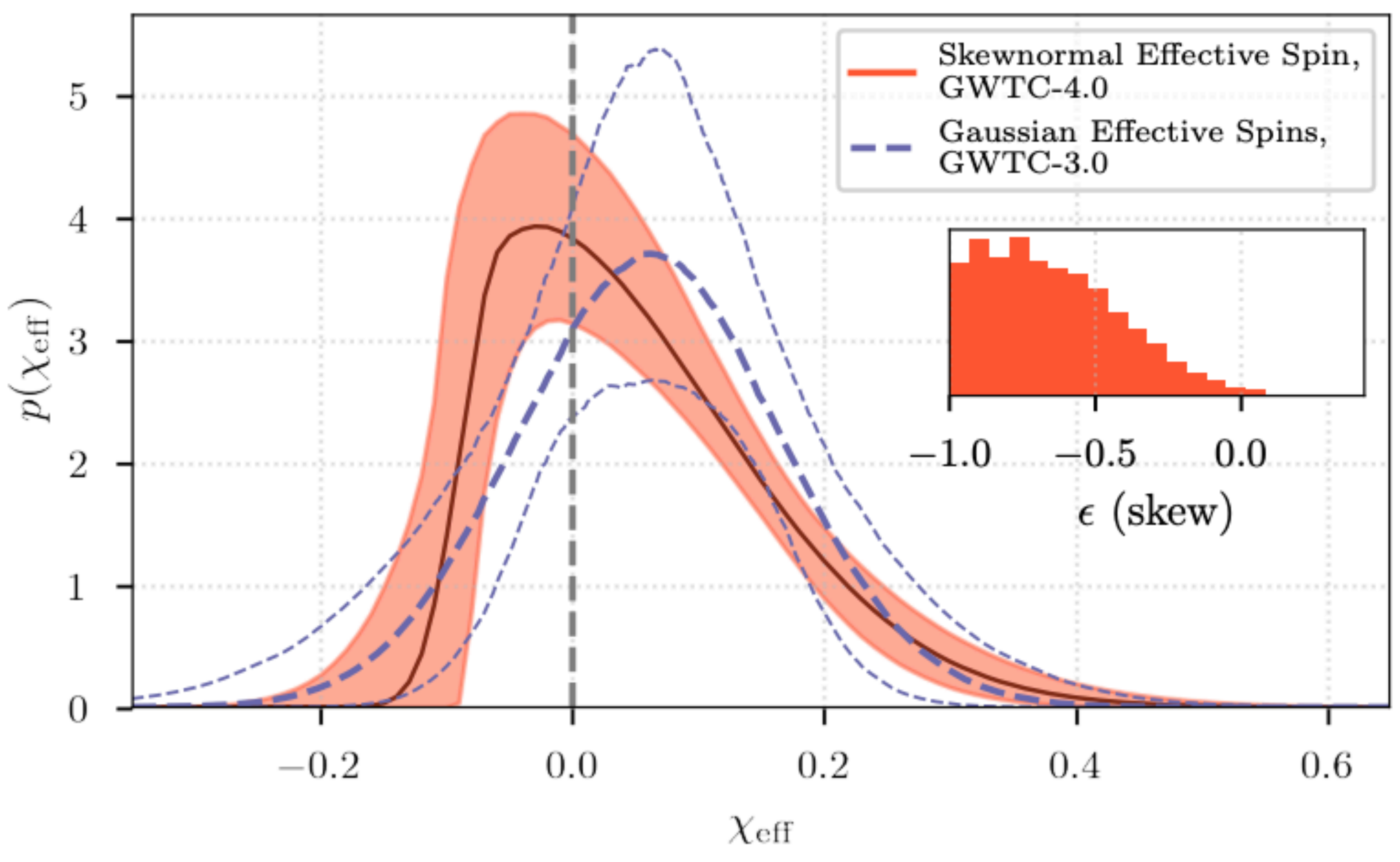

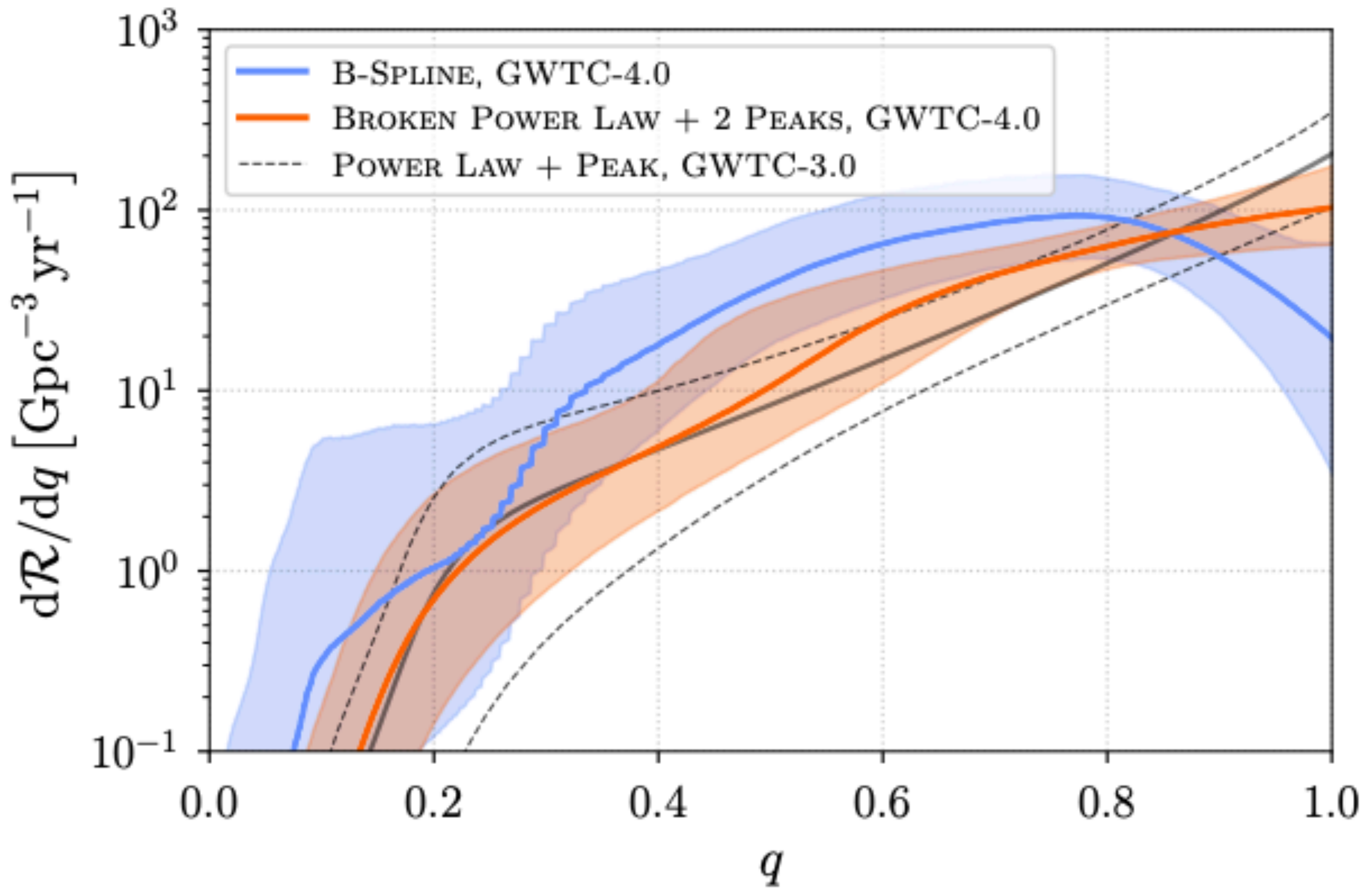

(GWTC4)

Population inference

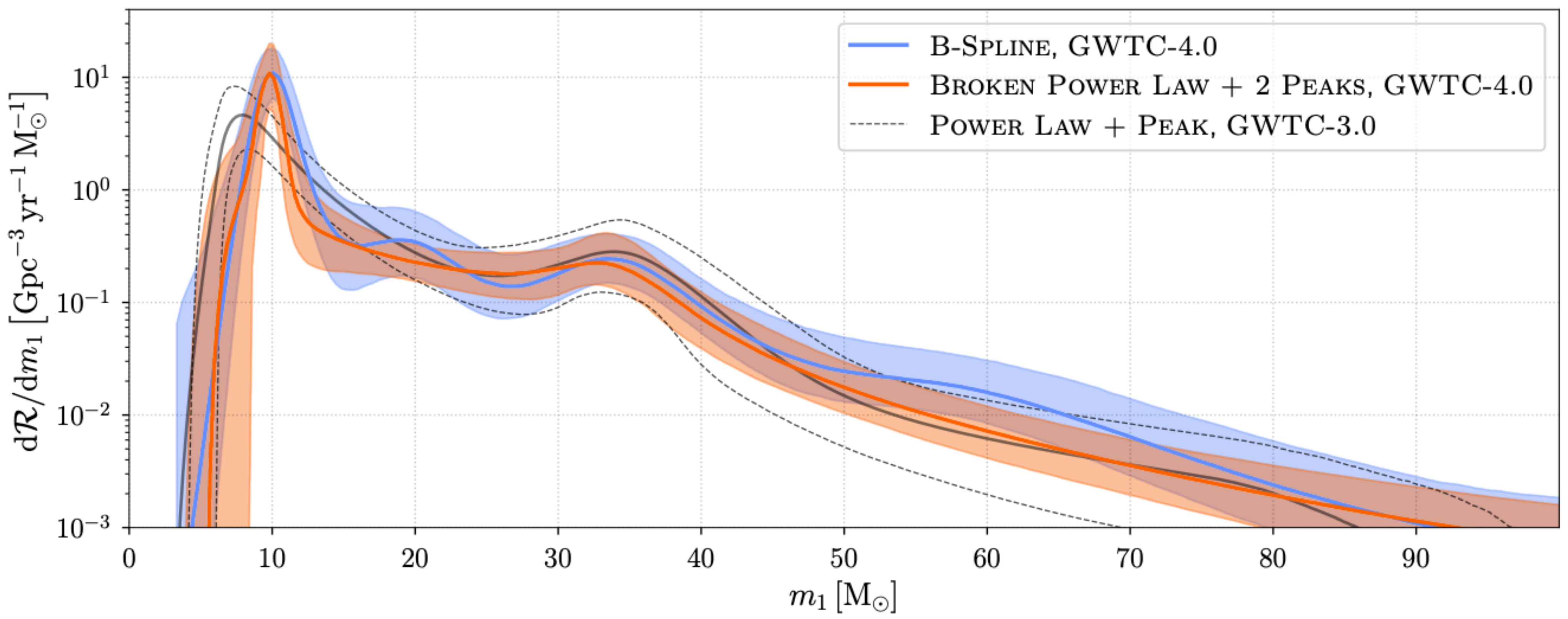

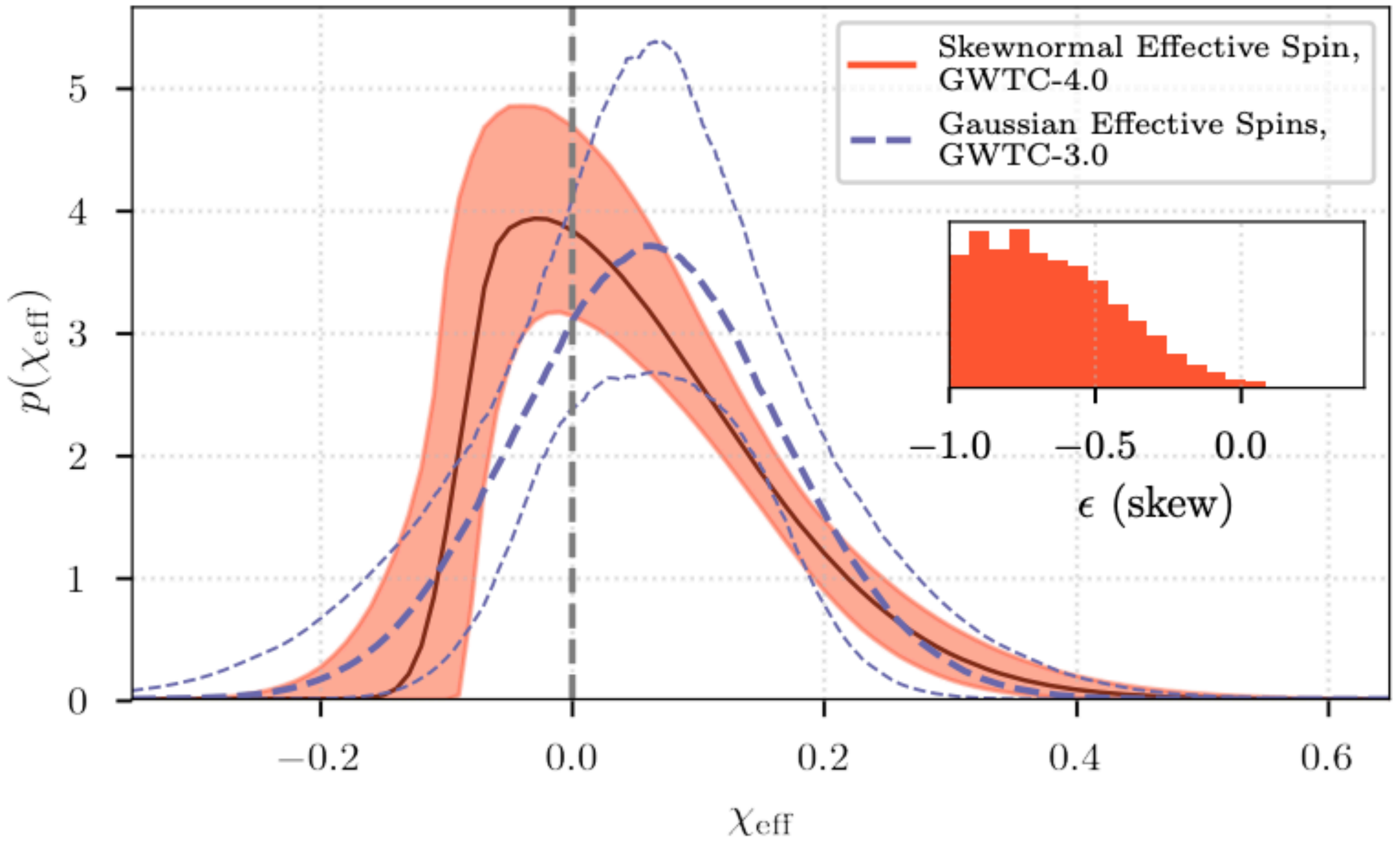

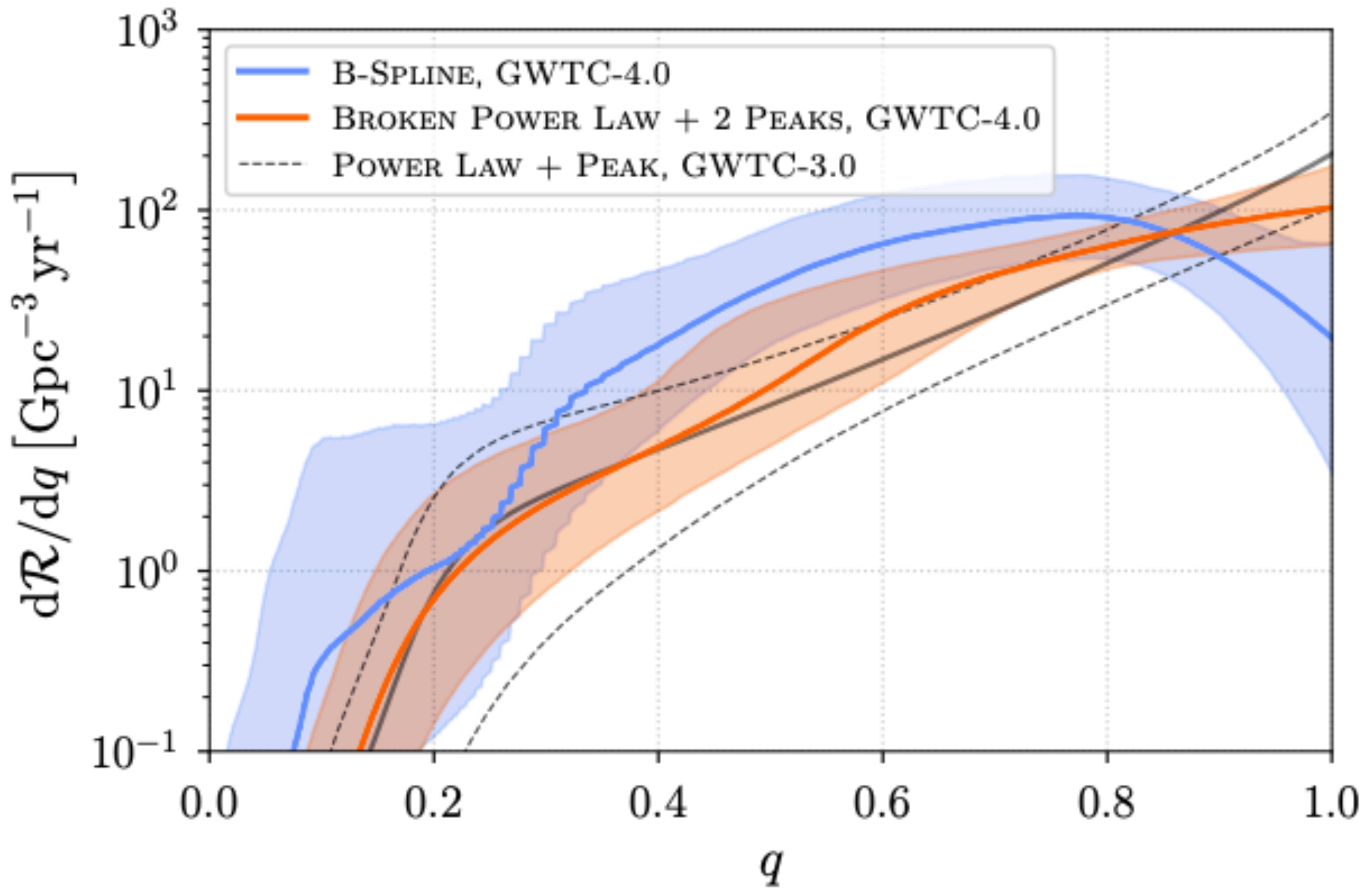

(GWTC4)

Future detectors

Future detectors

Space-based detectors:
LISA (Laser Interferometer Space Antenna)
Planned launch: 2035

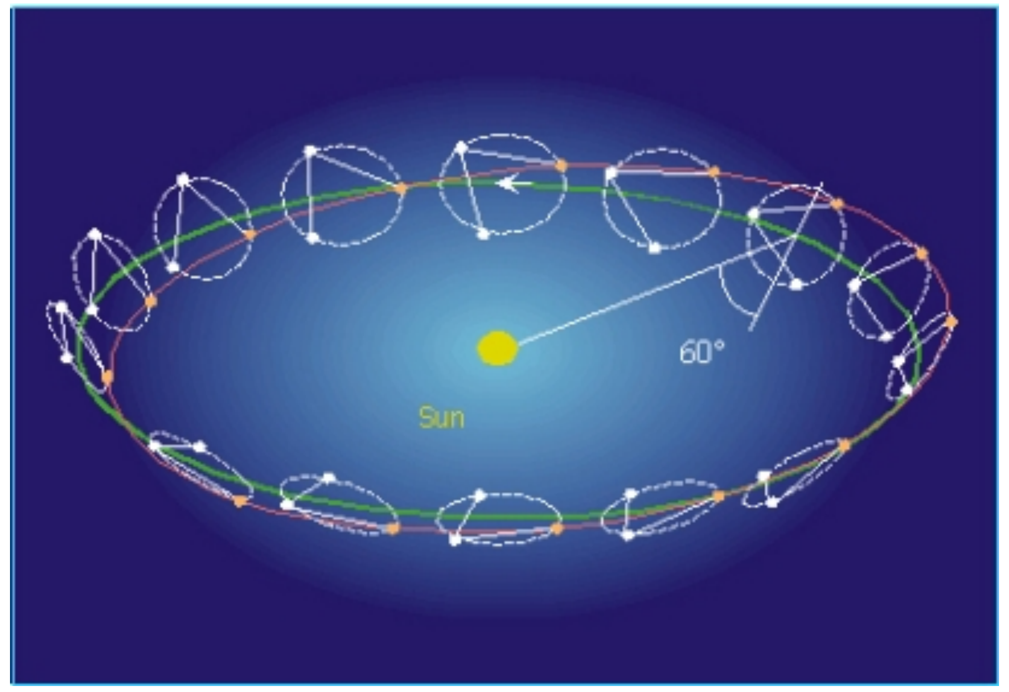

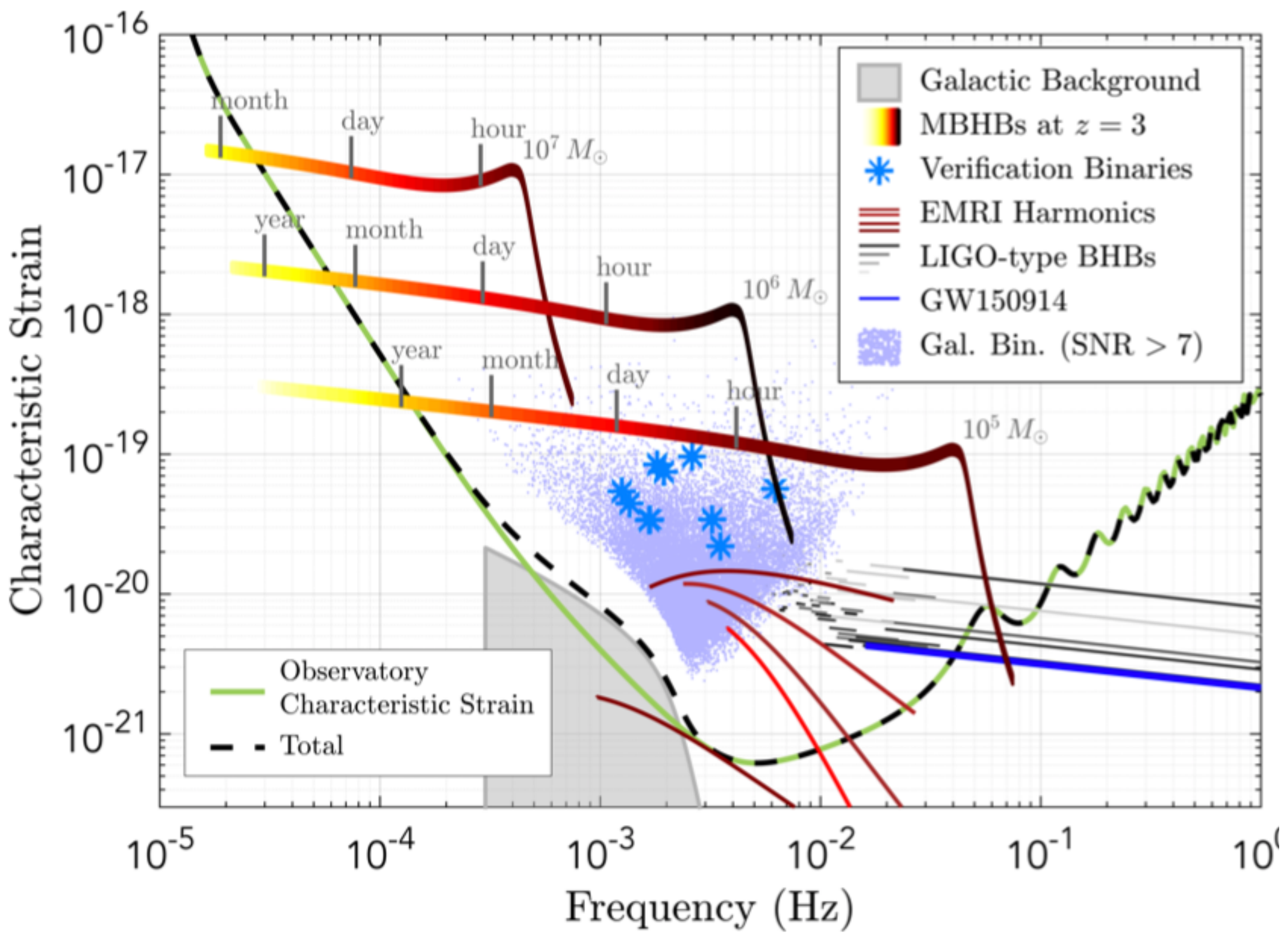

Future detectors

Space-based detectors:
LISA (Laser Interferometer Space Antenna)
Planned launch: 2035

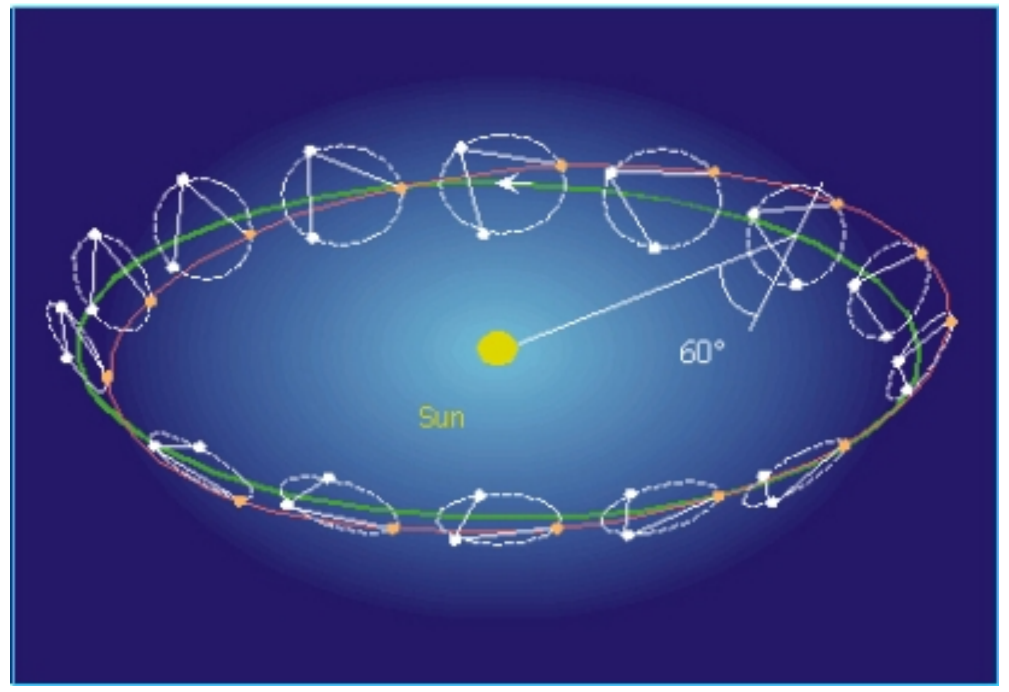

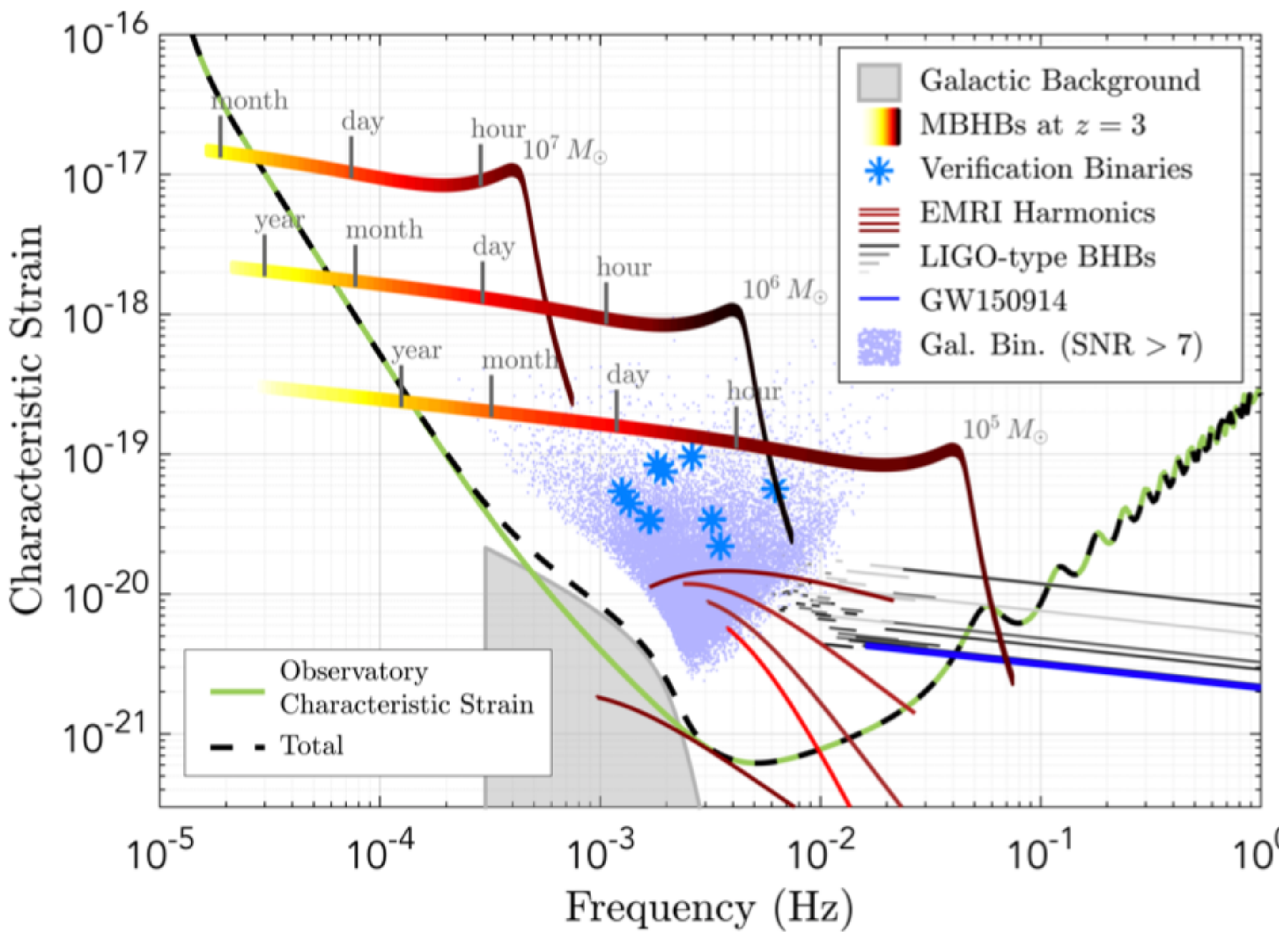

Third-generation ground-based detectors:
Einstein Telescope (Europe)
Planned completion: 2035

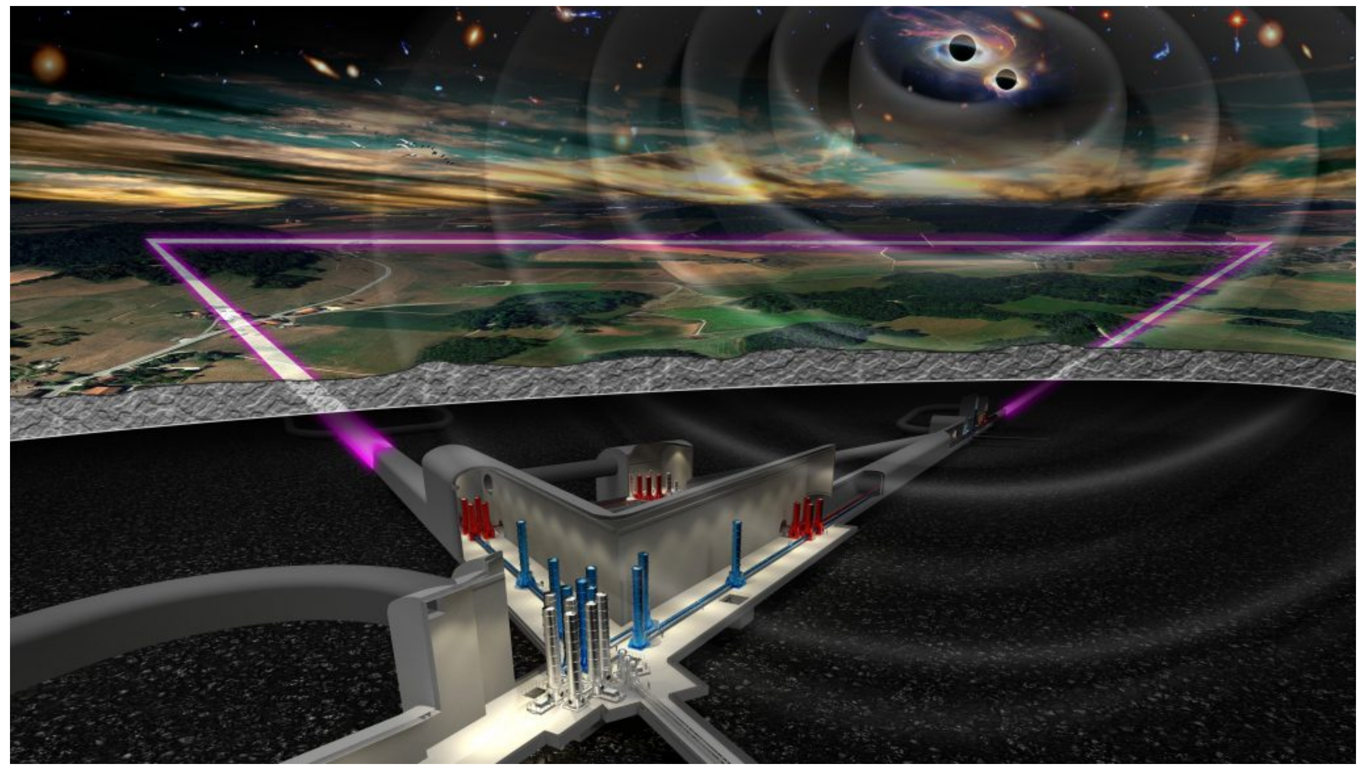

Cosmic Explorer (USA)
Planned completion: mid 2030s-2040s

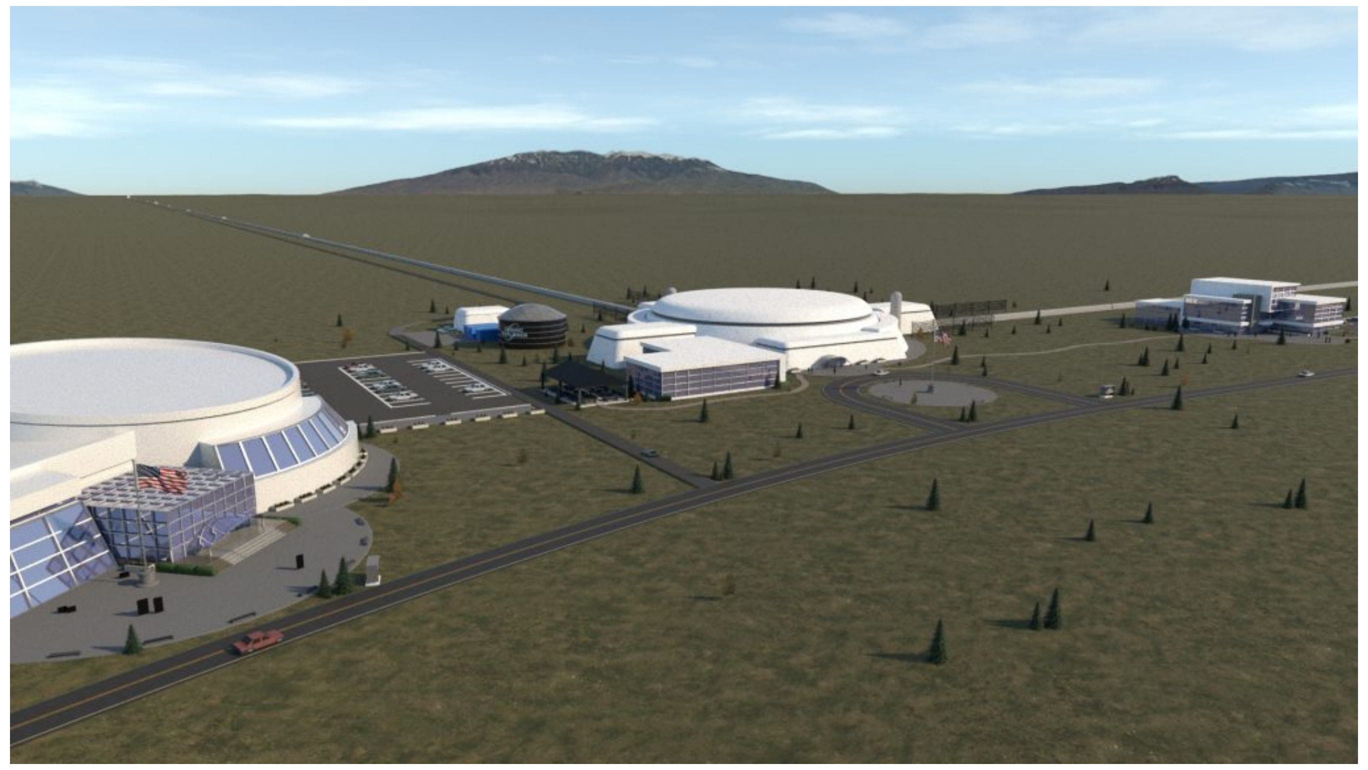

Future detectors

Space-based detectors:

LISA (Laser Interferometer Space Antenna)
Planned launch: 2035

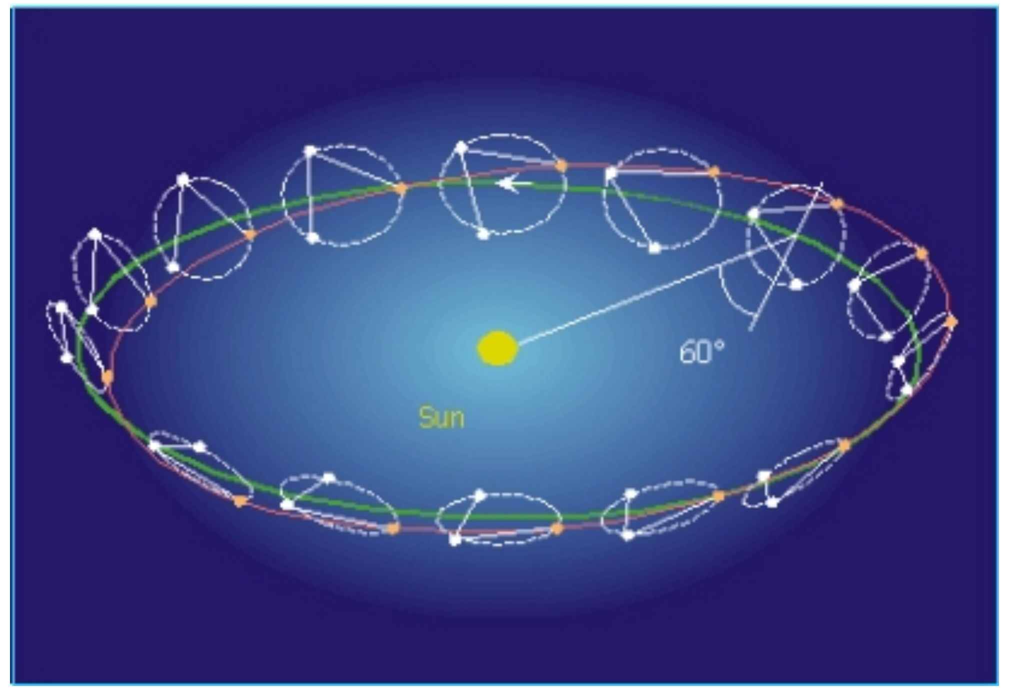

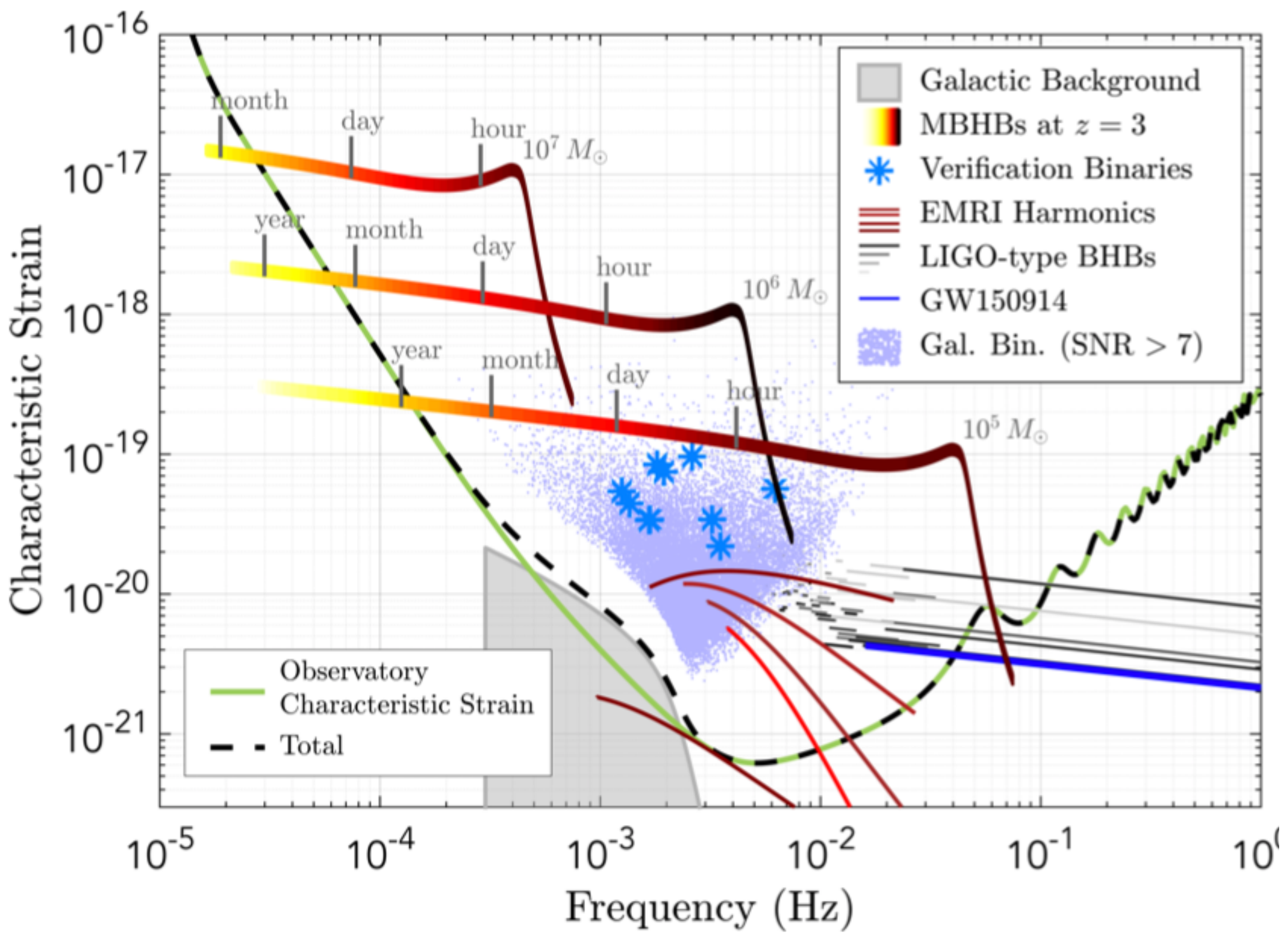

Third-generation ground-based detectors:

Einstein Telescope (Europe)
Planned completion: 2035

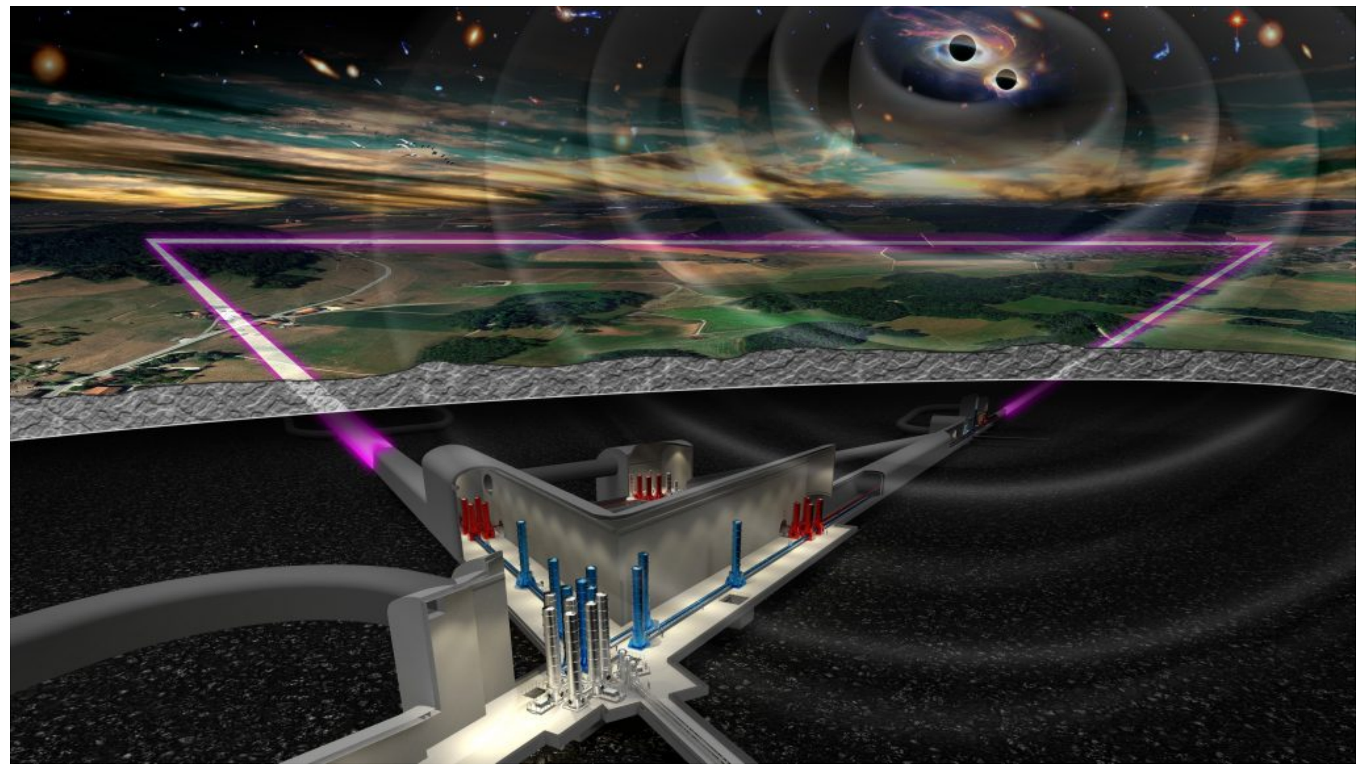

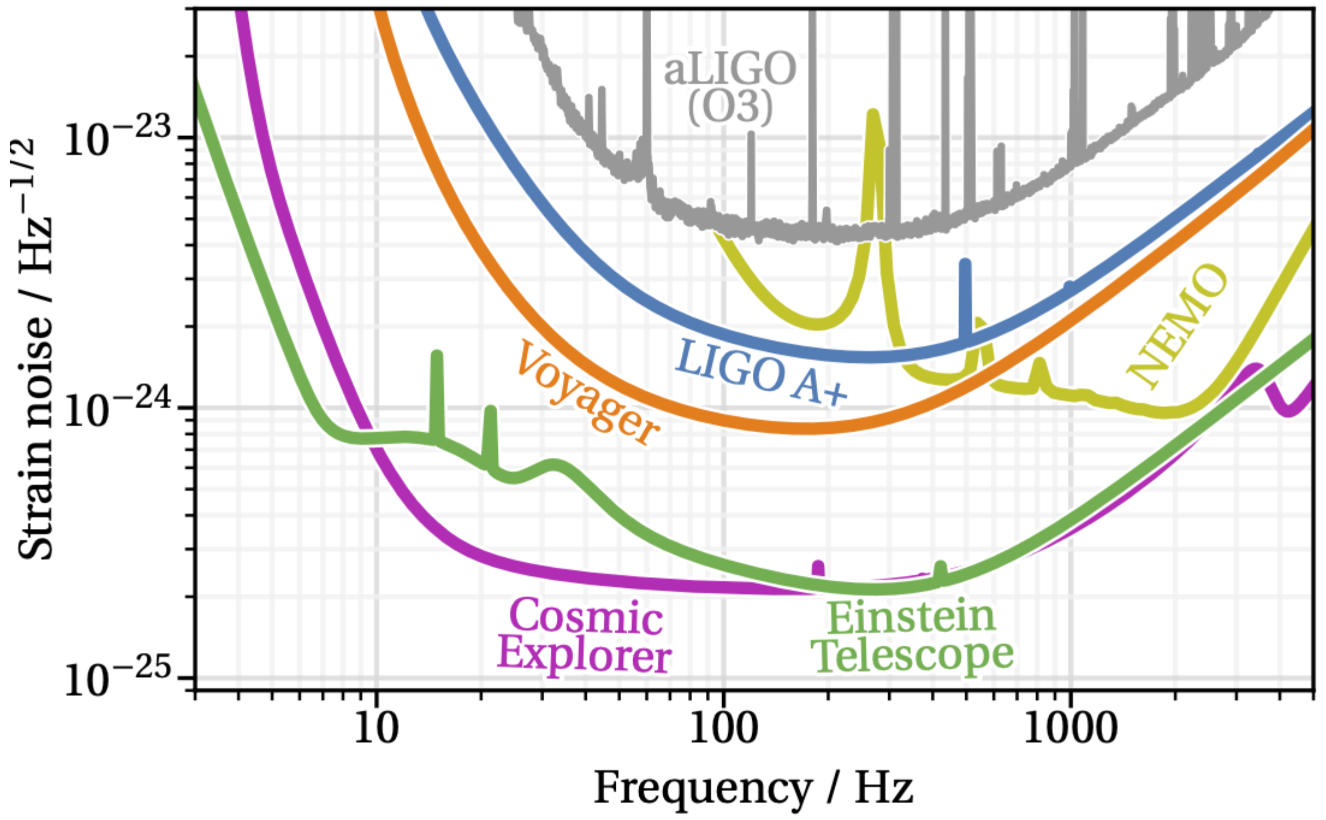

Cosmic Explorer (USA)
Planned completion: mid 2030s-2040s

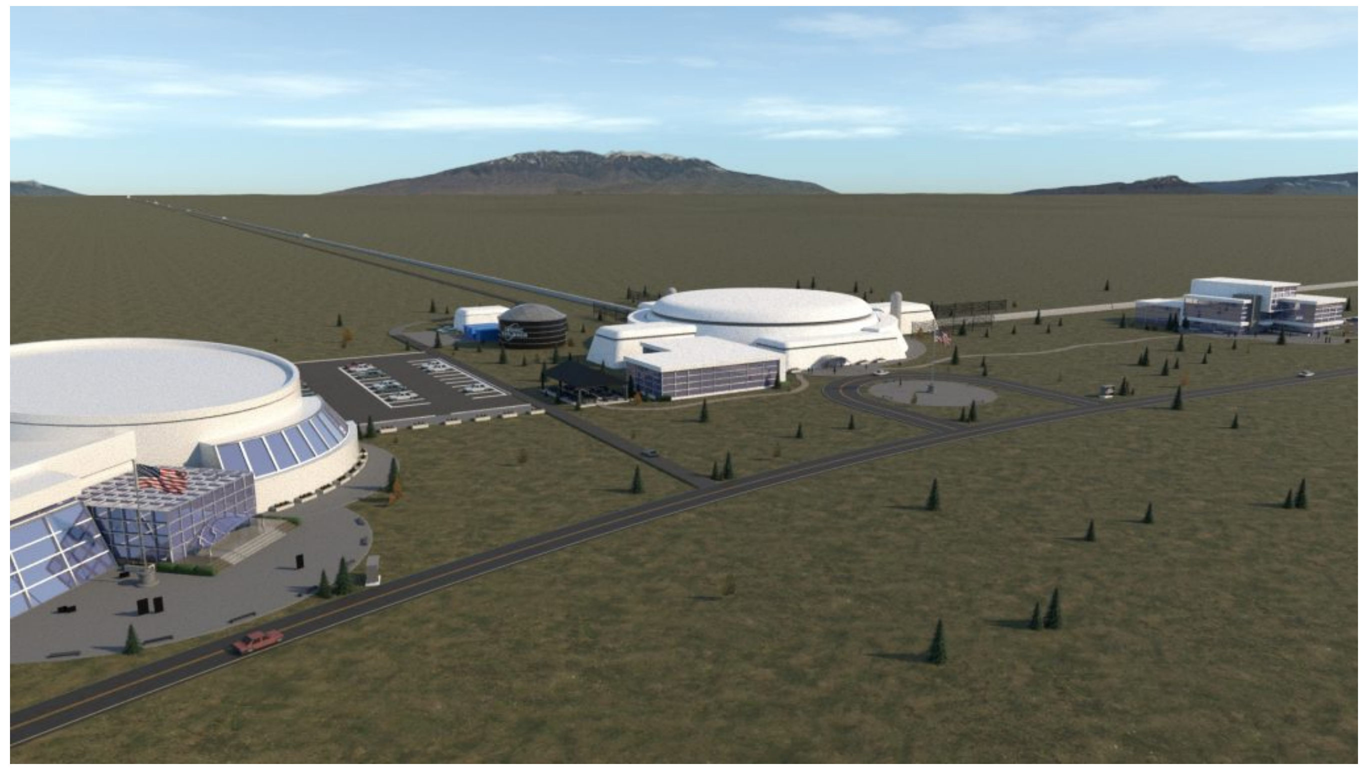

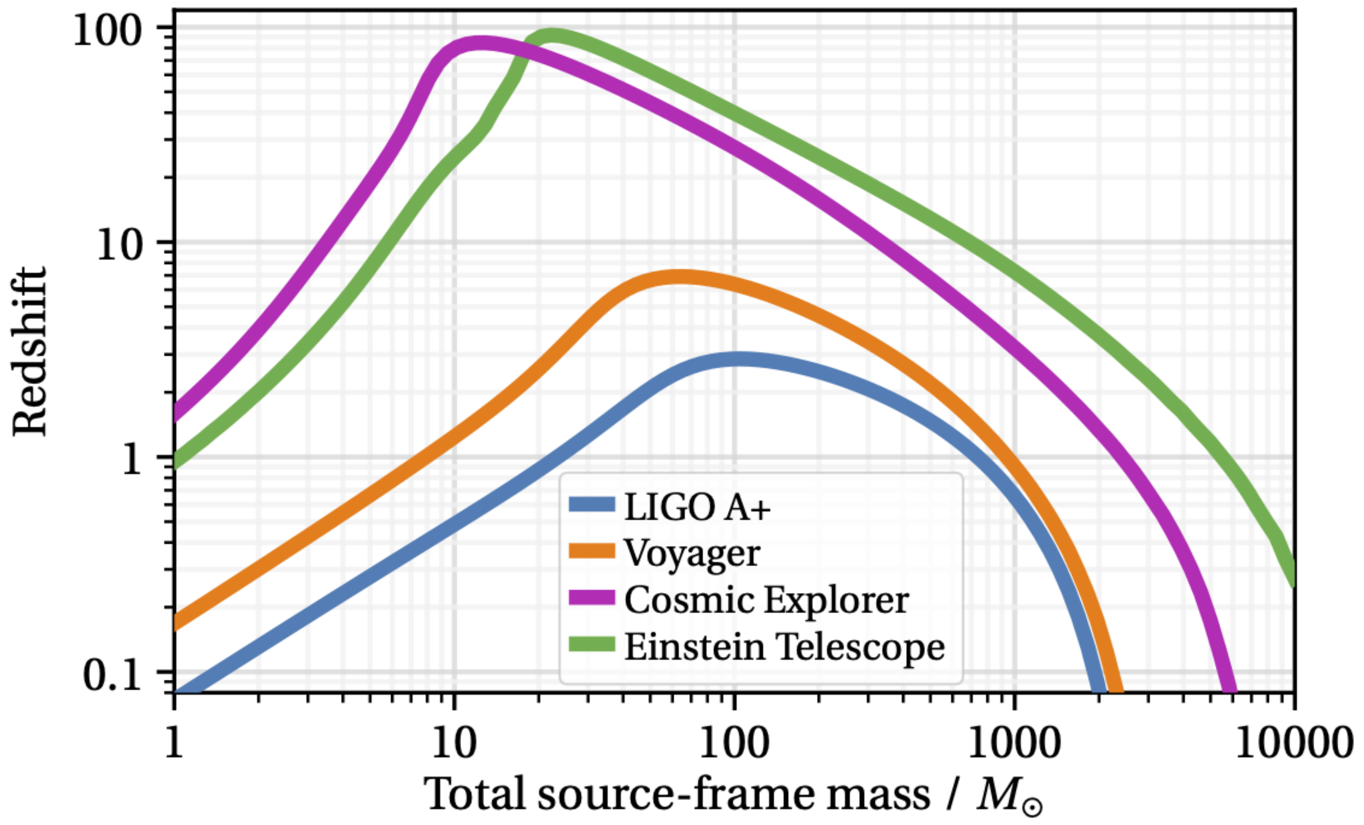

A new window into dark matter

A new window into dark matter

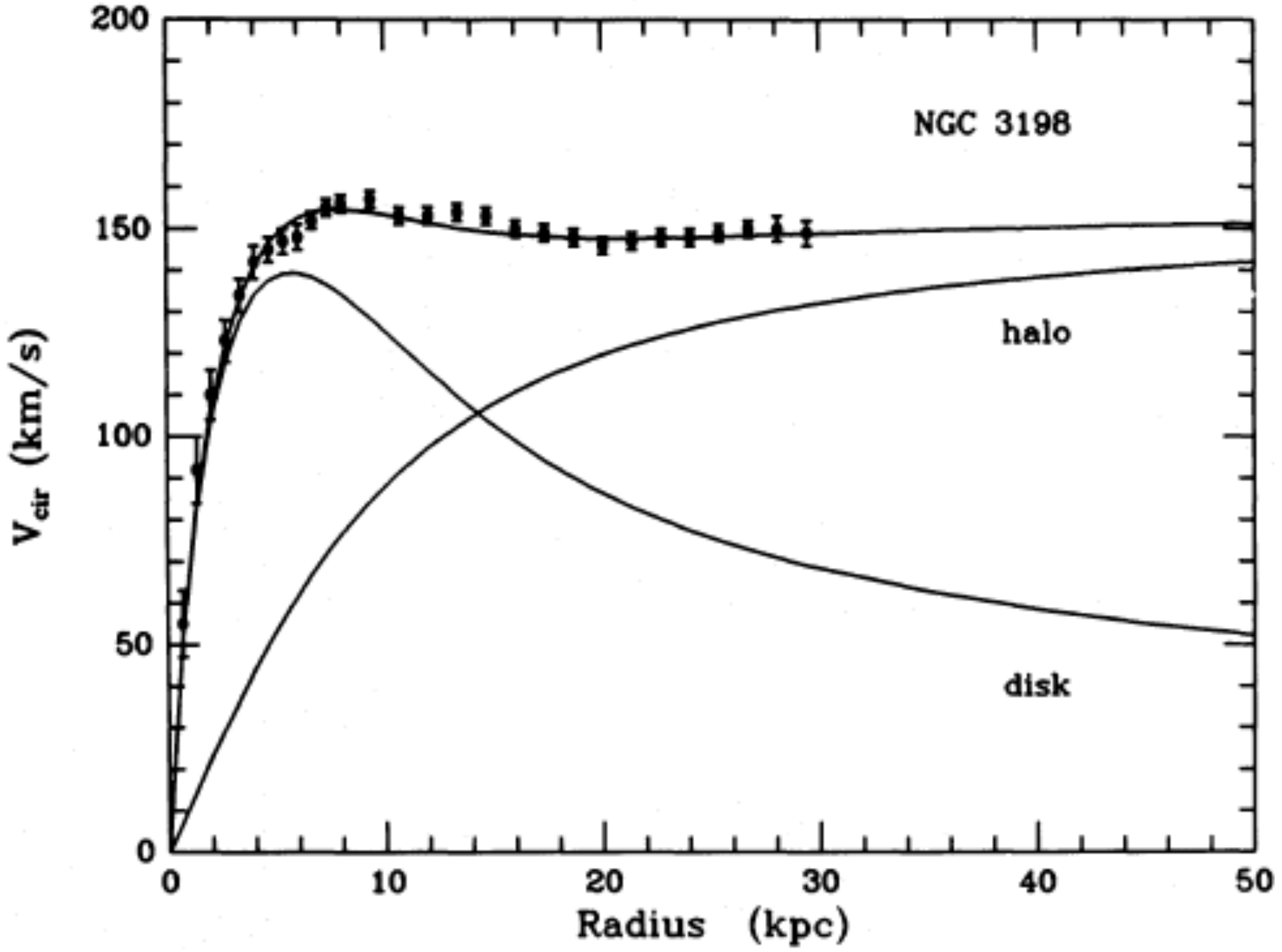

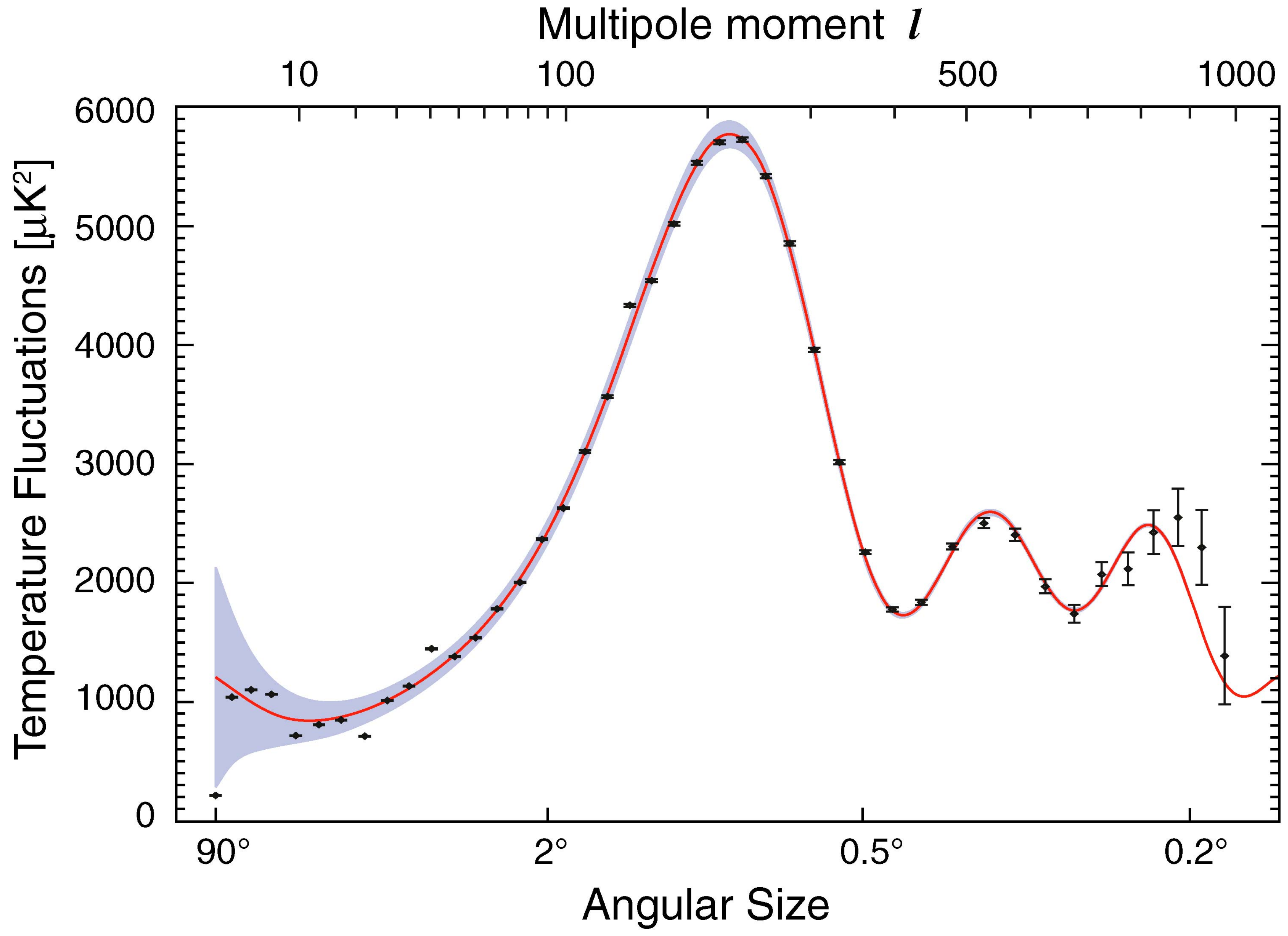

A new window into dark matter

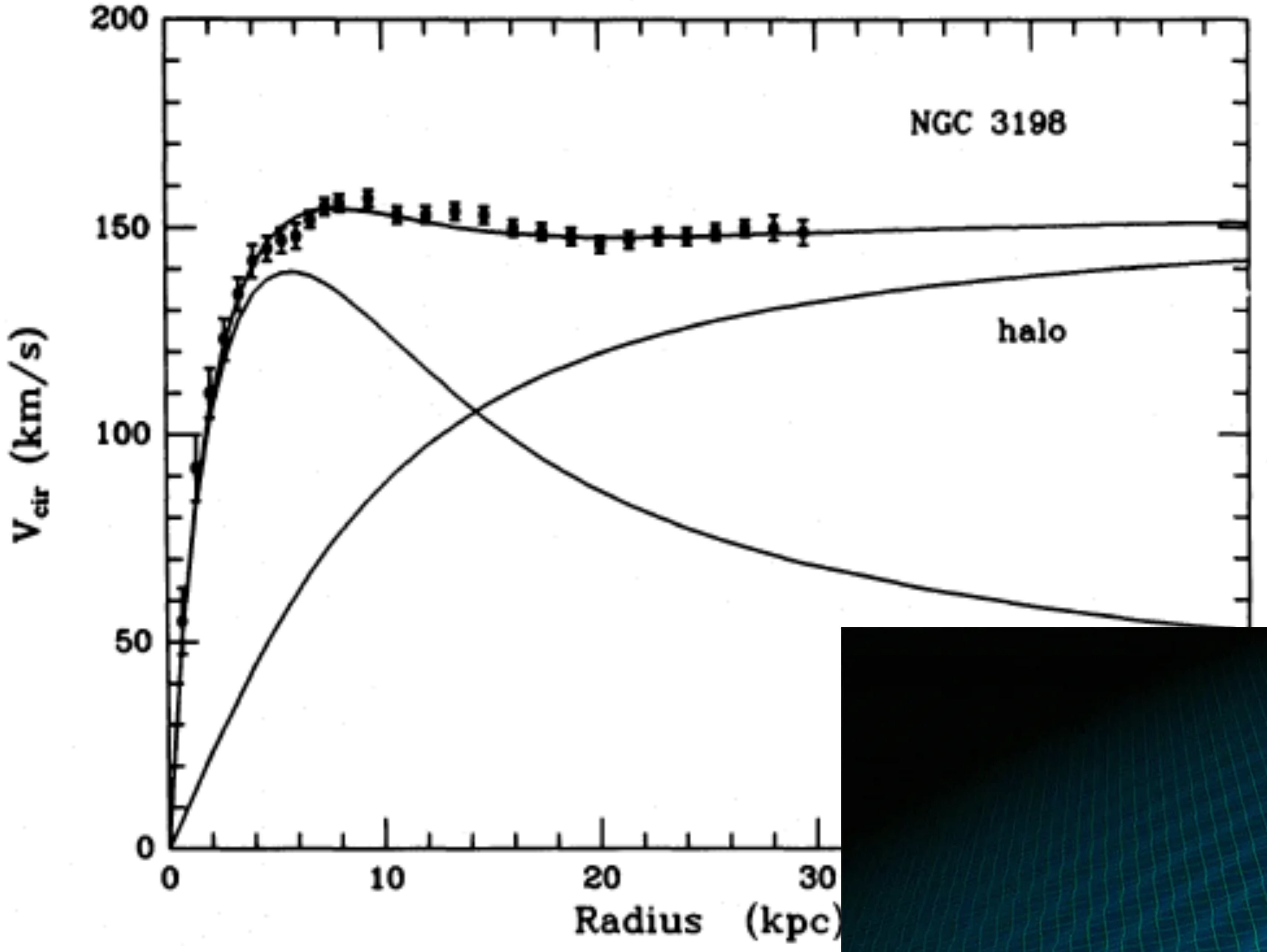

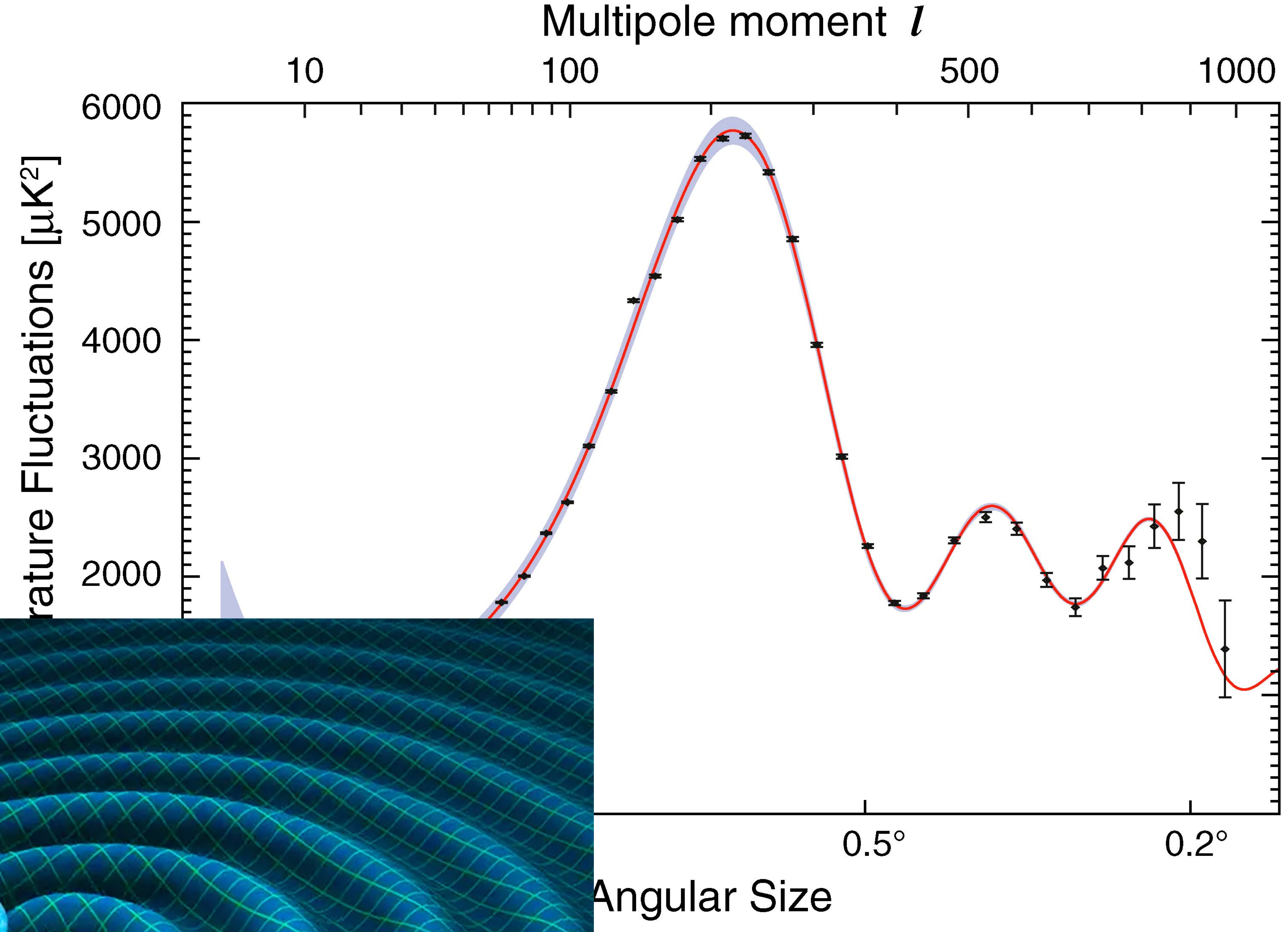

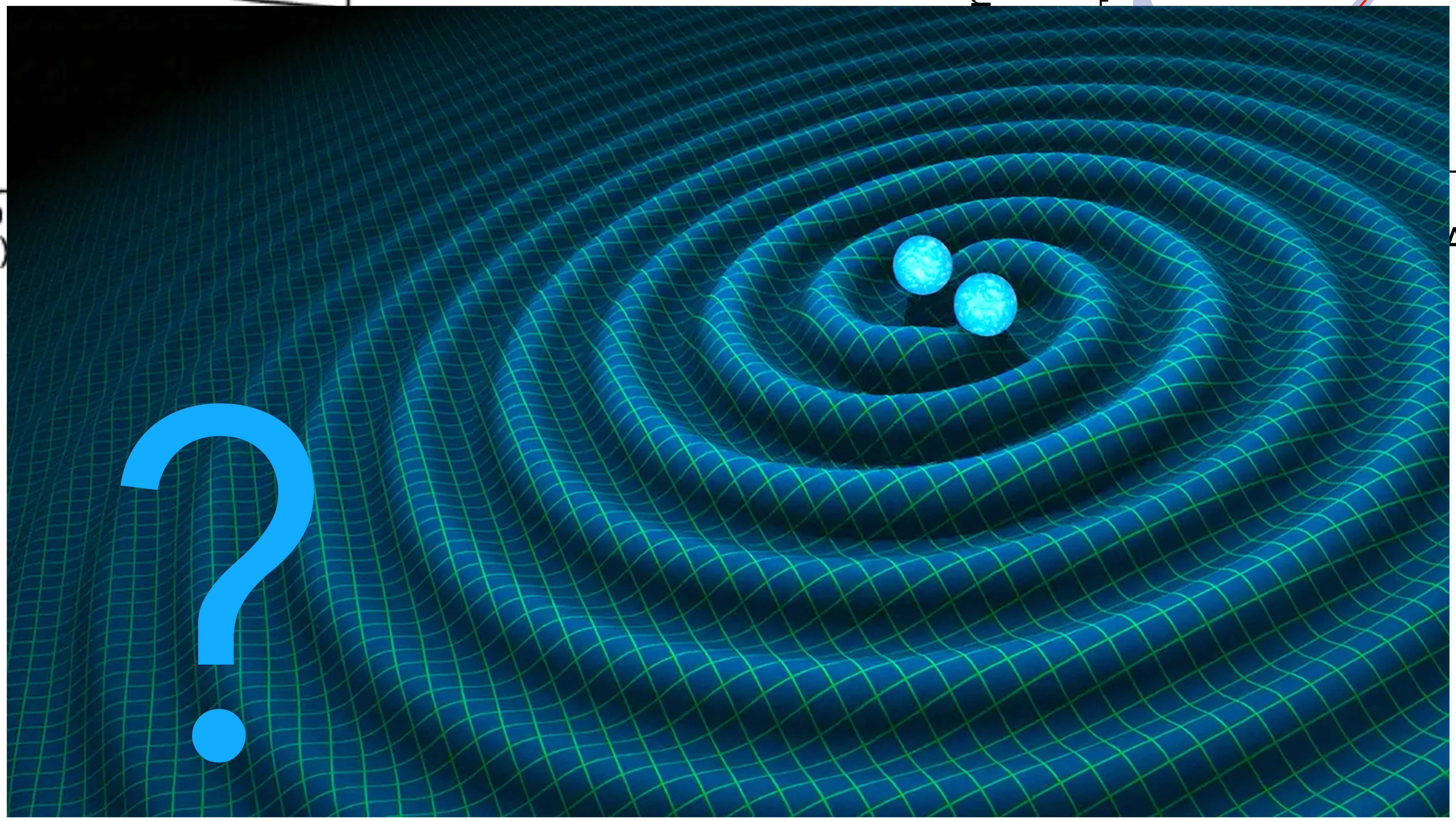

A new window into dark matter

A new window into dark matter

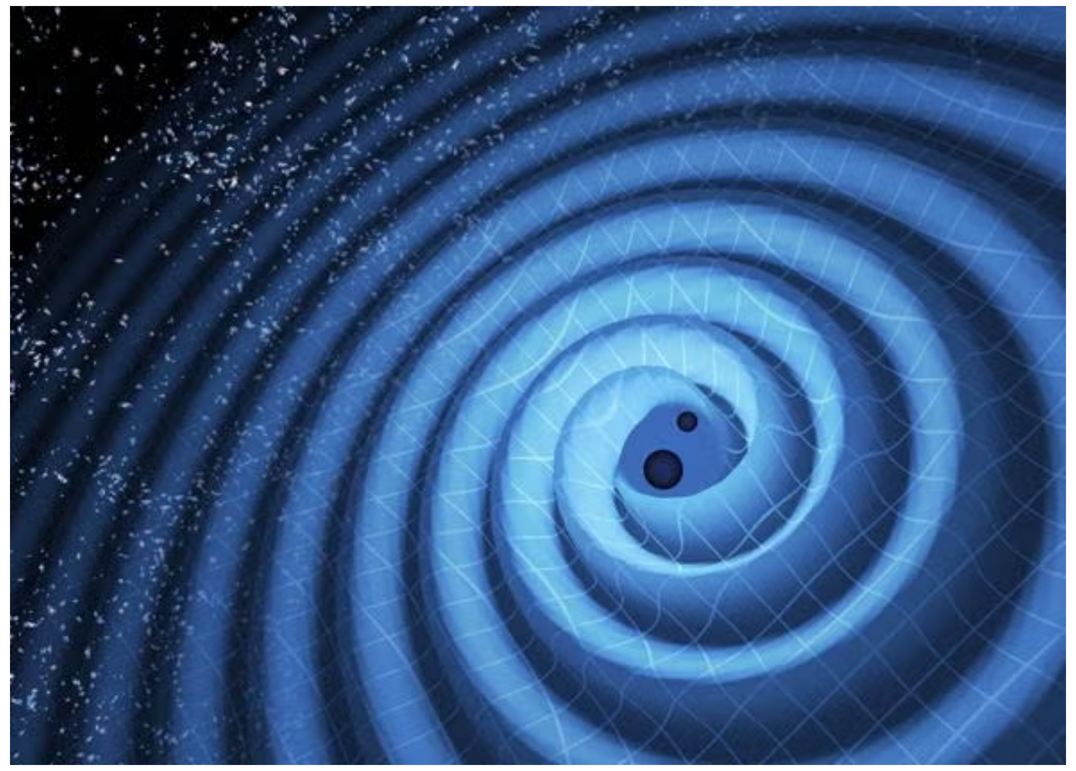

- Dark matter effects may modify the predicted evolution of compact binaries

A new window into dark matter

- Dark matter effects may modify the predicted evolution of compact binaries
- The population distribution of black hole masses could be used to constrain primordial black holes

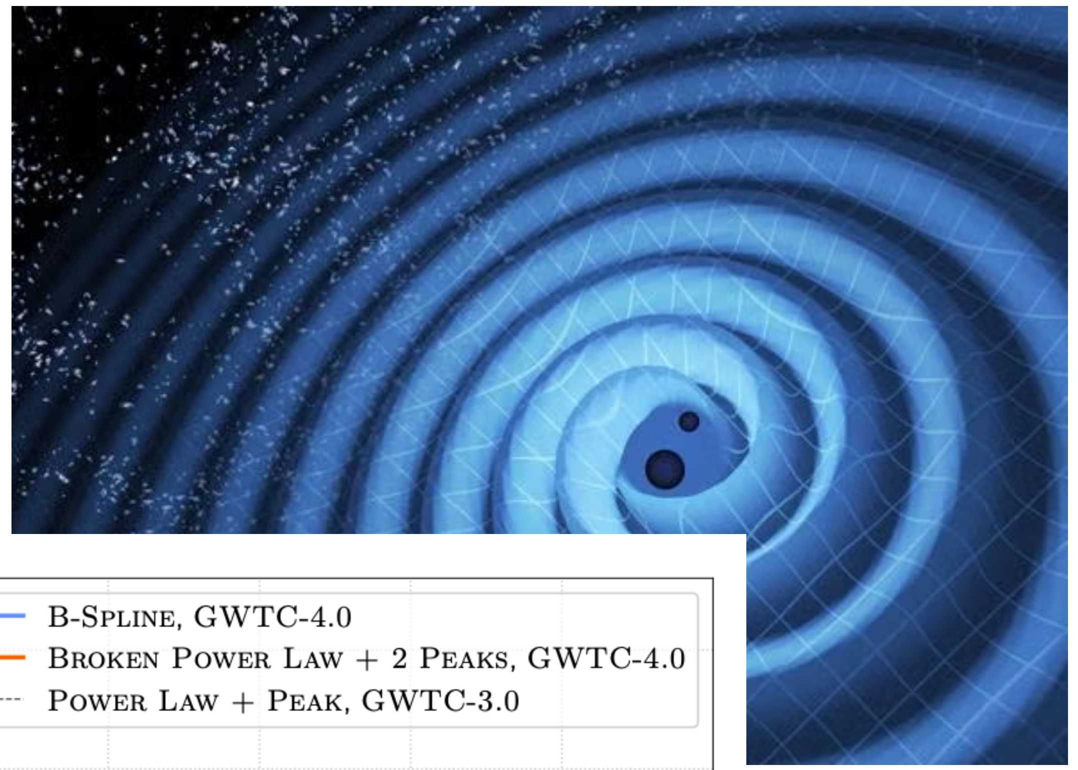

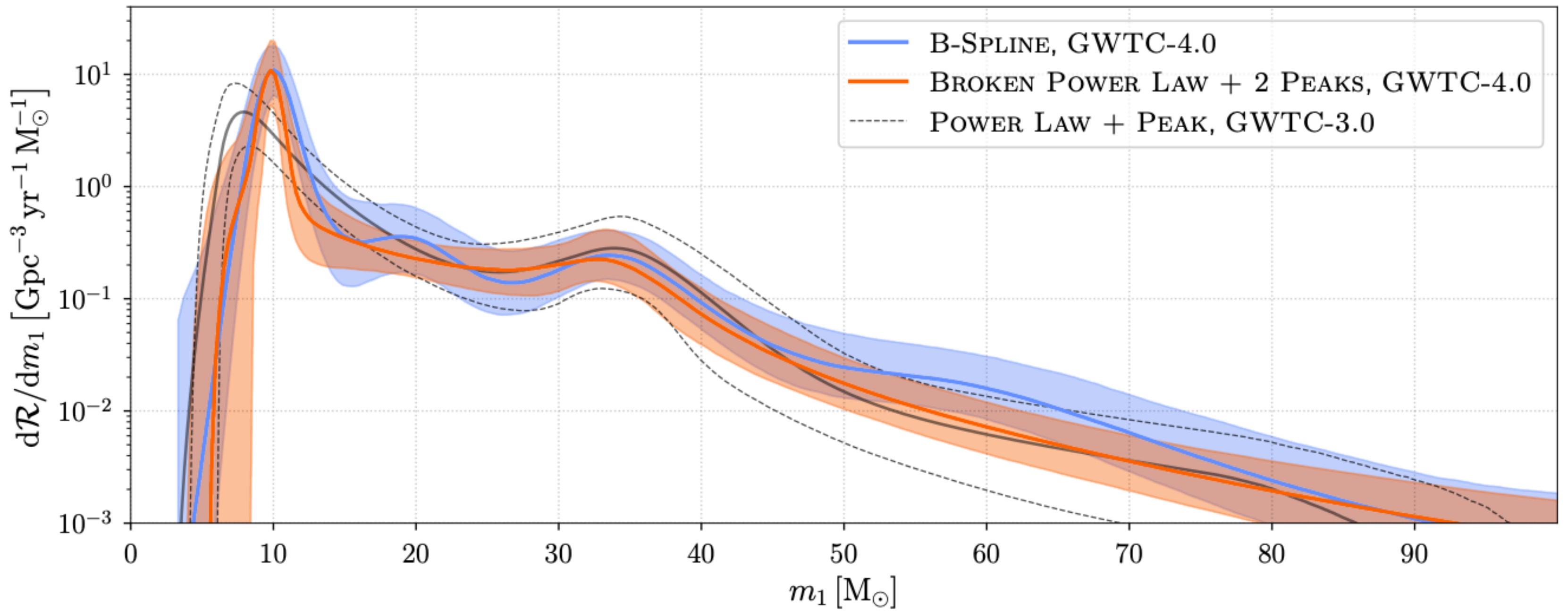

A new window into dark matter

- Dark matter effects may modify the predicted evolution of compact binaries
- The population distribution of black hole masses could be used to constrain primordial black holes
- Measurements of gravitational lensing could constrain the distribution of dark matter in our Universe

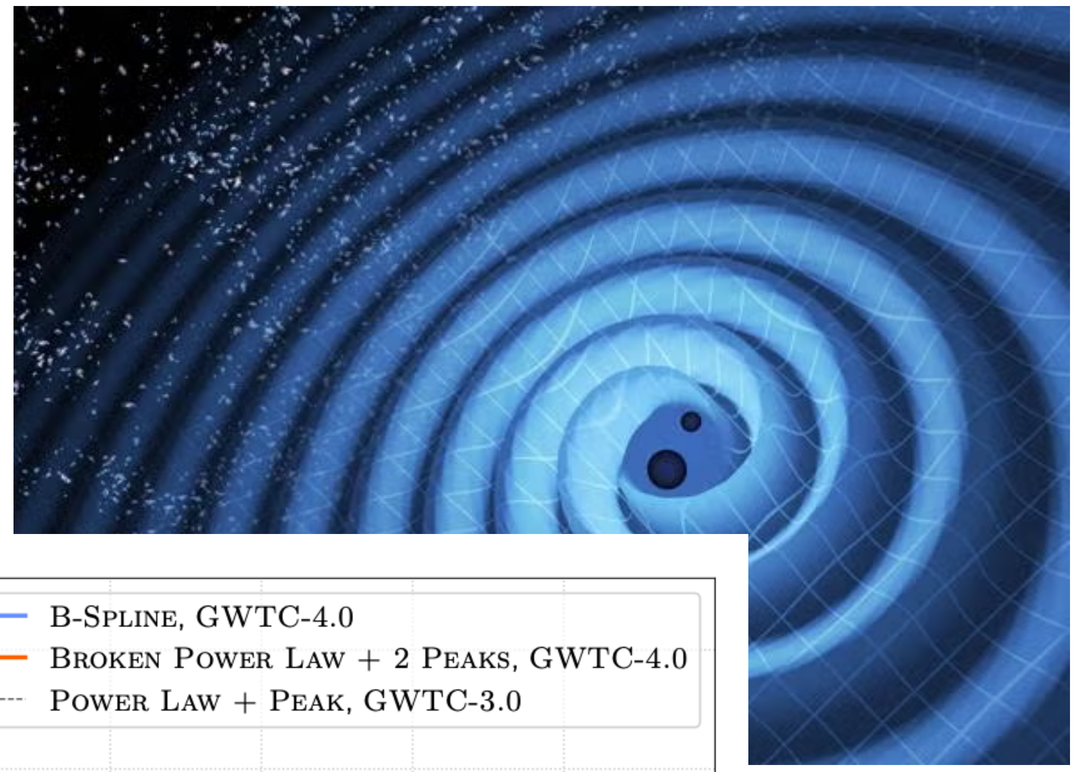

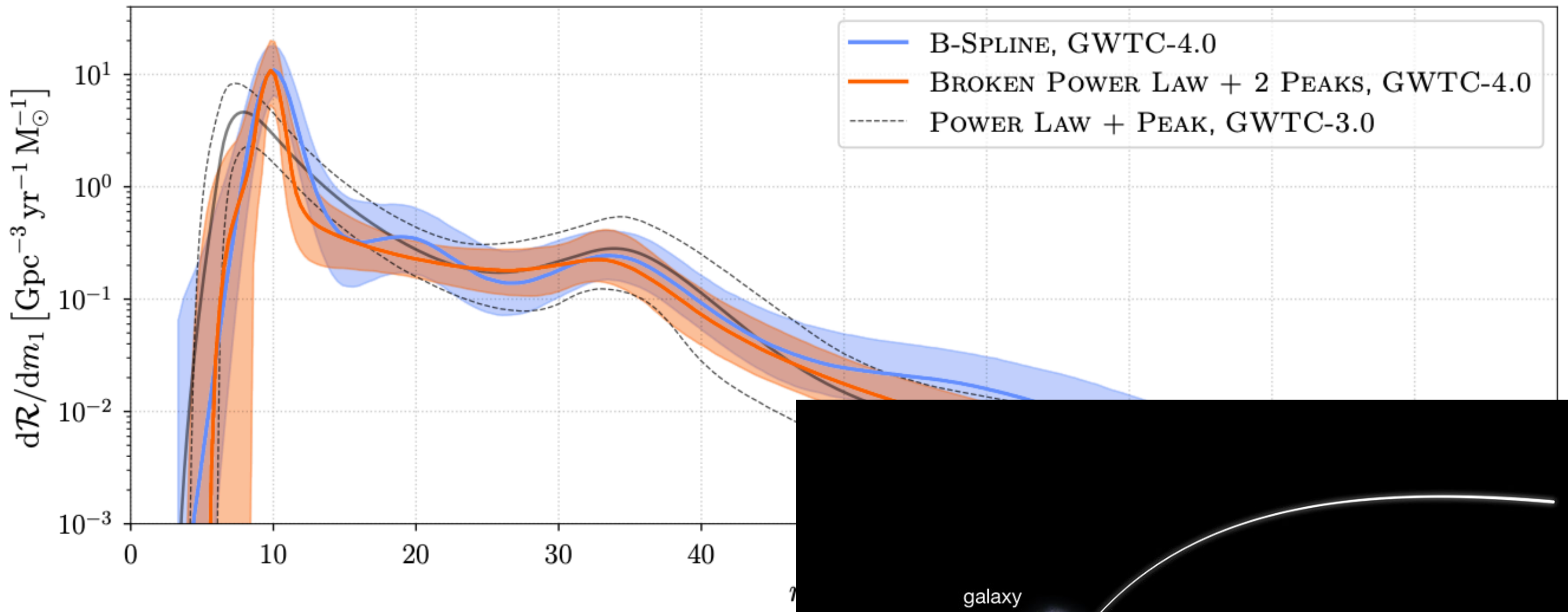

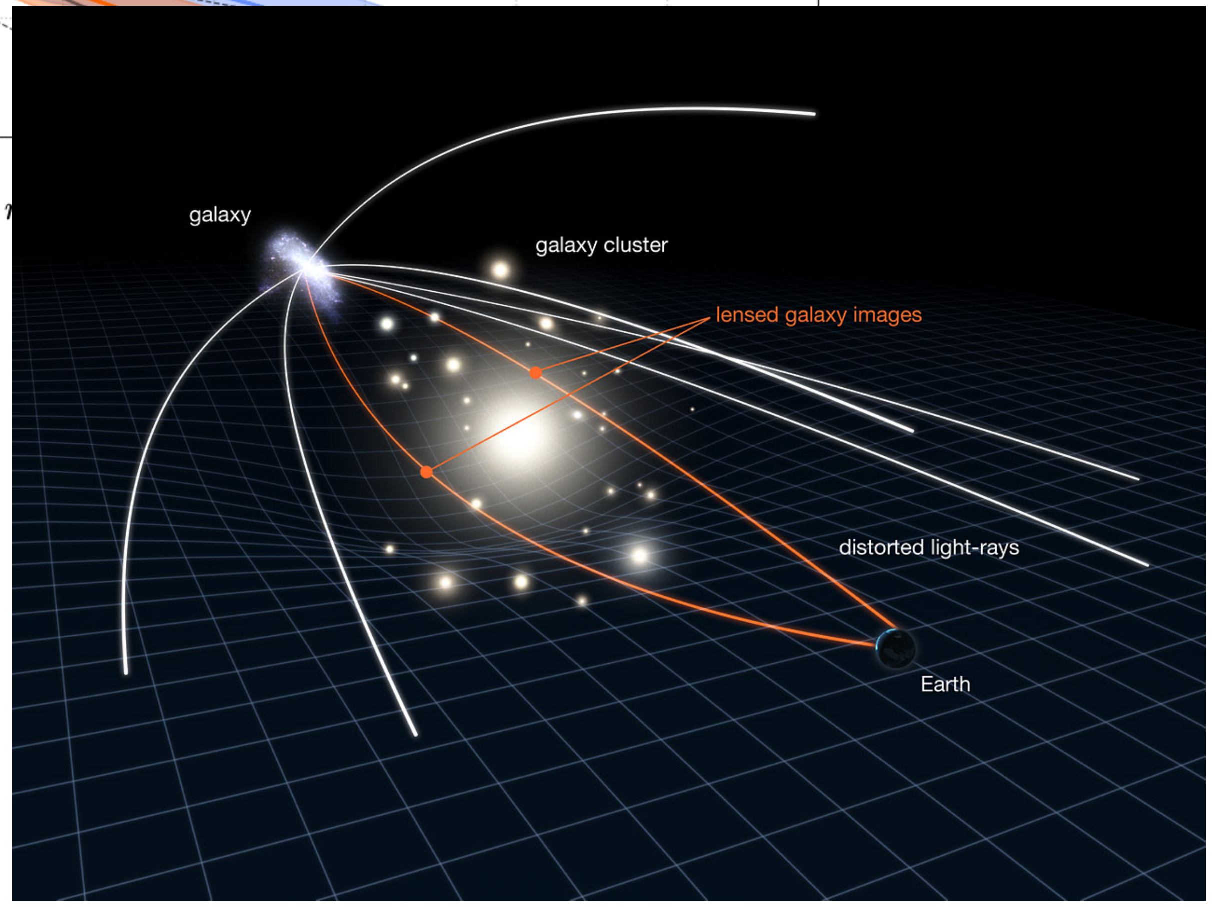

A new window into dark matter

- Dark matter effects may modify the predicted evolution of compact binaries
- The population distribution of black hole masses could be used to constrain primordial black holes
- Measurements of gravitational lensing could constrain the distribution of dark matter in our Universe
- Pulsar timing arrays could be used to probe the qualities of the dark matter in the Milky Way Galaxy

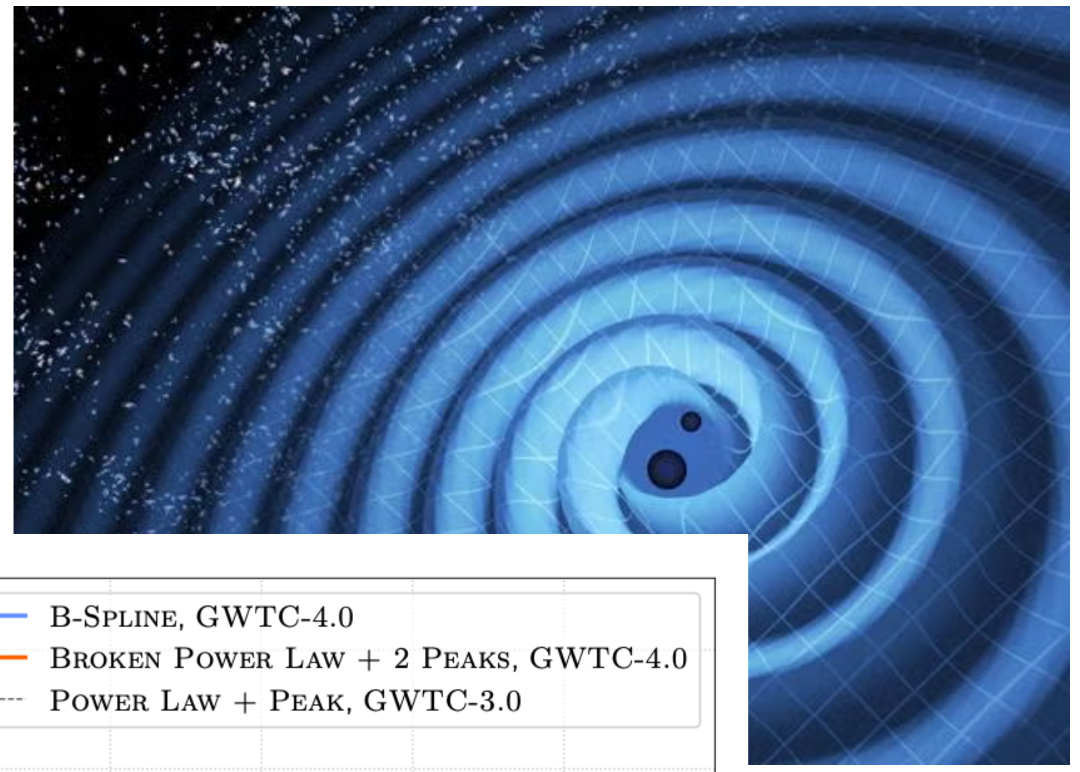

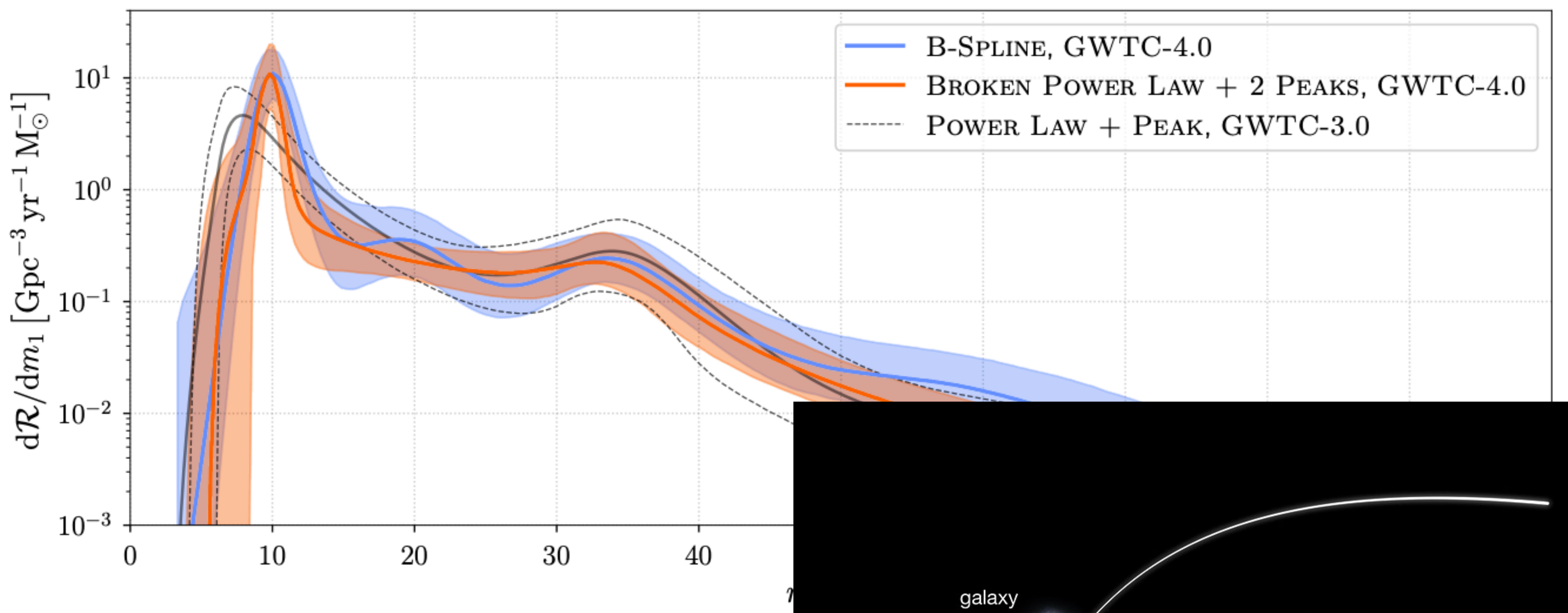

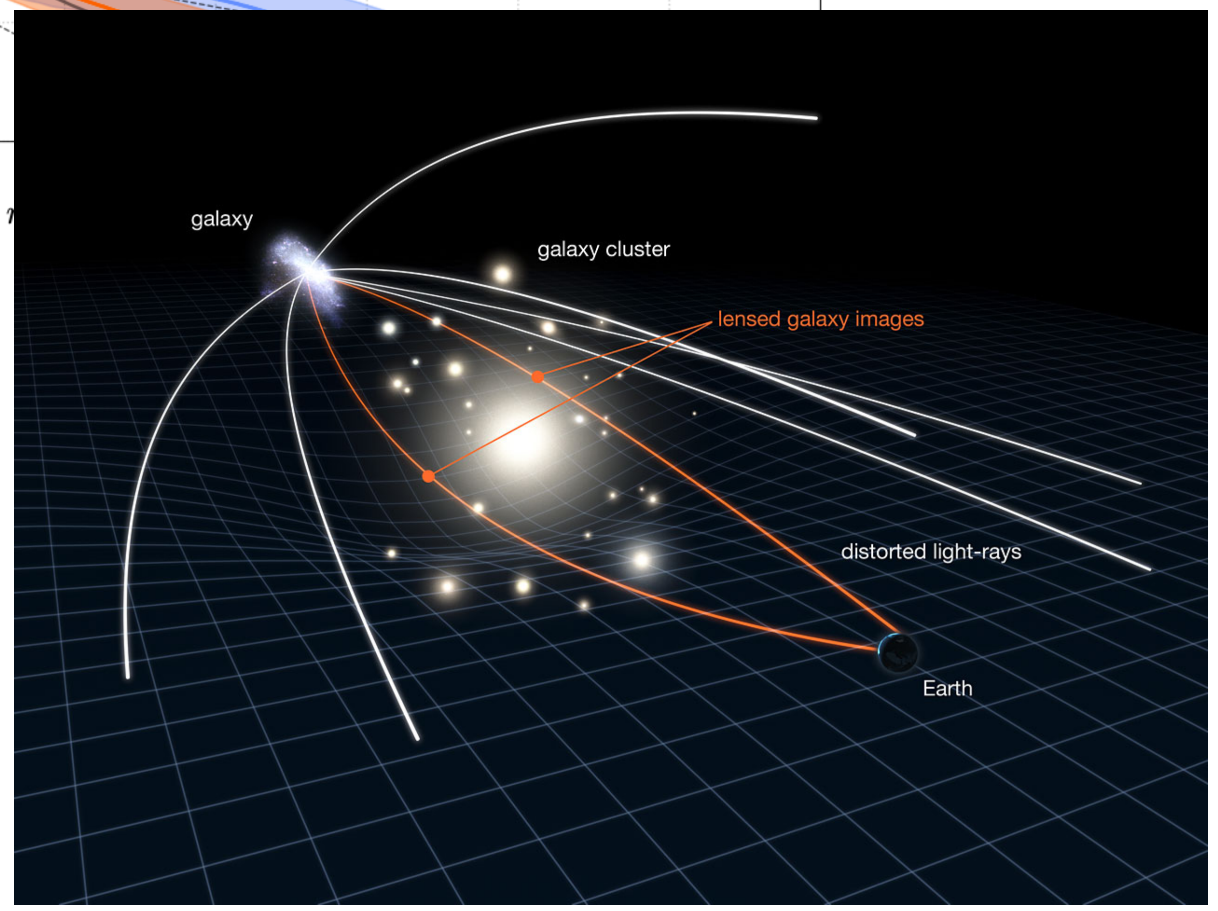

A new window into dark matter

- Dark matter effects may modify the predicted evolution of compact binaries
- The population distribution of black hole masses could be used to constrain primordial black holes
- Measurements of gravitational lensing could constrain the distribution of dark matter in our Universe
- Pulsar timing arrays could be used to probe the qualities of the dark matter in the Milky Way Galaxy
- …

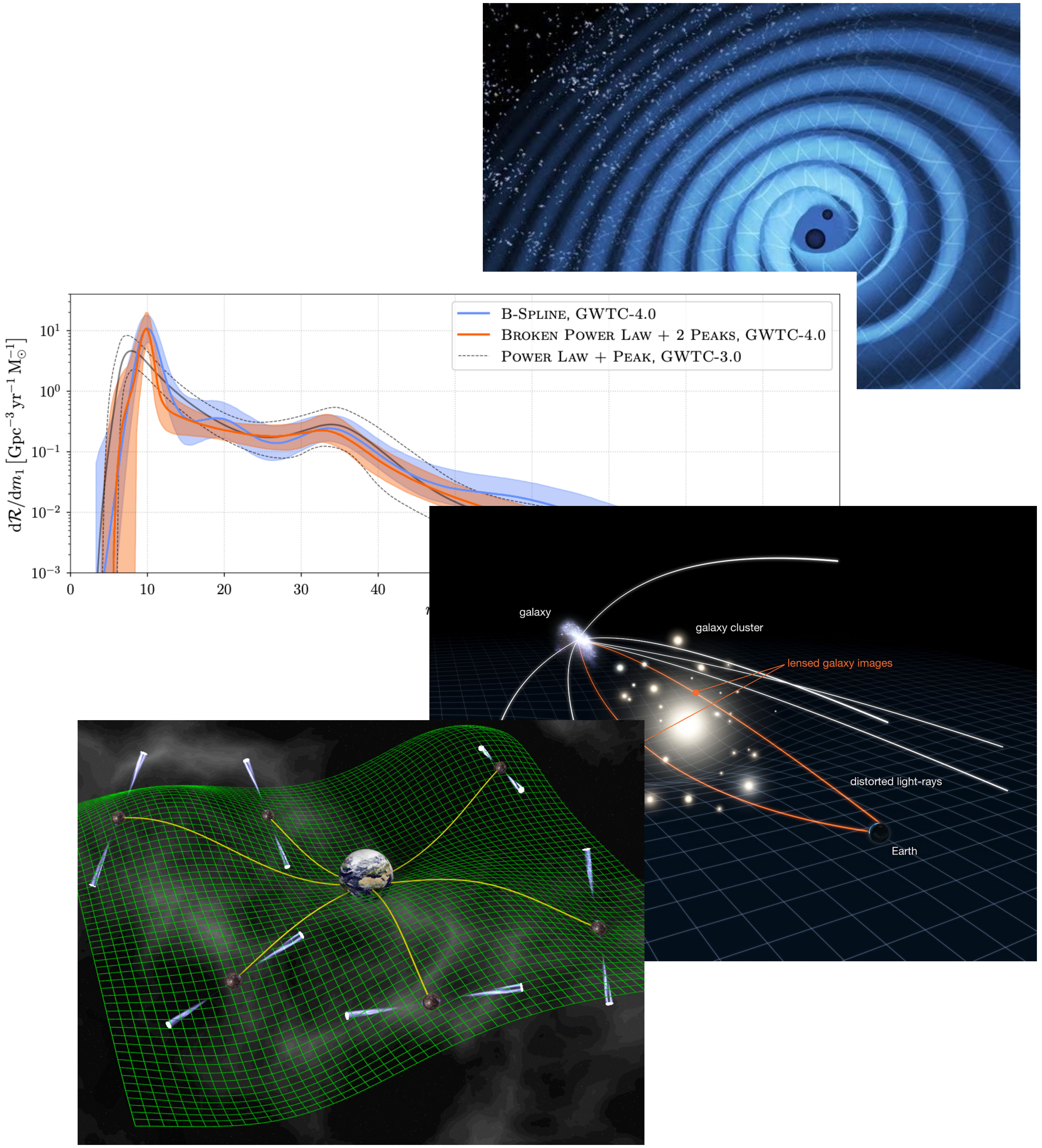

Testing gravity itself

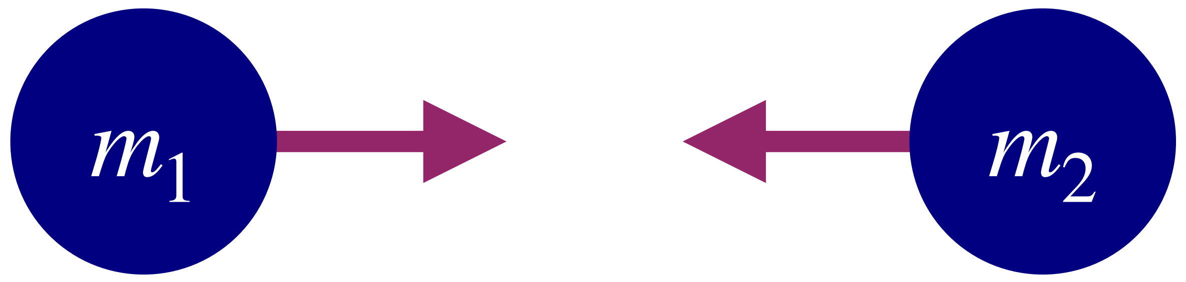

Testing gravity itself

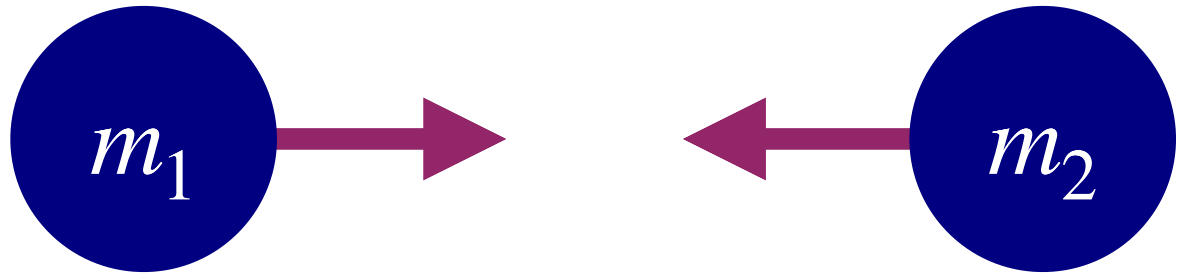

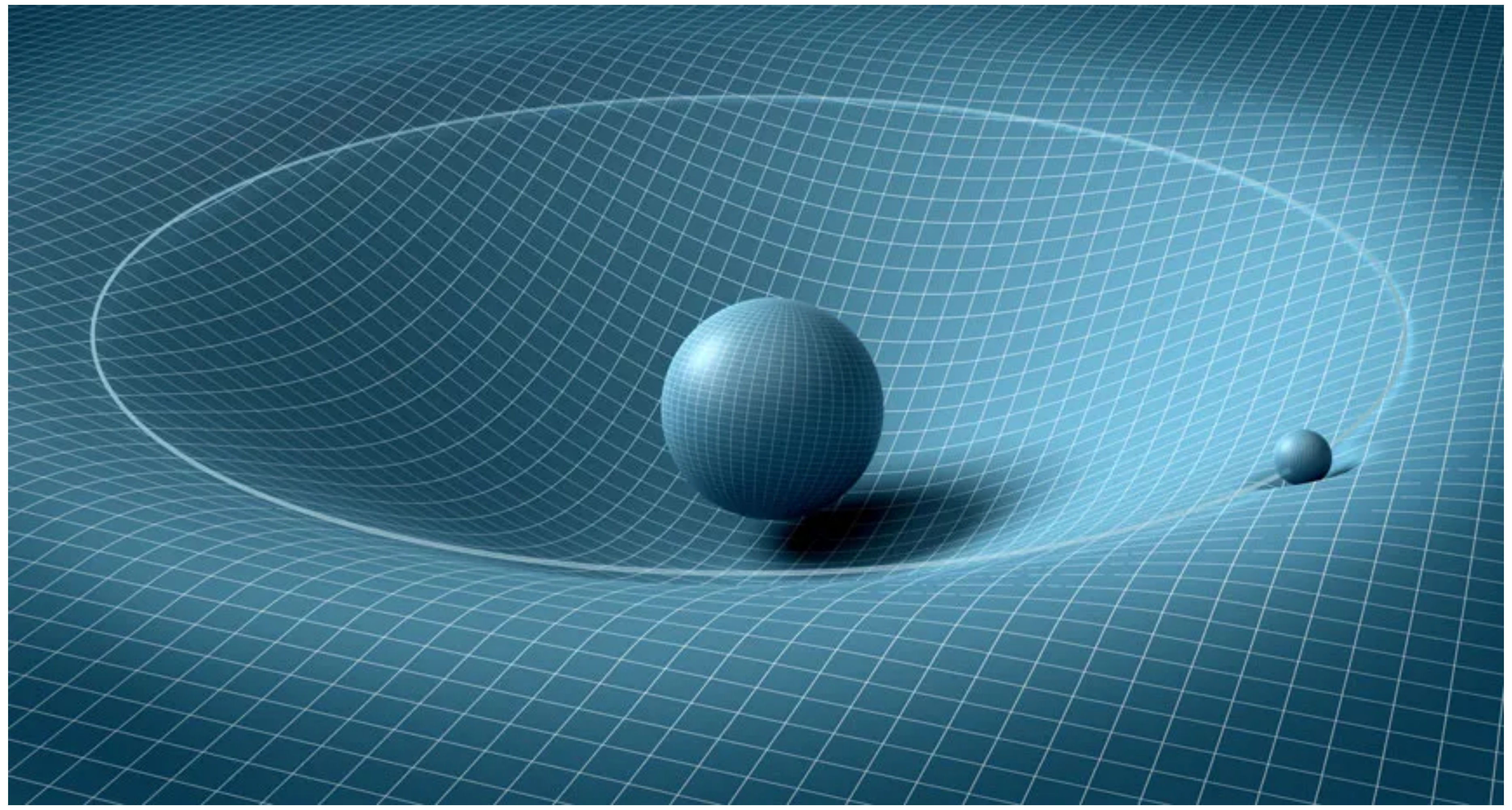

Testing gravity itself

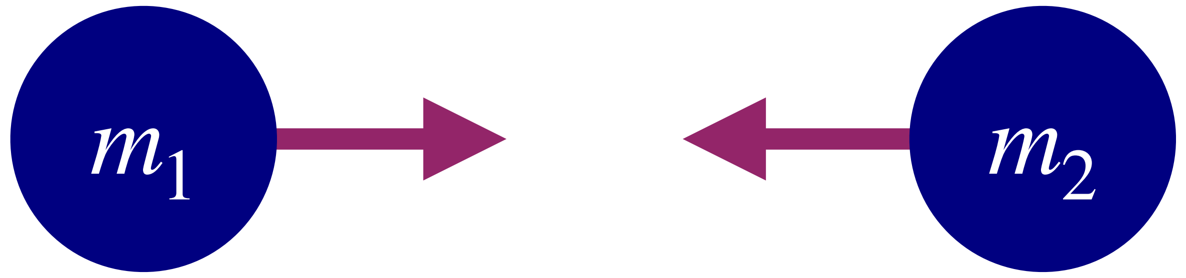

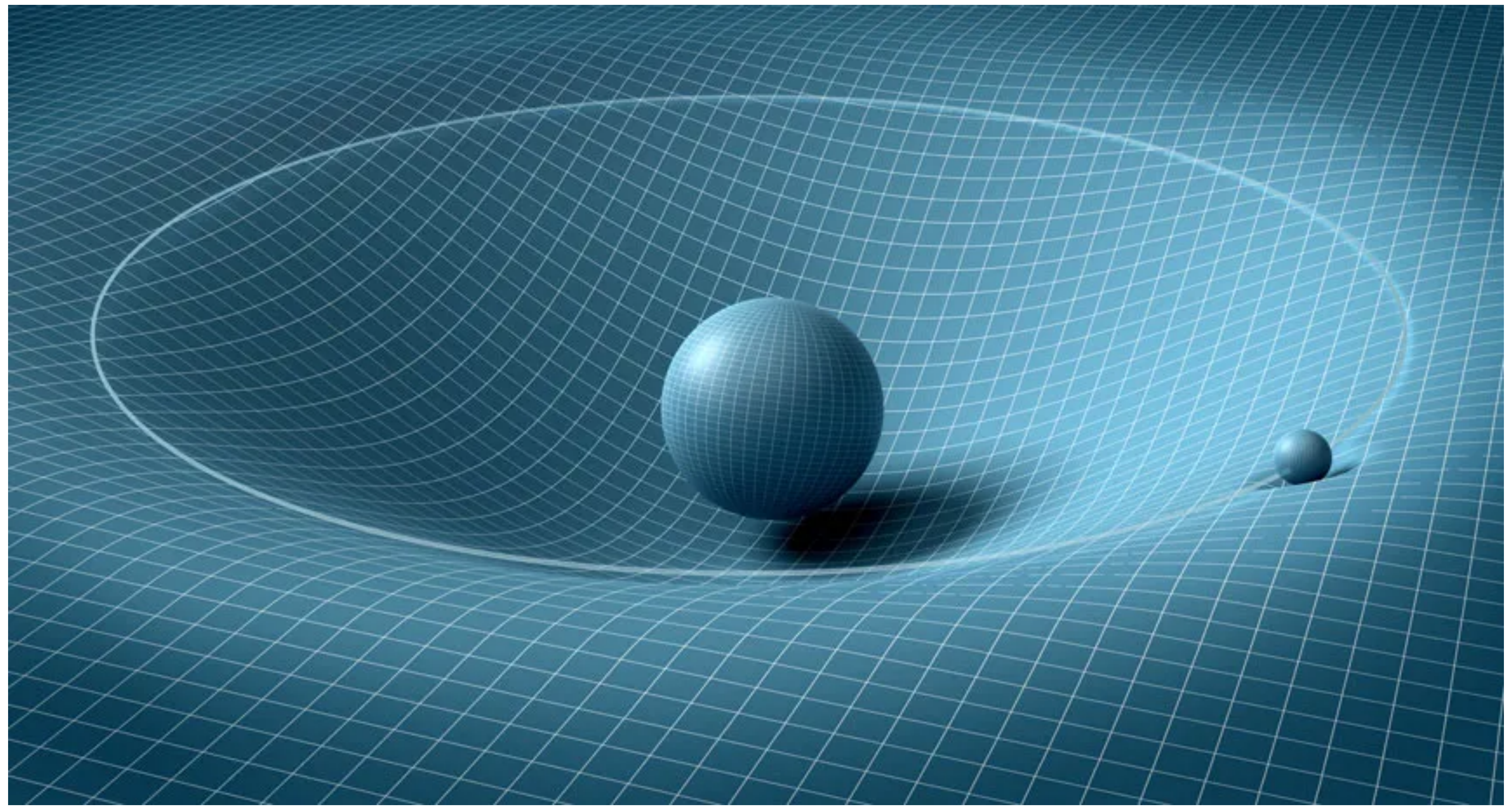

?

Useful links

"Gravitational Waves from Merging Compact Binaries: How Accurately Can One Extract the Binary's Parameters from the Inspiral Waveform?"

(https://arxiv.org/abs/gr-qc/9402014)

"The basics of gravitational wave theory"

(https://arxiv.org/abs/gr-qc/0501041)

Handbook of Gravitational Wave Astronomy

(https://link.springer.com/referencework/10.1007/978-981-16-4306-4)

"A Brief History of Gravitational Waves"

(https://arxiv.org/abs/1609.09400)

"An introduction to Bayesian inference in gravitational-wave astronomy"

(https://arxiv.org/abs/1809.02293

"Gravitational-wave sensitivity curves"

(https://arxiv.org/abs/1408.0740)